The Mitotic Role and Regulation of Kinesin-8 Klp5 and Klp6 in Fission Yeast

Amy Unsworth

Submitted towards the degree of Doctor of Philosophy

University College London
Department of Biology
London
WC1E 6BT

ProQuest LLC
789 East Eisenhower Parkway
P.O. Box 1346
Ann Arbor, MI 48106-1346

I declare that the work in this thesis is my own work

Dedication

I would like to dedicate this thesis to the memory of my father, John Roberts; to my mother, Pauline Roberts; and to my brother, Anthony Roberts. All have, in different ways, inspired and encouraged me to think scientifically.

"Do you not know?
Have you not heard?
The LORD is the everlasting God,
the Creator of the ends of the earth.
He will not grow tired or weary,
and his understanding no one can fathom.

He gives strength to the weary
and increases the power of the weak.

Even youths grow tired and weary,
and young men stumble and fall;

but those who hope in the LORD
will renew their strength.
They will soar on wings like eagles;
they will run and not grow weary,
they will walk and not be faint."

Isaiah 40: 28-31

Acknowledgements

I would like to thank Takashi Toda for giving me the opportunity to carry out my doctoral research in his lab, and for his supervision of this project. I would also like to thank members of the Cell Regulation Lab, past and present, who have offered me their support, encouragement and friendship during the course of my PhD. I thank Yasmine Mamnun for her unceasing helpfulness, Nathalie Spielewoy for taking the time to read my thesis and to discuss my results with me, and Chiho Ikebe for her kindness. I thank my excellent fellow students Karen Griffiths and Chii-Shyang Fong – my PhD has been made infinitely more enjoyable by having them to laugh with, discuss with and moan with! I also thank Chii-Shyang for his beautiful microtubule drawings which he has allowed me to use. I would also like to thank my ex-fellow student Bentley Lim for his friendship and for his wise advice.

I would also like to thank members of the other yeast labs, as they have been a wonderful group of people to work and play with. I would especially like to thank Rafael Carazo-Salas for his patience in teaching me Delta Vision microscopy. I am very grateful to the members of my thesis committee: Denise Sheer, Julie Cooper and Frank Uhlmann, who have been extremely helpful, supportive and enthusiastic about my project.

Finally, I would like to thank my friends and family who have encouraged me and kept me sane during the course of my PhD. I would especially like to thank my husband Paul, for always believing in me, and supporting me in so many ways over the years.

This work was funded by the Medical Research Council and by Cancer Research UK.

Abstract

Chromosome segregation in mitosis is mediated by the spindle, a structure consisting of microtubule fibres. Microtubules are inherently dynamic; that is, constantly growing and shrinking; and this property is utilised in the cell to create pushing and pulling forces. Cells contain an array of stabilising and destabilising factors to achieve precise spatial and temporal control of microtubule dynamics. During mitosis, this enables spindle elongation and shortening to be co-ordinated with chromosome segregation. It also facilitates the capture of kinetochores by microtubules.

Several kinesin subfamilies regulate microtubule dynamics, namely Kinesin-8, -13 and -14. Klp5 and Klp6 in fission yeast belong to the Kinesin-8 family, which are thought to function both as plus-end motors and as microtubule depolymerisers. Klp5 and Klp6 form a heterocomplex. They localise to cytoplasmic microtubules during interphase, and to kinetochores, the spindle, and the spindle midzone during mitosis. Deletion mutants are viable but show defects in chromosome congression and segregation, and activation of the spindle checkpoint.

We show that mitotic chromosome movements are abnormal in *Δklp5/Δklp6* cells, and that in the absence of spindle checkpoint function, chromosome missegregation may occur. We also show that Klp5/6 are required for maintenance of constant metaphase spindle length. We constructed rigor (ATPase) mutants and show their phenotype. We explore the significance of Klp5/6 heterocomplex formation for subcellular localisation and regulation of activity. We find that Klp5 and Kp6 are co-dependent for their localisation to the nuclear mitotic spindle, and that monomers are able to enter the nucleus, but cannot be retained. We identify a conserved NLS in Klp5 and Klp6. We consider whether heterocomplex formation is required solely for nuclear retention of Klp5 and Klp6, or if they contribute differing properties to the complex. We made N- and C-terminal deletions, and constructed Klp5 and Klp6 chimeric molecules. We found that the C-termini are dispensable, but that both Klp5 and Klp6 N-termini contribute essential and distinct functions to the Klp5/Klp6 heterocomplex.

Abbreviations

°C	degree(s) centigrade
AA	amino acid
ADP	adenosine diphosphate
APC	anaphase promoting complex
ATP	adenosine triphosphate
C	protein C-terminus
CC	coiled-coil
CDK	cyclin-dependent kinase
CFP	cyan fluorescent protein
DAPI	4',6-diamidino-2-phenylindole dihydrochloride
DNA	deoxyribonucleic acid
dNTP	deoxynucleotide triphosphate(s)
dsRED	*Discosoma* sp. red fluorescent protein
EDTA	ethylene diamine tetra-acetic acid
EGFP	enhanced green fluorescent protein
FL	full-length
GDP	guanosine diphosphate
GFP	green fluorescent protein
GTP	guanosine triphosphate
HA	hemagglutinin A
HU	hydroxyurea
int	integrated into genomic locus
IP	immunoprecipitation
kb	kilo base(s)
kD	kilo dalton(s)
Klp	kinesin like protein
LMB	leptomycin B
M	molar
MBC	methyl 2-benzimidazolecarbamate
mg	milligram(s)
Min	minute
ml	milliletre(s)
mM	millimolar
mRFP	monomeric red fluorescent protein

MT	microtubule
N	protein N-terminus
NES	nuclear export signal
ng	nanogram
NLS	nuclear localisation signal
PAGE	polyacrylamide gel electrophoresis
PCR	polymerase chain reaction
pH	puissance hyprogene
RNAi	ribonucleic acid interference
SAC	spindle assembly checkpoint
S.c.	*Saccharomyces cerevisiae* (budding yeast)
SDS	sodium dodecyl sulphate
Sec	second
S.p.	*Schizosaccharomyces pombe* (fission yeast)
SPB	spindle pole body
TBZ	thiabendazole
ts	temperature sensitive
WCE	whole cell extract
WT	wildtype
YE5S	rich fission yeast media
Δ	deletion
μg	microgram(s)
μl	microlitre(s)

Contents

Table of Figures

1 Introduction

Ever since Rudolf Virchow (1821 – 1902) famously proclaimed "Omnis cellula e cellula" (all cells are derived from cells), scientists have endeavoured to explain the remarkable phenomenon whereby cells reproduce by dividing. The process of cell division is essential for growth, repair and replenishment in multicellular organisms, and for the propagation of unicellular organisms. Cell division needs to be very precisely regulated to ensure that the different events proceed in a timely manner and in the correct order.

One crucial step during cell division is the equal segregation of DNA to daughter cells. Failure to achieve this results in aneuploidy and genomic instability, which are classic hallmarks of cancer in somatic cells, and which, in gametes, can lead to genetic disease. It is therefore of utmost interest and importance to study the highly conserved process of cell division, and its regulation.

1.1 Fission Yeast

The fission yeast *Schizosaccharomyces pombe* is a typical eukaryote, carrying out cellular processes such as transcription initiation, intron splicing, protein modification, and the mitotic cell cycle. Many of the mechanisms and molecules involved are conserved from yeast to humans, and fission yeast is therefore an ideal model for the characterisation and elucidation of these processes. In this study we use the fission yeast as a model organism to investigate the role of two kinesin-like proteins in regulation of microtubule dynamics and chromosome segregation.

Fission yeast is a unicellular ascomycete fungus, distantly related to the budding yeast *Saccharomyces cerevisiae*. Cells are rod-shaped, with a rigid cell wall. They grow by end-extension, reach a maximal length of 14-16μm, and then divide by medial fission. Fission yeast is ordinarily a haploid organism, with a genome size of approximately 14Mb, divided into three large chromosomes of 5.7, 4.7 and 3.5Mb (Fan *et al.*, 1989). Sequencing of the fission yeast genome was completed in 2002 (Wood *et al.*, 2002), revealing that it has 4824 genes. Fission yeast is a heterothallic organism, and under starvation conditions, cells of opposite mating types (i.e. h^+ and h^-) will conjugate to form diploid zygotes, which then immediately undergo meiosis and sporulation to produce four haploid spores contained within an ascus. This feature has facilitated strain crossing and genetic mapping.

Fission yeast is an excellent model organism. It readily undergoes homologous recombination, facilitating gene tagging, deletion and replacement. The ease with which complete gene deletions can be generated is a distinct advantage, as analysis of complete deletion phenotypes is simpler than analysis of partial knockdown phenotypes, as is required for RNAi experiments in higher eukaryotes. Conditional mutants, to investigate the function of essential genes, have also been used extensively in fission yeast.

1.2 Cytoskeleton

All eukaryotic cells have an internal cytoskeleton, which provides the cell with rigidity, and gives cells their characteristic shapes and structures, which are necessary for their proper function. The spindle, a major piece of machinery required to pull apart sister chromatids prior to cell division, is a cytoskeletal component. The cytoskeleton also provides a transport network, along which molecules and organelles can travel from one part of the cell to another. The cytoskeleton comprises three different kinds of polymer; actin filaments, microtubules (MTs) and intermediate filaments. Each type of polymer is composed of a different type of protein subunit. Fission yeast cytoskeletons consist only of MTs and actin cables and filaments.

1.2.1 Microtubules (MTs)

Microtubule (MT) polymers are made up of tubulin heterodimers, each consisting of one α-tubulin and one β-tubulin subunit. Each monomer subunit is able to bind one molecule of GTP nucleotide. The GTP in the α-tubulin subunit is deeply buried and stably bound, and cannot be hydrolyzed; in contrast the GTP bound to the β-tubulin subunit is exposed and can be hydrolyzed to GDP, and exchanged.

Tubulin heterodimers associate to form long protofilaments in which the tubulin heterodimers are all oriented in the same direction (Amos and Klug, 1974). These protofilaments then associate laterally with each other to make MTs, which are hollow cylindrical structures. MTs usually consist of 13 parallel protofilaments arranged in a ring (Evans *et al.*, 1985), although this number can vary. This structural arrangement means that MTs are inherently polar molecules, with α-tubulins exposed at one end (the 'minus end'), and β-tubulins exposed at the other (the 'plus end') (Mitchison, 1993; Hirose *et al.*, 1995; Fan *et al.*, 1996). As a result, the two different ends of a MT have distinct properties, which is important for their roles within the cell, as will be further explained later.

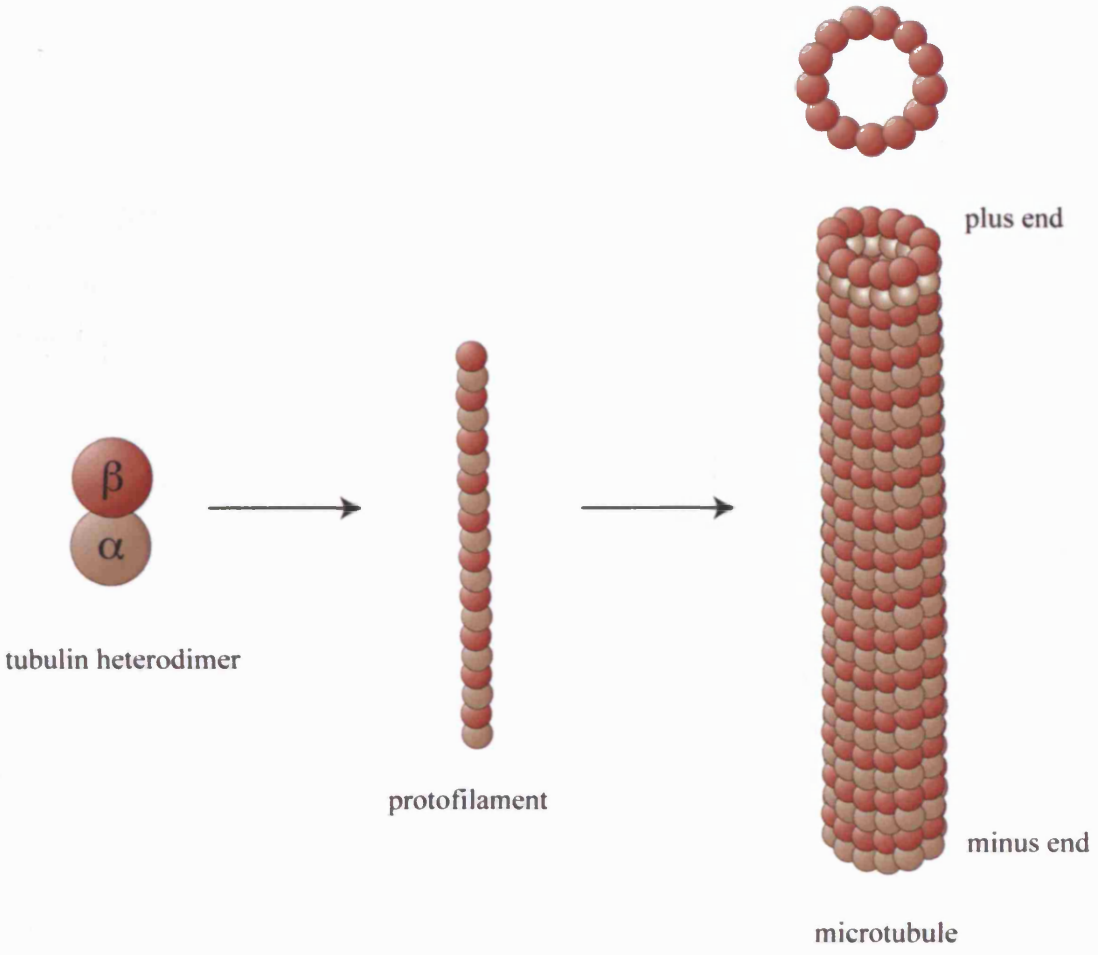

Figure 1.1 MT Structure

α- and β-tubulin monomers associate to form stable tubulin heterodimers. A protofilament consists of many heterodimers arranged with the same orientation. 13 parallel protofilaments associate laterally to form the cylindrical MT structure.

Fission yeast has four tubulin genes: two α-tubulin, *nda2* and *atb2*, one β-tubulin, *nda3* and one γ-tubulin, *gtb1/tug1* (see section 1.2.3).

1.2.2 Microtubule Dynamics

MTs undergo stochastic periods of growth and shrinkage, a property referred to as dynamic instability (Mitchison and Kirschner, 1984). The change to rapid shrinkage is called catastrophe, and the change to growth is called rescue. Once an αβ-tubulin subunit has been incorporated into the MT structure, the GTP bound to the β-tubulin can be hydrolysed to GDP (David-Pfeuty *et al.*, 1977; MacNeal and Purich, 1978). The dissociation rate constant of GDP tubulin is very large compared with that of GTP tubulin, meaning that a MT composed entirely of GDP tubulin will rapidly depolymerise. This is because the hydrolysis of GTP to GDP causes a conformational change within the tubulin subunits (Melki *et al.*, 1989). GTP tubulin subunits make strong and regular lateral contacts with each other, producing straight protofilaments. However, GDP tubulin protofilaments are curved, and can easily peel away from each other, resulting in depolymerisation of the MT. If a MT is growing rapidly, then additional GTP-containing subunits will be added to the lattice before the most recently added subunits have hydrolysed their GTP. This means that the tip of the MT always contains GTP, referred to as a 'GTP cap', which stabilises the MT structure, enabling it to continue growing (Mitchison and Kirschner, 1984). However, when the rate of GTP hydrolysis exceeds the rate of polymerisation, the subunits at the end of the MT will contain GDP, and the MT will be unstable and rapidly depolymerise, i.e. catastrophe occurs.

The property of dynamic instability is important for the *in vivo* functions of MTs. It enables the rapid remodelling of the MT cytoskeleton throughout the cell cycle (see section 1.2.4). It also allows MTs to rapidly explore three-dimensional space, which is especially important for the capture of kinetochores during early mitosis (see section 1.5.2).

1.2.3 Microtubule Organising Centres (MTOCs)

MTs can assemble *in vitro* from purified αβ-tubulin dimers, but this is a slow process. *In vivo*, the growth of new MTs is nucleated by protein complexes called MTOCs (Microtubule Organising Centres). In most animal cells, the centrosome is the sole MTOC. In fission yeast, the SPB (Spindle Pole Body, the centrosome equivalent) nucleates MT growth during interphase and mitosis; MTs are also nucleated from additional nuclear membrane-associated, cytoplasmic non-SPB sites during interphase, referred to as iMTOCs (interphase MTOCs). At the end of mitosis, the eMTOCs (equatorial MTOCs) nucleate MT growth at the septum.

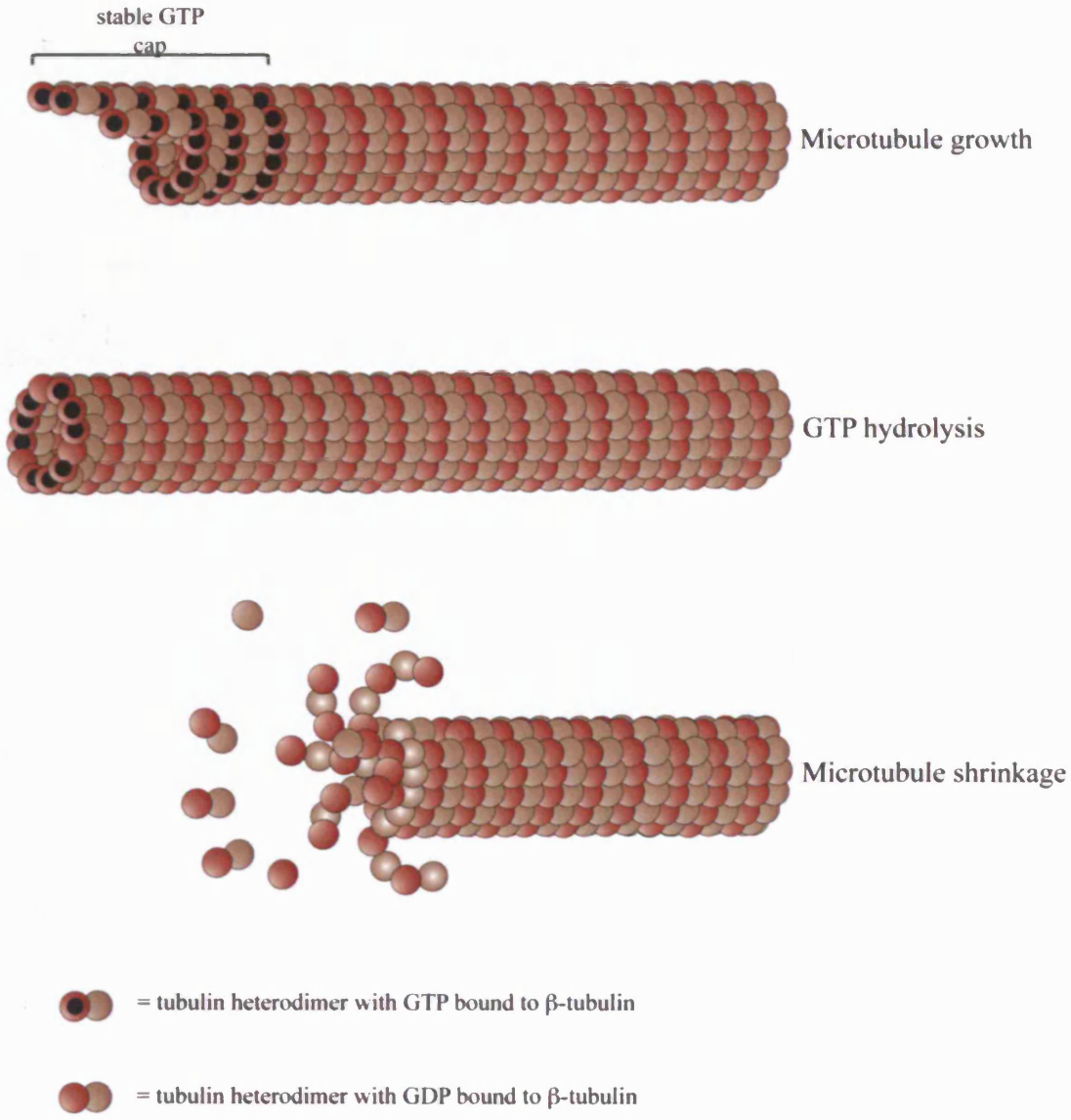

Figure 1.2 Microtubule Dynamic Instability

During periods of growth, stable GTP-tubulin heterodimers are added to the microtubule plus end. Once incorporated into the microtubule lattice, GTP hydrolysis occurs. GDP-tubulin is very unstable, but the GTP cap at the plus end of the microtubule ensures that a straight, stable microtubule structure is maintained. When the GTP in the GTP cap is hydrolysed to GDP, the microtubule undergoes catastrophe – a switch to shrinkage. GDP-tubulin protafilaments adopt a curved conformation, favouring disassembly of the microtubule structure.

The SPB resides on the cytoplasmic face of the nuclear envelope during interphase, where it nucleates cytoplasmic MTs. In fission yeast the SPB duplicates at the G1/S boundary, but the mother and daughter SBB remain joined by a bridge, and do not fully mature until exit from S phase (Uzawa *et al.*, 2004). At the onset of mitosis, the nuclear envelope invaginates, thereby allowing insertion of the duplicated SPBs into the nuclear membrane, so that they can nucleate intranuclear MTs to form the spindle during mitosis (Ding *et al.*, 1997).

One of the key players in MT organisation at MTOCs is a member of the tubulin family called γ-tubulin. γ-tubulin forms complexes with other proteins, which are accordingly named γ-tubulin complex proteins (GCP 1-6). The resulting protein complexes are referred to as the γ-TuC (γ-tubulin complex) or γ-TuSC (γ-tubulin small complex), found in yeast and metazoans, and the larger γ-TuRC (γ-tubulin ring complex) found only in metazoans, and so named because EM shows that the complex forms a ring structure (Raynaud-Messina and Merdes, 2007). There are currently two models suggesting how γ-tubulin nucleates MTs. In the 'template model', γ-tubulin molecules associate laterally to form a ring, onto which αβ-tubulin polymerises to make a MT. Alternatively, the 'protofilament model' suggests that γ-tubulin molecules associate longitudinally to form a protofilament-like structure, with which αβ-tubulin can associate laterally and longitudinally, making protofilaments that subsequently close to form the cylindrical MT structure. Evidence for both models has been reported (Erickson, 2000; Keating and Borisy, 2000; Moritz *et al.*, 2000; Wiese and Zheng, 2000). EM studies seem to show a γ-TuRC cap at MT minus ends, favouring the template model (Keating and Borisy, 2000; Moritz *et al.*, 2000; Wiese and Zheng, 2000). However, MTs can also be nucleated by the smaller γ-TuSCs (Verollet *et al.*, 2006), and there is no evidence that these can form rings.

The γ-TuSC consists of two copies of γ-tubulin (GCP1) and one copy each of GCP2 and GCP3 . The corresponding fission yeast homologues of these proteins are Gtb1, Alp4 and Alp6 (Horio *et al.*, 1991; Stearns *et al.*, 1991; Vardy and Toda, 2000). Three fission yeast homologues of the γ-TuRC proteins GCP4, GCP5 and GCP6 have also been found; Gfh1, Mod21 and Alp16, respectively (Fujita *et al.*, 2002; Venkatram *et al.*, 2004; Anders *et al.*, 2006).

1.2.4 Fission Yeast MT Cytoskeleton

The MT cytoskeleton has to undergo extensive reorganization as the cell transitions from interphase to mitosis, and back to interphase again (illustrated in Figure 1.3). In interphase, the MT cytoskeleton is essential for establishment of polarised growth at the cell ends (La Carbona *et al.*, 2006), for positioning the nucleus at the cell centre (Tran *et al.*, 2001), and

for distribution of organelles such as mitochondria (Yaffe *et al.*, 1996). During mitosis, MTs form the spindle to separate chromosomes prior to cell division.

There are three to four bundles of cytoplasmic MTs in an interphase fission yeast cell. These are oriented along the longitudinal axis, typically spanning more than half the cell length. They are positioned such that the dynamic plus-ends extend towards the cell tips, whereas the stable minus-ends overlap with each other in the vicinity of the nucleus (Drummond and Cross, 2000; Hoog *et al.*, 2007). The conserved Ase1 protein localises to MT overlap zones and is important for organising MTs into bundles (Loiodice *et al.*, 2005; Yamashita *et al.*, 2005). One EM study of MT bundle cross-sections suggests that there are two to five MTs per bundle (Carazo-Salas *et al.*, 2005), consistent with light microscopy observations, reporting 2-3 MTs per bundle, with 4-7 at the overlap zone (Sagolla *et al.*, 2003). MTs grow out towards the cell poles, pause there for several minutes, and then undergo catastrophe, shrinking back to the middle of the cell. However, catastrophe is only initiated when MTs touch the polar cortex of the cell, not if they touch the lateral cortex (Brunner and Nurse, 2000; Sagolla *et al.*, 2003; Grallert *et al.*, 2006).

Interphase MTs are nucleated from iMTOCs and the SPB at the nuclear periphery. However, it has been observed that many MT bundles are not in contact with the nuclear surface. In some other eukaryotes nucleated MTs are released from MTOCs by katanin, a MT severing protein (McNally and Vale, 1993). However, katanin does not exist in fission yeast. Recently it has been found that MT arrays in fission yeast can be organised independently of nuclear-associated MTOCs. Mto1 and Mto2 recruit γ-tubulin to cytoplasmic nucleation sites (Samejima *et al.*, 2005; Venkatram *et al.*, 2005), and Ase1 and the kinesin-like protein Klp2 are thought to fuse the newly nucleated MTs with pre-existing bundles (Carazo-Salas and Nurse, 2006; Daga *et al.*, 2006a).

At the onset of mitosis, cytoplasmic MT arrays disappear because the growth of new MTs is inhibited. Existing cytoplasmic MTs complete their cycle of growth/shrinkage and the mitotic spindle begins to form (Sagolla *et al.*, 2003). The SPBs nucleate spindle MTs, which become interdigitated at their plus ends by the action of Cut7, an essential member of the BimC/Kinesin-5 family (Hagan and Yanagida, 1992). As polymerisation at the MT plus-ends occurs, the spindle lengthens to span the nucleus by metaphase. A spindle typically consists of 12-14 pole-to-pole MTs nucleated from each SPB, with an additional 3-4 MTs connecting each of the six kinetochores to the SPB (designated kinetochore MTs, or k-fibres) (Ding *et al.*, 1993). Additional MTs that are not part of the spindle are also visible at this stage, although it is currently debatable whether these represent cytoplasmic astral MTs involved in spindle orientation (Gachet *et al.*, 2001; Oliferenko and Balasubramanian, 2002;

Gachet *et al.*, 2004; Rajagopalan *et al.*, 2004; Tournier *et al.*, 2004), or intranuclear MTs (Zimmerman *et al.*). Recent data indicates that the initial orientation of the spindle is dictated by interphase MT orientation, and is not dependent on astral MTs (Vogel *et al.*, 2007). The spindle lengthens substantially during anaphase B, and dynamic cytoplasmic astral MTs are visible extending at a tangent from the SPB. The spindle then starts to break down and MTs are nucleated from the eMTOCs in the centre of the cell to form the post-anaphase array (PAA) (Hagan and Hyams, 1988). The PAA initially appears as a ring localised to the cytokinetic actin ring (CAR), but MTs may then be released to create the characteristic PAA pattern. It has been suggested that the PAA functions to maintain the distance between the segregated daughter nuclei, keeping them away from the cell division site (Hagan and Hyams, 1988). However, mutant cells lacking a PAA (e.g. *mto1* mutants) apparently grow and divide normally. The physiological role of the PAA therefore remains to be elucidated; however, it has been established that the PAA structure must be disintegrated for interphase MTs to be reorganised at the beginning of the cell cycle (Zimmerman *et al.*, 2004b). Concomitant with PAA appearance is the enhanced nucleation of MTs from the SPB. Cytokinesis is completed, the daughter cells separate and the interphase configuration of cytoplasmic MT bundles is re-established.

1.2.5 Microtubule Associated Proteins (MAPs)

Although MTs are inherently dynamic, these dynamics are exquisitely regulated in the cell by an array of MT stabilising and destabilising factors, referred to as MAPs (Microtubule Associated Proteins). MAPs were originally identified as proteins that co-purify with tubulin from vertebrate brains. Although MAPs have subsequently been identified in non-neuronal cells, they are especially abundant in the brain. The majority of MAPs identified to date have MT stabilising activities. These include the Tau family of proteins, the major MAP in brain neuronal axons; paired filaments formed from this protein are a hallmark of Alzheimer's disease. Additional MT stabilisers in vertebrate cells are MAP1A and MAP1B; STOP; syncolin; tetkins (Pollard, 2004) and doublecortin (Moores *et al.*, 2004).

One of the best characterised MT destabilizing factors in vertebrates is Op18/stathmin, which is important for mitotic regulation. It functions by sequestering tubulin and promoting catastrophe. Overexpression is linked with tumourigenesis, and it is therefore an attractive target for the development of anti-cancer drugs. Another well characterised MT destabiliser is XKCM1/MCAK. Although non-motile, this protein belongs to a kinesin subfamily and

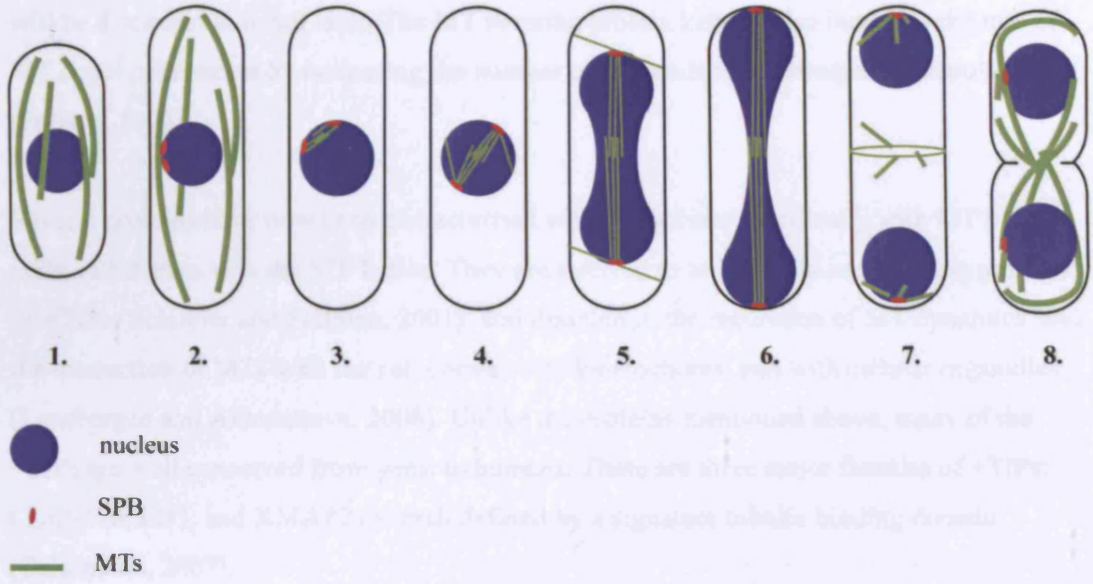

Figure 1.3 Changes in MT distribution throughout the cell cycle in fission yeast

Interphase cells have three to four bundles of cytoplasmic microtubule bundles oriented along the longitudinal axis (**1, 2.**). At the onset of mitosis, these disappear, and nuclear spindle microtubules are nucleated by the duplicated and separated SPBs (**3.**). The spindle lengthens, until it reaches a constant length of ~2.5μm at metaphase (**4.**). The spindle lengthens again during anaphase B, reaching a maximal length of 12-15μm (**5, 6.**) (Nabeshima *et al.*, 1998). The spindle then starts to break down and a post-anaphase array (PAA) of MTs is nucleated from eMTOCs (**7.**). This is followed by cytokinesis, and the re-establishment of cytoplasmic MT bundles in each of the two daughter cells (**8.**).

will be discussed in detail later. The MT severing protein katanin also increases the rate of MT depolymerisation by increasing the number of MT ends that subsequently depolymerise (Pollard, 2004).

Several proteins have now been characterised which associate specifically with MT plus ends, rather than with the MT lattice. They are referred to as MT plus-end tracking proteins, or +TIPs (Schuyler and Pellman, 2001), and function in the regulation of MT dynamics, and the interaction of MTs with the cell cortex, with kinetochores, and with cellular organelles (Lansbergen and Akhmanova, 2006). Unlike the proteins mentioned above, many of the +TIPs are well conserved from yeast to humans. There are three major families of +TIPs: CLIP-170, EB1, and XMAP215, each defined by a signature tubulin binding domain (Cassimeris, 2007).

The fission yeast CLIP-170 member, Tip1, is transported to MT plus ends by the Tea2 kinesin, where its accumulation is dependent on Mal3. The EB1 family (*S.c.* Bim1; *S.p.* Mal3) promote MT polymerisation (Morrison *et al.*, 1998; Tirnauer *et al.*, 1999; Rogers *et al.*, 2002). It has been shown that fission yeast Mal3 may stabilise MTs by localising to the weak MT seam (Sandblad *et al.*, 2006).

Members of the XMAP-215 (ch-TOG) family have been identified in humans (Charrasse *et al.*, 1995; Charrasse *et al.*, 1996; Charrasse *et al.*, 1998), animals, plants and yeasts. There are two XMAP-215 (ch-TOG) members in fission yeast: Dis1 and Alp14, and just one in budding yeast: Stu2. Dis1 and Alp14 are partially redundant, with single deletion mutants exhibiting temperature sensitivities; *Δalp14* is defective at high temperatures (Garcia *et al.*, 2001), whereas *Δdis1* is defective at low temperatures (Ohkura *et al.*, 1988). These proteins are required for cytoplasmic microtubule organisation and for proper bipolar spindle formation in mitosis (Nabeshima *et al.*, 1995; Nakaseko *et al.*, 1996 {Garcia, 2001 #64; Garcia *et al.*, 2001; Nakaseko *et al.*, 2001). Deletion of both *alp14* and *dis1* is lethal. It has been shown that the budding yeast ch-TOG member, Stu2, and recently, *C. elegans* Zyg9 and XMAP215, are able to bind to free tubulin heterodimers, and it has been suggested that they then load these to the MT plus end, thereby stabilising it and facilitating polymerisation (Al-Bassam *et al.*, 2006; Al-Bassam *et al.*, 2007; Slep and Vale, 2007).

MT motors i.e. kinesins and dyneins may also be considered as MAPs and in recent years, several kinesin subfamilies have been shown to regulate MT dynamics. These are discussed in detail in sections 1.6.4 and 1.6.5.

1.3 Chromosomes

The genomic DNA within a cell is divided between several separate DNA molecules, which are packaged into chromosomes. The number of chromosomes varies widely from organism to organism, for example diploid human cells have 46 chromosomes, consisting of 23 pairs, whereas haploid fission yeast cells have only three chromosomes. Chromosomes contain several types of functional DNA sequence in addition to their genes, such as a centromere, two telomeres, and many replication origins (~ one per 100kb of DNA) (Pollard, 2004).

1.3.1 Centromeres

A chromosome's centromere regulates its movements during mitotic and meiotic cell divisions. In higher eukaryotes, it may be visible as a constricted region in the centre of a chromosome. The centromere is the platform onto which the proteinaceous kinetochore structure (see following section) is built, which mediates attachment to spindle microtubules during cell division.

In budding yeast, just 125 bp of DNA consisting of three distinct centromeric DNA elements, CDEI, CDEII and CDEIII, define the centromere and hence the kinetochore assembly point (Hyman and Sorger, 1995). However, in other eukaryotes, sequence-specific DNA elements are not sufficient for centromere function. Instead, centromeres are large and complex; e.g. 35 – 110 Kb in *S. pombe* (Pidoux and Allshire, 2005); up to 4 Mb in humans (Carroll and Straight, 2006), and consist of long stretches of repetitive DNA organised into chromatin which has distinctive features. It is thought that centromeres are defined by epigenetic marks resulting in the formation of specialized chromatin regions.

S. pombe centromeres consist of a non-repetitive central core region (*cnt*) flanked by regions containing inverted repeats; innermost repeats (*imr*) and outer repeats (*otr*) (Takahashi *et al.*, 1992). The *cnt* and *imr* regions form the core upon which the kinetochore is assembled, whereas the *otr* forms heterochromatin – a type of highly condensed and transciptionally-repressed chromatin. Human centromeres contain arrays of tandemly repeated α-satellite DNA, also flanked by heterochromatin. It is thought that these regions of repeats provide favourable conditions for centromeric chromatin formation (Carroll and Straight, 2006).

An important feature of centromeric chromatin is the presence of a histone H3 variant (CenH3) within centromeric nucleosomes. Mutation of this protein causes failure of chromosome segregation e.g. (Takahashi *et al.*, 2000). This H3 variant is highly conserved between species, but is referred to by different names e.g. Cnp1 in *S. pombe,* and CENP-A

in humans (Morris and Moazed, 2007). It still remains to be elucidated how CenH3 is deposited at particular sites.

The heterochromatin flanking the central domain of a centromere is referred to as pericentric heterochromatin. The tails of histone proteins show characteristic post-translational modifications (sometimes referred to as the 'histone code') depending on whether they are found within a heterochromatic or euchromatic context. The tails of histones H3 and H4 in pericentric heterochromatin are hypoacetylated due to the activity of a number of histone deacetylases (HDACs). Additionally, Lysine 9 of histone H3 is methylated in heterochromatic regions by histone methylatransferases e.g. Clr4 in fission yeast. This modification enables the HP1 chromodomain protein (Swi6 in fission yeast) to bind.

It was first shown in fission yeast that the formation of 'silent' heterochromatin actually requires transcription from the silenced region and the RNA interference (RNAi) pathway (Reinhart and Bartel, 2002; Volpe *et al.*, 2002; Schramke and Allshire, 2003; Shankaranarayana *et al.*, 2003). RNAi is also thought to be important for pericentric heterochromatin formation in vertebrates (Fukagawa *et al.*, 2004; Kanellopoulou *et al.*, 2005). It is proposed that the RITS (RNA-induced transcriptional silencing) complex is directed by small siRNAs to associate with nascent transcripts and methylated H3K9 which propagates further H3K9 methylation and HP1/Swi6 binding (Pidoux and Allshire, 2005).

It has been shown that one function of pericentric heterochromatin is to mediate cohesion between sister chromatids. In fission yeast *swi6* mutants lose cohesion at the centromere (Bernard *et al.*, 2001; Nonaka *et al.*, 2002), and it seems likely that this function is conserved in vertebrate cells (Fukagawa *et al.*, 2004). It is also proposed that chromatin structure may be important for correct orientation of microtubule binding sites within the kinetochore (Pidoux and Allshire, 2005), thereby preventing merotelic orientations (see section 1.5.2). However, a recent publication shows that in PtK_1 cells, it is the forces exerted by kinetochore-MT attachments that are necessary to localise sister kinetochores correctly to opposite sides of the centromere (Loncarek *et al.*, 2007).

1.3.2 Kinetochores

The function of the kinetochore is to link the centromere to the plus-ends of spindle microtubules, so that the two sister chromatids can be pulled to opposite poles during mitosis. This seemingly simple task actually requires a huge assembly of different proteins and protein subcomplexes. In addition to mediating attachment, the kinetochore is able to monitor its own attachment status through the spindle assembly checkpoint (SAC). The

kinetochore also harnesses the force generated by microtubule polymerisation and depolymerisation to power chromosome movement.

The best-characterised kinetochores are those of budding yeast, which have >65 proteins, organised into 14 or more multi-protein subcomplexes, with a molecular mass of 5-10MDa (McAinsh *et al.*, 2003). Many of the constituent proteins are conserved in vertebrates (Meraldi *et al.*, 2006). Kinetochore proteins are often categorised according to their position within the kinetochore: *inner kinetochore* proteins directly contact centromeric DNA and provide a platform onto which other kinetochore proteins assemble; *microtubule binding* proteins such as motors, +TIPs and other MAPs (see section 1.2.5) are found at the kinetochore-microtubule interface; and *central kinetochore* proteins link the inner kinetochore components to the microtubule interaction surface (McAinsh *et al.*, 2003; Westermann *et al.*, 2007). Similarly, the vertebrate kinetochore has a multi-layered structure which has been described as a 'trilaminar plate' structure (Witt *et al.*, 1980; Ris and Witt, 1981), consisting of the inner kinetochore, an inner kinetochore plate, an outer kinetochore plate, and a fibrous corona layer. Kinetochore assembly is hierarchical, with the localisation of some protein complexes being dependent on the prior localisation of others.

The centromeric nucleosomal histone CenH3 (see previous section) is considered to be a component of the inner kinetochore. Mif2 (*S.c.*) (mammalian CENP-C, *S.p.* Cnp3) associates with CenH3 and with the central/inner kinetochore Mtw1 complex (Westermann *et al.*, 2003). In human cells it was recently shown that CENP-A nucleosomes recruit a CENP-A nucleosome associated complex (NAC) comprising three new human centromere proteins (CENP-M, CENP-N and CENP-T), along with the previously described CENP-U(50), CENP-C and CENP-H. The CENP-A-NAC then recruits inner kinetochore components such as CENP-I (*S.c.* Ctf3, *S.p.* Mis6) (Westermann *et al.*, 2003).

The central kinetochore Ndc80/Hec1 complex consists of four proteins all conserved from yeasts to humans. This complex is important for kinetochore-microtubule attachments, and is thought to provide an important link between proteins of the centromere/inner kinetochore, and proteins of the outer kinetochore. Studies in budding yeast, using an *ndc80* mutant, show that Ndc80 is not required for localisation of inner/central kinetochore proteins such as Mif2 and Mtw1; but it is required for localisation of outer kinetochore proteins such as microtubule binding proteins Dam1 and Stu2 (He *et al.*, 2001), and the motor proteins Cin8 and Kip1 (Tytell and Sorger, 2006).

The Mtw1/Mis12 complex is also proposed to have a 'linker' function (Westermann *et al.*, 2007), as is Spc105 (*S.p.* Spc7, metazoan KNL-1). Spc7 physically associates with the +TIP

Mal3 (Kerres *et al.*, 2004), and is also required for targeting of the Mis12 complex (Kerres *et al.*, 2007).

Another budding yeast linker complex, the Ctf3 complex (which contains the COMA subcomplex), is far less well conserved in other organisms. Limited sequence homology has been found between one member, Ctf3, and the human centromere protein CENP-I. There is some functional conservation between another budding yeast member, Chl4, the fission yeast protein Mis6, and metazoan CENP-H/I, as all are involved in depositing CENP-A at centromeres (Takahashi *et al.*, 2000; Mythreye and Bloom, 2003; Okada *et al.*, 2006).

The core kinetochore components outlined above function to recruit motor proteins and MAPs, which facilitate MT-kinetochore attachment, generate force, and mechanically couple the kinetochore to MT plus-end dynamics. Several MAPs that have been mentioned previously localise to the kinetochore, including members of the TOG, CLIP-170 and EB1 families. There has recently been great interest in the ten-component Dam1/DASH complex, initially characterised in budding yeast (Enquist-Newman *et al.*, 2001) (Jones *et al.*, 1999; Jones *et al.*, 2001) (Westermann *et al.*, 2005; Westermann *et al.*, 2006), and found to be conserved in fission yeast (Sanchez-Perez *et al.*, 2005) (Liu *et al.*, 2005). The budding yeast Dam1/DASH complex is able to form closed rings on microtubules *in vitro,* raising the possibility that it could act as a microtubule-coupling device to generate force at the MT plus-end. Structural analysis predicts that the ring should be able to slide along the MT lattice, enabling it to translate the mechanical energy from MT depolymerisation into directed kinetochore movement (Westermann *et al.*, 2006).

Many kinetochore proteins are regulated by phosphorylation, particularly by the Aurora B/Ipl1/Ark1 kinase, whose activity is important for resolution of incorrect kinetochore-microtubule attachments (see section 1.5.5). Aurora B kinase associates with other subunits to form the chromosomal passenger complex (CPC). The other subunits, INCENP, Survivin and Borealin, are non-enzymatic and control the localisation and activity of Aurora B. The CPC functions throughout mitosis, and its localisation is highly dynamic. It initially localises along chromosome arms, but then becomes concentrated at the inner centromeres during prometaphase and metaphase. At anaphase onset the CPC relocates to the spindle midzone, where it is required for cytokinesis (Ruchaud *et al.*, 2007).

Additionally, the components of the spindle checkpoint localise transiently to the kinetochore during checkpoint activation. This will be discussed in detail in section 1.5.4.

1.3.3 Cohesion

Once DNA replication is completed, the resulting two identical sister chromatids are held together by a protein complex called cohesin until they are segregated during mitosis (Guacci *et al.*, 1997; Tomonaga *et al.*, 2000; Michaelis *et al.*, 1997; Losada *et al.*, 1998). Cohesin consists of four subunits, Smc1, Smc3, Scc1 and Scc2, that are thought to adopt a ring-like configuration, which encloses the sister chromatids and holds them together (Nasmyth and Haering, 2005). The Scc1 subunit is cleaved at the metaphase-anaphase transition by separase (Ciosk *et al.*, 1998; Uhlmann *et al.*, 1999), allowing the sister chromatids to segregate to opposite poles.

In animal cells, centromeric cohesin is protected by shugoshin during early mitosis. Shugoshin recruits protein phosphatase 2A (PP2A) to centromeres, counteracting Polo kinase phosphorylation which leads to cohesin release (Rivera and Losada, 2006). Bub1 is also required for localisation of PP2A to the centromeres (Tang *et al.*, 2006). A similar, although not identical, pathway exists in fission yeast.

1.4 Cell Cycle

The cell cycle is a description of how cells grow and divide. It is important to elucidate how the various processes of cell growth, DNA synthesis and nuclear and cellular division are accomplished and how their integration is regulated. Disruption of cell cycle regulation has severe consequences; for example leading to tumour development and progression in cancer.

1.4.1 Fission Yeast Cell Cycle

As in higher eukaryotes, the fission yeast cell cycle is divided into four phases: G1 (gap phase 1), S (DNA synthesis), G2 (gap phase 2) and M (mitosis). Under rich nutritional conditions, G1 and S phases are very short, and fission yeast spends three-quarters of its time in a long G2 phase. This means that although it is a haploid organism, a cell usually contains two copies of each chromosome, so that a template is available for homologous repair of DNA strand breaks. Once a cell passes Start in late G1, it is committed to the mitotic cell cycle (Hartwell *et al.*, 1974). Passing Start requires that the previous mitosis has been successfully completed (Nurse and Thuriaux, 1977). However, if

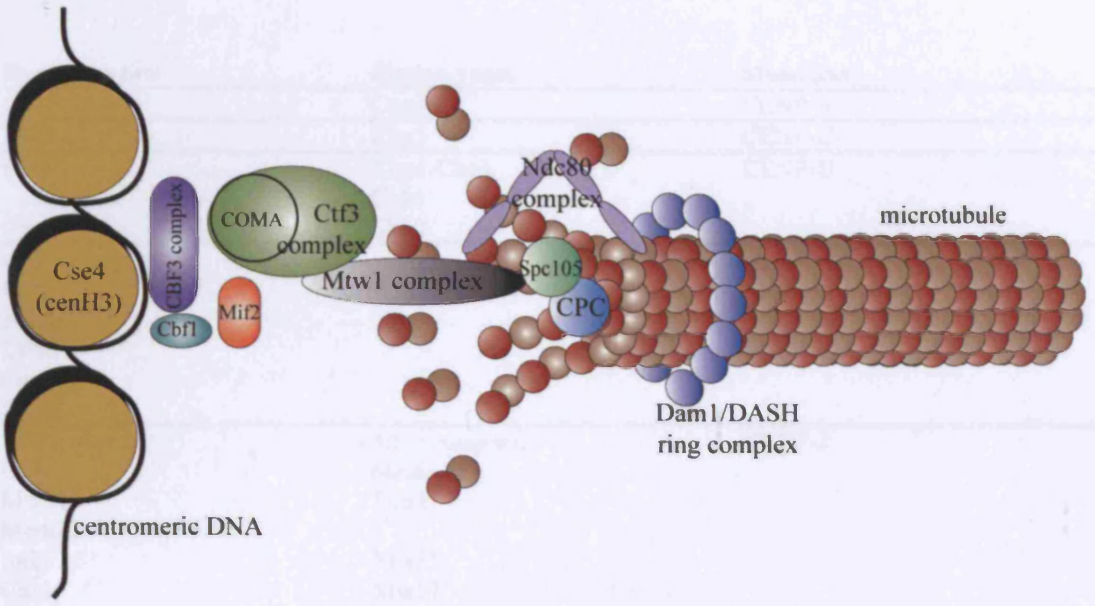

Figure 1.4 Structure of budding yeast kinetochore

Budding yeast	Fission yeast	Metazoan
Cse4	Cnp1	CENP-A
Mif2	Cnp3	CENP-C
Cbf1	Abp1/Cbp1	CENP-B
	Cbh1	
	Cbh2	
CBF3 complex:		
Cbf3		
Ndc10		
Ctf13		
Cep3		
Skp1		
Ctf3 complex:	*Mis6 complex:*	CENP-I
Ctf3	Mis6	
Mcm16	Sim4	
Mcm22		
Iml3	Mis15	
Chl4	Mis17	
Nkp-1	Fta1-7?	
Nkp-2	Fta1-7?	
Ctf19/COMA complex:		
Ctf19		
Okp1		
Mcm21	Mal2	
Ame1		
Mtw1/MIND complex:	*Mis12 complex:*	*Mis12 complex:*
Mtw1	Mis12	hMis12
Nnf1	Nnf1	hNnf1
Nsl1	Mis14	hNsl1
Dsn1	Mis13	hDsn1
Ndc80 complex:	*Ndc80 complex:*	
Ndc80	Ndc80	Hec1
Nuf2	Nuf2	hNuf2
Spc24	Spc24	hSpc24
Spc25	Spc25	hSpc25
Spc105	Spc7	hKNL-1
Dam1/DASH complex:	*Dam1/DASH complex:*	
Dam1	Dam1	
Dad1	Dad1	
Dad2	Dad2/Hos2	
Dad3	Dad3	
Dad4	Dad4	
Duo1	Duo1	
Ask1	Ask1	
Spc19	Spc19	
Spc34	Spc34	
Dad5/Hsk3	Dad5/Hsk3/Hos3	
Chromosomal Passenger Complex (CPC):	*Chromosomal Passenger Complex (CPC):*	*Chromosomal Passenger Complex (CPC):*
Ipl1	Ark1	Aurora B
Sli15	Pic1	INCENP
Bir1	Bir1/Cut17/Pbh1	Survivin
		Borealin/Dasra B

Table 1.1 Table of kinetochore components and complexes in budding yeast, fission yeast and metazoans

insufficient nutrients are available, cells either enter stationary phase (G0), or, in the presence of cells of the opposite mating type, undergo conjugation, meiosis and sporulation.

Once a cell has entered the mitotic cycle, the next major control point is at the G2-M boundary, governing when cells enter mitosis (Nurse and Bissett). Cells must have reached a certain size, and have completed DNA replication and repair. Fission yeast, like many unicellular eukaryotes, undergoes closed mitosis, meaning that the nuclear envelope does not break down (McCully and Robinow, 1971). Once cells enter mitosis, equal partitioning of genetic material and nuclear division is followed by cell division during cytokinesis. In rapidly-growing log-phase cultures, G1 and S phases are completed by the time the new daughter cells separate.

1.4.2 Cell Cycle Control

Regulation of the cell-cycle relies on the interdependent mechanisms of protein phosphorylation and proteolysis. The molecules involved in these mechanisms are highly conserved between all eukaryotes. Much of the seminal work in discovering how the cell cycle is regulated was carried out in fission and budding yeasts. The master controllers that drive progression through the cell cycle, ensuring completion of one stage before beginning the next, are complexes consisting of cyclins and cyclin-dependent protein kinases (Cdks), which phosphorylate a large number of substrates. The cyclins are regulatory subunits required for the kinase activity of the Cdks, and for targeting them to specific substrates. The timely action of cyclin/CDK complexes is ensured by several mechanisms: 1) ubiquitin-mediated cyclin degradation by the anaphase-promoting complex (APC); 2) reversible binding of inhibitor molecules; and 3) reversible inhibitory phosphorylation of the CDK itself.

Higher eukaryotic cells possess many Cdks, but fission yeast has only one essential one named Cdc2. Fission yeast has four cyclins (Cdc13, Cig1, Cig2 and Puc1). Cdc13 is required for the activity of Cdc2 at the onset of mitosis (Booher *et al.*, 1989; Moreno *et al.*, 1989) and is the only fission yeast cyclin that is essential for cell-cycle progression. Cdc2/Cdc13 activity is very low in G1 phase due to ubiquitin-mediated proteolysis of Cdc13 (Yamaguchi *et al.*, 1997), and because Cdc2 is inhibited by Rum1, a CDK inhibitor (Moreno and Nurse, 1994). Cdc2/Cdc13 activity levels then rise sufficiently to phosphorylate the substrates necessary for DNA replication during S phase.

During G2, the activity of Cdc2 is kept low by phosphorylation of the Tyr15 residue by Wee1. A very large increase in Cdc2/Cdc13 activity is required to drive cells from G2 into

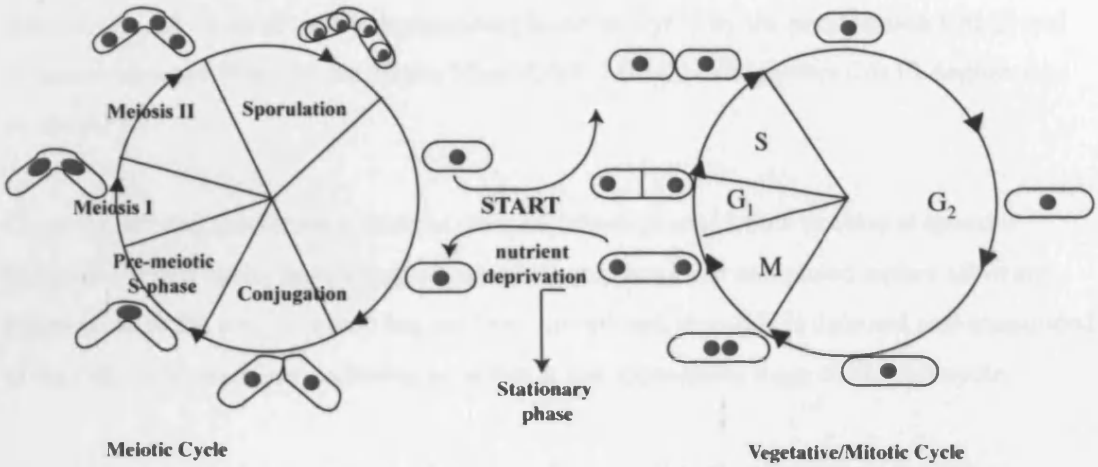

Figure 1.5 Life Cycle of Fission Yeast

At START/G1 cells must decide whether to enter mitosis or meiosis. In conditions of nutrient deprivation, cells remain in G1, or mate with a mating partner if one is available and subsequently undergo meiotic cell division to produce four spores. Cells committed to mitosis replicate their DNA during S phase and then proceed to G2. Fission yeast cells spend most of the time in G2. During M phase (mitosis) genetic material is segregated equally before cells undergo cytokinesis to create two new, genetically identical, daughter cells. The cell cycle then begins again.

mitosis, and this is achieved by dephosphorylation of Tyr15 by the phosphatase Cdc25 and by inactivation of Wee1 by the kinase Nim1/Cdr1. Mitotic exit requires Cdc13 degradation by the APC.

There are several surveillance systems, termed 'checkpoints' which operate at specific points in the cell cycle, monitoring whether one step has been completed before allowing progression to the next. If a step has not been completed, then this is detected and transduced to the cell cycle machinery, causing an arrest at the appropriate stage of the cell cycle.

Other kinases also play important roles in regulating cell cycle progression, including members of the Polo, Aurora and NiMA families, which are essential for progression of mitosis.

1.5 Mitosis

Mitosis is the division of a somatic cell to produce two genetically identical daughter cells. It is the most dynamic phase of the cell cycle; within a short period of time chromosomes are captured by the spindle, aligned and segregated to opposite poles, before the cell splits in two. Mitosis is also a dangerous phase of the cell cycle, because if chromosomes are not segregated accurately it can lead to aneuploidy, which has deleterious or deadly consequences for the daughter cells. The process therefore needs to be very tightly regulated.

1.5.1 Mitotic Phases

Mitosis consists of a number of different phases. During *prophase* chromosomes (consisting of sister chromatid pairs) condense, a process that requires histone protein phosphorylation, a protein complex called condensin (Hirano and Mitchison, 1994; Saka *et al.*, 1994), and DNA topoisomerase II (Gorbsky, 1994; Andreassen *et al.*, 1997). The network of interphase microtubules is broken down, and the duplicated centrioles (or SPBs in yeast) separate and nucleate spindle formation.

During *prometaphase*, the nuclear envelope disassembles in higher eukaryotes, but yeasts undergo a closed mitosis with the nuclear envelope intact. Highly dynamic MTs nucleated from the cell poles explore three-dimensional space by rapidly growing, shrinking, and then growing in a new direction. This facilitates the 'search and capture' of kinetochores by MT plus ends. Each human kinetochore captures about 20 MTs, whereas fission yeast kinetochores only capture 2-4 MTs, and budding yeast kinetochores attach to just a single

MT. When both kinetochores of a sister chromatid pair become attached to spindle MTs, bipolar orientation is achieved, and the chromosome aligns in the centre of the cell.

When all the chromosomes are attached and aligned in the centre of the cell, the cell is defined as being in *metaphase.* The spindle assembly checkpoint (SAC) functions at this stage to ensure that all kinetochores are properly attached, delaying progression to the next phase until this is achieved (see section 1.5.4).

During *anaphase* the sister chromatids are physically separated by cleavage of cohesin. They first move to opposite spindle poles (anaphase A); then the spindle lengthens, pushing the poles further apart (anaphase B).

In higher eukaryotes the nuclear envelope reforms during *telophase,* and the cleavage furrow starts to constrict. The cells are completely separated during *cytokinesis,* by contraction of the actin contractile ring. Fission yeast have rigid cell walls, and are separated by contractile ring contraction and by septum formation.

Fission yeast mitosis has also been described on the basis of spindle length and dynamics (Nabeshima *et al.*, 1998). During *phase 1* (corresponding to prophase) the spindle is formed and elongates to a length of ~2.5μm. In *phase 2* (prometaphase to anaphase A) this spindle length is maintained as constant. During *phase 3* (anaphase B) the spindle elongates, reaching a maximal length of 12-15μm.

1.5.2 Attachment and Tension

During chromosome segregation, one copy of each chromosome must be distributed to each pole prior to cell division. Failure to achieve this will cause daughter cells to receive an incorrect number of chromosomes, termed aneuploidy. This is very harmful for a cell, as essential genetic information may be lost, or gene dosages may be affected. Chromosome segregation is carried out by the spindle apparatus, which consists of many microtubules. Sister kinetochores on each chromosome must attach to microtubules emanating from either pole, such that they will be pulled apart to opposite poles once sister cohesion is lost. When both sister kinetochores within a chromosome are correctly attached, they have achieved *chromosome biorientation*, or *bipolar attachment.*

It is proposed that highly dynamic microtubules explore three-dimensional space during prometaphase to 'search and capture' kinetochores (Kirschner and Mitchison, 1986). This model is now being modified, to accommodate emerging evidence that MTs are also

nucleated within the vicinity of chromosomes (see section 1.7.3) (O'Connell and Khodjakov, 2007). As MT-kinetochore attachment is a stochastic process, different kinds of misattachments may occur, as illustrated in Figure 1.6. Correctly bioriented chromosomes are amphitelically attached (a). If one kinetochore becomes attached to microtubules from one pole, while its sister kinetochore remains unattached, this is referred to as monotelic attachment (b). If both sister kinetochores become attached to the same pole, it is referred to as syntelic attachment (c). Finally, if a single kinetochore becomes attached to microtubules emanating from both poles, it is referred to as merotelic attachment (d). Monotely, syntely and merotely could all cause chromosome missegregation, so it is important that the cell is able to correct these erroneous attachments (see section 1.5.5), and that correct amphitelic attachments are stabilised.

In fission yeast, the Pcs1 and Mde4 proteins have been implicated in the prevention of merotelic attachment in mitosis and meiosis II (Gregan *et al.*, 2007). It was proposed in the study that Pcs1 and Mde4 act to clamp together the microtubule binding sites within the kinetochore so that they are all oriented in one direction, thereby minimising formation of merotelic attachments.

Proper bipolar attachment results in the establishment of tension between sister kinetochores, as they are pulled in opposite directions, but remain cohesed. Incorrect monotelic or syntelic attachments fail to establish tension, and this can be sensed and corrected (see section 1.5.4). It has also been proposed that the sensing of inter-kinetochore tension can contribute to chromosome congression (see following section).

1.5.3 Congression

The alignment, or congression, of all the chromosomes to the metaphase plate at the spindle equator in metaphase is an impressive site in metazoan cells, but the molecular mechanisms underlying this phenomenon are not yet well understood. It seems that both the transport of chromosomes along MTs by motors, and the regulation of MT dynamics contribute to congression. It was originally thought that biorientation led to congression; and that this was because when equal but opposite pulling forces were applied to sister kinetochores, they would align in the centre of the cell (Ostergren, 1951). However, evidence accumulated against this theory, for example, monotelically attached chromosomes exhibit movements both towards (P) and away from (AP) the pole to which they are attached (Rieder and Salmon, 1994).

Chromosome congression in metazoan cells proceeds in the following manner: laterally attached kinetochores are rapidly transported towards the poles, where additional, end-on attachments are formed. The chromosome then exhibits P and AP oscillations, until it biorients and congresses to the cell centre (Kapoor and Compton, 2002). P movement is likely due to pulling forces at the kinetochore, whereas AP movement is probably a combination of pushing forces at the kinetochore, and of polar ejection forces acting on the chromosome arms, generated by the Kid (Kinesin-10) family of kinesins (Funabiki and Murray, 2000; Levesque and Compton, 2001; Tokai-Nishizumi *et al.*, 2005). A pool of the minus-end directed motor protein dynein localises to kinetochores during mitosis, where it plays a role in chromosome congression by driving the poleward (P) kinetochore movement during chromosome oscillations, facilitating biorientation (Li *et al.*, 2007).

Recently, an interesting study revealed that chromosomes can congress to the metaphase plate before biorientation in mammalian cells (Kapoor *et al.*, 2006). Monooriented chromosomes initially accumulate at spindle poles during prometaphase (Lampson *et al.*, 2004), and are then transported along the kinetochore fibres of other, already bioriented chromosomes by the kinesin-7 motor protein, CENP-E. Once they reach the cell equator, the likelihood of being captured by microtubules from the opposite pole is presumably increased, leading to biorientation.

Other models of congression have focused primarily on the dynamic properties of kinetochore MTs, and how these are regulated. One suggestion is that the kinetochore acts as a 'tensiometer' that can detect the tension between sister kinetochores and effect directed chromosome movement accordingly (Skibbens *et al.*, 1993; Skibbens *et al.*, 1995; Skibbens and Salmon, 1997). Another possibility is that kinetochore-MT dynamics could be regulated according to chromosome position e.g. via a concentration gradient of molecules influencing MT dynamics. One approach used to test these possibilities was to use computer simulations of MT dynamics to find the best fit with experimental data from budding yeast (Gardner *et al.*, 2005). The model which best reproduced experimental results consists of kinetochores able to regulate MT dynamics by sensing tension, and by sensing spindle position via a catastrophe gradient.

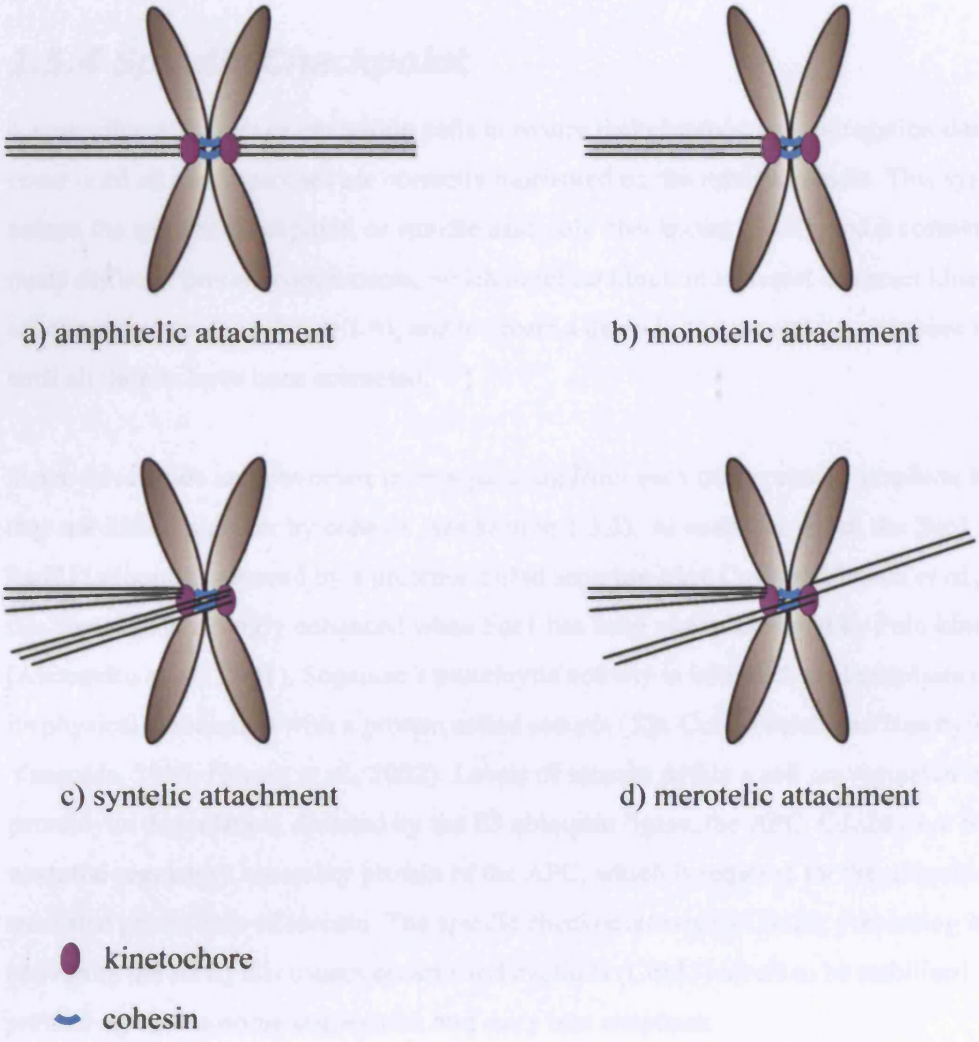

Figure 1.6 Different states of kinetochore-microtubule attachment

a) correct bipolar attachment. **b) – d)** various types of erroneous kinetochore-microtubule attachments. **a)** Amphitelic attachment: correctly bi-oriented chromosomes, with each kinetochore attached to microtubules from just one pole. **b)** Monotelic attachment: only one kinetochore is attached. **c)** Syntelic attachment: both sister kinetochores are attached to the same pole. **d)** Merotelic attachment: one or both kinetochores become attached to microtubules emanating from both pole.

1.5.4 Spindle Checkpoint

A surveillance system exists within cells to ensure that chromosome segregation does not occur until all chromosomes are correctly bioriented on the mitotic spindle. This system is named the spindle checkpoint, or spindle assembly checkpoint (SAC), and it consists of many different protein components, which together function to detect incorrect kinetochore attachment states (see Figure 1.6), and to create a delay in the metaphase-anaphase transition until all defects have been corrected.

Sister chromatids are prevented from separating from each other prior to anaphase because they are linked together by cohesin (see section 1.3.3). At anaphase onset, the Scc1 (*S.p.* Rad21) subunit is cleaved by a protease called separase (*S.p.* Cut1) (Uhlmann *et al.*, 1999); this cleavage is strongly enhanced when Scc1 has been phosphorylated by Polo kinase (Alexandru *et al.*, 2001). Separase's proteloytic activity is inhibited until anaphase onset by its physical association with a protein called securin (*S.p.* Cut2) (Salah and Nasmyth, 2000; Yanagida, 2000; Hornig *et al.*, 2002). Levels of securin within a cell are regulated by proteloytic degradation, directed by the E3 ubiquitin ligase, the APC. Cdc20 (*S.p.* Slp1) is an essential regulatory accessory protein of the APC, which is required for the ubiquitin-mediated proteolysis of securin. The spindle checkpoint targets Cdc20, preventing it from activating the APC; this causes securin and cyclin B (Cdc13) levels to be stabilised, thereby preventing chromosome segregation and entry into anaphase.

Components of the spindle checkpoint were first identified in two independent screens in budding yeast (Hoyt *et al.*, 1991; Li and Murray, 1991), which revealed that mutations in several genes prevented cells from arresting in mitosis in the presence of spindle poison drugs. These genes include the *MAD* (mitotic-arrest deficient) genes *MAD1, MAD2* and *MAD3 (BUBR1* in humans), and the *BUB* (budding uninhibited by benzimidazole) genes *BUB1* and *BUB3*. Bub1 and BubR1 are protein kinases. It is thought that MAD2, BUBR1/MAD3 and BUB3 form a complex with CDC20 (termed the MCC, Mitotic Checkpoint Complex), which binds to the APC and prevents it from ubiquitinating securin and cyclin B (Sudakin *et al.*, 2001). Additional components of the spindle checkpoint include the kinases MPS1 (Mph1 in *S. pombe*) and Aurora B/Ipl1/Ark1; spindle checkpoint function in higher eukaryotes also requires the RZZ complex (ROD-ZW10-ZWILCH), $p31^{comet}$, protein kinases such as MAPK, CDK1, NEK2 and PLK1, and the microtubule motors CENP-E (kinesin-7) and dynein (Musacchio and Salmon, 2007).

During prometaphase, Cdc20 and the MCC components exhibit dynamic localisation to the kinetochore, suggesting that the kinetochore functions as a catalytic platform for production

of active MCC complex, which then acts as a diffusible 'wait anaphase' signal. It is not yet well understood how the MCC inhibits APC activity; one possibility is that the MCC binds the APC as a pseudosubstrate via the KEN-box motif in BUBR1/MAD3 (King *et al.*, 2007). The currently-favoured model for how kinetochore recruitment of MCC components results in the formation of the mature complex is the 'MAD2-template model' (De Antoni *et al.*, 2005). MAD1 is stably bound to the kinetochore during prometaphase and is required for kinetochore localisation of MAD2. Both proteins leave the kinetochore when MT attachment is established. Structural studies revealed that MAD2 exists as two different conformers; 'open' (O-MAD2) and 'closed' (C-MAD2) (Luo *et al.*, 2004). MAD2 binding to MAD1 triggers a conformational change to C-MAD2, and this stable MAD1-C-MAD2 complex acts as a receptor for a rapidly cycling population of O-MAD2. It has been proposed that MAD1-C-MAD2 acts as a template, converting O-MAD2 to C-MAD2 (De Antoni *et al.*, 2005). The binding of O-MAD2 to Cdc20 is fairly energetically unfavourable, but binding by C-MAD2 might be more favourable, overcoming the energy barrier to fire the checkpoint. This could trigger a positive-feedback loop such that formation of a small amount of C-MAD2-CDC20 promotes further C-MAD2-CDC20 formation (Musacchio and Salmon, 2007).

It is well established that the spindle checkpoint is activated in response to either attachment or tension defects of the kinetochore-microtubules, although it is difficult to discern whether these signals are monitored separately, or whether there is some interdependency. Tension clearly cannot be generated without attachment, and it has been found that tension in turn stabilizes attachment (King and Nicklas, 2000). However, several studies have shown that different subsets of SAC components are recruited to the kinetochore depending on whether there are tension or attachment defects. Mad1 and Mad2 localise to unattached kinetochores, but not those lacking tension (Waters *et al.*, 1998), whereas Bub1 and BubR1/Mad3 localise to kinetochores lacking attachment or tension (Skoufias *et al.*, 2001; Logarinho *et al.*, 2004). However, Mad1 and Mad2 are absolutely required for checkpoint activation, so the tension/attachment pathways must converge.

It is now emerging that Bub1 plays several different roles during mitosis, making it difficult to specify its precise role in the spindle checkpoint. Bub1 acts to recruit a number of checkpoint and motor proteins to the kinetochore, such as Mad1, Mad2, BubR1, CENP-E and Plk1. A study in *Xenopus* showed that Bub1 is important for the localisation of the CPC (Aurora B, survivin and INCENP), and that it phosphorylates INCENP (Boyarchuk *et al.*, 2007). It has also been observed that Bub1 is necessary for chromosome congression; in human cells, 90% of chromosomes failed to congress in a Bub1 RNAi knockdown experiment. Serious congression defects persist even if entry into anaphase is artificially

delayed (Meraldi and Sorger, 2005). In fission yeast, deletion of *bub1* causes lagging chromosomes and increased chromosome missegregation (Bernard *et al.*, 1998). Fission yeast Bub1 kinase activity is required for spindle checkpoint function. Bub1 is itself phosphorylated by Cdc2, which is important for the activation of Bub1 in the checkpoint (Yamaguchi *et al.*, 2003).

Once chromosomes are correctly bioriented, the checkpoint must be switched off. In metazoans, MAD1, MAD2, the RZZ complex and MPS1 are removed from the kinetochores in a dynein-dependent manner, while BUBR1 activity is regulated by CENP-E. The inhibitory MAD2-CDC20 complex seems to be dissociated by non-degradative ubiquitylation of CDC20 (de Gramont *et al.*, 2006). Additionally, it is thought that the destruction of cyclin B at anaphase onset, leading to the inactivation of Cdk1, plays a role in inhibiting the checkpoint response (D'Angiolella *et al.*, 2003; Potapova *et al.*, 2006).

1.5.5 Correction of erroneous MT-kinetochore attachments

The establishment of MT-kinetochore attachments is a stochastic process, resulting in many incorrect attachments. The spindle checkpoint is able to detect defects in attachment or tension and impose a metaphase arrest, allowing the cell time to correct any errors; but what is the actual mechanism of error correction? Monotelically oriented chromosomes do not contain incorrectly attached kinetochores; they simply need time to establish connections to the opposite pole. In contrast, syntelically and merotelically oriented chromosomes possess incorrect MT-kinetochore attachments that need to be destabilised. The Aurora B kinase plays an important role in this process, co-ordinating tension and attachment by sensing tension defects and phosphorylating key substrates at the kinetochore to promote detachment of erroneous MT attachments.

In budding yeast, syntelic kinetochore-MT attachments are maintained throughout most of the cell-cycle. Once SPBs have duplicated and separated, one of the kinetochores needs to sever its attachment to the mother SPB and establish attachment to the daughter SPB. Ipl1/Aurora B kinase is necessary to promote turnover of syntelic attachments, thereby promoting biorientation and preventing monopolar segregation (Tanaka *et al.*, 2002). One of the key downstream targets of Ipl1 is Dam1/DASH (Kang *et al.*, 2001; Courtwright and He, 2002), a complex which is thought to mediate the interaction between kinetochore and microtubule. Phosphorylation of Dam1 by Ipl1 may disrupt the binding of Dam1 to the core kinetochore component Ndc80, causing detachment of the

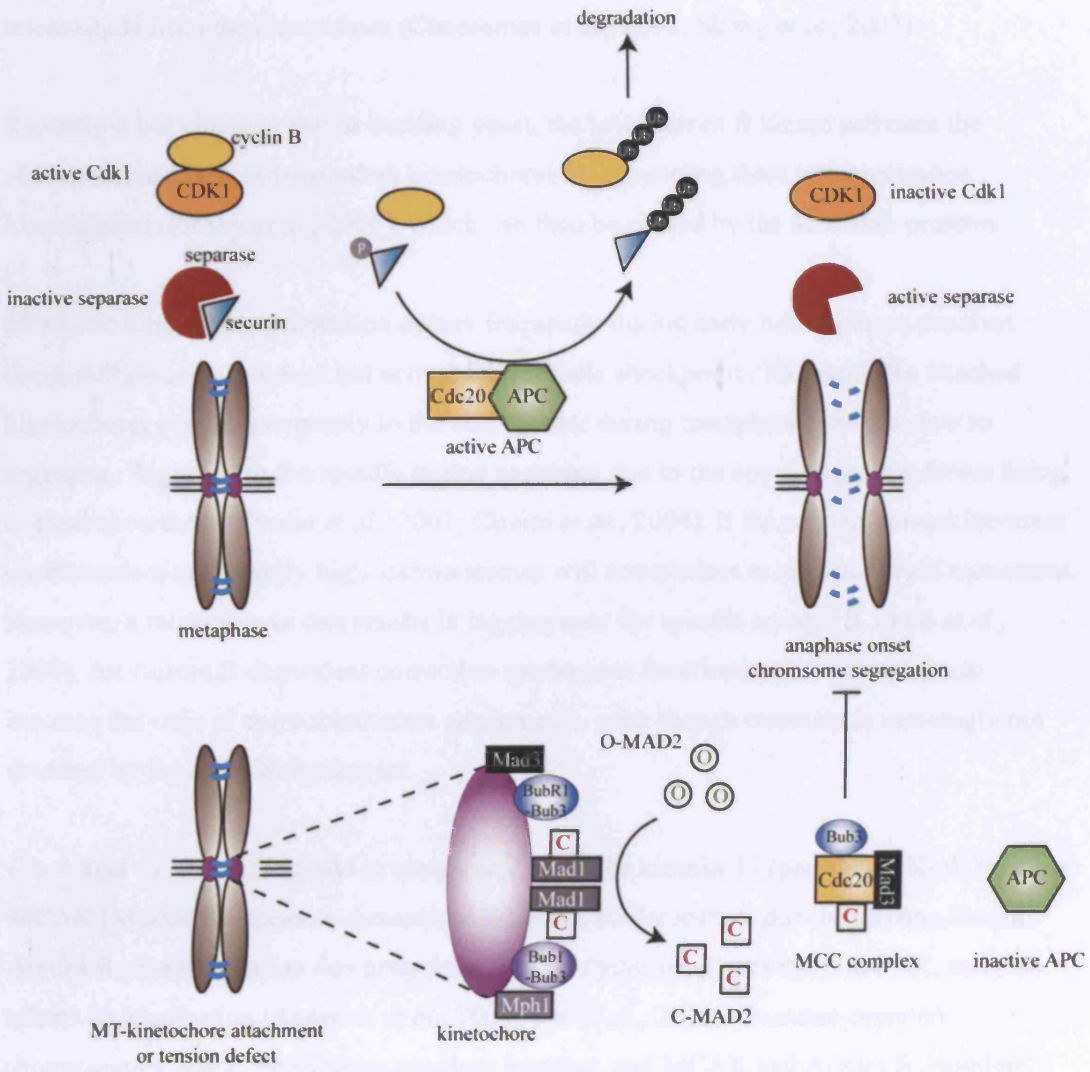

Figure 1.7 Mechanism of spindle checkpoint activation

Sister chromatids are held together by cohesin until correct MT-kinetochore attachments are formed. Chromosome segregation is achieved by cleavage of the Scc1 subunit of cohesin by separase, once inhibition of separase by securin is relieved. Securin is phosphorylated by Plk1, and then ubiquitinated by the E3 ligase APC/C, which targets it for degradation. Cdk1 activity is also reduced by ubiquitin-mediated proteolysis of the cyclin B subunit. If a defect in MT-kinetochore attachment or tension exists, the Mad, Bub, and Mph1 checkpoint components localise to the kinetochore, forming a catalytic platform for formation of the MCC complex, which inhibits the Cdc20 subunit of the APC thus preventing securin and cyclin B degradation, which delays chromosome segregation and anaphase onset. See text for further details.

microtubule from the kinetochore (Cheeseman *et al.*, 2002; Shang *et al.*, 2003).

Recently it has emerged that in budding yeast, the Ipl1/Aurora B kinase activates the checkpoint response at tensionless kinetochores by converting them into unattached kinetochores (Pinsky *et al.*, 2006), which can then be sensed by the Mad/Bub proteins.

Merotelic kinetochore orientation occurs frequently during early mitosis in mammalian tissue culture cells, but does not activate the spindle checkpoint . Merotelically attached kinetochores congress normally to the cell equator during metaphase, and are slow to segregate, 'lagging' on the spindle during anaphase due to the opposed pulling forces being exerted upon them (Cimini *et al.*, 2001; Cimini *et al.*, 2004). If the ratio of correct:incorrect attachments is sufficiently high, chromosomes will nonetheless exhibit poleward movement. However, a ratio close to one results in lagging near the spindle equator (Cimini *et al.*, 2004). An Aurora B-dependent correction mechanism functions prior to anaphase to increase the ratio of correct:incorrect attachments, even though merotely is seemingly not detected by the spindle checkpoint.

One target of Aurora B kinase in metazoan cells is the kinesin-13 (previously KinI) member MCAK (Mitotic Centromere-Associated Kinesin), a microtubule depolymerising kinesin. Aurora B phosphorylation downregulates the depolymerising activity of MCAK, and also affects its localisation (Andrews *et al.*, 2004; Lan *et al.*, 2004). In mono-oriented chromosomes, sister centromeres are close together, and MCAK and Aurora B completely co-localise. Once attachment is established, centromeres are stretched apart, and a portion of MCAK becomes localised to the kinetochores, away from Aurora B, but close to PP1 phosphatase, which could activate MCAK's depolymerase activity (Gorbsky, 2004).

It has now been shown that Aurora B and MCAK become enriched at sites of merotelic attachment, and inhibition of Aurora B kinase activity increases the frequency of merotelic attachments (Knowlton *et al.*, 2006). However, phospho-MCAK is not enriched at merotelic sites; this indicates that the population of MCAK localised there is dephosphorylated with active depolymerising activity, but means that the functional relationship between Aurora B and MCAK is not entirely clear.

It has been shown that kinetochore-MT turnover is greatly diminished in prometaphase when Auorora B is inhibited (Cimini *et al.*, 2006), and now the kinetochore Ndc80/Hec1 complex is emerging as another key target for Aurora B phosphorylation. In human cells non-phosphorylable Hec1 mutants showed increased frequencies of merotelic attachments (Ciferri *et al.*, 2005), and *in vitro* phosphorylation of budding yeast Ndc80 inhibits its MT-

binding ability (Cheeseman *et al.*, 2006). These data suggest that Auorora B phosphorylation of Ndc80 could lead to the release of mis-attached microtubules. Perhaps once released, the MT is depolymerised by MCAK to clear the way for correct attachments to be made (Cimini, 2007).

1.5.6 Anaphase

At anaphase onset, cohesion between sister chromatids is lost and they separate, migrating to opposite cell poles. During anaphase A, chromatids move towards the poles, and during anaphase B the spindle lengthens to further increase the distance between the segregated chromatids. The depolymerisation of kinetochore MTs is thought to power anaphase A movement, although the molecules responsible for this remain largely unidentified. In *Drosophila*, two Kinesin-13 members, KLP59C and KLP10A, were found to be required for poleward movement of chromosomes during anaphase A (Rogers *et al.*, 2004). KLP59C depolymerises kinetochore-MTs from the kinetochore-associated plus end, whereas KLP10A depolymerises from the poles.

Microtubules are highly dynamic during prometaphase/metaphase, but they become stabilised during anaphase B, allowing the mitotic spindle to lengthen. In budding yeast, activation of the phosphatase Cdc14 by separase is necessary for this stabilisation, linking chromosome segregation to spindle elongation (Higuchi and Uhlmann, 2005) (Sullivan and Uhlmann, 2003). Cdc14 dephosphorylates a number of key spindle midzone proteins (see below) including Ase1 and the Sli15/INCENP subunit of the CPC. Additionally, the Ask1 subunit of the budding yeast DASH complex is dephosphorylated by Cdc14 (Higuchi and Uhlmann, 2005), which may contribute to the suppression of MT dynamic instability.

During anaphase B, the central spindle is formed: an arrangement of anti-parallel non-kinetochore microtubules bundled at their plus-ends at the spindle midzone. MT polymerisation and sliding at this region cause the spindle to elongate during anaphase B, pushing the poles further apart (Khodjakov *et al.*, 2004). The central spindle is required for cytokinesis in animal cells (Wheatley and Wang, 1996). The microtubule bundling protein Ase1/PRC1 is required for proper central spindle formation, as is the Aurora B containing CPC, which, in metazoans, localises a MT-bundling protein complex called centralspindlin, consisting of the CYK-4/MgcRacGAP Rho-family GAP and the ZEN-4/MKLP1 kinesin-6 motor protein (McCollum, 2004).

1.6 Kinesins

The first kinesin (kinesin-1, or conventional kinesin) was identified as a translocator protein present in squid giant axons (Vale *et al.*, 1985). Since then, proteins belonging to the kinesin superfamily of microtubule-based motors have been found to be involved in numerous cellular processes, including the transport of organelles, vesicles, chromosomes, protein complexes, and microtubules; some are also involved in regulation of microtubule dynamics. Kinesins are able to hydrolyse ATP and convert the energy generated into mechanical movement.

1.6.1 Kinesin Structure

All kinesins contain a globular kinesin domain, which houses both ATPase and the microtubule-binding activities. This catalytic core consists of ~360 residues, which are highly conserved between different species, and between different members of the kinesin superfamily. The kinesin domain is most often located at the N-terminus of the protein, but may also be found in the middle, or at the C-terminus. The canonical Kinesin-1 functions as a homodimer; each constituent kinesin subunit consists of a globular head (the kinesin domain) at the N-terminus, followed by a central stalk region consisting of coiled-coils, which mediate dimerisation of Kinesin-1. A tail region is located at the C-terminus of the molecule and is important for interactions with cargoes. Metazoan Kinesin-1 possesses two additional light chains that also mediate interactions with cargo, but fungal kinesins lack associated light chains.

Kinesin Domain

Structural studies of the kinesin domain reveal that it consists of a central β sheet flanked by three α helices on either side. The catalytic core of kinesin shares common motifs with myosin and G-proteins (Vale, 1996). Nucleotide is bound by a pocket surrounded by several highly conserved loops. The switch I loop lies close to the α- and β-phosphates of the bound nucleotide, and the P-loop and switch II loop lie close to the γ-phosphate that is lost upon ATP hydrolysis (Amos and Hirose, 2007). Residues important for kinesin's interaction with the microtubule were found by mutational analysis (Woehlke *et al.*, 1997), and are located primarily in loop L12 and helix α5, and loops L7/L8. Most of the mutations that abolished MT binding were in positively charged residues, suggesting that ionic interactions make a major contribution to the kinesin-tubulin interaction. From EM maps, it is generally agreed that the switch II-helix α4 rests in the groove between α- and β-tubulin, and that loops L11 and L12 directly interact with tubulin (Amos and Hirose, 2007).

Kinesins bind microtubules strongly when bound to ATP, and detach from microtubules upon hydrolysis to ADP. These cycles of attachment and detachment enable kinesin to walk along the microtubule. It is thought that the α4 helix plays a critical role in communicating conformational changes from the nucleotide-binding pocket to the rest of the molecule. The short region between the head and the stalk domains is termed the 'neck', and may contain features specific to a particular kinesin family. It may be important for determining motor directionality (Endow and Waligora, 1998), or for regulating activity (Miki *et al.*, 2005).

Coiled-Coil Domain

The coiled-coil is a very common protein interaction motif that has been found in motor proteins, DNA binding proteins, extracellular proteins, and viral fusion proteins. A coiled-coil is a rod-like structure consisting of two to five α-helices. Hydrophobic residues occur with a regular periodicity such that they localise to one side of the helix, which forms the interface for protein-protein interactions. The remaining hydrophilic residues are exposed to solvent. If residues within a coiled-coil are designated with letters from $a - g$, the hydrophobic residues are found to repeat at *a* and *d* positions, a pattern that was first described for the coiled-coil of tropomyosin (Sodek *et al.*, 1972). Ionic attractions between the *e* and *g* residues influence the specificity of the coiled-coil interaction (O'Shea *et al.*, 1993; Lee *et al.*, 2003).

Tail Domain

In contrast to the kinesin domain, the tail domains of different kinesins are highly diverged. They are thought to confer the specificity required for interaction with cargoes. It has also been shown that the tail domain plays a role in regulating the activity of the kinesin domain (Coy *et al.*, 1999; Friedman and Vale, 1999; Stock *et al.*, 1999). When the tail is not bound to cargo, it folds back to associate with the head domain, thereby partially inhibiting kinesin's ATPase activity. This folded form appears able to bind microtubules, but can only move slowly along them.

1.6.2 Kinesin Dimerisation and Movement

Kinesin is a highly processive motor, taking hundreds of 8nm steps along the microtubule lattice before dissociating, and hydrolyzing one molecule of ATP per step (Hua *et al.*, 1997; Noji *et al.*, 1997; Schnitzer and Block, 1997). Experiments with engineered

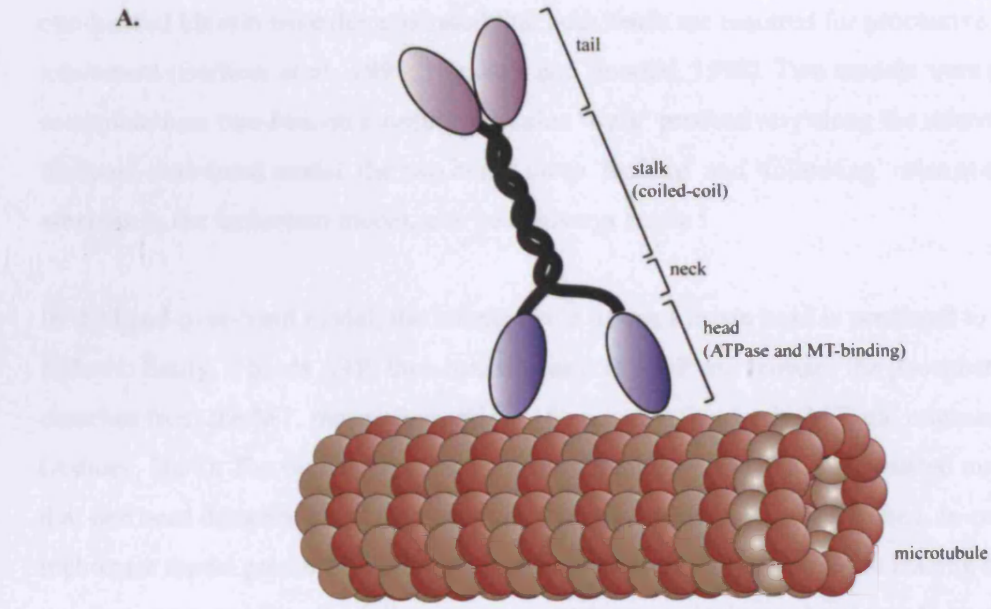

Figure 1.8 Structural Features of Kinesins

A. Cartoon showing features of a generalised kinesin dimer on a microtubule (not drawn to scale). **B.** Helical view of two α-helices associating to form a coiled-coil. Positively charged residues are located at the *a* and *d* positions of each helix, forming a hydrophobic surface favouring protein interaction. Interactions between residues at the *e* and *g* positions confer the specificity of the protein interaction. Taken from (Lee *et al.*, 2003). **C.** Cartoon to illustrate the structure of the highly conserved kinesin domain. Important features depicted are the nucleotide-binding pocket, consisting of the Switch I, Switch II and P-loop motifs; and the microtubule interaction surface, consisting of loops L7/L8 and L11/12 and the α4 and α5 helices. Taken from (Amos and Hirose, 2007).

one-headed kinesin have demonstrated that both heads are required for processive movement (Berliner *et al.*, 1995; Hancock and Howard, 1998). Two models were proposed to explain how two-headed kinesin molecules 'walk' processively along the microtubule. In the hand-over-hand model, the two heads swap 'leading' and 'following' roles at every step, whereas in the inchworm model, one head always leads.

In the hand-over-hand model, the kinetic cycle of one kinesin head is predicted to be as follows: firstly, it binds ATP, then hydrolyses it to ADP and releases the phosphate. Then it detaches from the MT, moves forward by 16nm, reattaches to the MT and releases the ADP (Asbury, 2005). The two heads must function identically, but in a co-ordinated manner so that one head detaches from the MT while the other remains firmly attached. In contrast, the inchworm model predicts that the two heads behave differently, with the leading head taking one 8nm step, and then the following head catching up. Only one head would be an active ATPase.

There is strong evidence favouring the hand-over-hand model. For example, if heterodimers are constructed with one mutant head that hydrolyzes ATP slowly, the molecule is seen to 'limp' along the microtubule (Kaseda *et al.*, 2003). However, rather surprisingly, it has been shown that heterodimers of this type are still capable of long-distance movement (Asbury, 2005).

Recently, it was shown that the budding yeast Kinesin-14, Kar3, forms a heterodimer with the nonmotor protein Vik1 (Allingham *et al.*, 2007). Vik1 has a kinesin-like globular domain, but it lacks a nucleotide-binding region. It can, however, bind to microtubules very efficiently, and seems to mediate microtubule binding of the heterodimer. Two proposed models for Kar3/Vik1 motility both require that the entire molecule dissociates from the microtubule at points in the cycle.

The Kif3A/Kif3B kinesins (Kinesin-2) also form a heterodimer and are involved in intraflagellar transport and golgi trafficking. The two heads have distinct properties, as demonstrated by constructing homodimers; a Kif3A/A homodimer moves more slowly than the WT heterodimer, whereas a Kif3B/B homodimer moves quickly but shows reduced processivity (Zhang and Hancock, 2004). It is suggested that the Kif3B head accelerates detachment of the Kif3A head.

1.6.3 Kinesin Families

Kinesin nomenclature was standardised in 2004 (Lawrence *et al.*, 2004). There are currently 14 recognized kinesin families; the Kinesin-1 to Kinesin-12 families have a kinesin domain located at the N-terminus, and plus-end directed motor activity. The Kinesin-13 family members (formerly KinI) have a kinesin domain placed in the middle of the protein sequence, and are non-motile. Kinesin-14 family members have the kinesin domain located at the C-terminus end of the protein, and possess minus-end directed motility.

Microtubule destabilizing activity has been attributed to three kinesin families; namely, kinesin-8, kinesin-13 and kinesin-14. These kinesins are therefore able to regulate microtubule dynamics. Most microtubule-destabilizing kinesins characterised so far have been shown to play important roles during mitosis; for example, in centrosome separation, spindle formation, chromosome congression and segregation, central spindle formation and cytokinesis. The kinesin-8 and -13 families are described in greater detail in following sections.

The completed genome sequence of fission yeast contains nine members of the conserved kinesin superfamily, listed in Table 1.2 below. Fungal genomes do not contain any members of the microtubule depolymerising Kinesin-13 family, but do possess members of both Kinesin-8 and Kinesin-14 families, members of which have been shown to possess microtubule depolymerising activity in budding yeast (Sproul *et al.*, 2005; Gupta *et al.*, 2006; Varga *et al.*, 2006).

***S. pombe* kinesin**	**Kinesin family**
Klp3	Kinesin-1
Cut7	Kinesin-5
Klp4	(not determined)
Klp5	Kinesin-8
Klp6	Kinesin-8
Pkl1	Kinesin-14
Klp2	Kinesin-14
Tea2	Kinesin 7?
SPBC2D10.21c	Kinesin-6

Table 1.2 Kinesin superfamily proteins in fission yeast

1.6.4 Kinesin-13 Family

Kinesin-13 proteins are the best-characterised microtubule depolymerases. They are well conserved amongst higher eukaryotes, but do not exist in yeasts. The first time that microtubule depolymerising activity was attributed to a member of the kinesin superfamily was to the Kinesin-13 member MCAK (also described in section 1.5.5) (Walczak *et al.*, 1996; Maney *et al.*, 1998; Desai *et al.*, 1999).

The Kinesin-13 catalytic core is highly similar to other kinesins, but it is located in the middle of the protein sequence, instead of at the N- or C-terminus. Motifs required for ATPase activity and microtubule interaction are conserved with other kinesins (Moores *et al.*, 2003; Moores and Milligan, 2006). There are additionally some Kinesin-13 specific features: a class-specific neck of highly charged residues is located N-terminal to the kinesin domain, and loop L2 contains an insert of three conserved residues: KVD, required for initiation of microtubule depolymerisation (Moores *et al.*, 2003; Shipley *et al.*, 2004). Another three conserved residues, KEC, are found in a region important for MT-binding adjacent to the L12/α5 region (Woehlke *et al.*, 1997; Shipley *et al.*, 2004). The very N-terminus of Kinesin-13s contains a domain for subcellular targeting, e.g centromere targeting of MCAK and KIF2A.

The currently favoured model for Kinesin-13 microtubule depolymerisation is that the ATP-bound form of the motor increases the curvature of the microtubule protofilaments, a conformation that favours tubulin subunit dissociation and hence catastrophe (see section 1.2.2) (Desai *et al.*, 1999; Moores *et al.*, 2002; Moores *et al.*, 2006). The α4 helix, known to be important for energy transduction in kinesins, is thought to be directly involved in microtubule depolymerisation. The positively charged neck region may also be important for tubulin bending (Moores and Milligan, 2006). Kinesin-13 members function as protein homodimers *in vivo*, but a monomeric neck+motor construct can recapitulate WT-like depolymerisation activity both *in vitro* and *in vivo* (Maney *et al.*, 2001; Ovechkina *et al.*, 2002), although full-length dimeric MCAK is a more efficient depolymerase (Hertzer *et al.*, 2006). It is not currently clear exactly why Kinesin-13s associate as homodimers; one possibility is that it facilitates processive depolymerisation (Helenius *et al.*, 2006).

Kinesin-13 members are able to depolymerise microtubules from either end. They localise to microtubule ends by rapid passive diffusion along the microtubule lattice (Helenius *et al.*, 2006), as well as targeting to the kinetochore/centromere in a microtubule-independent manner. The C-terminus of MCAK is thought to inhibit the lattice-stimulated ATPase activity of the kinesin domain, because when the C-terminus is truncated, ATPase activity is increased (Moore and Wordeman, 2004a).

The human genome contains three distinct kinesin-13 members; Kif2a, Kif2b and MCAK (Kif2c). MCAK is the best characterised; it localises to centrosomes, kinetochores and the spindle midzone (Wordeman and Mitchison, 1995) and is known to be phosphorylated by Aurora B kinase and to contribute to the destabilisation of erroneous kinetochore-microtubule attachments (see section 1.5.5). Perturbation of its function leads to an increase in lagging chromosomes (Maney *et al.*, 1998; Kline-Smith *et al.*, 2004). Kif2a is required for proper bipolar spindle formation. Its localisation at the centrosomes contributes to polewards flux, which plays a role in the poleward movement of chromosomes in anaphase (Ganem and Compton, 2004). Kif2b has recently been reported to participate in bipolar spindle assembly, chromosome movement and cytokinesis. It localises to kinetochores and the spindle midzone (Manning *et al.*, 2007). Kinesin-13s in *Drosophila* and *Xenopus* have also been identified and characterised.

1.6.5 Kinesin-8 Family

The Kinesin-8 family of microtubule depolymerising kinesins is conserved from yeast to humans (see Figure 1.9). All members characterised so far play roles in mitotic cell division. The kinesin domain of Kinesin-8 proteins is well conserved with other kinesins. Additionally, there are two conserved regions N-terminal to the kinesin domain which seem to be specific to Kinesin-8s (first two lines, Figure 1.9).

The budding yeast member, Kip3, was the first Kinesin-8 to be characterised biochemically, and was shown to differ from Kinesin-13 members, because it is both a plus-end directed motor and a depolymerase, and its depolymerisation activity is plus-end specific (Gupta *et al.*, 2006; Varga *et al.*, 2006). Kip3 is necessary for positioning of the mitotic spindle – a function that seems to be specifically required in budding yeast (Cottingham and Hoyt, 1997), and for regulation of interphase MT dynamics; *Δkip3* cells exhibit decreased rates of MT growth and shrinkage in G1. It also binds directly to core kinetochore components and is required for synchronous poleward movements of chromosomes in anaphase. It is suggested that it couples MT plus end depolymerisation to release of tension at centromeres upon cohesin cleavage (Tytell and Sorger, 2006). One intriguing, and unique, aspect of the Kinesin-8 Kip3 function is that it depolymerises MTs in a length-dependent manner; longer MTs are depolymerised faster than short MTs (Varga *et al.*, 2006). Kip3 was found to be a highly processive motor (about 20 times more so than Kinesin-1 (Walczak, 2006)), and it walks towards the plus end faster than the rate of plus-end MT polymerization. This means that the longer the MT is, the more Kip3 molecules will have accumulated at its plus end, where they subsequently induce its depolymerisation (Varga *et al.*, 2006).

Kip3 requires ATP hydrolysis to power its plus-end directed motor movement, but could promote low levels of MT depolymerisation in the absence of ATP (Gupta *et al.*, 2006). In contrast, Kinesin-13s require ATP for depolymerization (Moores *et al.*, 2002). All kinesins' ATPase activity is stimulated by MTs, but ATPase activity of both Kinesin-8s and Kinesin-13s is also stimulated by tubulin-dimer (Walczak, 2006).

Klp67A is a kinesin-8 member characterised in *Drosophila*. It is required for proper chromosome congression and segregation in mitosis and meiosis I (Goshima and Vale, 2003; Savoian *et al.*, 2004). Mutant *klp67A* primary spermatocytes exhibit disorganised spindle structure with dense, overgrown MTs. Central spindles do not form correctly in anaphase, and cytokinesis frequently fails (Gandhi *et al.*, 2004; Savoian *et al.*, 2004; Gatt *et al.*, 2005). It thus seems that Klp67A is required to destabilise MTs before anaphase onset, but is subsequently required for stabilisation of the central spindle (Gatt *et al.*, 2005).

The human kinesin-8 member, Kif18a, is also required for chromsome congression. Kif18a depleted cells have longer spindles in mitosis, with scattered, unaligned chromosomes (Zhu *et al.*, 2005). Kif18a was shown, like budding yeast Kip3, to possess both plus-end directed motor activity and MT depolymerizing activity (Mayr *et al.*, 2007). Kif18a localises to the plus ends of kinetochore microtubules during mitosis, where it probably regulates MT dynamics to contribute to chromosome congression. Chromosome velocities are reported to be slower in the absence of Kif18a. MTs in *Δkip3* cells (described above) show increased dynamicity, whereas cells depleted for Kif18a appear to have suppressed MT dynamics (Stumpff and Wordeman, 2007).

The fission yeast genome contains two Kinesin-8 members, *klp5* and *klp6*. The protein sequences have 50% identity and 69% similarity between them. Klp5 and 6 form a heterocomplex (Garcia *et al.*, 2002a; Li *et al.*, 2003) and localise to cytoplasmic microtubules, mitotic spindles and the spindle midzone. When cells are arrested in metaphase, they localise at the kinetochore (Garcia *et al.*, 2002a). ChIP showed that Klp5 binds to outer repeats of the centromere (*otr*) in metaphase arrested cells in a microtubule-dependent manner (Garcia *et al.*, 2002a).

Deletions of *klp5*, *klp6* or both are viable. Single and double deletions have identical phenotypes: cells are on average 20% longer (Garcia *et al.*, 2002a) and cytoplasmic microtubules are long and curl around the edge of these cells (West *et al.*, 2001; Garcia *et al.*, 2002a). Deletion mutants are resistant to microtubule destabilizing drugs (West *et al.*, 2001; Garcia *et al.*, 2002a) and to cold shock treatment, suggesting that they are microtubule depolymerising factors (Garcia *et al.*, 2002b). Chromosomes in *klp* mutants do not congress

properly prior to anaphase onset (West *et al.*, 2002), but after a Mad2-dependent delay, usually segregate correctly (Garcia *et al.*, 2002a). Nonetheless, 10-20% of anaphase cells in *klp* mutants display lagging chromosomes (Garcia *et al.*, 2002a). *klp5* mutants show an elevated rate of minichromosome loss (Garcia *et al.*, 2002a); when spindle checkpoint delay is prevented by deletion of *mad2*, an extremely high rate of loss is observed (Garcia *et al.*, 2002b). Examination of kinetochore localisation of spindle checkpoint proteins in *klp5* mutants revealed that some kinetochores contain Bub1 only, while some contain both Mad2 and Bub1 (Garcia *et al.*, 2002b). Overexpression of Klp5 or 6 causes severe chromosome segregation defects (Garcia *et al.*, 2002a). Somewhat surprisingly, *Δklp5/6* is synthetic lethal with deletions of the microtubule stabilizing proteins Alp14 and Dis1 (TOG homologues) (Garcia *et al.*, 2002b). The kinetochore localization of Klp5 is reduced in *alp14* mutants (Garcia *et al.*, 2002b). It has been proposed that Klp5/Klp6 and Alp14/Dis1 collaborate in the formation and maintenance of a bipolar spindle by regulating spindle microtubule dynamics (Garcia *et al.*, 2002b).

Deletion of *klp5/klp6* is also synthetic lethal with components of the Dam1/DASH kinetochore complex (Sanchez-Perez *et al.*, 2005). Microscopic analysis of double *klp/dam1* mutants showed that spores are able to germinate, but arrest with a cut phenotype i.e. undergo septation in the absence of proper chromosome segregation. Klp5/Klp6 and Dam1/DASH are both required to establish a proper bipolar spindle, but their roles in this process are distinct; it has been suggested that the DASH complex corrects syntelic attachments, whereas Klp5/6 correct merotelic attachments (Sanchez-Perez *et al.*, 2005).

klp5 and *klp6* were also isolated in a screen for *scd1* interacting genes (Li *et al.*, 2003). Scd1 is a guanine nucleotide exchange factor for the Ras-like protein Cdc42. Double mutant *klp/scd1* cells showed cytokinetic defects.

Another kinesin-8 member, KipB, has been identified in *Aspergillus nidulans* (Rischitor *et al.*, 2004). *kipB* mutants are highly resistant to microtubule destabilizing treatments, show bent spindles during mitosis, and decreased depolymerisation of MTs in both interphase and mitosis. KipB localises to microtubules, and can be seen moving towards the plus ends. These data are all consistent with the idea that KipB functions as a depolymerase and as a plus-end directed motor, similar to other Kinesin-8 proteins.

The protein sequences of Klp5 and Klp6, like other members of the Kinesin-8 family, do not possess features that are important for Kinesin-13 depolymerisation, namely the positively charged neck domain, and the highly conserved KVD motif. This, along with the fact that Kinesin-8s have both motor and depolymerase activities, suggests that the mechanism for

Kinesin-13 depolymerisation differs from the Kinesin-8 mechanism. However, both families show ATPase stimulation by microtubules and by tubulin dimer, suggesting some similarity of mechanisms too.

1.7 Nuclear Transport

The nuclear envelope acts as a selectively permeable barrier between the nucleoplasm and the cytoplasm. Various cellular events are regulated by controlling whether molecules can be imported into, or exported from, the nucleus. This requires their passage through channels called nuclear pore complexes (NPCs), which are composed of ~30 proteins. Small proteins (up to ~60kD) can pass through by passive diffusion, but larger molecules need to be actively transported. In metazoans, the nuclear envelope breaks down at the beginning of mitosis. However, yeasts undergo a closed mitosis in which the nuclear envelope is maintained, meaning that components required for chromosome segregation need to be imported into the nucleus during mitosis.

1.7.1 Overview of Nuclear Transport Systems

Proteins that are imported into the nucleus contain a nuclear localisation signal (NLS) that is recognised by an adaptor molecule. Classical NLSs consist of a short sequence of 3-5 basic amino acids, which may also be associated with a proline or glycine. A bipartite NLS has an additional basic dipepetide located ten residues upstream of the basic sequence. The adaptor, an importin α, binds directly to the NLS-containing protein (the cargo), and this complex is then bound by a receptor, an importin β, which mediates passage of the heterotrimeric complex through the NPC. It is also possible for the importin β to bind the cargo directly. Export of proteins from the nucleus to the cytoplasm occurs in an analogous manner, mediated by exportin β family members, which bind to nuclear export signals (NES) in protein cargoes. NESs are not as easily defined as NLSs. The best characterised exportin is CRM1, which exports proteins containing a leucine-rich NES (Fornerod *et al.*, 1997; Fukuda *et al.*, 1997; Ossareh-Nazari *et al.*, 1997; Stade *et al.*, 1997).

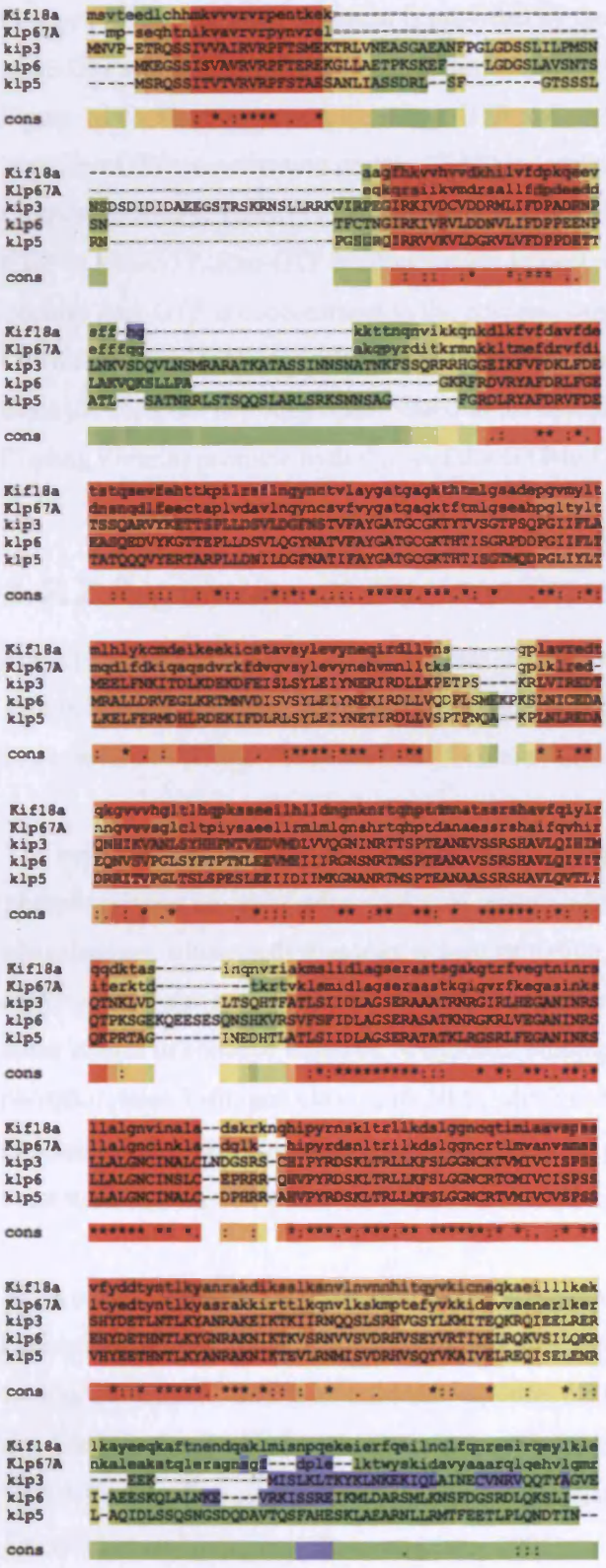

Figure 1.9 Alignment of Kinesin-8 N-termini (kinesin domain)

Conservation between human Kif18a, *Drosophila* Klp67A, *S. cerevisiae* Kip3, and *S. pombe* Klp5 and Klp6. Alignment done using T-coffee (Swiss Institute of Bioinformatics).

Energy for active nuclear transport is provided by the hydrolysis of GTP, catalysed by the small GTPase, Ran. Ran also provides directionality for nuclear import and export (see Figure 1.10). The conversion from Ran-GTP to Ran-GDP is favoured in the cytoplasm, because a GTPase-activating protein (GAP) is located there. In contrast, a Ran-GEF (guanine exchange factor) is located in the nucleus or on the chromatin and converts Ran-GDP to Ran-GTP. Ran-GTP binding causes import receptors to release their cargo, and because Ran-GTP is concentrated in the nucleus, cargo is only released in the nucleus. Conversely, Ran-GTP promotes the binding of cargo to export receptors in the nucleus. Once the complex has been translocated to the cytoplasm, Ran-GAP and RanBP1 (Ran Binding Protein) promote hydrolysis of the GTP to GDP, causing the cargo to be released.

1.7.2 Regulation of Nuclear Transport

Some proteins contain both nuclear import and export signals. Such proteins may constantly shuttle between the cytoplasm and the nucleus, or rate of import or export may be modified as necessary to change the subcellular location of the protein (Alberts *et al.*, 2002).

The best understood mechanism that regulates nuclear transport of proteins is the phosphorylation or dephosphorylation of protein substrates by different protein kinases or phosphatases, whose activities may in turn be tightly regulated or co-ordinated with important cellular events. Phosphorylation of residues proximal to the NLS or NES can either reduce or enhance importin or exportin binding. The protein kinase CK2 phosphorylates T-antigen close to its NLS, which enhances importin α/β binding 100-fold (Hubner *et al.*, 1997; Xiao *et al.*, 1997). Conversely, phosphorylation near the NLS of the yeast transcription factor Pho4 inhibits its nuclear import (Kaffman *et al.*, 1998).

NLSs or NESs may be masked within a cargo protein (i.e. intramolecular masking) to reduce their accessibility to importins/exportins. For example, the NLS is masked in a precursor form of NF-κB, but during an immune response, the C-terminus is phosphorylated and degraded, so that the NLS is revealed in the mature form of NF-κB (Riviere *et al.*, 1991). NLS/NES intramolecular masking can also be mediated by conformation changes caused by disulphide bond formation (Poon and Jans, 2005).

Alternatively, NLS/NES activity may be regulated by intermolecular masking, whereby binding of an additional molecule prevents interaction with importins/exportins. A classic example of this mechanism is the binding of calcineurin to the NES of the transcription factor NF-AT4 at high calcium concentrations, preventing its export from the nucleus

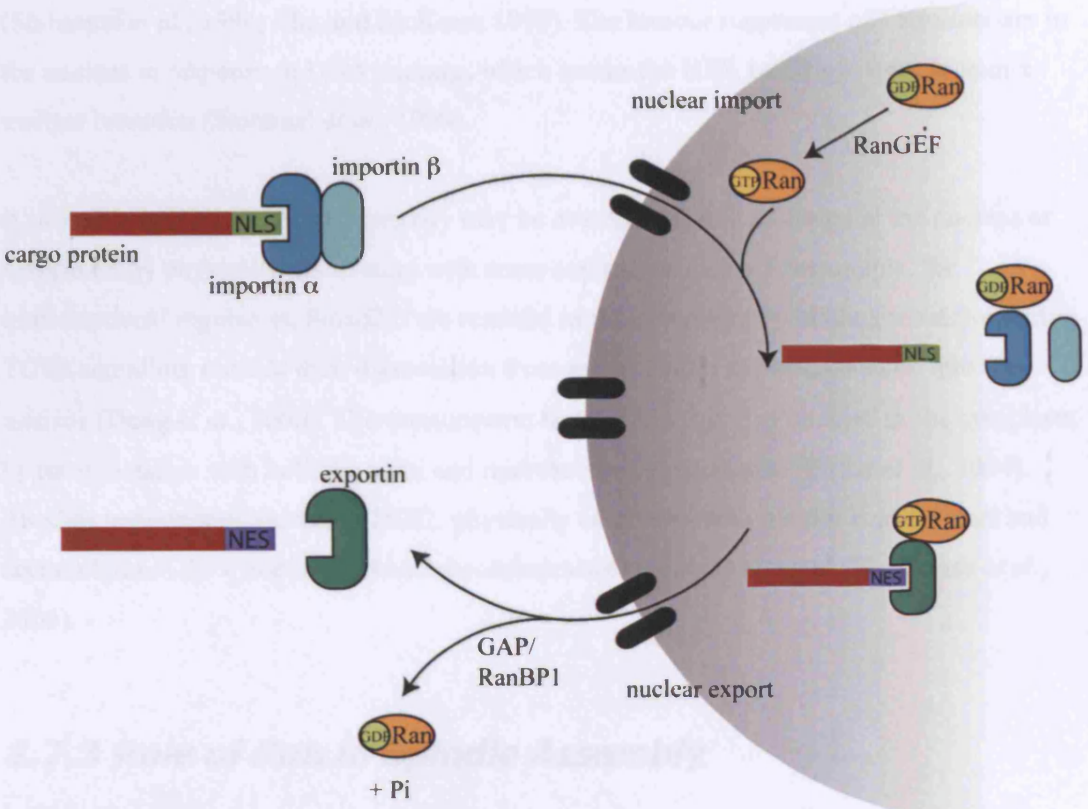

Figure 1.10 Model for nuclear import and export

Nuclear import: an NLS-containing cargo protein is bound by importin α/β adaptor complex, which mediates its passage through the nuclear pore complexes (NPCs). In the nucleus, the RanGEF (nucleotide exchange factor) ensures that a high proportion of Ran is complexed with GTP, rather than GDP. Ran-GTP binds to the importin α/β complex, causing them to release their cargo in the nucleus. Nuclear export: an NES-containing cargo protein is bound by an exportin associated with Ran-GTP. This complex can be transported from the nucleus to the cytoplasm through the NPCs. In the cytoplasm, the Ran-GAP (GTPase activating protein) and RanBP1 (Ran Binding Protein) promote hydrolysis of the GTP to GDP, which causes the cargo protein to be released.

(Shibasaki *et al.*, 1996; Zhu and McKeon, 1999). The tumour suppressor p53 tetramerises in the nucleus in response to DNA damage, which masks the NES, resulting in the protein's nuclear retention (Stommel *et al.*, 1999).

A protein's intrinsic NLS/NES activity may be overcome if it is anchored in the nucleus or cytoplasm by physically associating with some cellular structure. For example, the transcriptional regulators, Smad2/3 are retained in the cytoplasm by binding to microtubules. TGFβ signalling induces their dissociation from microtubules and translocation into the nucleus (Dong *et al.*, 2000). The transcription factor PREP2 is also retained in the cytoplasm by its association with both the actin and microtubule cytoskeletons (Haller *et al.*, 2004). Another transcription factor, RUNX2, physically associates with tubulin heterodimers and accumulates in the cytoplasm when microtubules are stabilised by taxol (Pockwinse *et al.*, 2006).

1.7.3 Role of Ran in Spindle Assembly

In recent years, it has emerged that Ran plays an important role in spindle assembly. The Ran-GEF (RCC1), which generates Ran-GTP, is chromatin-bound throughout the cell-cycle (Ohtsubo *et al.*, 1989; Moore *et al.*, 2002), and its activity is thought to be regulated by phosphorylation (Hutchins *et al.*, 2004). This results in a Ran-GTP gradient being concentrated around the chromosomes in metazoan cells. In *Xenopus* egg extracts, high levels of Ran-GTP cause microtubule polymerisation and spindle formation (Carazo-Salas *et al.*, 2001; Wilde *et al.*, 2001). It is proposed that Ran-GTP activates factors required for spindle assembly, such as TPX2, NuMA and HURP, by releasing them from importin α/β binding in the vicinity of chromosomes. Microtubules nucleated immediately adjacent to kinetochores can be captured much more easily than in the classical 'search-and-capture' model. The chromosomes with their associated K-fibres must then be integrated into the spindle.

These findings suggest that the closed mitosis of yeasts and the open mitosis of other eukaryotes may not in fact be so different. Yeast cells are probably too small to establish a Ran-GTP gradient around individual chromosomes; however, a closed mitosis ensures compartmentalisation of high Ran-GTP concentration in the nucleus. In both yeast and animal mitoses, components required for spindle formation have to be released from importin α/β binding; the only difference in yeast is that these components must first pass through the NPCs in the nuclear membrane.

1.8 This Thesis

This thesis describes the study of the mitotic role of Kinesin-8 Klp5 and Klp6 proteins in fission yeast. Kinesin-8 proteins are of great interest, as their function seems to be conserved from yeast to man. Analysis of *Δklp* mutants in fission yeast is very informative, because we can be certain that the proteins are completely absent. In contrast, studies using RNAi in higher organisms can be more difficult to interpret, given that some phenotypes may result from only partial knockdown. Klp5/6 are known to play roles at the kinetochore, and fission yeast is also an excellent model for dissection of kinetochore function. Its genetic tractability means that a number of useful molecular tools are available, and additionally, its centromeres are larger and more complex than those of budding yeast, and it is therefore a better model of higher eukaryote centromeres.

Cartoon representations of Klp5 and Klp6 are shown in Figure 1.11. The colour-coding in this figure is used throughout this thesis, to enable the reader to easily understand results obtained using different constructs. Regions of homology are shown by coloured blocks, and distinctions between Klp5 and Klp6 kinesin and coiled-coil domains are made by cross-hatching Klp6 domains. Homology of the Klp5/Klp6 kinesin domains with e.g. MCAK or Kinesin-1 begins at position ~100. However, Klp5 and Klp6 show identity with each other, and with other Kinesin-8 proteins throughout the N-terminus i.e. before the coiled-coil (see Figure 1.9), so in this thesis, the entire N-terminus is referred to as the kinesin domain.

Klp5 and Klp6 usually localise to the nucleus during mitosis. Early on in this study, it was found that Klp5 cannot localise to the nucleus in *Δklp6* cells, and that Klp6 cannot localise to the nucleus in *Δklp5* cells (results presented in Chapter 3). This means that a *Δklp5* strain is essentially a double deletion as far as nuclear mitotic function is concerned, as is a *Δklp6* strain. This is useful in the sense that we can assume that the mitotic phenotype of *Δklp5* and *Δklp6* cells is the same. Throughout this thesis, the general terms Klp or *klp* are used to describe a phenotype attributable to either *Δklp5*, *Δklp6* or *Δklp5Δklp6* cells.

Project Aims:

There were two major aims that we set out to address in this project. These were:

1) To further characterise the phenotype of *Δklp* mutants during mitosis, with the aim of elucidating the mitotic role Klp5/Klp6.

2) To determine why Kinesin-8 Klp5 and Klp6 function as a heterodimer. More specifically, to establish whether the Klp5 N-, Klp5 C-, Klp6 N- and Klp6 C-termini domains make distinct contributions to the overall function of the Klp5/Klp6 heterocomplex. If this were the case, to determine what properties each domain contributes.

Presentation of Results in this Thesis:

The results presented in this thesis are divided into two sections, roughly corresponding to the two major project aims described above. In the first section, localisation data gained from live cell imaging is presented. Additionally, the mitotic phenotype of *Δklp5* and *Δklp6* mutants is analysed. We look specifically at kinetochore movement and at metaphase spindle length, and at the necessity of various spindle checkpoint components for viability of *Δklp* strains. We also describe the construction of Klp5 ATPase mutants and their subsequent characterisation.

In the second section of this thesis we turn our attention to the function of Klp5/6 heterodimerisation. We find that heterodimerisation is significant for correct localisation of Klp5 and Klp6 to the nucleus during mitosis. We describe the identification of NLSs in Klp5 and Klp6, and discuss possible regulatory mechanisms for nuclear import and export. We also explore whether the Klp5 and Klp6 kinesin domains are interchangeable, or whether they each contribute distinct properties to the Klp5/6 heterodimer that are required for proper function. This question is investigated by the construction and characterisation of Klp5 and Klp6 N homodimers.

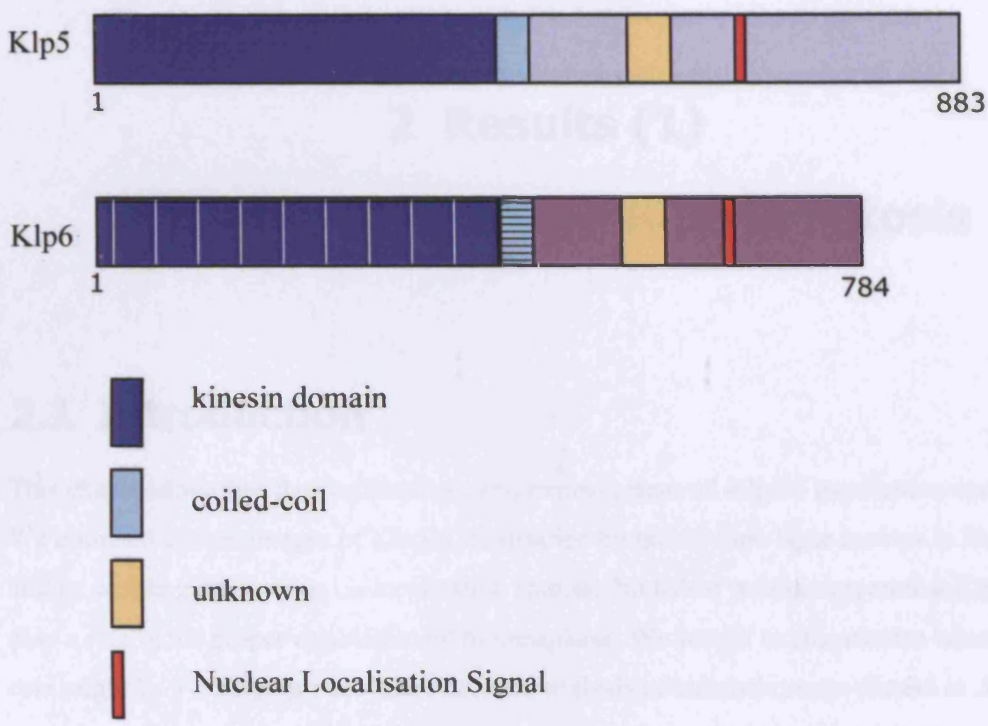

Figure 1.11 Cartoon of Klp5 and Klp6 domains

Representation of various domains within Klp5 and Klp6 proteins, as used throughout this thesis. Coloured blocks show regions of homology. The C-termini tails are highly diverged and therefore represented by different colours; lilac for Klp5 and purple for Klp6. The Klp5 and Klp6 kinesin domains and coiled-coil domains are distinguished by cross hatching; the Klp6 domains are cross-hatched, whereas the Klp5 domains are not.

2 Results (1)

The Role of Klp5 and Klp6 in Mitosis

2.1 Introduction

This chapter describes the continuation, and improvement of, Klp5/6 localisation studies. We obtained clearer images of Klp5/6 localisation by taking time-lapse movies in live cells, and by carrying out various co-localisation studies. Published results suggest that Klp5/Klp6 play a role in the proper establishment of metaphase. We sought to characterise what this role might be by carrying out a more detailed analysis of kinetochore movement in *Δklp* mutants, and examining the *Δklp* phenotype in the absence of a functional spindle checkpoint.

2.2 Localisation Data

2.2.1 Live localisation of Klp5-GFP

Immunofluorescence studies on fixed cells show that Klp5 that is C-terminally tagged with GFP (Klp5-GFP) localises to mitotic kinetochores and spindle during metaphase, and to the spindle midzone during anaphase (Garcia *et al.*, 2002a; Garcia *et al.*, 2002b). Since then, the lab has acquired a more advanced microscope system for the observation of live cells. In this study, Klp5-GFP localisation was observed live using the Delta Vision system (Applied Precision, Issaquah, WA). Sad1 is a constitutive component of the SPB, and Sad1-dsRED was used to visualise the SPBs. The time-lapse images shown in Figure 2.1 confirm that Klp5-GFP localises to the spindle during mitosis, but becomes restricted to the central spindle during anaphase. The dot-like localisation (such as that visualised at 240s) may indicate kinetochore localisation, although it could also be localisation to MT plus-ends, rather than *bona fide* kinetochore localisation. However, ChIP has shown that Klp5 binds to outer repeats of the centromere (*otr*) in metaphase arrested cells, and Klp5-GFP colocalises with Nuf2-CFP in metaphase arrested cells (Garcia *et al.*, 2002a). These previous data suggest that Klp5 does indeed localise to kinetochores.

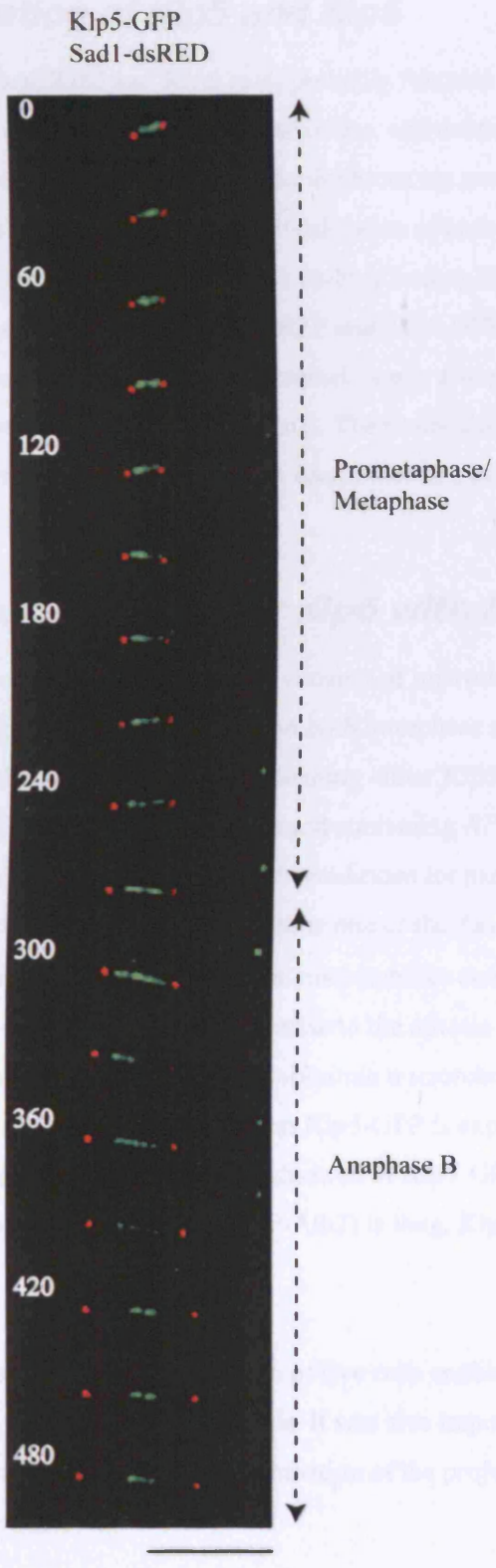

Figure 2.1 Localisation of Klp5-GFP and Sad1-dsRED

Time-lapse images of Klp5-GFP and Sad1-dsRED acquired every 30s during mitosis. Images were deconvolved and projections made. Time shown in seconds. Approximate stages of mitosis are indicated to the right. Scale bar = 10μm.

2.2.2 Co-localisation of Klp5 and Klp6

According to published data, Klp5 and Klp6 most probably function as a heterodimer. Co-immunoprecipitation shows that they physically associate, and deletion of *klp5,* or *klp6,* or a double deletion shows the same phenotype, and the deletions are non-additive (Garcia *et al.*, 2002a). To further corroborate this data, the live localisation of both Klp5 and Klp6 was examined using Klp5-2mRFP and Klp6-GFP. The co-localisation of Klp5 and Klp6 is shown in Figure 2.2. It can be seen that Klp5-2mRFP and Klp6-GFP co-localise precisely; regions of greater fluorescence intensity in one channel nearly always correspond to regions of greater fluorescence intensity in the other channel. The co-localisation of Klp5/Klp6 is consistent with the notion that they associate with each other as a kinesin heterodimer.

2.2.3 Co-localisation of Klp5 or Klp6 with tubulin

Klp5-GFP localises to the mitotic spindle, which consists of microtubules. The localisation of either Klp5-GFP or Klp6-GFP was visualised in both interphase and mitosis in conjunction with microtubules. For this, cells containing either Klp5-GFP or Klp6-GFP at the endogenous loci were transformed with a plasmid containing *RFP-atb2*$^{+}$ under the thiamine-repressible *nmt1* promoter, and grown in conditions for partial repression, as described elsewhere (Yamashita *et al.*, 2005). Atb2 is one of the fission yeast α-tubulin subunits, and by fluorescently tagging this protein, microtubules can be visualised. Figure 2.3 shows that both Klp5-GFP and Klp6-GFP localise to the mitotic spindle and to cytoplasmic microtubules. The localisation to cytoplasmic microtubules (Figure 2.3, cells iv) and viii)) is weak and quite difficult to detect when Klp5-GFP is expressed from its endogenous locus. Cell iii) clearly shows the localisation of Klp5-GFP to the spindle midzone; although the spindle (visualised by RFP-Atb2) is long, Klp5-GFP only localises to the central region.

These localisation data obtained from observation of live cells enable us to be sure of the localisation data reported previously for fixed cells. It was also important to gain proficiency in live cell analysis, as it was crucial for the continuation of the project.

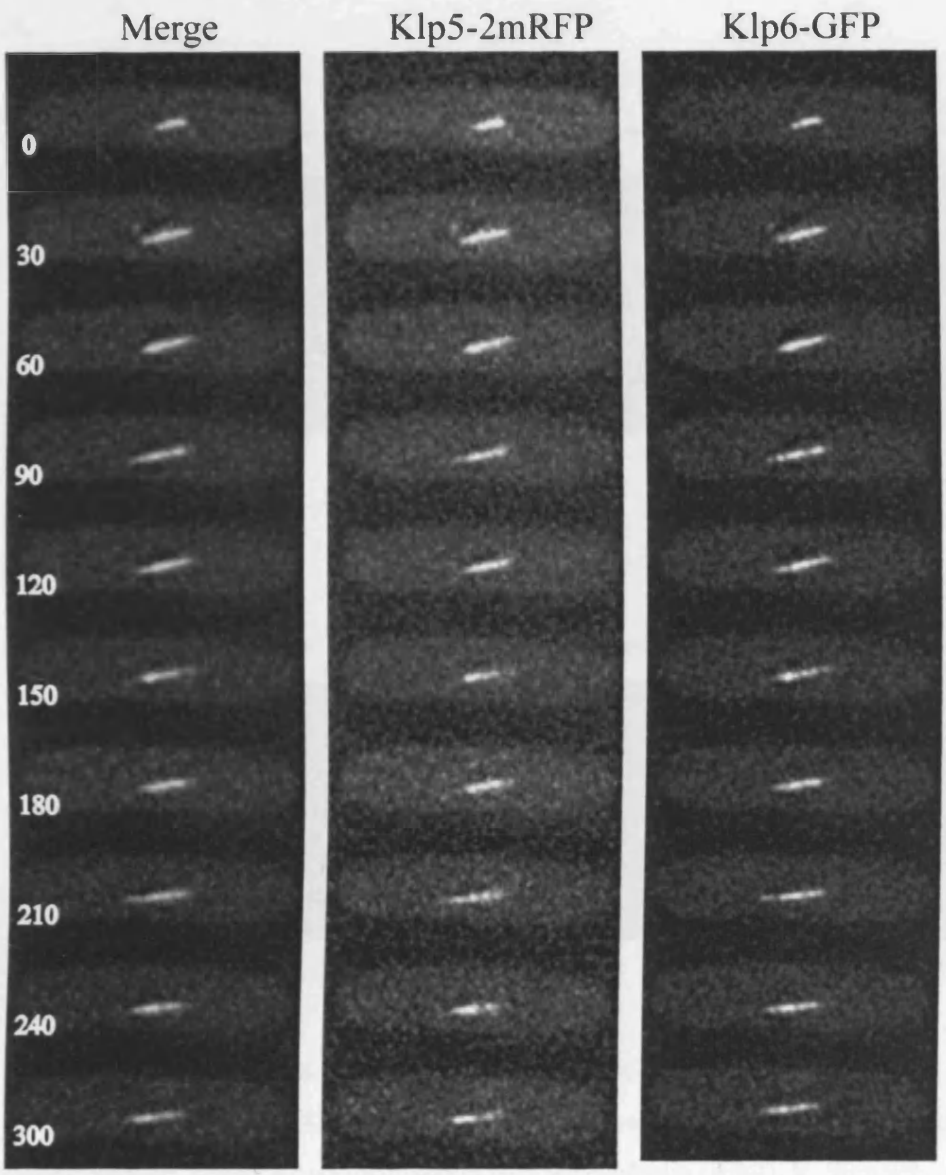

Figure 2.2 Co-localisation of Klp5-2mRFP and Klp6-GFP

Time-lapse images of Klp5-2mRFP and Klp6-GFP were taken every 30s during mitosis. Scale bar = 10μm. Time is shown in seconds.

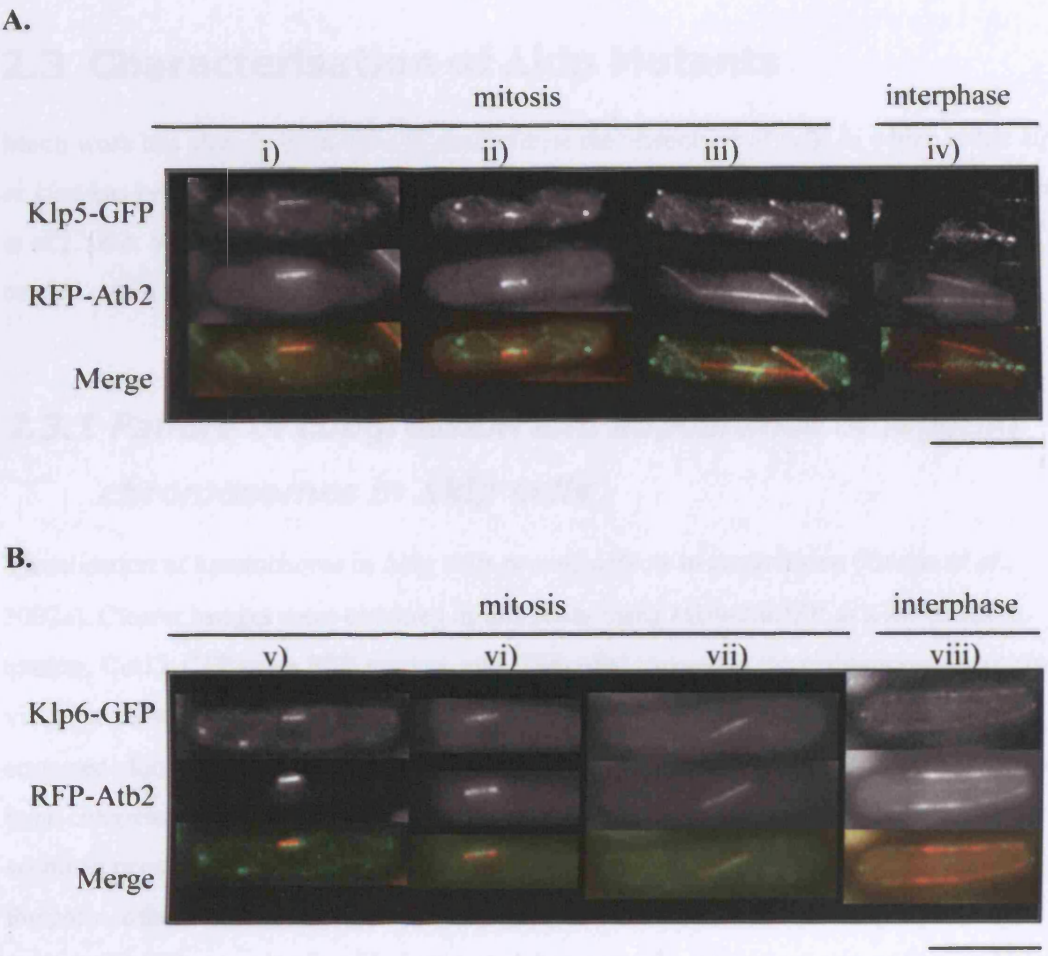

Figure 2.3 Localisation of Klp5-GFP or Klp6-GFP with RFP-Atb2

Still images of live cells. **A.** Klp5-GFP localises to cytoplasmic microtubules and to the mitotic spindle, shown by co-localisation with RFP-tubulin (Atb2). **B.** Similarly, Klp6-GFP localises to cytoplasmic microtubules and the mitotic spindle. Scale bar = 10μm

2.3 Characterisation of Δklp Mutants

Much work has already been done to characterise the phenotype of cells in which either *klp5* or *klp6* has been deleted (West *et al.*, 2001; Garcia *et al.*, 2002a; Garcia *et al.*, 2002b; West *et al.*, 2002; Sanchez-Perez *et al.*, 2005). In this study, some additional experiments were carried out to try and further our understanding of the role of Klp5/6 during mitosis.

2.3.1 Failure of congression and appearance of lagging chromosomes in Δklp cells

Visualisation of kinetochores in Δ*klp* cells reveals defects in congression (Garcia *et al.*, 2002a). Clearer images were obtained in this study using Mis6-2mRFP as a kinetochore marker, Cut12-CFP as an SPB marker, and GFP-Atb2 (tagged at the endogenous locus) to visualise the mitotic spindle. Figure 2.4 shows that kinetochores in the Δ*klp5* mutant are scattered along a spindle which is much longer than a wildtype pre-anaphase spindle. There is no congression at the spindle equator prior to chromosome segregation, and segregation seems to occur asynchronously; while some sister chromatids have completely segregated to the poles, others remain near the centre of the spindle. Two pairs of sisters complete segregation 180 seconds after filming started, but one or both kinetochores of the remaining pair of sister chromatids are still lagging on the spindle at 620 seconds (yellow arrowhead). In 5 of 5 movies of Δ*klp5* cells, some lagging on the spindle is observed. Although lagging chromosomes have been observed previously for *klp* mutants, the reported frequency is only 2.4% for Cen1-GFP (Sanchez-Perez *et al.*, 2005). It is possible that microtubule dynamics are slightly perturbed in the GFP-Atb2 strain, and this, in conjunction with the deletion of *klp5*, causes an increase in the frequency of lagging chromosomes. Therefore, Mis6-2mRFP movement was also observed in a strain lacking GFP-Atb2 (data not shown). In this strain too, sister chromatids appear to segregate asynchronously and laggards are observed. The phenotype observed in this strain is markedly different to the wildtype situation, in which chromosomes segregate synchronously on a shorter spindle (Figure 2.4, right-hand side).

2.3.2 Analysis of centromere II movement

When all six of the fission yeast kinetochores are visualised using a kinetochore marker such as Mis6 (see previous section), it can be difficult to distinguish which kinetochores belong to sister chromatids. The dynamics of sister chromatid movement are therefore very difficult to follow. To overcome this problem, strains with only centromere II marked with GFP were constructed. These strains contain the *LacO* array from *E. coli* integrated just 5kb from

centromere II, and GFP-LacI-NLS expressed from another locus, which binds to the array (Nabeshima *et al.*, 1998; Straight *et al.*, 1998; Ding *et al.*, 2004). Sad1-dsRED is used as a marker for the SPBs. The time-lapse images of live cells in Figure 2.5 show clear differences between the movements of sister chromatids in Δ*klp6* mutants compared with wildtype. In wildtype cells, sister chromatids display characteristic 'breathing' movements, moving towards and away from each other. They are then seen to congress in the centre of the cell, before segregating to opposite poles. Δ*klp6* mutants also display breathing movements, but the sister chromatid pair shuttles across the spindle, being first in the vicinity of one SPB, then moving over to the opposite pole. Chromosomes segregate correctly, but proper congression never occurs. Instead, the sister chromatids segregate while located close to one pole; one *cen2-GFP* focus remains at that pole, while the other is seen moving rapidly across the entire spindle length to join the other SPB.

This type of analysis provides a clearer picture of the effect of *klp* deletion during mitosis. However, it is not immediately obvious how it corresponds to the observations of all six kinetochores visualised by Mis6-2mRFP (Figure 2.4). After the onset of chromosome segregation in a *Δklp6* mutant, one sister chromatid has to traverse the length of the spindle to reach the opposite pole. It is possible that if this moment is captured in a still image, with one sister at a pole and the other in the middle of the spindle, it could be classified as a lagging chromosome. However, this is clearly different to the type of laggard that is described in the Mis6-2mRFP analysis. Lagging chromosomes visualised with Mis6-2mRFP lag for prolonged periods of time on the spindle, rather than rapidly moving towards one of the poles. Perhaps different chromosomes differ in their behaviour, and chromosome II is not prone to lag on the spindle. The analysis of Mis6-2mRFP does show that only one pair of sisters lags, and perhaps this rarely or never corresponds to *cen2*.

Additional kymographs for the comparison of *cen2-GFP* behaviour in WT and Δ*klp6* cells are shown in Figure 2.6. **A.** and **B.** respectively. Quantification of these phenotypes is shown in Figure 2.11. All five representative wildtype cells show congression of the *cen2-GFP* signal in the centre of the cell, followed by rapid segregation to opposite poles. A total of ten Δ*klp6* cells were filmed in this experiment. 8 of 10 cells show no congression at the cell centre, but go on to segregate *cen2-GFP* correctly. Of these, seven cells showed the 'shuttling' phenotype described above, where both *cen2-GFP* foci are seen to move across the spindle between opposite poles (Figure 2.6 **B.** ii) – v)). In the other cell, the two *cen2*-GFP foci associate solely with one SPB, as if monopolar segregation had occurred, but then the *cen2*-GFP signal finally separates, and one of the centromeres moves to the opposite pole (Figure 2.6 **B.** vi)). 1 of 10 cells shows a more wildtype-like segregation, although the spindle is considerably longer and anaphase onset is delayed (Figure 2.6 **B.** i)). Finally, 1 of

10 cells shows a 'spindle collapse' phenotype, in which duplicated and separated SPBs move back towards each other (Figure 2.6 **B.** vii)). Unfortunately, because of fluorescence bleaching, it was not possible to address whether cells exhibiting spindle collapse later reattempt chromosome segregation. The growth rate of *Δklp* cells is indistinguishable from that of wildtype cells, suggesting all *Δklp* cells do ultimately segregate their chromosomes correctly.

Chromosome movement is clearly defective in *Δklp* cells; one possible explanation for this is that there is an increase in defective kinetochore-microtubule attachments, meaning that chromosomes do not biorient properly, thus explaining the lack of congression. We speculated that correct segregation is ultimately achieved because activation of the spindle checkpoint allows for repair of any defective kinetochore-microtubule attachments. This hypothesis is tested in the following section.

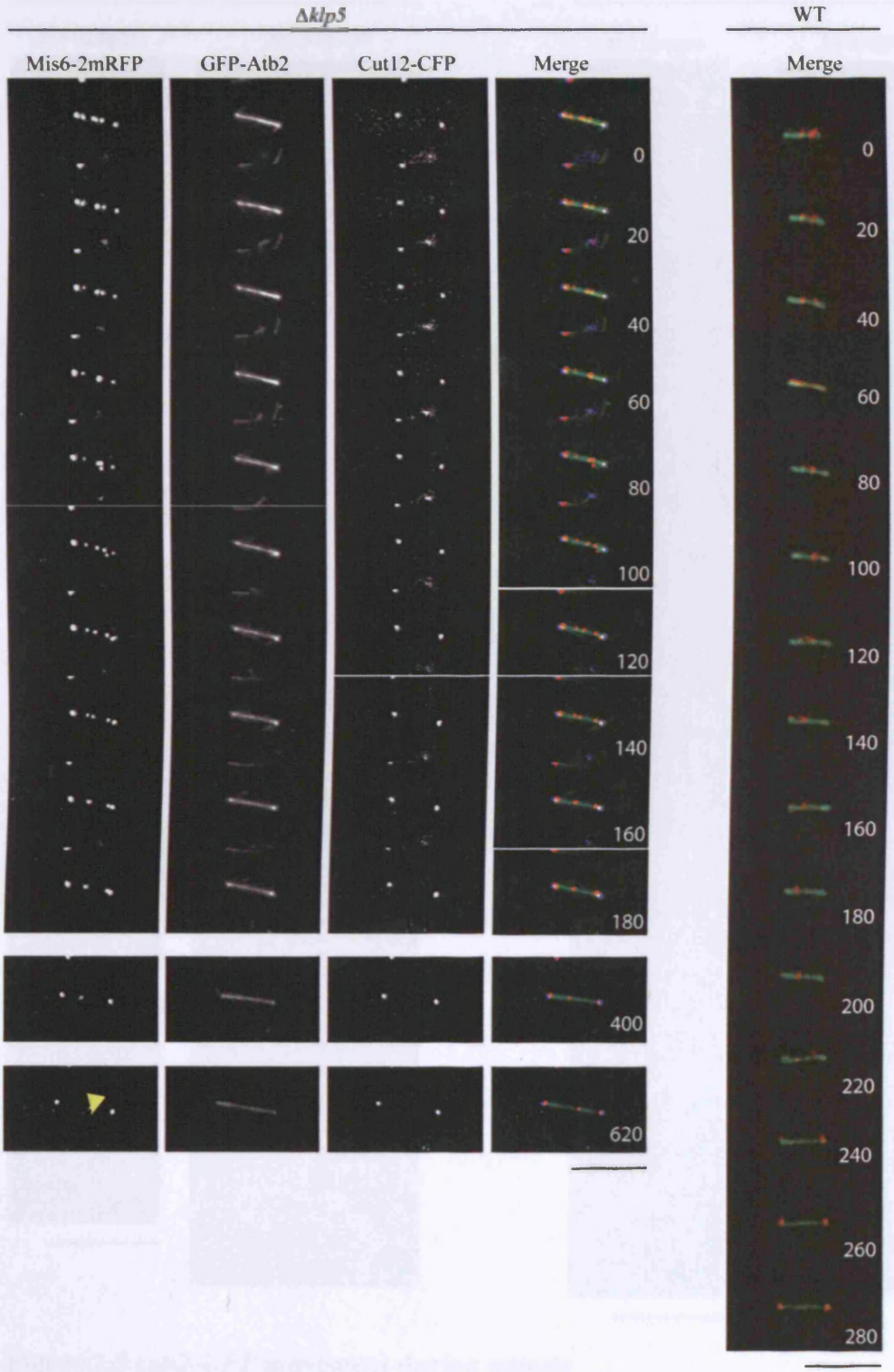

Figure 2.4 *Δklp5* mutants show defects in chromosome congression

Live imaging of Mis6-2mRFP (kinetochore marker), Cut12-CFP (SPB marker) and GFP-Atb2 (tubulin) during mitosis in Δ*klp5* cells. Lagging chromosome marked with yellow arrowhead (620s). An example of wildtype is shown on the right for comparison. Time is shown in seconds. Scale bar = 10μm.

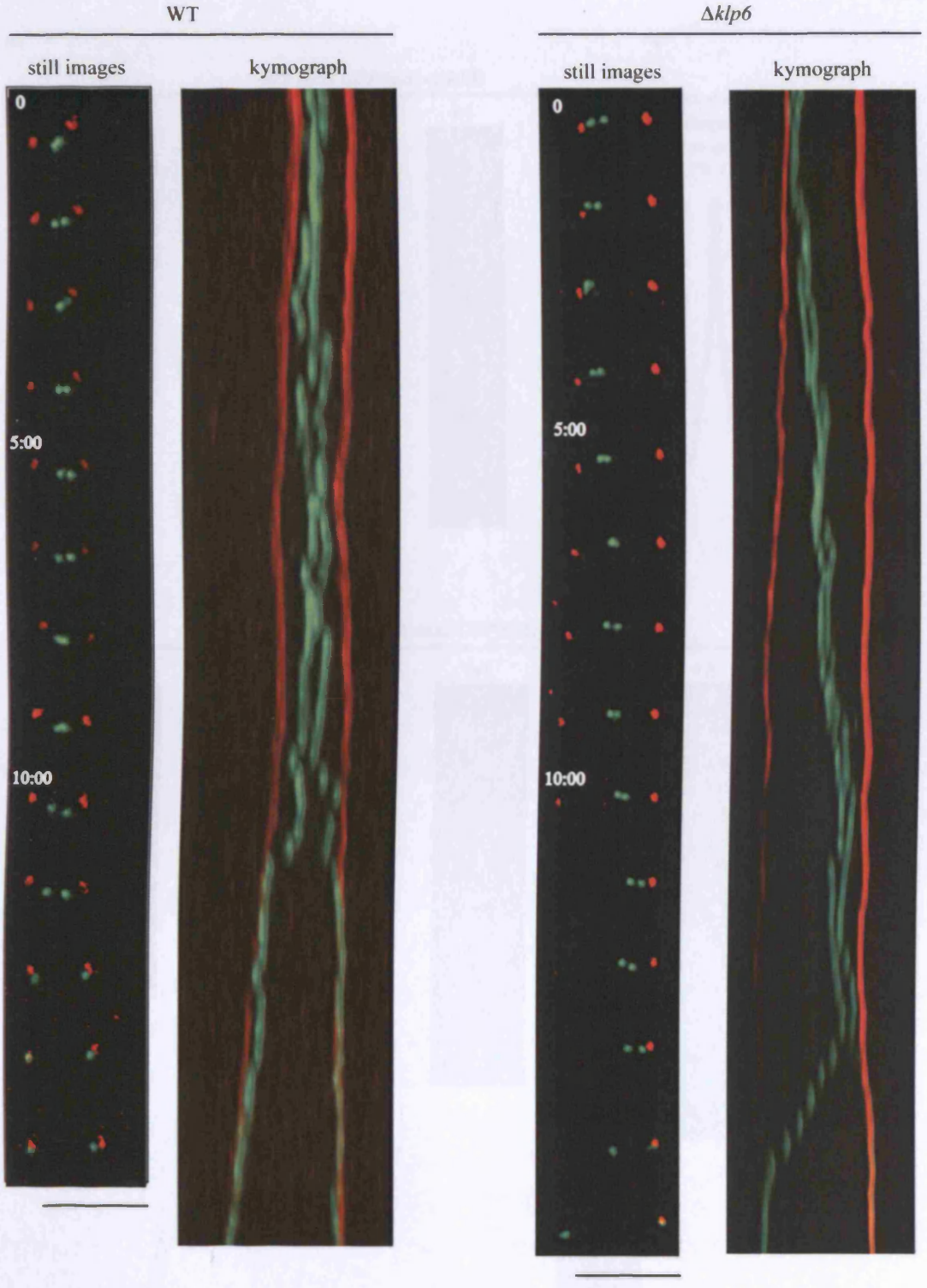

Figure 2.5 *cen2-GFP* movement during mitosis

Images taken every 30 seconds, still images shown for every 1 minute. Kymographs generated from same time-lapse movie as still images (see Materials and Methods). Scale bar = 5μm

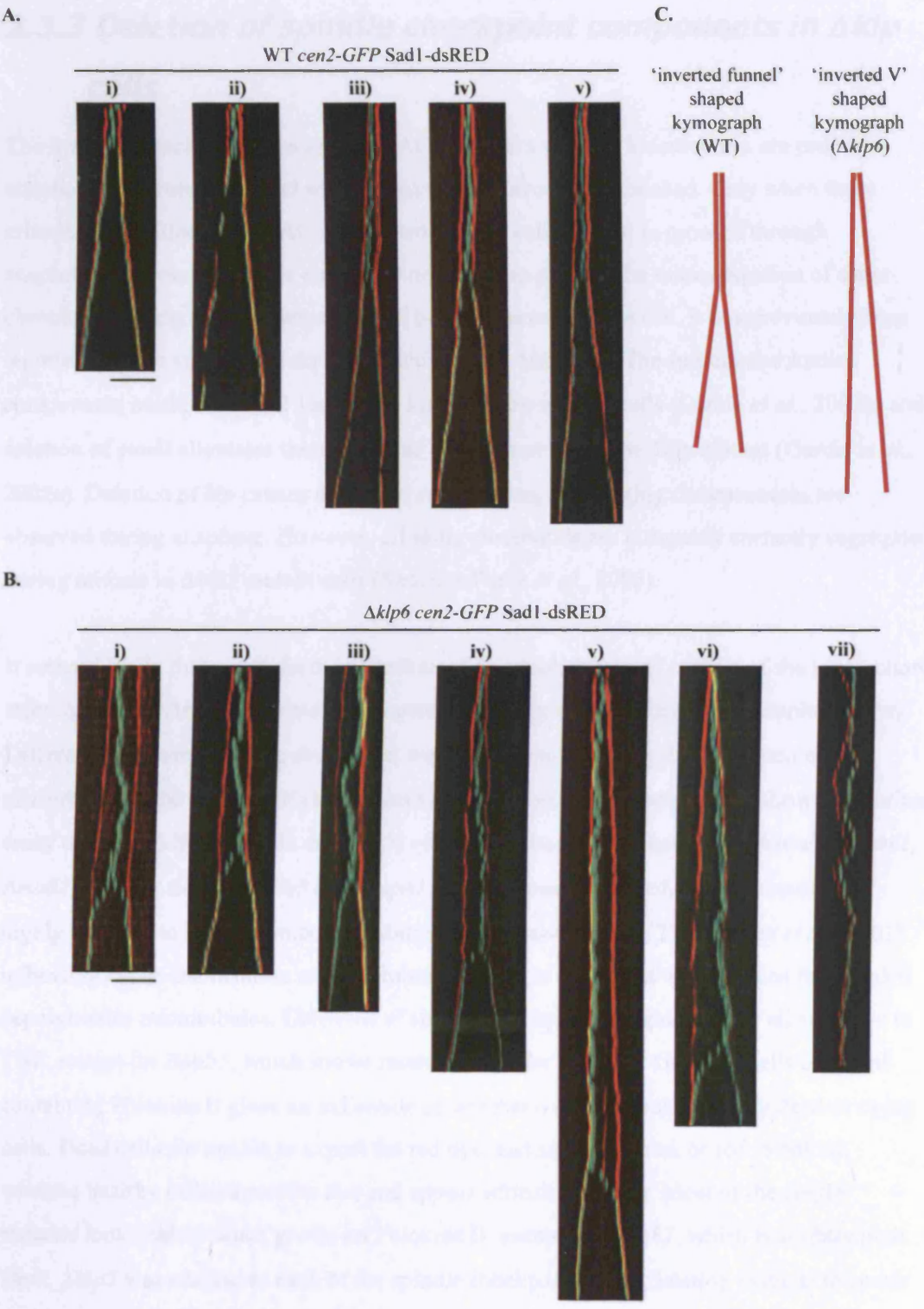

Figure 2.6 Kymographs of *cen2-GFP* movement in WT and Δ*klp6* cells

A, B. Kymographs of *cen2-GFP* movement in individual **A.** WT or **B.** *Δklp6* cells. Time-lapse images were taken every 30secs, deconvolved and projected, then kymographs were generated. Scale bar = 5μm. **C.** Traces of Sad1-dsRED signal (SPB) from WT (**A.** iv)) and *Δklp6* cells (**B.** vi)), showing characteristic 'inverted funnel' or 'inverted V' shapes.

2.3.3 Deletion of spindle checkpoint components in Δklp cells

The Spindle Attachment Checkpoint (SAC) monitors whether kinetochores are properly attached to microtubules, and whether tension is correctly established. Only when these criteria are fulfilled is the SAC inactivated and the cell allowed to proceed through anaphase. This mechanism is extremely important to prevent the missegregation of sister chromatids during mitosis, which would be very harmful to the cell. It has previously been reported that the spindle checkpoint is activated in Δ*klp* cells. The spindle checkpoint components Mad2 and Bub1 localise to kinetochores in Δ*klp* cells (Garcia *et al.*, 2002b) and deletion of *mad2* alleviates the metaphase arrest observed in the Δ*klp* mutant (Garcia *et al.*, 2002a). Deletion of *klp* causes defects in congression, and lagging chromosomes are observed during anaphase. However, all sister chromatids are ultimately correctly segregated during mitosis in Δ*klp5* mutant cells (Sanchez-Perez *et al.*, 2005).

It seemed likely that any defects in attachment or establishment of tension of the kinetochore microtubules in Δ*klp* cells were being corrected during the SAC-imposed metaphase delay. Different components of the checkpoint were deleted to see if the Δ*klp* phenotype were exacerbated in the absence of checkpoint function. Figure 2.7 (upper panel) shows a dilution assay of single Δ*klp5* mutants and single mutants of the spindle checkpoint, namely Δ*mad1*, Δ*mad2*, Δ*mad3*, Δ*bub1*, Δ*bub3* and Δ*mph1*. As previously reported, Δ*klp5* mutants are highly resistant to the microtubule inhibiting drug thiabendazole (TBZ) (West *et al.*, 2001) indicating hyper-stabilisation of microtubules, which is consistent with the idea that Klp5/6 depolymerise microtubules. Deletions of spindle checkpoint components are all sensitive to TBZ, except for Δ*bub3*, which shows resistance similar to Δ*klp5*. Growing cells on plates containing Phloxine B gives an indication of whether a colony contains many dead or dying cells. Dead cells are unable to export the red dye, and so appear pink or red in colour, whereas healthy cells export the dye and appear whitish in colour. Most of the single mutants look healthy when grown on Phloxine B, except for Δ*mph1*, which is slightly pink. Next, Δ*klp5* was crossed to each of the spindle checkpoint single deletion mutants to create double mutant strains. These are shown in the lower panel in Figure 2.7. There is a genetic interaction between Δ*klp5* and Δ*mad1*, and between Δ*klp5* and Δ*bub1*. These double mutants grow dark pink on Phloxine B plates and exhibit a slow growth phenotype. The TBZ resistance of the Δ*klp5*Δ*mad1* resembles wildtype; the strong TBZ resistance of the single Δ*klp5* mutant is lost. The Δ*klp5*Δ*bub1* double mutant is sensitive to TBZ, similar to the Δ*bub1* single mutant, and completely losing the TBZ resistance phenotype of the single Δ*klp5* mutant. The Δ*klp5*Δ*mph1* mutant is even more TBZ sensitive than the single Δ*mph1*

mutant, although the double mutant cells do not appear to be any more sick than the single Δ*mph1* mutant cells.

Mad2 localises to unattached kinetochores, whereas Bub1 localises to tensionless kinetochores (Zhou *et al.*, 2002a; Zhou *et al.*, 2002b) (Skoufias *et al.*, 2001) (Westermann *et al.*, 2005; Westermann *et al.*, 2006). As previously reported for the tubulin mutant *atb2-983* (Asakawa *et al.*, 2006) and *mal3* mutants (Asakawa *et al.*, 2005), Δ*klp5* mutants seem to genetically interact with only a subset of spindle checkpoint components. This suggests that Bub1, and perhaps Mad1 and Mph1 are required if the defects present in Δ*klp5* are to be corrected.

2.3.4 Chromosome missegregation is increased in Δklp5Δbub1 double mutants

It has already been published that the checkpoint proteins Mad2 and Bub1 localise to kinetochores in *Δklp* mutants, and that there is a Mad2-dependent metaphase delay. Presumably, some type of defect in kinetochore attachment is corrected during this SAC-imposed delay. To analyse whether defects do occur in the absence of Klp function, and whether prevention of the SAC delay allows these defects to persist, the missegregation frequency of *cen2*-GFP was calculated in WT, Δ*klp6*, Δ*klp6Δmad2*, Δ*klp6Δbub1*, *Δmad2* and *Δbub1* strains. As described above, centromeres move between poles in Δ*klp* strains, although they eventually segregate correctly. This means that even if two *cen2*-GFP foci are visualised at one SPB in fixed cells, missegregation has not necessarily occurred. It is possible that the cell was fixed at a time when both *cen2*-GFP foci were at one pole, although they subsequently segregated correctly. To avoid over-estimating the number of missegregation events, cells were synchronised by using HU to block in S-phase, then releasing them to progress through the cell-cycle. Cells were methanol fixed at various timepoints after release, and the *cen2*-GFP segregation pattern was scored in septated cells, as visualised by calcofluor staining. A 2:0 segregation pattern was counted as missegregation, and a 1:1 pattern was counted as correct segregation. Figure 2.8 shows that there is a huge increase in the missegregation of *cen2*-GFP in Δ*klp6Δbub1* mutant cells (30% missegregation) compared to both Δ*klp6* and *Δbub1* single mutants (4% and 7.7% missegregation, respectively). In contrast, deletion of *mad2* in Δ*klp6* cells does not increase the missegregation frequency of *cen2*-GFP when compared with the frequency seen in single Δ*mad2* cells. This analysis reveals that that the Bub1 component of the SAC is critical for proper chromosome segregation in cells lacking Klp5.

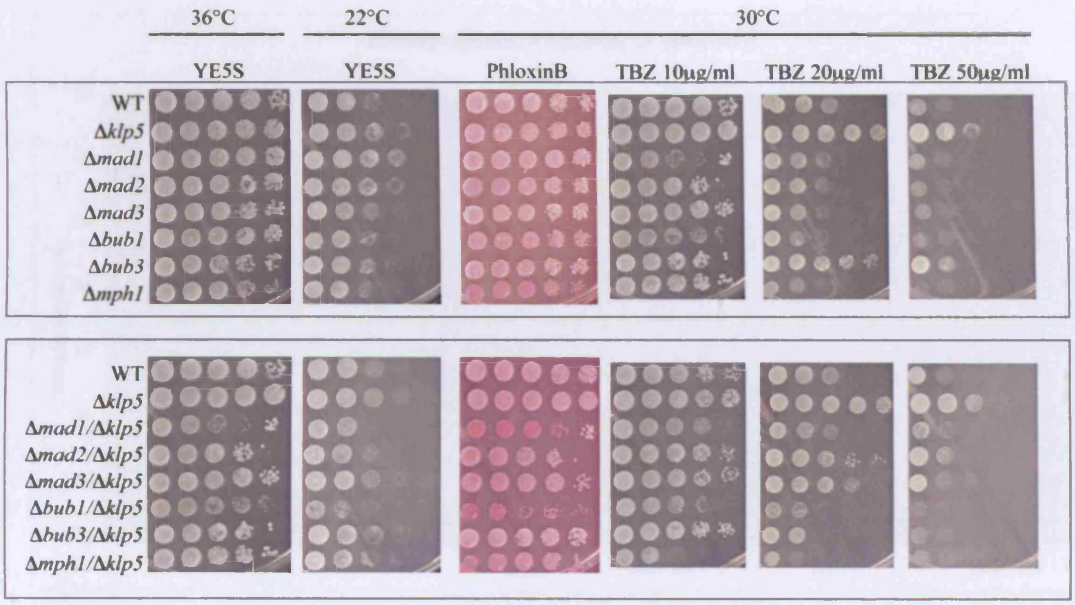

Figure 2.7 Dilution assay showing genetic interaction of Δ*klp5* with deletion of spindle checkpoint components

Ten-fold serial dilutions were spotted onto YE5S plates, with additions as shown. Plates were incubated for two days at the indicated temperatures.

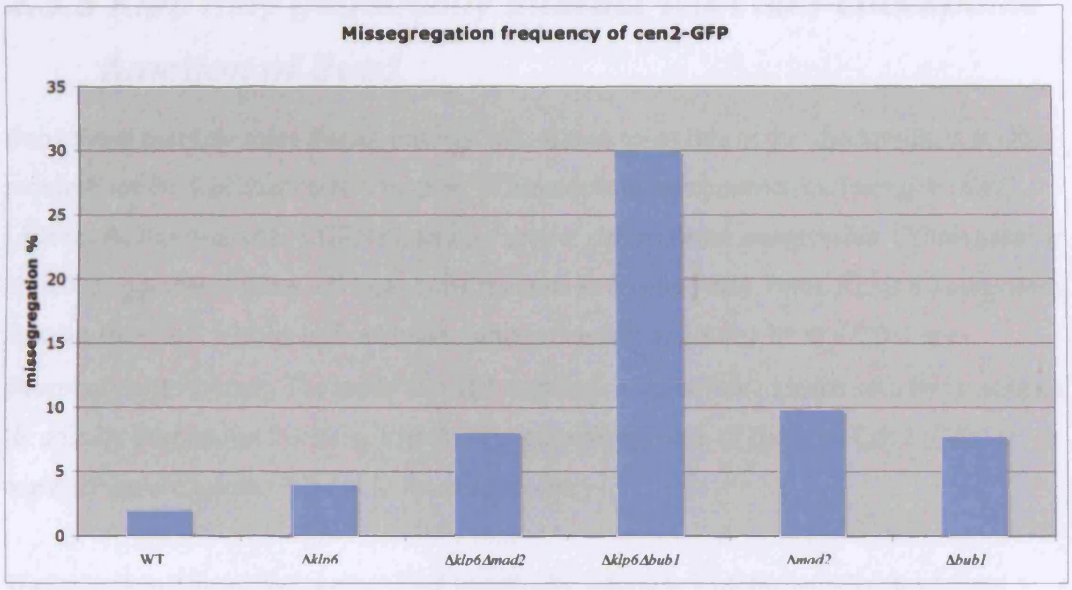

Figure 2.8 Missegregation frequency of cen2-GFP

The missegregation frequency was calculated for the strains shown by scoring the segregation pattern of Cen2-GFP in septated cells. Missegregation corresponds to a 2:0 segregation pattern of Cen2-GFP. *n=100*

2.3.5 Klp5 may genetically interact with non-checkpoint function of Bub1

Bub1 plays multiple roles during mitosis. In addition to its role in the checkpoint, it is also required for the localisation of a number of kinetochore components, including the CPC (Aurora B, survivin and INCENP), and for proper chromosome congression. (Yamaguchi *et al.*, 2003) generated three different *bub1* mutants in fission yeast: Bub1 KD is a kinase dead mutant; Bub1 ΔK has the entire kinase domain deleted; and Bub1 P* is a CDK non-phosphorylable mutant. The study showed that fission yeast Bub1 kinase activity is required for spindle checkpoint function, and that the phosphorylation of Bub1 by Cdc2 (Cdk) is required for activation of Bub1 in the checkpoint.

We wanted to determine whether *klp5* genetically interacts with the spindle checkpoint functions of *bub1*, or whether the interaction is due to non-checkpoint functions of *bub1*. To do this, a *Δklp5* strain was crossed to the three different *bub1* mutant alleles described above. Growth of these double mutant strains was compared with that of the single mutants, and with the synthetically sick *Δklp5 Δbub1* double mutant at different temperatures and concentrations of TBZ (see Figure 2.9 **B.**). A deletion of *klp5* in conjunction with any of the *bub1* mutants is not nearly as sick as the *Δklp5 Δbub1* double mutant; indeed deletion of *klp5* does not appear to exacerbate the phenotype of any of the *bub1* mutants. Rather surprisingly, the Bub1 P* mutant (which cannot be phosphorylated by Cdc2) appears to be temperature sensitive, even though *bub1* deletion mutants do not show any temperature sensitivity. One explanation is that the P* mutant is constitutively activated; however, (Yamaguchi *et al.*, 2003) reported that phosphorylation is required for activation, rather than inactivation, of Bub1 in the spindle checkpoint. The temperature sensitivity of the P* mutant is rescued by deletion of *klp5*. These results are rather puzzling. However, what is clear is that the genetic interaction observed between *klp5* and *bub1* is not due to loss of Bub1 kinase activity, nor is it related to the activity of Bub1 that requires Cdc2 phosphorylation for activation. As both Bub1 kinase activity and Cdc2 phosphorylation are required for function of the spindle checkpoint, it seems that *klp5* may genetically interact with a non-checkpoint function of *bub1*. This would also explain why the genetic interaction between *klp5* and *mad2* is so different from that of *klp5* and *bub1*.

A.

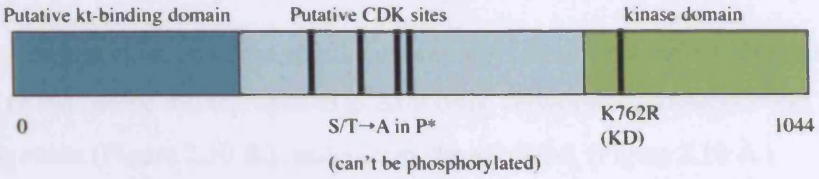

B.

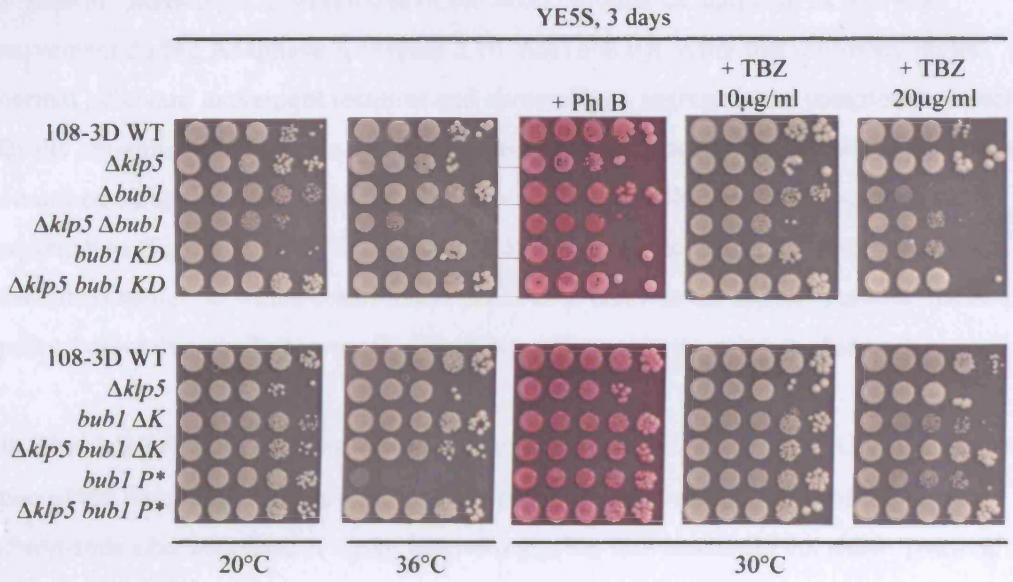

Figure 2.9 Klp5 genetic interaction with different Bub1 mutants

A. Cartoon showing domain structure of Bub1, including kinetochore binding domain, CDK phosphorylation sites, and the Bub1 kinase domain. (Yamaguchi *et al.*, 2003) created three different *bub1* mutants: 1) *bub1 KD* = Bub1 kinase-dead (K762R), 2) *bub1 ΔK* = deletion of kinase domain, 3) *bub1 P** = Bub1 phosphodead i.e. mutation of S/T>A in CDK sites. **B.** Dilution assay showing genetic interaction of *klp5* with the different *bub1* mutants. Growth temperatures and additions as shown.

2.3.6 Cen2-GFP analysis in checkpoint-deficient cells

Having established that deletion of the spindle checkpoint component Bub1 led to much higher rates of chromosome missegregation in *Δklp* cells, centromere movement was analysed in this strain (Figure 2.10 **B.**), and also in *Δmad2Δklp6*. (Figure 2.10 **A.**) Quantification of these analyses is shown in Figure 2.11. In *Δmad2Δklp6*, 11 of 11 cells eventually segregated the *cen2-GFP* signal correctly, in a 1:1 ratio. Of these, 2 of 11 showed a 'paused' phenotype, in which one of the sister chromatids pauses in its poleward movement during Anaphase A (Figure 2.10. **A.** i) and ii)). After this stationary period, normal poleward movement resumes and chromosome segregation is completed correctly. Of the remaining nine cells in which no pausing took place, 5 of 9 showed the phenotype described earlier, in which both centromeres associate exclusively with one pole until segregation (Figure 2.10. **A.** iii) and iv)). 4 of 9 showed the 'shuttling' phenotype also described earlier, in which centromeres are seen to traverse the spindle between the two poles, before eventually segregating from one pole; no congression is observed.

In *Δbub1Δklp6*, 7 of 10 cells eventually segregated *cen2-GFP* correctly. Out of these seven, two of the time-lapse movies showed slow polewards movement of one of the sister chromatids after anaphase A onset. Interestingly, the movement did not show 'pausing' as described above for the *Δmad2Δklp6* strain, but was continuous (Figure 2.10. **B.** i) and ii)). In one of these cells, shuttling between poles was observed prior to segregation, and in the other cell, both centromeres associated with just one pole before segregation. 1 of 10 cells showed monopolar missegregation of the *cen2-GFP* signal ie. both centromeres remained associated with one pole and never segregated. 2 of 10 cells showed the 'spindle collapse' phenotype described previously in the *Δklp6* single deletion strain. This suggests that the high rate of *cen2-GFP* missegregation seen in the *Δbub1Δklp6* strain is caused by both monopolar segregation events, and by failure to generate a stable mitotic spindle.

These observations confirm that Bub1 is more important than Mad2 for survival of *Δklp* mutants, and reveal the type of segregation defects caused by deletion of Klp6. Interestingly, Mad2 is also required in some cases for proper poleward movement of chromosomes in cells lacking Klp6, but it is not required for correct segregation. This explains why no genetic interaction between *Δklp* and *Δmad2* was seen in the dilution assay (Figure 2.7), as the synthetic phenotype of Klp and Mad2 does not affect cell viability.

2.3.7 Length of spindle at anaphase onset

It is clear from the kymographs of WT, *Δklp6*, *Δmad2Δklp6* and *Δbub1Δklp6* (shown in Figure 2.6 and Figure 2.10) that spindle length, as determined by distance between Sad1-dsRED foci, is increased in strains containing *Δklp6*. Careful observation also reveals that the dynamics of spindle elongation differ between WT and *Δklp* cells. In WT cells, the spindle forms upon SPB separation and grows to a length of ~2.5μm. This length is maintained as constant until the spindle elongates again during anaphase to reach a maximal length of ~15μm (Nabeshima *et al.*, 1998). This results in a characteristic kymograph shape, which I describe as being an 'inverted funnel' (eg. Figure 2.6 **A.** iv)). The distance between the SPBs (marked by Sad1-dsRED) is constant for some time prior to anaphase onset, forming the constricted section of the funnel. In contrast to this, *Δklp6* kymographs are characterised by their 'inverted V' shape. The inter-SPB distance does not remain constant at any point; instead it gradually and continually increases (eg. Figure 2.6 **B.** vi)). Traces of these two shapes are shown in Figure 2.6 **C.**

Next, the length of the spindle at anaphase onset was measured in the kymographs previously presented in Figure 2.6 and Figure 2.10. Anaphase onset was defined as the time point at which the two *cen2-GFP* signals first start segregating to opposite poles. Figure 2.12 and Table 2.1 show spindle length at anaphase onset. The average spindle length in WT cells was 2.52 ± 0.14μm, consistent with published data (Nabeshima *et al.*, 1998; Goshima *et al.*, 1999), and the standard deviation from this value was very small. In contrast, the average spindle length at anaphase onset in *Δklp6* cells was over twice as long, at 5.19 ± 1.08μm. The standard deviation from this value is also far greater, indicating that the length of the spindle in this strain is very variable. The 'inverted V' shape of the kymograph (described earlier) suggests that the spindle elongates at a constant rate throughout metaphase. It is known that *Δklp* mutants exhibit a Mad2-dependent metaphase delay (Garcia *et al.*, 2002a), but the extent of the delay is presumably variable depending on how long the error correction process takes. It could be that this accounts for the high variability seen in spindle length at anaphase onset in *Δklp6* cells; the longer the metapahase delay, the longer the spindle length at anaphase onset. If this metaphase delay is relieved by deleting *mad2*, then the average spindle length is reduced considerably (3.68 ± 0.47μm), as is the standard deviation, although both remain higher than for WT cells. If *bub1* is deleted in conjunction with *klp6*, then only a small reduction in spindle length (4.73 ± 0.33) is observed compared to the single *Δklp6* mutant.

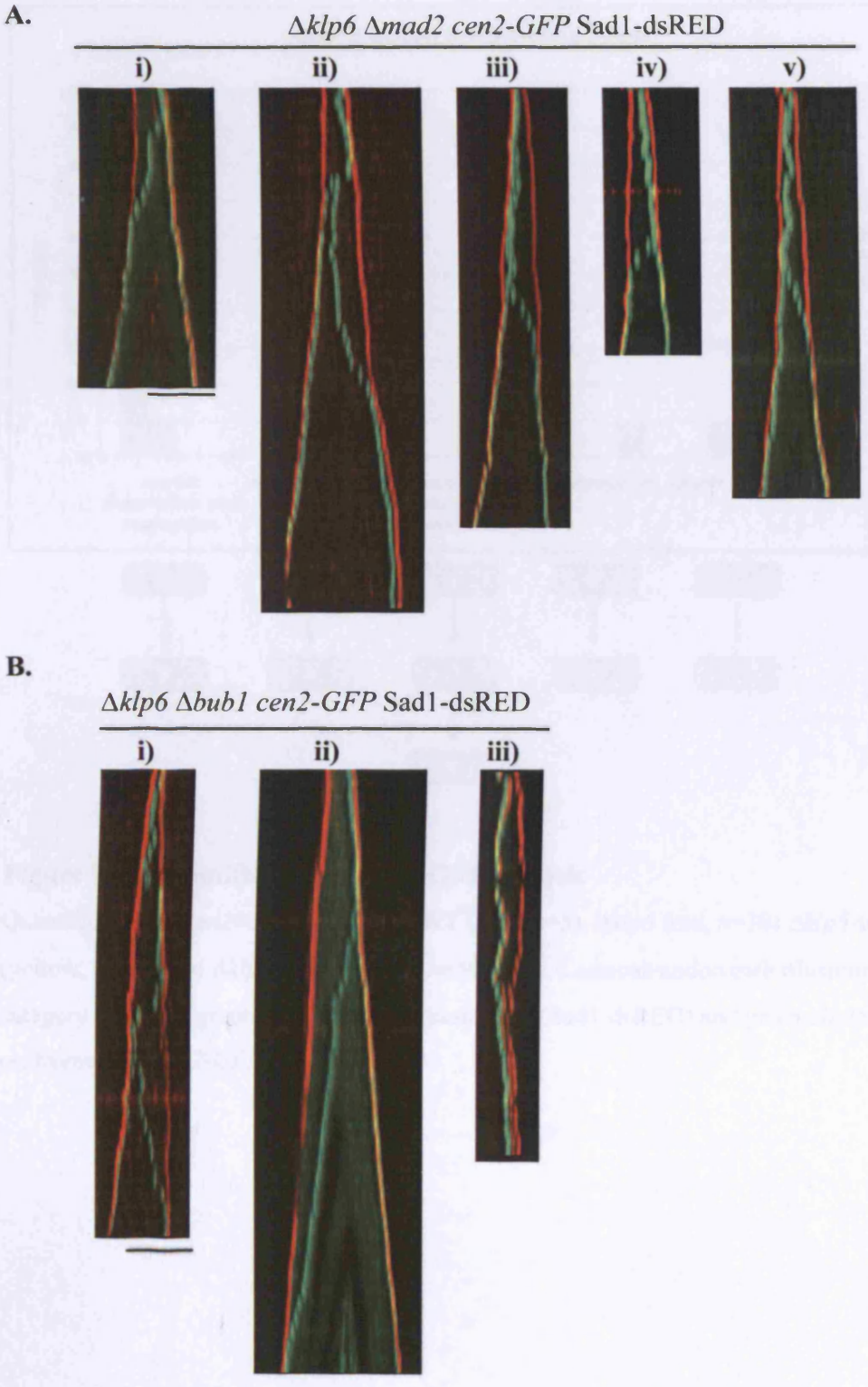

Figure 2.10 *cen2-GFP* analysis in checkpoint deficient *Δklp* cells.

A. i) – v) shows examples of *cen2-GFP* movement in *Δklp6Δmad2* cells. **B.** i) – iii) shows examples of *cen2-GFP* movement in *Δklp6Δbub1* cells. Scale bar = 5μm.

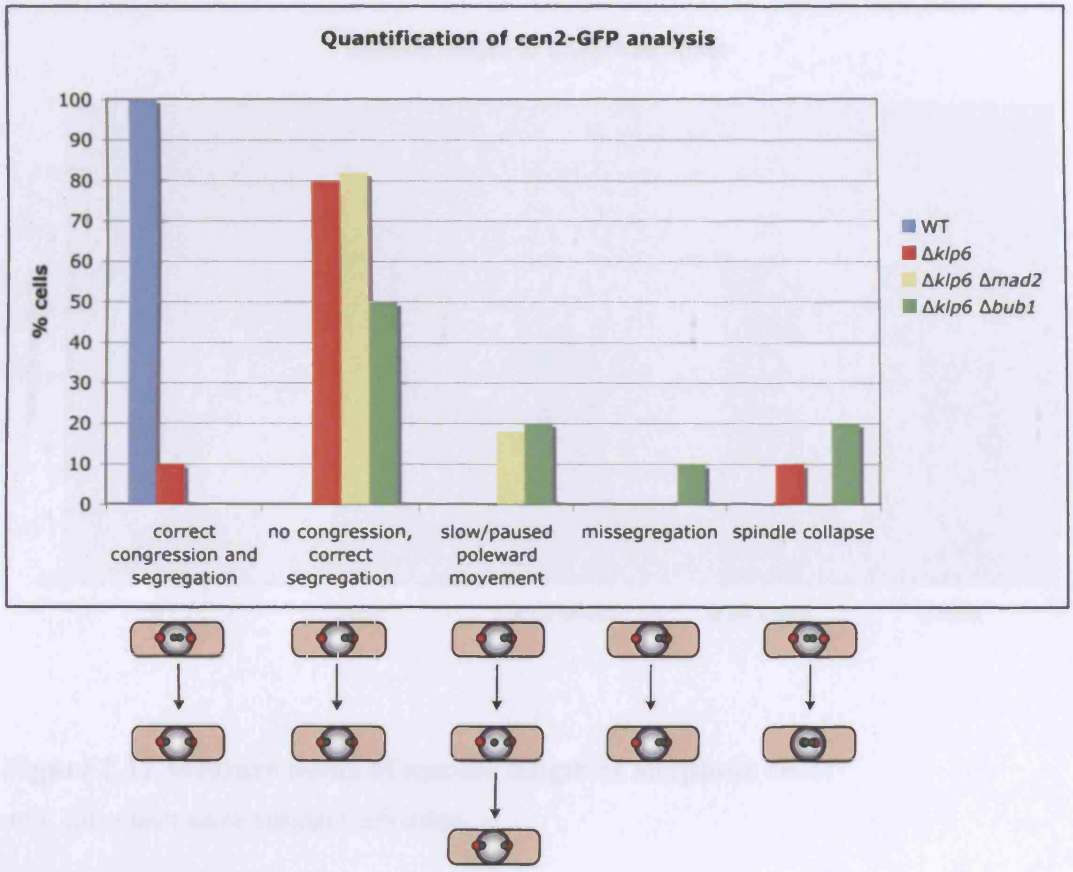

Figure 2.11 Quantification of cen2-GFP analysis

Quantification of *cen2-GFP* analysis in WT (blue, *n*=5), *Δklp6* (red, *n*=10) *Δklp6Δmad2* (yellow, *n*=11), and *Δklp6Δbub1* (green, *n*=10) cells. Cartoons underneath illustrate each category shown in graph; red circles represent SPB (Sad1-dsRED) and green circles centromere II (*cen2*-GFP).

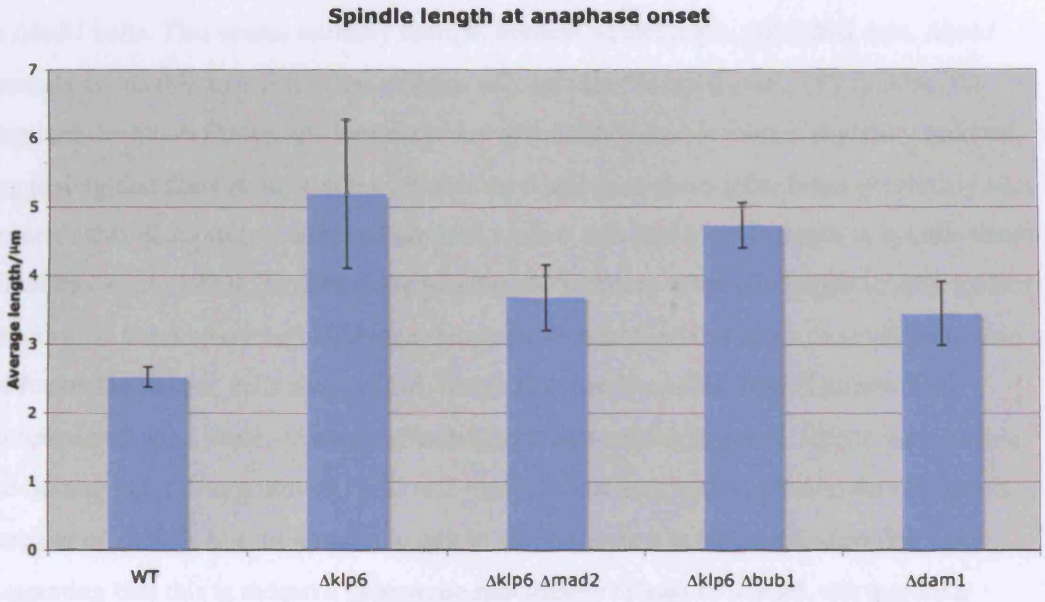

Figure 2.12 Measurements of spindle length at anaphase onset

n=5. Error bars show standard deviation.

	WT	*Δklp6*	*Δklp6Δmad2*	*Δklp6Δbub1*	*Δdam1*
Spindle length at anaphase onset (μm)	2.52 ± 0.14	5.19 ± 1.08	3.68 ± 0.47	4.73 ± 0.33	3.45 ± 0.46

Table 2.1 Measurements of spindle length at anaphase onset

One possible interpretation of this result is that a spindle checkpoint arrest can be maintained in *Δbub1* cells. This seems unlikely though, because according to published data, *Δbub1* mutants are unable to arrest in the absence of a spindle (Bernard *et al.*, 1998). Also, the standard deviation for spindle lengths in the *Δklp6Δbub1* double mutant is greatly reduced, suggesting that there is not a delay of variable duration in these cells. It has previously been reported that disruption of kinetochore components can lead to an increase in spindle length (Goshima *et al.*, 1999). To determine whether the increase in spindle length in *Δklp* mutants was similar to a mutant with disrupted kinetochore structure, this same quantification was performed in *Δdam1* cells as a control. Dam1 is a member of the DASH kinetochore complex in fission yeast. Average spindle length at anaphase onset is slightly increased in the *Δdam1* kinetochore mutant (3.45 ± 0.46μm), consistent with published data (Sanchez-Perez *et al.*, 2005), but the spindle length in *Δklp6* mutants is far greater than this value, suggesting that this is indeed a phenotype specifically related to Klp5/6, not merely a consequence of kinetochore disruption.

2.3.8 Deletion of klp5/6 rescues cut9-665 and nuc2-663 ts mutants

The observations described in the previous section raise the possibility that Klp5/6 are required for the maintenance of constant metaphase spindle length, which would be consistent with their proposed role as microtubule depolymerising kinesins. To further address this point, an attempt was made to compare metaphase spindle dynamics in WT and *Δklp5* cells using FRAP (Fluorescence Recovery After Photobleaching). FRAP has previously been used to detect the stabilisation of microtubule dynamics at the metaphase to anaphase transition (Mallavarapu *et al.*, 1999), so if there is stabilisation of the metaphase spindle in the absence of Klp5/6 depolymerising activity, this should be detectable using FRAP. Essentially we might expect to see anaphase-like microtubule dynamics during metaphase. Metaphase spindles in *Δklp* are longer and more variable in length than in WT (see previous section), so to ensure that *bona fide* metaphase spindles were being observed, it was necessary to try and arrest the cells in metaphase. WT and *Δklp5* strains containing GFP-Atb2 were crossed to the temperature sensitive (ts) mutant *cut9-665*, which arrests cells in metaphase at the non-permissive temperature (36°C) (Samejima and Yanagida, 1994). Cut9 and Nuc2 are both subunits of the APC complex (Yamada *et al.*, 1997), whose ubiquitin ligase activity is required for the destruction of Cut2 (securin) (Funabiki *et al.*, 1996), and the B-type cyclins, Cdc13 (Yamano *et al.*, 1996) and Cig2 (Yamano *et al.*, 2000) necessary for progression into anaphase. Surprisingly, it was found that *Δklp5* partially rescues the *cut9-665* mutant at 36°C. The double mutant *cut9-665Δklp5* grows much better

at 36°C than the single *cut9-665* mutant (Figure 2.13 **A.**) and chromosome segregation occurs at 36°C in the double mutant, unlike the single mutant (Figure 2.13 **B.**).

As the *cut9-665* allele is unable to impose a metaphase arrest in *Δklp5* mutants, *nuc2-663*, another APC/C ts mutant, was crossed to WT and *Δklp5* strains containing GFP-Atb2. Again, this ts allele was rescued at 36°C by *Δklp5* (data not shown). We were therefore unable to use either the *cut9-665* or the *nuc2-663* alleles to arrest *Δklp5* cells in metaphase. It is not currently clear why a *klp* deletion rescues APC ts mutants.

An attempt was made to carry out FRAP in non-arrested cells, but it proved difficult to obtain images of *Δklp5* mutant cells that were convincingly in metaphase, because of the elongated spindle phenotype.

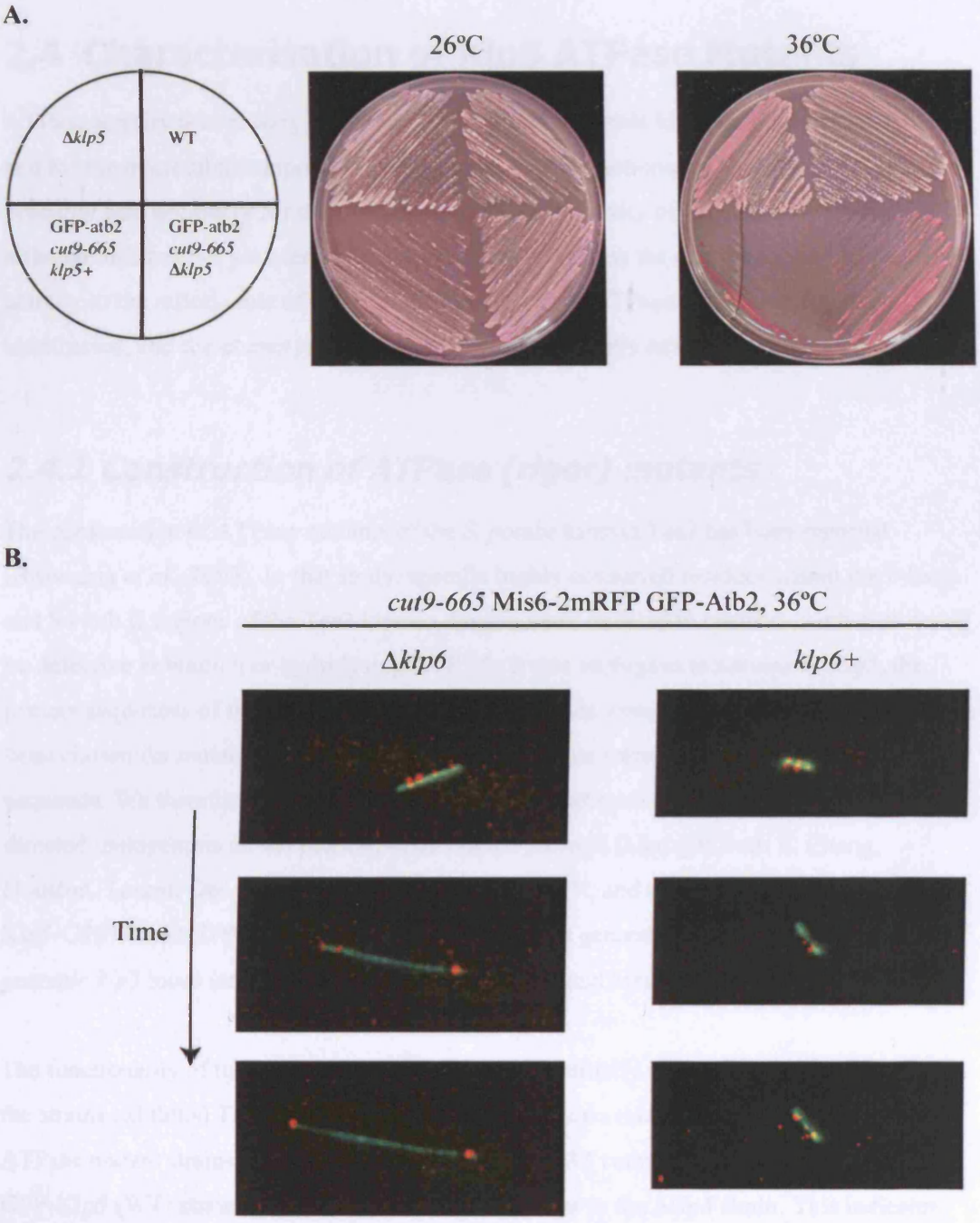

Figure 2.13 *Δklp6* rescues *cut9-665* ts mutants

A. Strains (as shown) streaked on phloxine B plates and incubated at either the permissive temperature for the *cut9-665* mutant (26˚C), or at the restrictive temperature (36˚C). **B.** Live cell imaging during mitosis of kinetochores (Mis6-2mRFP) and microtubules (GFP-Atb2) in *cut9-665* ts mutants at 36˚C, in either a *Δklp6* or a *klp6+* background.

2.4 Characterisation of Klp5 ATPase Mutants

ATPase activity is necessary for directed movement of motile kinesins along microtubules, and for the microtubule-depolymerisation activity of the non-motile Kinesin-13 MCAK. It is probably also necessary for the MT depolymerisation activity of Kinesin-8 members, although this has not yet been shown definitively. To assess the contribution of ATPase activity to the mitotic role of the Klp5/6 complex, Klp5 ATPase (rigor) mutants were constructed, and the phenotypes of the mutants subsequently analysed.

2.4.1 Construction of ATPase (rigor) mutants

The construction of ATPase mutants of the *S. pombe* kinesin Tea2 has been reported (Browning *et al.*, 2003). In that study, specific highly conserved residues within the P-loop and Switch II regions of the Tea2 kinesin domain were mutated to create mutants that would be defective in binding or hydrolysing ATP. To create analogous mutations in Klp5, the protein sequences of the Klp5 and Tea2 kinesin domains were aligned. The residues that had been chosen for mutation to make Tea2 ATPase mutants were conserved in the Klp5 kinesin sequence. We therefore decided to make identical mutations in Klp5, by performing site-directed mutagenesis on the pREP41-EGFP-Klp5 plasmid (kind gift from E. Chang, Houston, Texas). One P-loop mutant, GFP-Klp5-T151N, and two Switch II mutants, GFP-Klp5-G297A and GFP-Klp5-E299A were successfully generated and integrated into the genomic *klp5* locus (see Figure 2.14 **A.** and Materials and Methods).

The functionality of these Klp5 ATPase mutants was initially assessed by testing whether the strains exhibited TBZ resistance. Figure 2.14 **B.** shows that all three of the integrated ATPase mutant strains show increased resistance to TBZ compared to the control integrated GFP-Klp5 (WT) strain, but that they are not as resistant as the Δ*klp5* strain. This indicates that Klp5 function is compromised in the ATPase mutants, although not completely abolished. It is also evident that the integrated GFP-Klp5 (WT) strain is slightly more TBZ resistant than WT. This is probably because N-terminal tagging of the kinesin with GFP has a small effect on its function.

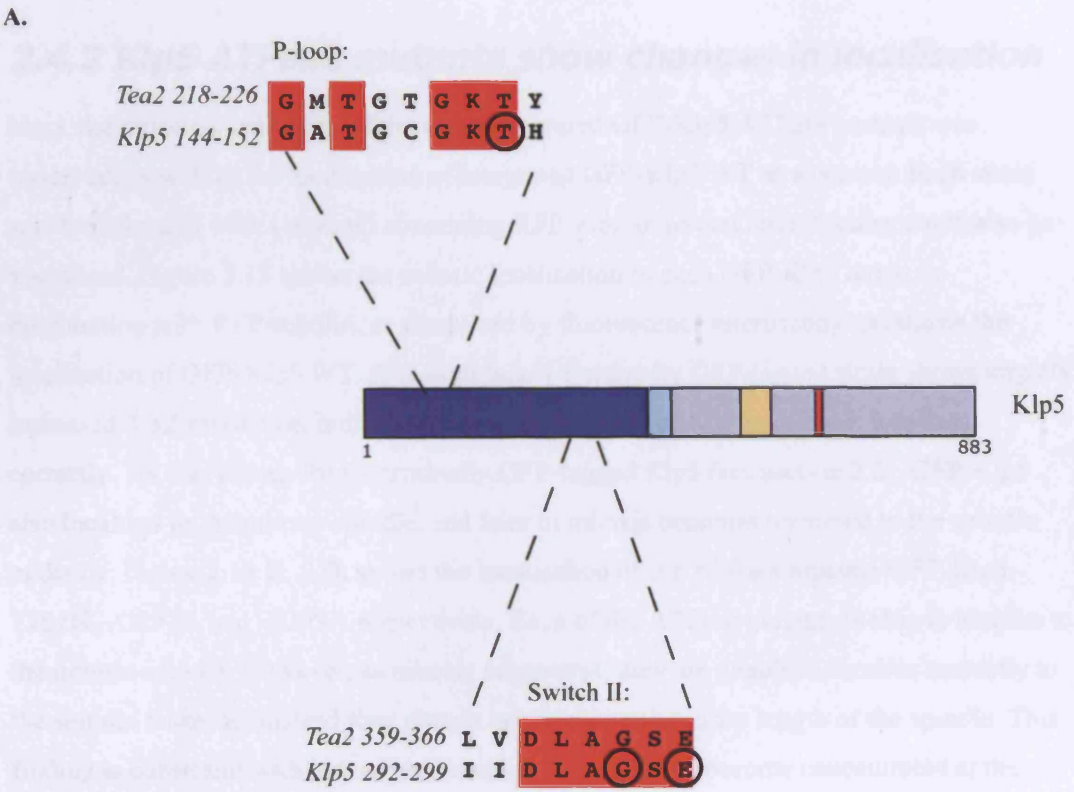

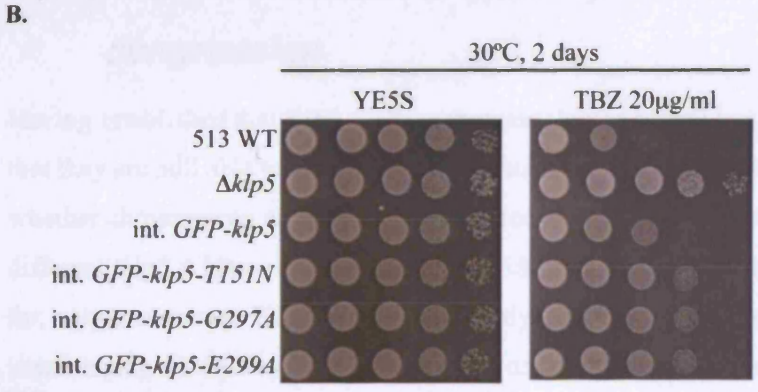

Figure 2.14 Klp5 ATPase Mutants

A. Cartoon showing positions of conserved P-loop and Switch II motifs of the kinesin nucleotide binding pocket within the kinesin domain. Amino acid sequences of Tea2 kinesin and Klp5 are aligned and conserved P-loop or Switch II residues are highlighted in red. Residues that were mutated in Klp5 in this study are circled in black. **B.** Dilution assay showing increased TBZ resistance of Klp5 ATPase mutants integrated at the genomic locus under the native promoter. Ten-fold serial dilutions were spotted onto YE5S plates, with additions as shown. Plates were incubated for two days at 30°C.

2.4.2 Klp5 ATPase mutants show changes in localisation

Next, the mitotic localisation of the three integrated GFP-Klp5 ATPase mutants was observed, as well as the localisation of integrated GFP-Klp5 WT as a control. Each strain was transformed with a plasmid containing RFP-tubulin so that microtubules could also be visualised. Figure 2.15 shows the mitotic localisation of each GFP-Klp5 strain in conjunction with RFP-tubulin, as visualised by fluorescence microscopy. **A.** shows the localisation of GFP-Klp5 WT. Although this N-terminally GFP-tagged strain shows slightly increased TBZ resistance, indicating some perturbation of Klp function, it localises correctly. As was shown for C-terminally GFP-tagged Klp5 (see section 2.2), GFP-Klp5 also localises to the mitotic spindle, and later in mitosis becomes restricted to the spindle midzone. Figure 2.15 **B. – D.** shows the localisation of the ATPase mutants GFP-Klp5-T151N, -G297A and -E299A respectively. Each of the ATPase mutants is able to localise to the mitotic spindle. However, as mitosis progresses, they are unable to localise correctly to the spindle midzone; instead they remain bound along the entire length of the spindle. This finding is consistent with loss of motor activity; for Klp5 to become concentrated at the spindle midzone (which consists of overlapping MT plus ends) it probably requires plus-end directed motor activity.

2.4.3 Klp5 ATPase activity is required for chromosome congression

Having established that Klp5 ATPase mutants show a partial loss of function phenotype, but that they are still able to localise to the nuclear mitotic spindle, we next checked to see whether chromosome movement was affected if Klp5 ATPase activity is disrupted. As the different Klp5 ATPase mutants had shown identical phenotypes in analyses performed thus far, only one mutant, Klp5-T151N, was analysed for chromosome movement. Klp5-T151N was integrated into the *klp5* genomic locus under the native promoter without the N-terminal GFP. Kinetochores were visualised by using Mis6-2mRFP, microtubules visualised with GFP-Atb2 and SPBs with Cut12-CFP. Figure 2.16 shows fluorescence microscopy still images taken from time-lapse movies of both WT and Klp5-T151N cells. It is clear that kinetochores in the Klp5-T151N cell are scattered and dispersed across a long spindle, just as in *Δklp5* cells (see Figure 2.4). This was observed in all cells visualised (>10). We therefore conclude that Klp5 ATPase activity is required for proper chromosome congression.

A.

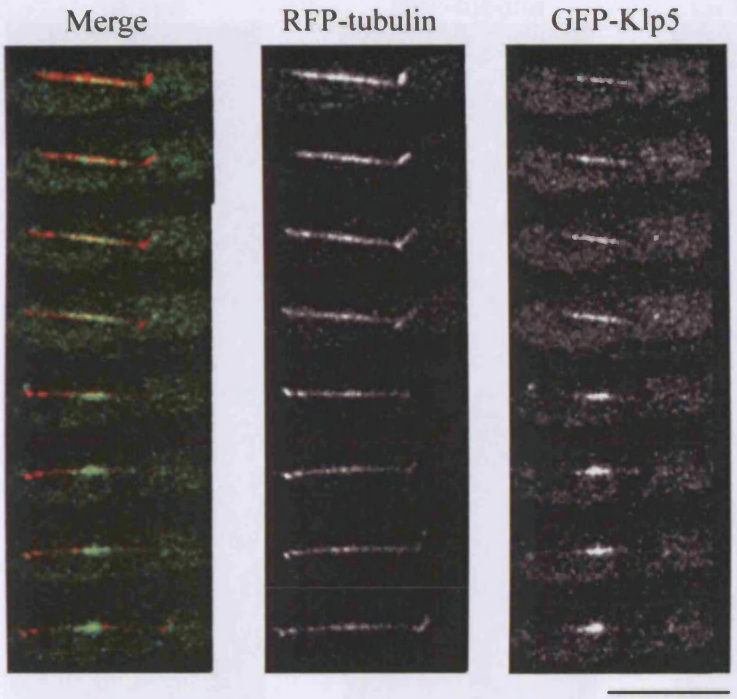

B.

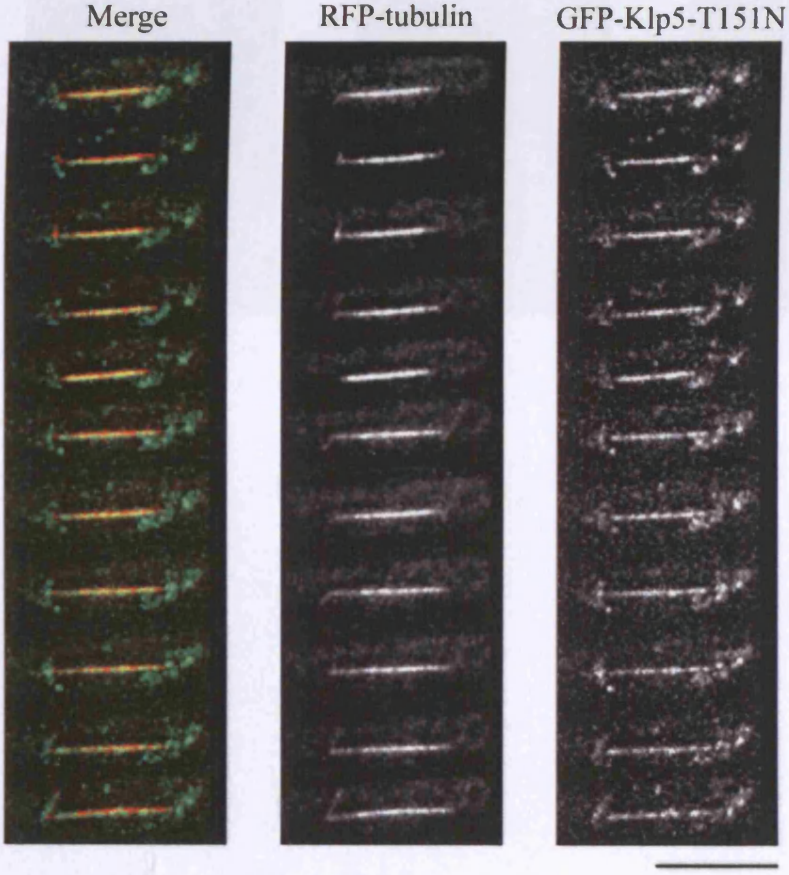

C.

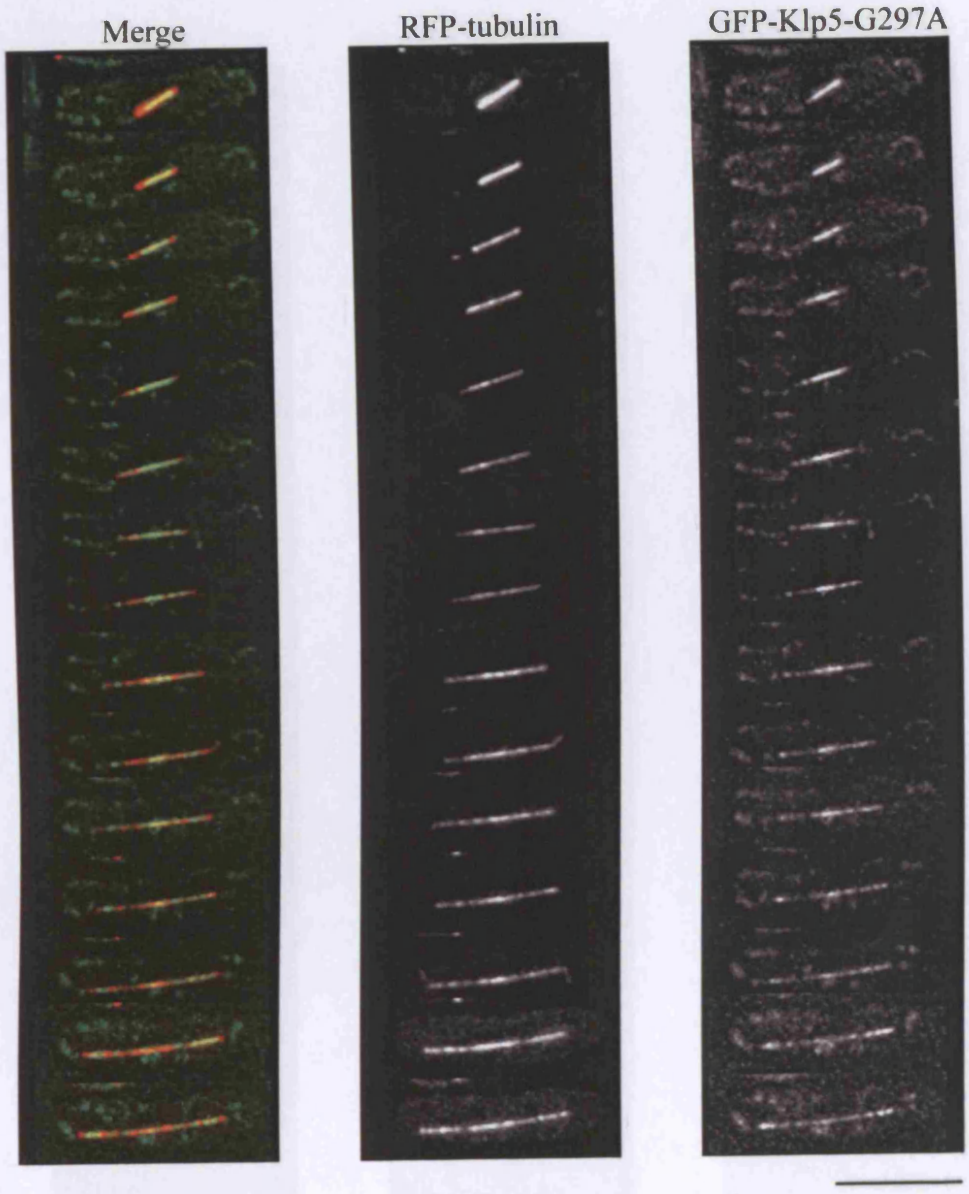

D.

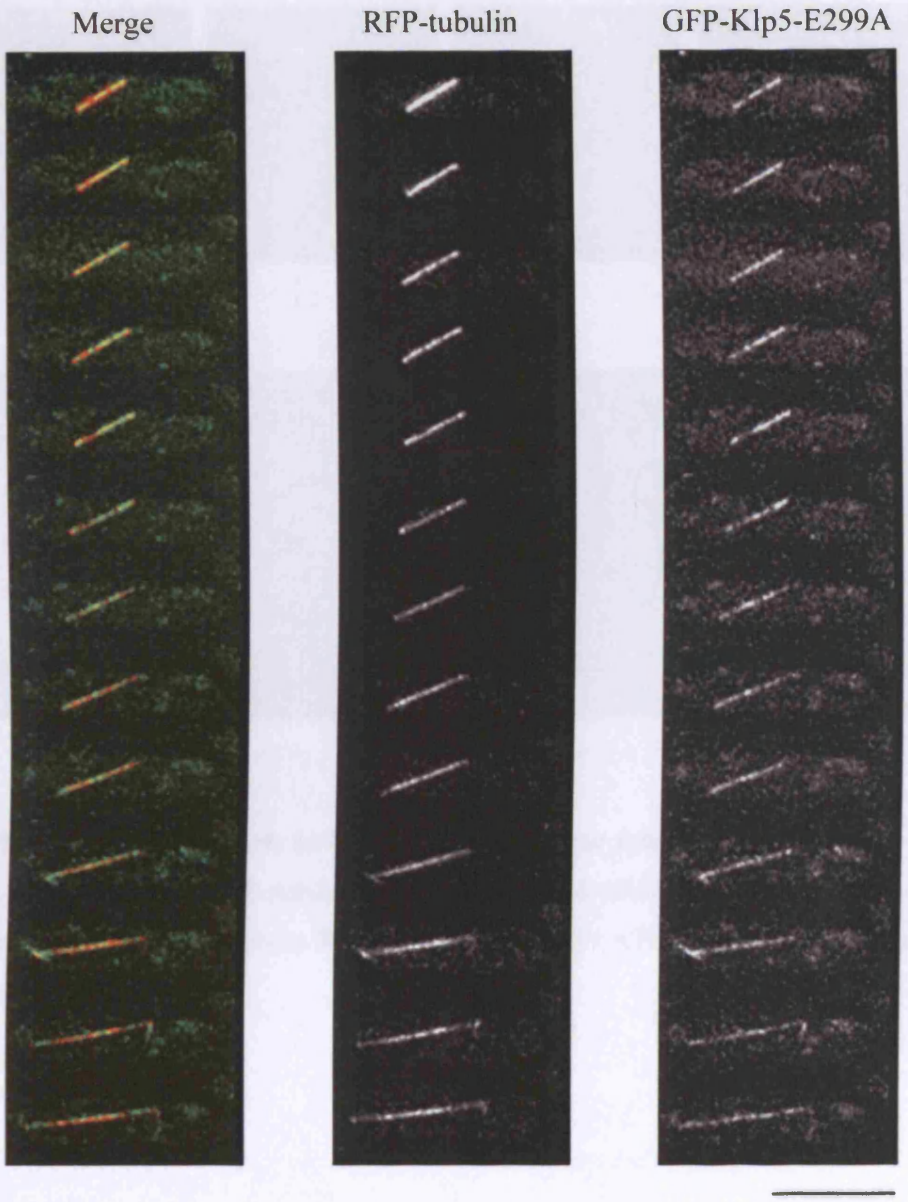

Figure 2.15 Localisation of Klp5 ATPase mutants

A. – D. All constructs were integrated into the *klp5* genomic locus under the native promoter. GFP-Klp5 and RFP-tubulin were visualised by fluorescence microscopy. Images taken every 30 secs. Scale bar = 10μm. **A.** Localisation of GFP-Klp5 (WT). **B.** Localisation of the ATPase mutant, GFP-Klp5-T151N. **C.** Localisation of the ATPase mutant, GFP-Klp5-G297A. **D.** Localisation of the ATPase mutant, GFP-Klp5-E299A.

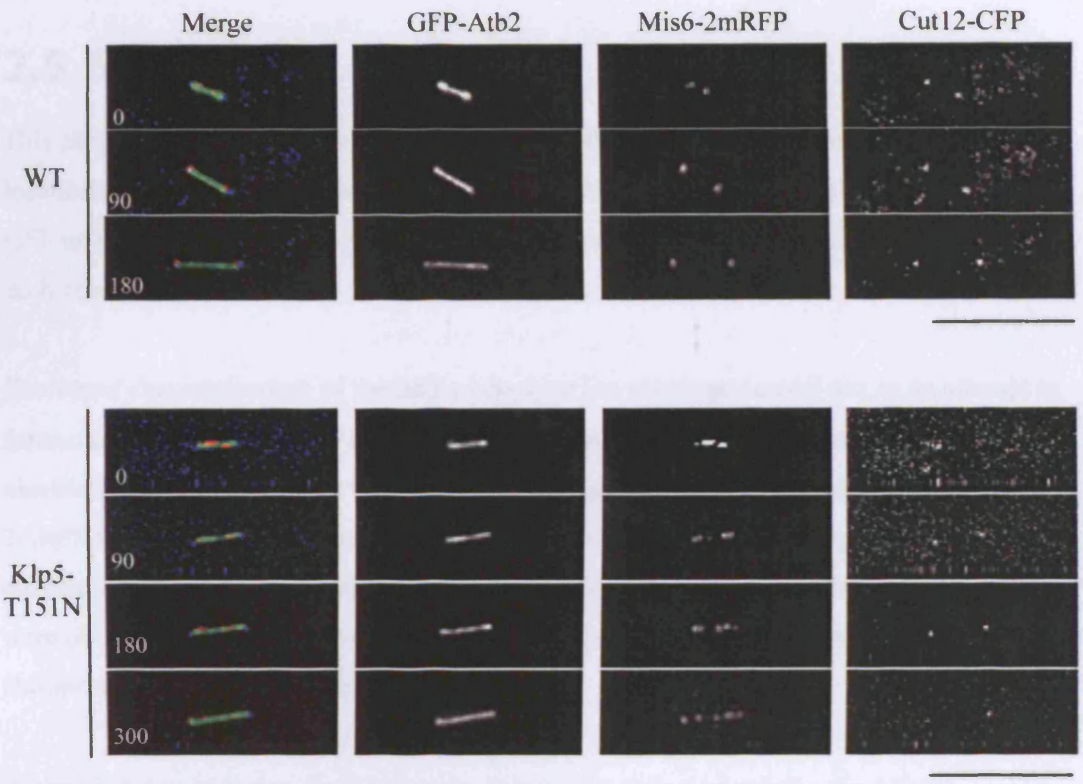

Figure 2.16 Congression defects in Klp5-T151N ATPase mutant

Localisation of microtubules (GFP-Atb2), kinetochores (Mis6-2mRFP) and SPBs (Cut12-CFP) were compared during mitosis in WT and the Klp5-T151N ATPase mutant. Scale bar = 10μm. Time shown in seconds.

2.5 Summary

This chapter has described the study of Klp5/6 localisation in live cells, examining the co-localisation of Klp5-GFP with the SPB marker Sad1-dsRED, the co-localisation of Klp5-GFP or Klp6-GFP with RFP-Atb2 (tubulin), and the co-localisation of Klp5 and Klp6 with each other.

Continued characterisation of the *Δklp* phenotype has also been carried out, in an attempt to further understand the role of Klp5/6 during mitosis. Live analysis of chromosome movement during mitosis has been performed using two systems; the first utilised Mis6-2mRFP to mark all six kinetochores; the second utilised the *cen2-GFP* system to visualise the centromeres of just one pair of sister chromatids. Abnormal chromosome movements were observed, both for congression and for segregation, although ultimately, correct chromosome segregation is achieved in *Δklp* cells.

A genetic interaction was found between *Δklp5* and a subset of spindle checkpoint components, namely *Δbub1, Δmad1* and *Δmph1*. The frequency of chromosome missegregation was compared in WT, *Δklp6, Δklp6Δmad2* and *Δklp6Δbub1* mutants, and was found to be greatly elevated in the *Δklp6Δbub1* double mutant. Analysis of single centromere movement was also carried out in these same strains, and some instances of delayed poleward movement of a single centromere were observed in *Δklp6* cells that were also lacking either the Mad2 or the Bub1 checkpoint proteins. It is possible that *klp5* genetically interacts with a non-checkpoint function of *bub1*, because there is no genetic interaction between *klp5* and specific *bub1* mutant alleles that are defective for spindle checkpoint function.

The dynamics of spindle elongation were also found to be affected in *Δklp* mutants. Constant spindle length is not maintained during metaphase; instead the spindle length continues to increase at a steady rate, so that chromosome segregation occurs on greatly elongated spindles.

An attempt to impose a metaphase arrest in *Δklp* cells by crossing to the APC/C ts mutants *cut9-665* or *nuc2-663* was unsuccessful. *Δklp* appears to partially rescue the ts phenotype of these mutants.

Mutation of the highly conserved P-loop and Switch II motifs of the Klp5 kinesin nucleotide binding pocket to create ATPase mutants resulted in compromised Klp function. Klp5

ATPase mutants showed increased resistance to TBZ. They localised to the nuclear mitotic spindle, but were unable to localise correctly to the spindle midzone in late mitosis. Chromosome congression was also perturbed in these mutants.

2.6 Discussion

Klp5 and Klp6 localise to cytoplasmic microtubules during interphase and to the spindle during mitosis. Klp5 and Klp6 also localise as several dots along the spindle prior to anaphase onset, although it can be difficult to distinguish these from background spindle staining. This is thought to correspond to kinetochore localisation, although it could also represent localisation to microtubule plus-ends. Kip3, the budding yeast homologue of Klp5/6, has been shown to have microtubule plus-end directed motor activity and to localise to growing microtubule plus-ends (Gupta *et al.*, 2006; Varga *et al.*, 2006). Published data indicates that Klp5-Myc binds to the outer repeats of the centromere (*otr)* in a microtubule-dependent manner in metaphase-arrested cells (Garcia *et al.*, 2002a), suggesting that Klp5 is actually loaded onto the kinetochores, most probably from the microtubule plus-end. Klp5 and Klp6 are not seen segregating to the SPBs with the kinetochores during anaphase A, but instead remain on the spindle, becoming restricted to the spindle midzone during anaphase B. This localisation is similar to that of the chromosomal passenger complex (CPC), which consists of Aurora B kinase, INCENP and Survivin (and also Borealin in human cells). The CPC plays roles during chromosome congression and cytokinesis (Adams *et al.*, 2001). Indeed, it has been shown that Klp5 is a target for Aurora B phosphorylation (J. Kamenz and S. Hauf, personal communication), but the biological significance of this has not yet been determined.

It is clear from the results presented in this chapter that proper chromosome congression does not occur in Δ*klp* mutants, but the underlying molecular explanation for this phenotype has not yet been fully elucidated. It is unlikely that kinetochores in *Δklp* mutants are not attached to spindle microtubules, as all of the kinetochores are aligned along the same axis as the spindle itself. Detached kinetochores would most likely be seen outside of this axis, for example, as visualised after centromere inactivation in an elegant budding yeast experimental system (Tanaka *et al.*, 2005). The predominant phenotype in *Δklp* mutants of centromere shuttling between poles suggests that there must be some kind of attachment to both poles. We would also expect to see higher rates of chromosome missegregation when the spindle checkpoint component *mad2* is deleted if there were an attachment defect in *Δklp* mutants.

It is possible that kinetochores are attached in *Δklp* mutants, but that this attachment is incorrect. An increase in the frequency of lagging chromosomes in *Δklp* mutants has been reported previously (Garcia *et al.*, 2002a; Sanchez-Perez *et al.*, 2005). The vast majority of lagging chromosomes in fission yeast are single chromatids and are indicative of merotelic attachment (Pidoux *et al.*, 2000; Gregan *et al.*, 2007). The analysis of kinetochore behaviour using the *cen2-GFP* system in this chapter indicates that a single chromatid is frequently visualised in the middle of the spindle, while its sister has already segregated to one of the poles. In the single *Δklp6* mutant, the movement of a single chromatid across the spindle towards its destination SPB is rapid, and it is difficult to imagine that this corresponds to merotelic attachment; however it is possible that it corresponds to a newly corrected kinetochore that was merotelically attached. When one sister kinetochore is merotelically attached and the other attached correctly, as a cohesed pair they contain more attachments to one pole than the other, and this could result in them both moving closer to that pole, as is seen in *Δklp6* cells. Once the incorrect attachments have been detached and proper bipolar attachment is achieved, the checkpoint delay would be alleviated, and cohesin cleaved, allowing the sister chromatid located at the wrong pole to rapidly segregate to the correct pole. This model could explain why sister chromatids are always seen to segregate from within the vicinity of one pole in *klp* mutants.

In contrast, some slow-moving or paused single kinetochores are observed in *Δklp6Δbub1* or *Δklp6Δmad2* strains respectively, and these may well represent uncorrected merotelic attachments. The fact that they are only visualised when the spindle checkpoint is compromised would suggest that in WT cells this type of defect can be detected by the checkpoint, and that alternative mechanisms exist within the cell for their correction during the checkpoint-imposed delay. However, it has been reported that in human cells the spindle checkpoint is unable to detect lagging (probably merotelic) chromosomes (Cimini *et al.*, 2003) because Mad2 does not localise to anaphase lagging chromosomes. The reasoning is that the spindle checkpoint must have been satisfied for depletion of kinetochore Mad2 to occur. Fission yeast only have 2-4 MTs attached per kinetochore, so one merotelic attachment will result in a far greater imbalance of force across sister kinetochores than in metazoan cells. Merotelic attachment might therefore be detectable as a tension defect by the spindle checkpoint in fission yeast, although it is not detectable in metazoan cells.

(Cimini *et al.*, 2003) observe that a large number of kinetochores are merotelically attached in prometaphase, but that most of these are corrected prior to anaphase onset. Those that do persist into anaphase also usually segregate correctly because the attachments to the correct pole outnumber the attachments to the incorrect pole (Cimini *et al.*, 2004). The depolymerising Kinesin-13, MCAK, contributes to the turnover of incorrect attachments,

regulated by Aurora B kinase, in metazoan cells (Andrews *et al.*, 2004; Knowlton *et al.*, 2006; Huang *et al.*, 2007). It is reasonable to postulate that the microtubule depolymerising activity of Klp5/6 could contribute to the removal of incorrect attachments, and that in its absence, these incorrect attachments persist. An additional, slower-acting mechanism may function during a SAC-imposed metaphase delay, and it is only when the SAC delay is prevented, that the incorrect attachments can be visualised. It has been proposed that the Dam1/DASH complex functions in conjunction with Klp5/Klp6 to promote correct chromosome biorientation; *Δdam1 Δklp* is synthetic lethal (Sanchez-Perez *et al.*, 2005), and ts mutants of *dam1* (*dam1-A8*) in a *Δklp* background show severe chromosome segregation defects and require the checkpoint for survival (K. Griffiths, PhD thesis). Perhaps Dam1/DASH also functions to detach erroneous MT-kinetochore attachments, and the absence of both the Klp5/6 and the Dam1/DASH pathway is lethal for the cell as it is unable to correct errors.

An alternative explanation for the abnormal kinetochore movements and lack of congression seen in *Δklp* mutants, is that kinetochores are correctly attached, but that tension is not correctly established. In line with this explanation, it was found that depletion of human Kinesin-8 (Kif18a) induces loss of tension across sister kinetochores. Kif18a is proposed to drive metaphase chromosome congression by regulating the dynamics of kinetochore MTs (Mayr *et al.*, 2007). However, an *increased* interkinetochore distance has been reported for *Δklp5/6* mutants (West *et al.*, 2002), consistent with our own qualitative observations, which is not indicative of tensionless kinetochores.

Chromosome poleward movement is thought to be driven by the force of microtubule depolymerisation in fission yeast (Grishchuk and McIntosh, 2006). Microtubule depolymerisation occurs at the plus and minus ends in mammalian cells, but only at the plus end in yeast (Mallavarapu *et al.*, 1999). The depolymerising activity responsible for the poleward movement of kinetochores in anaphase A in yeast must therefore be located at the kinetochore. Klp5/6 have depolymerising activity and are located at the kinetochore, but results in this chapter show they are unlikely to contribute to poleward chromosome movement, because chromatids are seen travelling rapidly towards their destination SPB after segregation in *Δklp* mutants.

Although Mad2 localises to *Δklp* kinetochores, and deletion of *mad2* causes abnormal kinetochore movement (pausing) in some *Δklp* cells, it does not result in chromosome missegregation, and so no genetic interaction is observable in terms of a growth defect. The genetic interaction of *Δklp5* with *Δbub1,* but not with some other SAC components, including *Δmad2,* could be accounted for by two possibilities. There is evidence suggesting

that there are two branches of the spindle checkpoint, one that senses attachment, and the other tension (Skoufias *et al.*, 2001). Perhaps *Δklp5* mutants only require a subset of SAC components for their viability, or one branch of the spindle checkpoint. However, there is increasing evidence from human cells showing that Bub1 plays important roles independent of its role in the checkpoint, including targeting Shugoshin (Kitajima *et al.*, 2005) and the CPC (Boyarchuk *et al.*, 2007) to the kinetochore. The other possible explanation is that *klp5* genetically interacts with non-checkpoint functions of *bub1*, a notion that is supported by the fact that *Δklp5* is not synthetically sick with specific mutant alleles of *bub1* affecting its checkpoint function. Klp5/6 and Bub1 may function in parallel pathways for the error correction of merotelic attachments. Increased frequencies of lagging chromosomes are seen in *Δbub1* single mutants (Bernard *et al.*, 1998), even if an anaphase delay is artificially imposed on the cell to give it time to correct erroneous attachments. In human cells, Bub1 and Aurora B are required for localisation of hSgo2, which is required for the localisation of the Kinesin-13 depolymerase, MCAK (Huang *et al.*, 2007), which depolymerises incorrect MT-kinetochore attachments. Perhaps in fission yeast Bub1 also recruits components required for error correction to the kinetochores. The genetic interaction between *bub1* and *klp5/6* indicates that they probably function in different pathways that are partially redundant, which would suggest that Bub1 is not involved in the localisation of Klp5/6.

Because fission yeast kinetochores attach to only 2-4 microtubules in total, formation of just two incorrect attachments per kinetochore, if left uncorrected, could presumably result in chromosome missegregation. In metazoan cells, it is extremely unlikely that merotelic attachments would ever result in chromosome missegregation, because this would require a huge number of erroneous attachments to be made. We propose that Klp5/6 and Bub1 function, in distinct pathways, to prevent merotelic kinetochore-microtubule attachments. When both are deleted, many more merotelic attachments exist within the cell. If the ratio of correct:incorrect kinetochore-MT attachments is low (i.e. the kinetochore has more attachments to the 'wrong' pole) then the kinetochore will segregate to the wrong pole (see Figure 2.17 for further explanation of this model).

Our results suggest that Klp5/6 are required for maintenance of proper metaphase spindle length. Microtubules comprising the metaphase spindle are highly dynamic, although the overall length is maintained as constant. This requires a precise balance of microtubule polymerising and depolymerising activities, and we propose that Klp5/6 contribute to the deploymerisation activity required for maintenance of constant metaphase spindle length. In the absence of Klp5/6, spindles are observed to increase in length at a constant rate during metaphase, presumably because the polymerisation activity is unopposed. It has previously been shown that *mis6* and *mis12* kinetochore mutants exhibit increased metaphase spindle

lengths (Goshima *et al.*, 1999), although they do not possess MT depolymerising activity. It is possible then, that the increase in spindle length observed in *Δklp* mutants is simply due to disruption of the kinetochore. However, *mis6* and *mis12* mutants only show a 35-60% increase in metaphase spindle length, whereas *klp* mutants show >100% increase, demonstrating that deletion of Klp5/6 has a more pronounced effect than that caused simply by kinetochore disruption. Additionally, it seems that Klp5 ATPase mutants also have elongated metaphase spindles, although these mutants probably do not disrupt kinetochore structure. Another possibility is that an intact kinetochore structure is required for proper Klp5/6 localisation, and that the reason that kinetochore mutants exhibit long metaphase spindles is because Klp5/6 fail to localise. We attempted to address whether Klp5/6 localised to the kinetochore in ts *mis6* and *mis12* mutants at the restrictive temperature; however, it was not possible to distinguish between Klp5-GFP spindle staining and *bona fide* kinetochore localisation by fluorescence microscopy. Consistent with our results, an analysis of a number of components regulating MT dynamics and MT sliding in *Drosophila* S2 cells showed that metaphase spindle length was particularly sensitive to knock-down or overexpression of Kinesin-8. (Goshima *et al.*, 2005)

A kinesin-8 member found in *Drosphila*, Klp67A, shows a similar localisation pattern to Klp5/6. It is required for destabilisation of MTs prior to anaphase onset, but is subsequently required for stabilisation of the central spindle during anaphase. Perhaps Klp5/6 function in a similar manner at the spindle midzone, and Klp5/6 depolymerisation activity is switched off at anaphase onset to allow spindle elongation. It is difficult to postulate a function for Klp5/6-mediated MT depolymerisation during anaphase B, because the spindle elongates via polymerisation and MT sliding at the spindle midzone, which is the site of Klp5/6 localisation. As mentioned earlier, Klp5 is phosphorylated by Aurora B, and one of the proven phosphorylation sites is located in the Klp5 motor domain. Phosphorylation in this region is a possible mechanism by which motor / depolymerisation activity of Klp5 could be regulated.

If Klp5/6 do indeed function to correct merotelic attachments, as well as to regulate global MT dynamics, then their function appears to be more analogous to the Kinesin-13 MCAK than the Kinesin-8 Kif18a in human cells. Yeast genomes do not contain Kinesin-13 members, yet fission yeast kinetochores can become merotelically attached, and these incorrect attachments need to be turned over. In higher eukaryotes the MT depolymerising activity of MCAK contributes to this process, so it seems likely that in fission yeast, in the absence of Kinesin-13 activity, the Kinesin-8 proteins Klp5 and Klp6 fulfil this role.

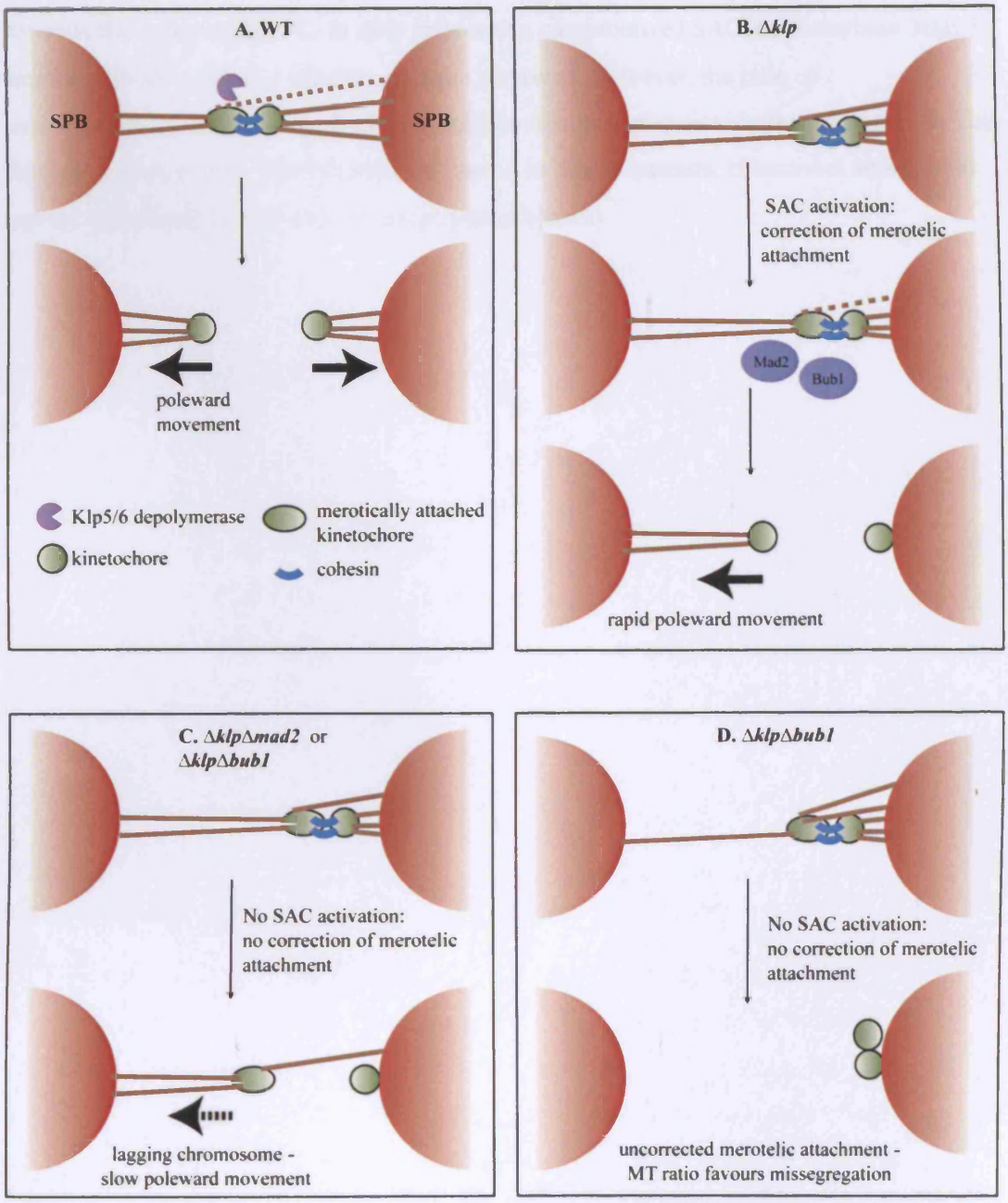

Figure 2.17 Model showing role of Klp5/6 in correction of merotelic attachments, leading to proper congression

Schematic showing just one chromosome pair.

A. In WT cells, the MT depolymerisation activity of Klp5/6 functions during prometaphase to ensure that erroneous attachments are corrected. An equal balance of forces across the kinetochore promotes congression, and segregation after cohesin cleavage. **B.** In *Δklp* cells, depolymerisation of incorrectly attached kinetochores cannot occur during prometaphase. This results in unequal forces across the kinetochore, causing the chromosome pair to localise close to one SPB. The spindle checkpoint is activated and correction of the merotelic attachment achieved by a slower-acting alternative mechanism active during the metaphase arrest. Once corrected, cohesin is cleaved and the chromatid moves rapidly

towards the opposite pole. **C.** In *Δklp* cells with a compromised SAC, no metaphase delay is imposed, so the merotelic attachment is not corrected. However, the ratio of correct:incorrect attachments (here 2:1) ensures correct segregation during anaphase. **D.** The frequency of merotelic attachments is increased in *Δbub1* mutants. If incorrect attachments outnumber correct attachments, missegregation occurs.

3 Results (2)

The Function of Klp5/6 Heterodimerisation

3.1 Introduction

Klp5 and Klp6 are unusual members of the Kinesin-8 family, because they are the only members reported thus far that associate as a heterodimer, rather than a homodimer. This gives us a unique opportunity to explore the significance of Kinesin-8 dimerisation, as it is possible to examine the behaviour of one 'half' of the dimer in the absence of its partner. It is also interesting to distinguish whether Klp5 and Klp6 have different properties, and if so, what the significance of these are for the function of the Klp5/6 complex.

3.2 Spatio-Temporal Localisation of Klp5/6

3.2.1 Klp5/6 localisation interdependency

In the previous chapter it was shown that Klp5-GFP or Klp6-GFP localise to the spindle during mitosis in wildtype cells. Next, as an initial step in addressing the role of Klp5/6 association, the localisation of Klp5-GFP was examined in a *Δklp6* background, and vice-versa i.e. the localisation of Klp6-GFP in a *Δklp5* background. Simultaneous visualisation of microtubules was achieved by transforming strains with a plasmid containing RFP-*atb2*+ under the thiamine repressible *nmt1* promoter. Cells were observed under partial repression of the *nmt1* promoter, as previously described (Yamashita *et al.*, 2005).

Figure 3.1 **A.** compares the localisation of Klp5-GFP in wildtype cells (upper panel, cells i) – iv), shown in previous chapter) with the localisation in *Δklp6* cells. It is clear that Klp5-GFP still localises to cytoplasmic microtubules during interphase when *klp6* is deleted (Figure 3.1 **A.** viii)); but intriguingly, localisation of Klp5-GFP to the nuclear spindle during mitosis is abolished (cells v) – vii)). This is particularly visible in cell vii), where Klp5-GFP is seen localising to cytoplasmic astral microtubules, but not to the nuclear spindle. It is also noticeable that the nucleus is dark in appearance in the *Δklp6* strain, suggesting that Klp5-GFP may well be excluded from the nucleus.

The reciprocal experiment was also carried out, to determine whether Klp6-GFP is dependent on Klp5 for its localisation. Figure 3.1 **B.** shows that Klp6-GFP can also localise to cytoplasmic microtubules during interphase in the absence of Klp5 (cells vii) and viii)). However, no localisation of Klp6-GFP to the nuclear mitotic spindle was observed in the *Δklp5* strain (cells v) and vi)). Klp5 and Klp6 are therefore interdependent for localisation to the nuclear spindle during mitosis.

3.2.2 Klp5- and Klp6-GFP are targets of Crm1, and can enter the nucleus independently of each other

The interdependency of Klp5 and Klp6 for localisation to the nucleus during mitosis could be for one of the following reasons: 1) for promotion of nuclear import or 2) for inhibition of premature nuclear export. To distinguish between these two possibilities, nuclear export was inhibited in each strain observed in the previous experiment. This was achieved by using Leptomycin B (LMB), which specifically inhibits NES (Nuclear Export Signal)-dependent nuclear export by binding exportin-1 (Crm1 in fission yeast) (Fornerod *et al.*, 1997; Fukuda *et al.*, 1997). If a Klp-GFP protein is able to enter the nucleus, then nuclear accumulation of the GFP signal should be observed upon incubation with LMB; however, if a Klp-GFP protein cannot enter the nucleus, then incubation with LMB will not cause nuclear GFP accumulation. Figure 3.2 **A.** shows Klp5-GFP localisation 90 minutes after LMB addition in both WT and *Δklp6* cells. Microtubules are visualised with RFP-Atb2, as described in previous sections. In WT mitotic cells, there is clear localisation to the nuclear spindle, although not to the nucleoplasm (Figure 3.2 **A.** i) and ii)). WT interphase cells show some nuclear accumulation, but this is not very strong (Figure 3.2 **A.** iii) and iv)). In mitotic *Δklp6* cells, Klp5-GFP can be seen localising to the nuclear spindle (Figure 3.2 **A.** v) and vi)); Klp5-GFP localisation is thus restored in *Δklp6* cells if Crm1-mediated nuclear export is inhibited. However, similar to WT cells, there is very little nuclear accumulation of Klp5-GFP in interphase *Δklp6* cells (Figure 3.2 **A.** vii) and viii).

Figure 3.2 **B.** shows the reciprocal experiment; Klp6-GFP localisation 90 minutes after LMB addition in both WT and *Δklp5* cells. WT mitotic cells show clear localisation of Klp6-GFP to the nuclear spindle Figure 3.2 **B.** i) – iii). In contrast to Klp5-GFP, Klp6-GFP shows very strong nuclear accumulation during interphase in WT cells (Figure 3.2 **B.** iv). In mitotic *Δklp5* cells, Klp6-GFP is also seen localising to the nuclear spindle; similar to Klp5-GFP, the mitotic nuclear localisation is restored in the absence of Crm1-mediated nuclear export (Figure 3.2 **B.** v) – vii)). Klp6-GFP also shows very strong nuclear accumulation in *Δklp5* interphase cells (Figure 3.2 **B.** viii).

These results show that the mitotic localisation of Klp5-GFP or Klp6-GFP in the absence of the partner Klp protein is altered by addition of LMB, demonstrating that both Klp5-GFP and Klp6-GFP are targets of the Crm1-mediated nuclear export pathway. Restoration of Klp5-GFP localisation to the nuclear mitotic spindle in the absence of Klp6 upon LMB addition indicates that Klp5-GFP is able to enter the nucleus independently of Klp6 during mitosis, but is not retained under normal conditions. The same is true for Klp6-GFP; addition of LMB shows it is able to enter the nucleus in the absence of Klp5.

Qualitative observations of nuclear accumulation in interphase suggest that more Klp6-GFP enters the nucleus than Klp5-GFP. To quantify this observation, line profiles of fluorescence intensity across the length of a cell were created (see Materials and Methods). This was done for five interphase cells in each strain described above, 60 minutes after LMB addition. The resulting graphs are shown in Figure 3.3. The cartoon of a fission yeast cell shows the positioning of the lines, passing through the centre of the cell along its longitudinal axis. The central region of each graph corresponds to the centre of each cell, where the nucleus is located. These graphs clearly illustrate the difference in nuclear accumulation between Klp5-GFP and Klp6-GFP (compare Figure 3.3 **A.** and **C.**) It is also apparent that the levels of Klp5-GFP or Klp6-GFP nuclear accumulation are unaffected by the presence or absence of *Δklp6* or *Δklp5*, respectively (compare Figure 3.3 **A.** and **B.**, and **C.** and **D.**) This shows that Klp6-GFP enters interphase nuclei, as well as mitotic nuclei (above), independently of Klp5. Very low levels of Klp5-GFP accumulate in interphase nuclei, and this is independent of Klp6. This raised the interesting possibility that nuclear entry of Klp5 is cell-cycle regulated.

3.2.3 Expression levels of Klp5 and Klp6

One formal possibility for the increased nuclear accumulation of Klp6-GFP in interphase nuclei is that Klp6 is expressed at higher levels during interphase than Klp5. Klp5 and Klp6 expression should be the same at the transcriptional level, because their transcription is regulated by the same transcription factor, Ace2 (Rustici *et al.*, 2004). However, they could be differently regulated at translational or post-translational levels. Western blot analysis (N. Koonrugsa, PhD thesis; my data, not shown) indicates that Klp6-HA is not expressed at higher levels than Klp5-HA in asynchronous cultures. By comparison with levels of Cut2-HA, whose expression has been determined as 20 000 molecules per cell, it was estimated that there are ~31 600 molecules of Klp5-HA per cell, compared with ~20 000 molecules of Klp6-HA per cell (N. Koonrugsa). As asynchronous cultures consist of ~90% interphase cells, this shows that increased nuclear accumulation of Klp6 during interphase is unlikely to be because more Klp6 is present in interphase cells.

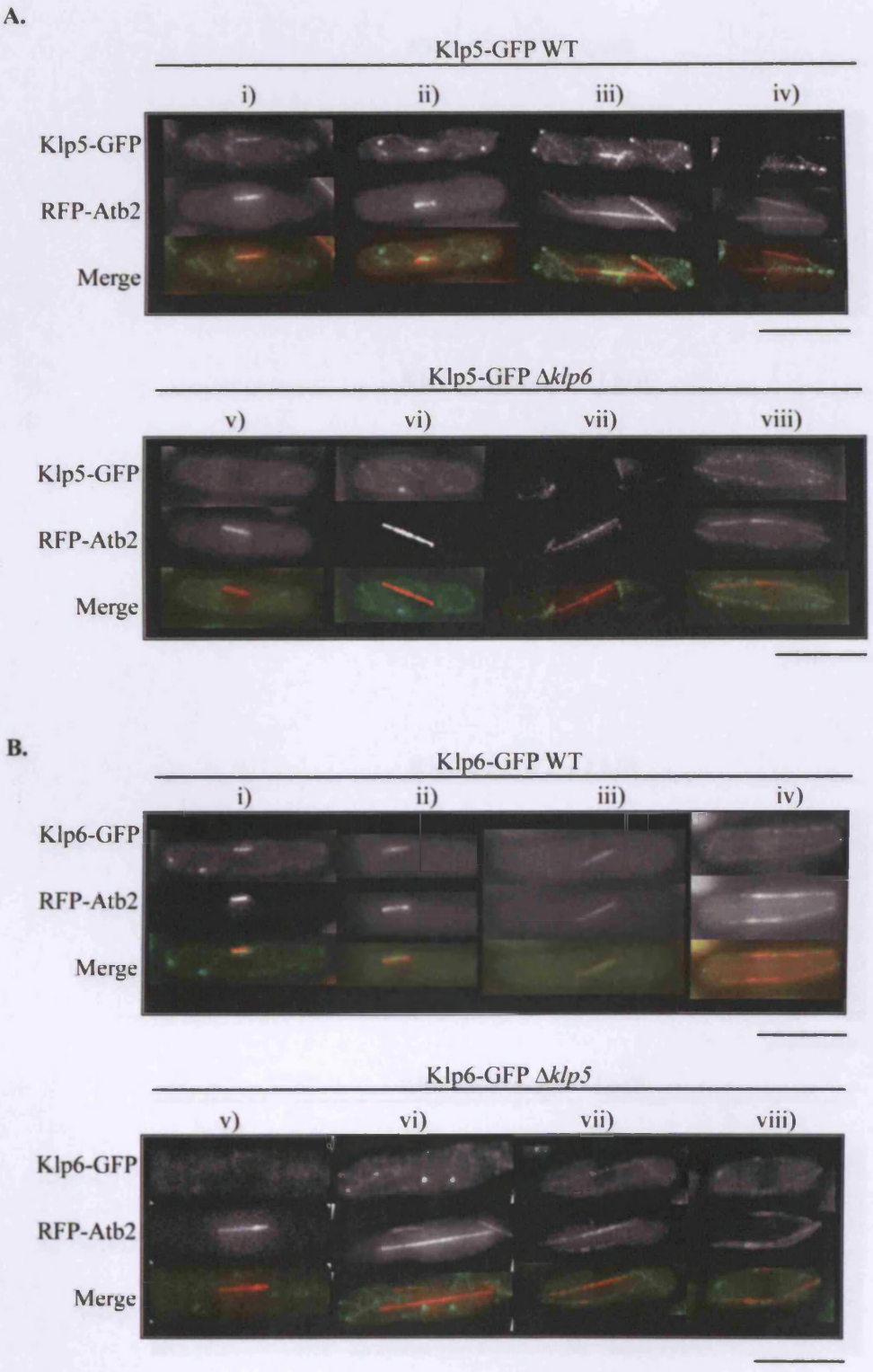

Figure 3.1 Interdependency of Klp5 and Klp6 for nuclear mitotic localisation

A. Klp5-GFP localises to cytoplasmic MTs and the mitotic spindle, as shown by co-localisation with tubulin-RFP. Klp5-GFP does not localise to the mitotic spindle in the absence of Klp6, but still localises to cytoplasmic MTs. **B.** Klp6-GFP shows a similar localisation pattern, failing to localise to the mitotic spindle in the absence of Klp5. Scale bar=10μm

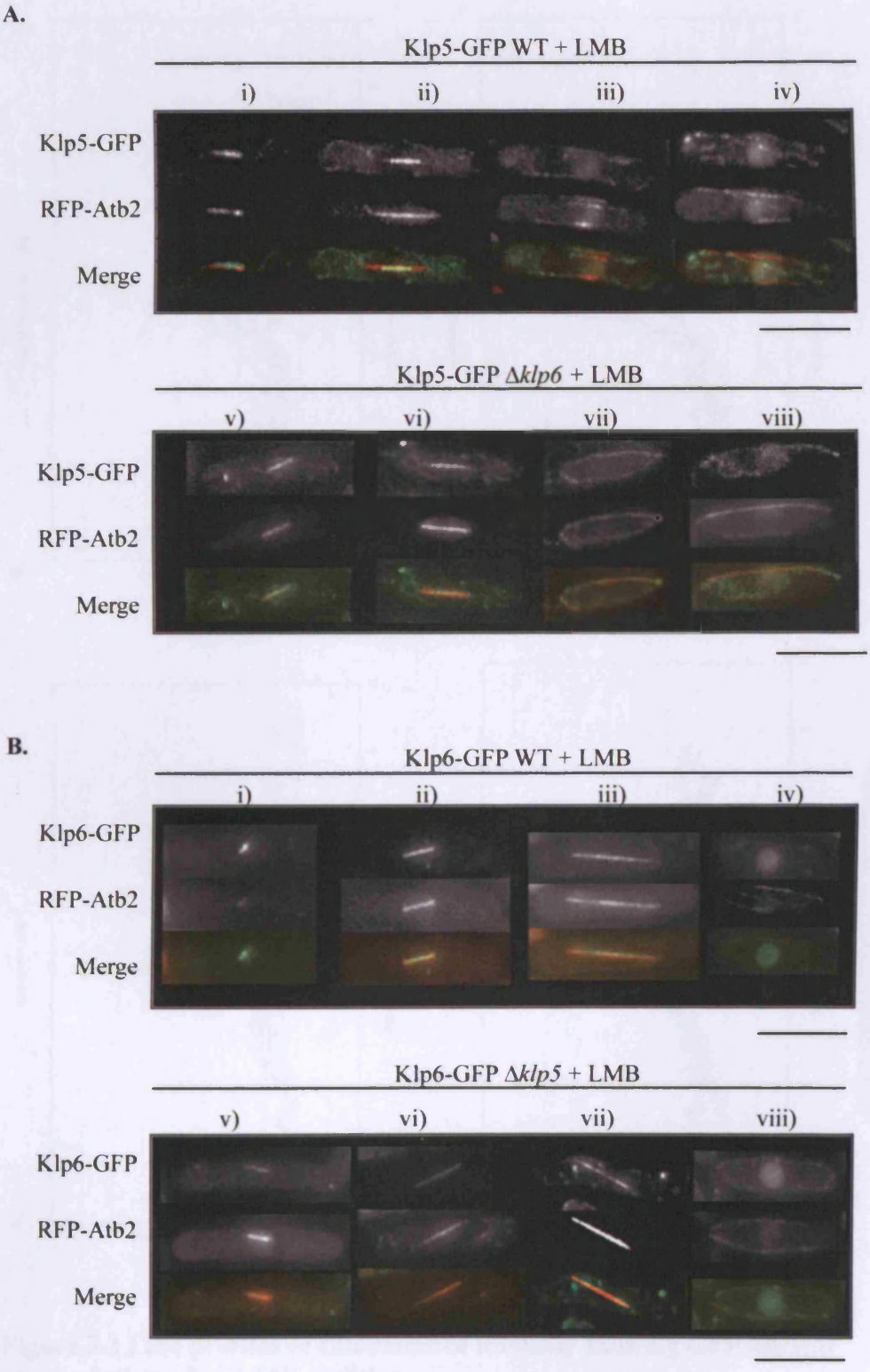

Figure 3.2 Addition of Leptomycin B to examine nuclear entry of Klp5 and Klp6

Images taken 90mins after LMB addition. **A.** Klp5-GFP shows low levels of nuclear accumulation in interphase cells in both WT and *Δklp6* backgrounds. Localisation to the nuclear mitotic spindle is restored in *Δklp6* cells. **B.** Klp6-GFP shows strong nuclear accumulation in both WT and *Δklp5* interphase cells. Localisation to nuclear mitotic spindle is restored in *Δklp5* cells.

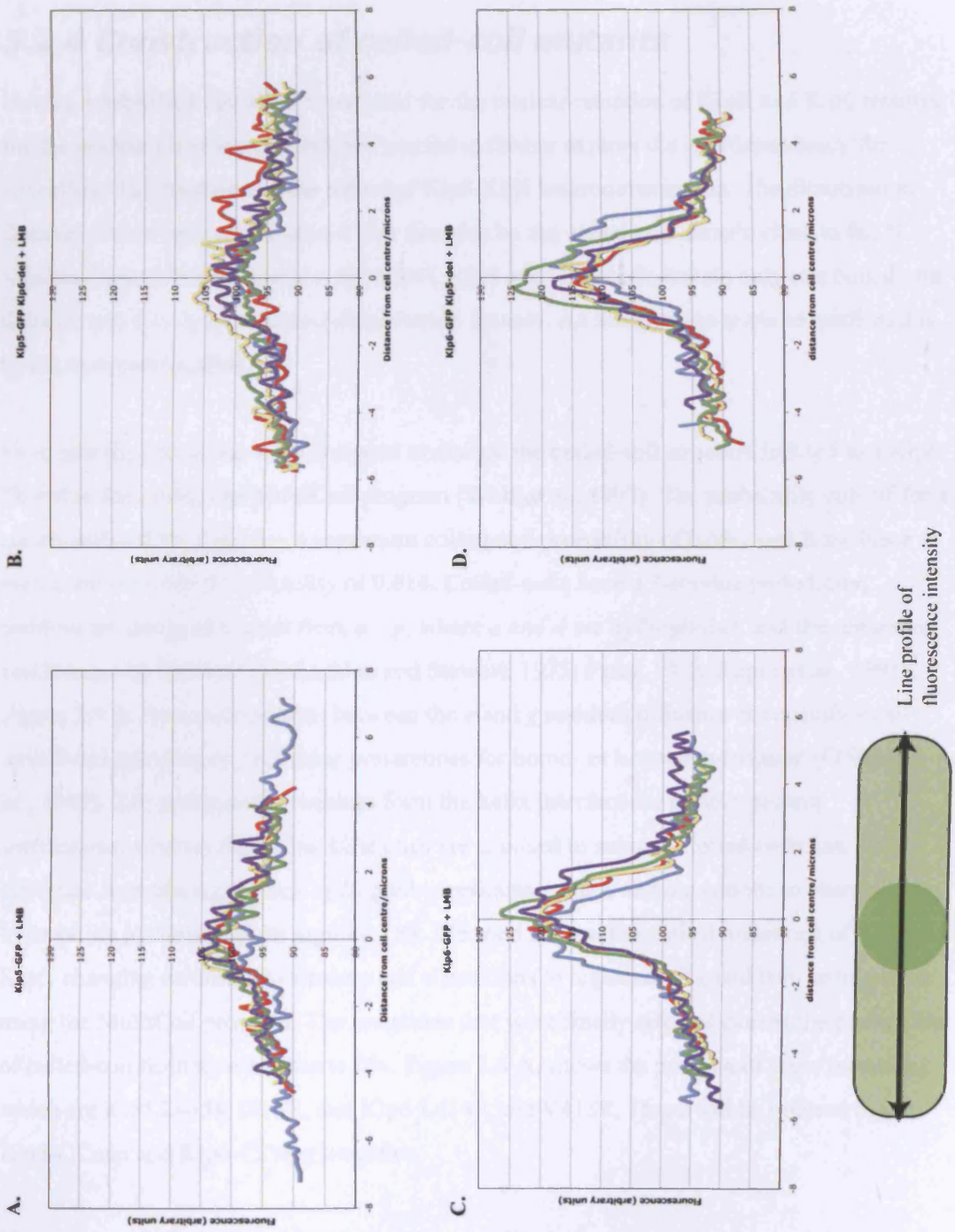

Figure 3.3 Line profiles of fluorescence intensity showing GFP nuclear accumulation after LMB addition

A line was drawn along the longitudinal axis of each cell (n=5 for each strain) and the fluorescence intensity calculated using ImageJ software.

3.2.4 Construction of coiled-coil mutants

Having established that Klp5 is required for the nuclear retention of Klp6, and Klp6 required for the nuclear retention of Klp5, we wanted to further explore the interdependency for subcellular localisation and the nature of Klp5/Klp6 heterodimerisation. The dimerisation domain of conventional Kinesin-1 was found to be the coiled-coil domain close to the N-terminal kinesin head (Huang *et al.*, 1994). Klp5 and Klp6 both contain only one coiled-coil domain, and this is the assumed dimerisation domain. An attempt was made to confirm this by immunoprecipitation.

First, specific mutations were designed to disrupt the coiled-coil structure in Klp5 and Klp6. This was done using the MultiCoil program (Wolf *et al.*, 1997). The probability cut-off for a coiled-coil is 0.50; Klp5 has a maximum coiled-coil probability of 0.686, and Klp6 has a maximum coiled-coil probability of 0.614. Coiled-coils have a 7-residue periodicity; residues are assigned a letter from *a* – *g*, where *a* and *d* are hydrophobic, and the remaining residues are hydrophilic (McLachlan and Stewart, 1975; Parry, 1982; Lupas *et al.*, 1991), Figure 3.4 **A.**. Ionic interactions between the *e* and *g* residues influence the specificity of coiled-coil interactions, including preferences for homo- or heterodimerisation (O'Shea *et al.*, 1993). The hydrophobic residues form the helix interface for protein-protein interactions, whereas the hydrophilic ones are exposed to solvent. Coiled-coils can be disrupted by mutating the key hydrophobic residues at the *a* and *d* positions to charged hydrophilic residues such as arginine (R). We tried several theoretical mutations of Klp5 and Klp6, changing residues at various *a* and *d* positions to arginines (R), and then testing these using the MultiCoil program. The mutations that were finally selected caused the probability of coiled-coil formation to drop to 0%. Figure 3.4 **A.** shows the position of these mutations, which are Klp5 L415R I419R, and Klp6 L414R and V418R. These will be referred to as Klp5-CCmut and Klp6-CCmut hereafter.

Having identified which residues to mutate, site-directed mutagenesis was carried out on the pREP41-EGFP-Klp5 and pREP41-EGFP-Klp6 plasmids (kind gift from E. Chang, Houston, Texas). The pREP41 plasmid contains the moderately-strong *nmt41* promoter which is induced in the absence of thiamine. Unfortunately, attempts to construct Klp6-CCmut were unsuccessful, but Klp5-CCmut was constructed successfully and confirmed by sequencing. To confirm whether the coiled-coil domain of Klp5 is indeed the Klp5/Klp6 dimerisation domain, a co-immunoprecipitation (IP) experiment was carried out. The pREP41 plasmids harbouring either GFP-Klp5 WT or GFP-Klp5-CCmut were transformed into WT (untagged) or Klp6-HA strains. These cultures were grown in the absence of thiamine to induce expression from the plasmid-borne *nmt41* promoter. Cell extracts were then made

and immunoprecipitation perfomed using an α-GFP antibody. Subsequent Western-blot analysis revealed successful immunoprecipitation of GFP-Klp5 WT and CC-mut, and co-immunoprecipitation of Klp6-HA (Figure 3.4 **B.**) The amount of Klp6-HA co-immunoprecipitated with GFP-Klp5-CCmut is greatly reduced compared to that with GFP-Klp5 WT (compare lanes 8 and 10 of left-hand gel), suggesting that the coiled-coil of Klp5 does mediate its interaction with Klp6. However, it was not possible to detect GFP-Klp5 in the whole-cell extract (WCE) (lanes 1 - 5, right-hand gel), so it cannot be confirmed that input levels of GFP-Klp5 were equal in all reactions, although total protein concentrations were equalised, and input levels of Klp6-HA were equal (lanes 2,3 and 5, left-hand gel). This result suggests that the Klp5 coiled-coil domain is required for heterodimerisation, but for the reason described above, it does not unequivocally confirm it. Several attempts to repeat the experiment under different conditions proved unsuccessful.

3.2.5 Klp6 coiled-coil domain is required for function, but does not contain a Nuclear Export Signal (NES)

Experiments thus far have shown that Klp5 and Klp6 do not require each other for import into the nucleus, but that they do require each other for retention in the nucleus; it seems that deletion of one Klp leads to premature nuclear exit of the remaining Klp molecule, accounting for the loss of localisation to the mitotic spindle. We reasoned that the Klp5/Klp6 physical interaction might provide an intermolecular masking mechanism of Nuclear Export Signals (NES) located within the molecules, similar to that reported for p53 (Stommel *et al.*, 1999). In the absence of one Klp, perhaps the NES of the other is exposed and is therefore exported rapidly from the nucleus.

It is likely that the coiled-coil domains mediate the heterodimerisation of Klp5 and Klp6 (see previous section); if the intermolecular masking mechanism were correct, it would be reasonable to suppose that the NESs were also located within this domain. Klp5 and Klp6 are targets of Crm1, as demonstrated by their sensitivity to LMB. Most Crm1 substrates contain a short, leucine rich NES, roughly conforming to the consensus Φ-x_{2-3}-Φ-x_{2-3}-Φ-x-Φ, where Φ represents a hydrophobic L,I,V,F or M residue, and x is any amino acid (Fornerod and Ohno, 2002; la Cour *et al.*, 2004). This requirement for regularly spaced hydrophobic residues is remarkably similar to the periodicity of hydrophobic residues seen in coiled-coils (see previous section). It therefore seemed possible that the exposed (i.e. non-dimerised) coiled-coils of Klp5 and Klp6 could interact with Crm1, resulting in their nuclear export.

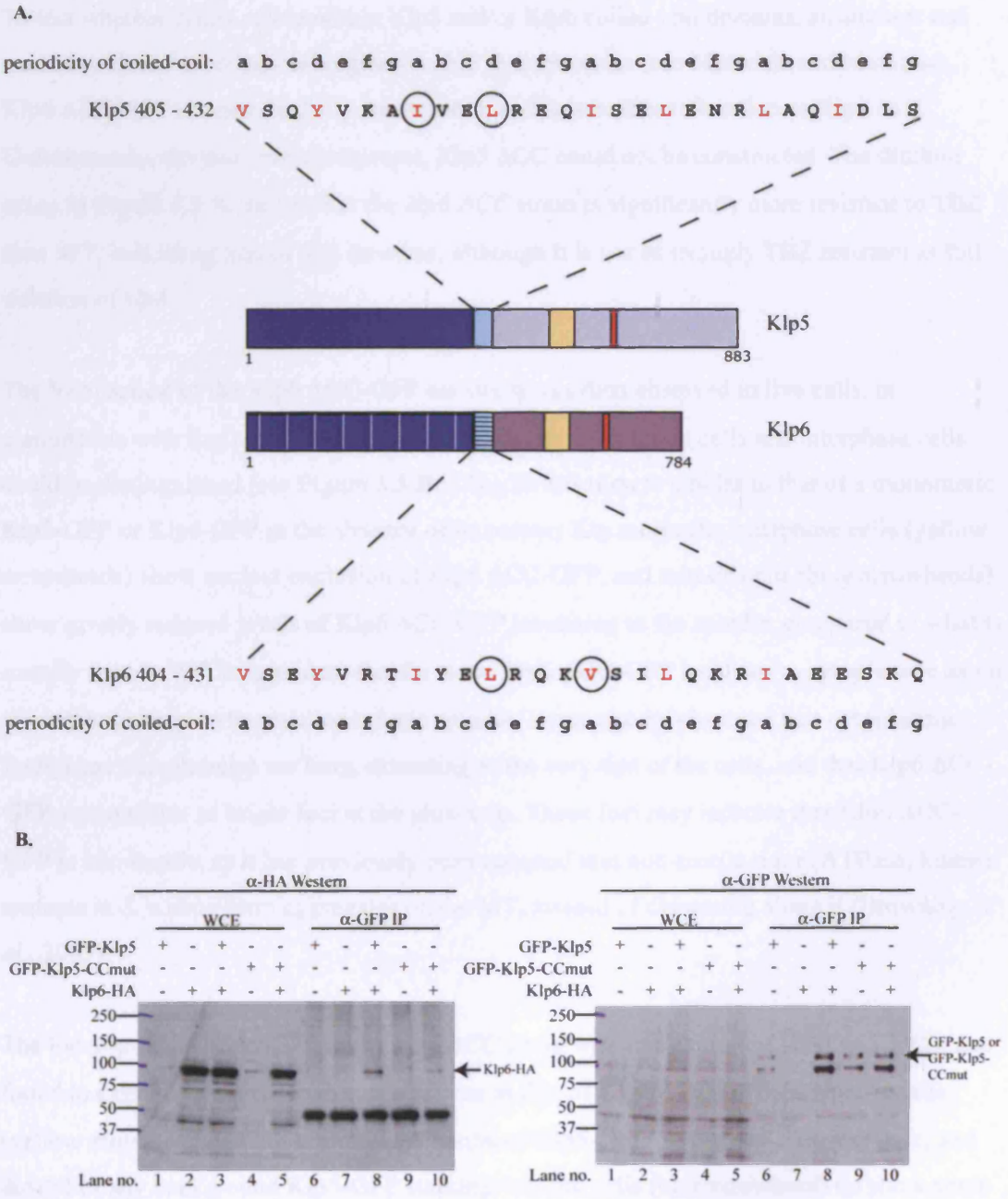

Figure 3.4 Klp Coiled-Coil Mutants

A. Cartoon shows position of coiled-coil domain (light blue) in Klp5 and Klp6. Amino acid sequence and periodicity (see text for details) shown above (Klp5) and below (Klp6). Hydrophobic residues corresponding to positions *a* and *d* (see periodicity of coiled-coil) are shown in red. Residues mutated to arginine (R) to create coiled-coil mutants are circled. **B.** Immunoprecipitation to compare interaction between Klp6-HA and either GFP-Klp5 WT or GFP-Klp5-CCmut.

To test whether NESs reside within Klp5 and/or Klp6 coiled-coil domains, an attempt was made to delete the coiled-coil regions within these proteins (see Materials and Methods). Klp6 Δ402-431 was successfully constructed, and is hereafter referred to as Klp6 ΔCC. Unfortunately, despite several attempts, Klp5 ΔCC could not be constructed. The dilution assay in Figure 3.5 **A.** shows that the *klp6 ΔCC* strain is significantly more resistant to TBZ than WT, indicating loss of Klp function, although it is not as strongly TBZ resistant as full deletion of *klp6*.

The localisation of the Klp6 ΔCC-GFP construct was then observed in live cells, in conjunction with Sad1-dsRED to mark the SPBs, so that mitotic cells and interphase cells could be distinguished (see Figure 3.5 **B.**). The localisation is similar to that of a monomeric Klp5-GFP or Klp6-GFP in the absence of its partner Klp molecule; interphase cells (yellow arrowheads) show nuclear exclusion of Klp6 ΔCC-GFP, and mitotic cells (blue arrowheads) show greatly reduced levels of Klp6 ΔCC-GFP localising to the spindle, compared to what is usually seen in WT. It is evident that far more Klp6 ΔCC-GFP localises to cytoplasmic astral microtubules than to the nuclear mitotic spindle. It can also be observed that cytoplasmic interphase microtubules are long, extending to the very tips of the cells, and that Klp6 ΔCC-GFP accumulates as bright foci at the plus-ends. These foci may indicate that Klp6 ΔCC-GFP is non-motile, as it has previously been reported that non-motile rigor (ATPase) kinesin mutants in *S. pombe* form aggregates on the MT, instead of dispersing along it (Browning *et al.*, 2003).

The localisation of Klp5-GFP in the *klp6 ΔCC* strain was also examined (Figure 3.5 **C.**), and found to exhibit the same localisation pattern as that of Klp6 ΔCC-GFP. Interphase cells (yellow arrowheads) exhibit nuclear exclusion of Klp5-GFP, as the nuclei appear dark, and devoid of any background Klp5-GFP staining. Mitotic cells (blue arrowhead) do show some localisation of Klp5-GFP to the spindle, but this is very weak compared to the cytoplasmic astral microtubule staining seen in the same cell.

This analysis shows that the Klp6 coiled-coil domain is required for efficient nuclear localisation of both Klp6 itself, and of Klp5.We suggest that this is because the physical interaction between Klp5 and Klp6 is required for nuclear retention of Klp5 and this is abolished in the *klp6 ΔCC* strain. Our hypothesis that the Klp5 and Klp6 coiled-coil domains might contain NESs that are masked upon dimerisation has not been proved. It could not be addressed whether the Klp5 coiled-coil domain contains an NES, as the coiled-coil could not be deleted. The experiments with LMB demonstrated that Klp6-GFP shuttles between the nucleus and the cytoplasm during interphase. If the functional NES were deleted, it should result in nuclear accumulation of the protein. No such accumulation was observed for Klp6

ΔCC-GFP; in fact this molecule is excluded from the nucleus. We therefore conclude that the Klp6 coiled-coil does not contain a functional NES.

3.2.6 Identification of Nuclear Localisation Signals (NLS) in Klp5 and Klp6

Having established that Klp5 and Klp6 are both able to enter the nucleus, the mechanism of their nuclear transport was further explored. A search for possible Nuclear Localisation Signals (NLS) within Klp5 and Klp6 was carried out by submitting the protein sequences to PSORT (http://psort.nibb.ac.jp/). This revealed that both Klp5 and Klp6 contain a classical NLS within a conserved region in their C-terminal tails (Figure 3.6).

To test whether these were genuine localisation signals, arginine residues within each putative NLS were mutated to alanines (Sato and Toda, 2007) to create the Klp5 R693A R695A and Klp6 R673A R675A mutants, designated Klp5-NLSmut and Klp6-NLSmut, respectively). This was achieved by site-directed mutagenesis (see Materials and Methods) of the plasmids pREP41-EGFP-klp5 and pREP41-EGFP-klp6 (gift from E. Chang). *Δklp5Δklp6* double mutant cells were transformed with pREP41-EGFP plasmids containing either Klp5 WT, Klp5-NLSmut, Klp6 WT or Klp6-NLSmut. This host strain was chosen so that the nuclear import competency of the Klp5 WT and Klp5-NLSmut proteins could be assessed independently of their interaction with Klp6, and vice versa. Experiments were carried out in thiamine-free media, to induce expression from the *nmt41* promoter.

To determine whether the GFP-Klp5-NLSmut and GFP-Klp6-NLSmut proteins enter the nucleus, firstly, the localisation patterns of individual GFP-Klps were observed under induced (+thiamine) conditions. Next, LMB was added to inhibit nuclear export (Fornerod *et al.*, 1997). If no nuclear localisation was observed even in the presence of LMB, it would prove that these proteins were defective in nuclear import, and that their NLSs had been correctly identified and mutated. Figure 3.7 **A.** compares the nuclear import of WT GFP-Klp5 and GFP-Klp5-NLSmut. In each case, the same field of cells is shown before addition of LMB (-LMB), and 60 minutes after additon of LMB (+LMB). Klp5-GFP expressed from the endogenous locus shows very little nuclear accumulation in interphase cells (Figure 3.2 and Figure 3.3). However, under these conditions, with GFP-Klp5 overexpressed by induction of the *nmt41* promoter, there is very obvious nuclear accumulation (Figure 3.7, right). In contrast, GFP-Klp5-NLSmut does not show any nuclear accumulation in interphase cells upon LMB addition, although some localisation to the mitotic spindle is visible. This is a rather puzzling result, as mutation of the putative NLS in

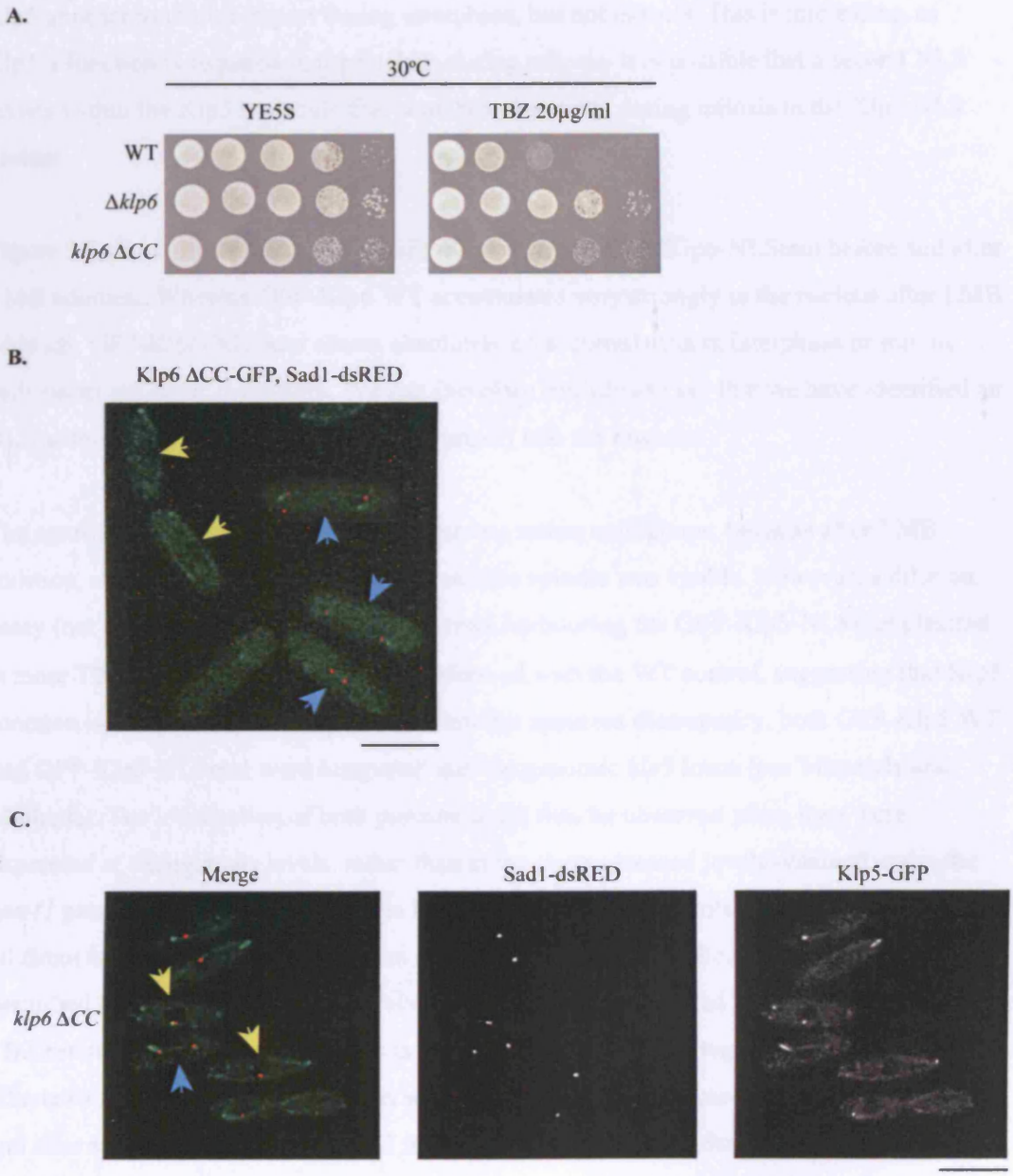

Figure 3.5 Klp6 Coiled-coil deletion

A. Dilution assay showing increased TBZ resistance of Klp6 ΔCC strain compared to WT. Ten-fold serial dilutions were spotted onto YE5S plates, with additions as shown. Plates were incubated at 30°C. **B.** Fluorescence microscopy showing localisation of Klp6 ΔCC-GFP, in conjunction with Sad1-dsRED to mark the SPBs. Examples of mitotic cells are marked with a blue arrowhead, and examples of interphase cells are marked with a yellow arrowhead. **C.** Field of cells visualised by fluorescence microscopy, showing localisation of Klp5-GFP in the *klp6 ΔCC* strain, in conjunction with Sad1-dsRED. Scale bar = 10µm.

Klp5 appears to inhibit import during interphase, but not mitosis. This is interesting, as Klp5's function is required in the nucleus during mitosis. It is possible that a second NLS exists within the Klp5 molecule that somehow functions during mitosis in the Klp5 NLS mutant.

Figure 3.7 shows the localisation of GFP-Klp6 WT and GFP-Klp6-NLSmut before and after LMB addition. Whereas GFP-Klp6 WT accumulates very strongly in the nucleus after LMB addition, GFP-Klp6-NLSmut shows absolutely no accumulation in interphase or mitotic cells under the same conditions. We can therefore confidently say that we have identified an NLS within Klp6 that is necessary for its import into the nucleus.

The result obtained for GFP-Klp5-NLSmut was rather ambiguous, because after LMB addition, some localisation to the nuclear mitotic spindle was visible. However, a dilution assay (not shown) indicated that a *Δklp5* strain harbouring the GFP-Klp5-NLSmut plasmid is more TBZ resistant than the strain transformed with the WT control, suggesting that Klp5 function is compromised. To try and address this apparent discrepancy, both GFP-Klp5 WT and GFP-Klp5-NLSmut were integrated into the genomic *klp5* locus (see Materials and Methods). The localisation of both proteins could thus be observed when they were expressed at endogenous levels, rather than at the overexpressed levels obtained under the *nmt41* promoter. The dilution assay in Figure 3.8 **A.** shows that integrated GFP-Klp5-NLSmut is more resistant to TBZ than GFP-Klp5 WT, again, indicating that function is perturbed in the Klp5 NLSmut. It is also evident that the integrated GFP-Klp5 strain is more TBZ resistant than WT; perhaps this is because N-terminal GFP tagging of Klp5 slightly affects its function. These two strains were then viewed by fluorescence microscopy, before and after addition of LMB (Klp5 WT in Figure 3.8 **B.** ; Klp5-NLSmut in Figure 3.9) Int.GFP-Klp5 is visible on mitotic spindles before and after LMB addition, as would be expected. It also shows low levels of accumulation in interphase nuclei after LMB addition. Figure 3.9 shows the co-localisation of int.GFP-Klp5-NLSmut with RFP-Atb2 (tubulin) before and after LMB treatment. This clearly demonstrates that int.GFP-Klp5-NLSmut is not visible on mitotic spindles before LMB treatment. Additionally, interphase nuclei appear dark, indicating nuclear exclusion. However, in the presence of LMB, localisation of int.GFP-Klp5-NLSmut to the mitotic spindle was observed, although no accumulation in interphase nuclei was seen. This result is the same as that obtained using pREP41-GFP-Klp5-NLSmut (Figure 3.7). The localisation of the Klp5-NLSmut to the mitotic spindle in the presence of LMB is therefore not a consequence of overexpression.

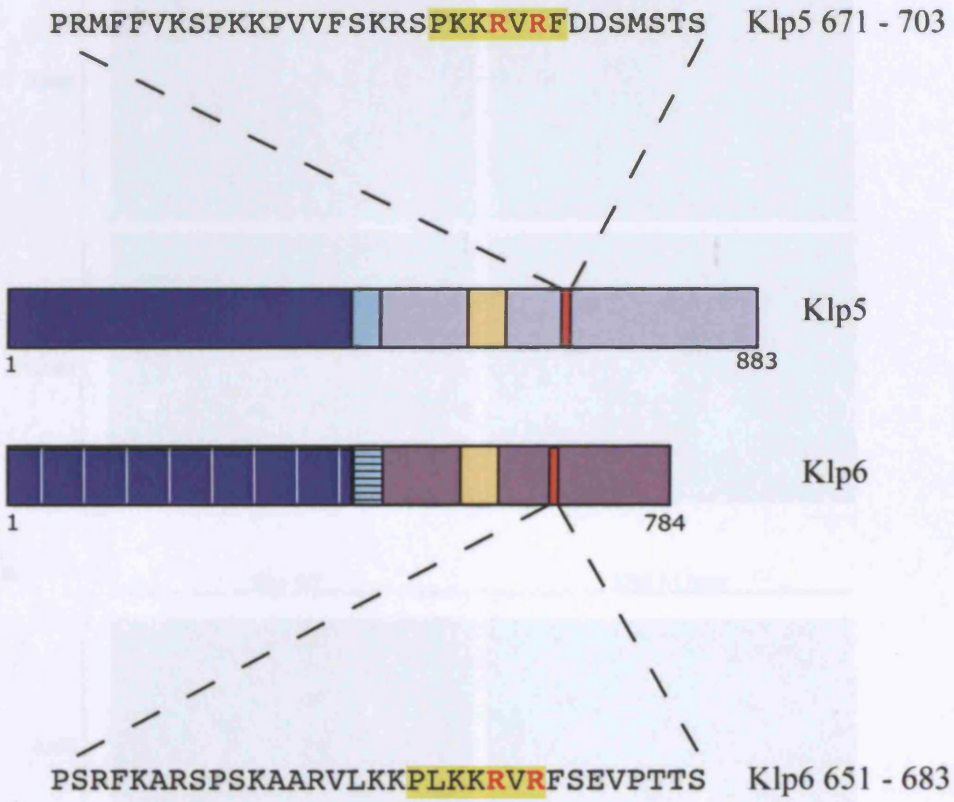

Figure 3.6 Nuclear Localisation Signals within conserved region of Klp5 and Klp6 C-terminal tails

Coloured blocks refer to regions of homology between Klp5 and Klp6. NLSs were identified using PSORT software. Amino acid sequences of NLSs are highlighted in yellow. Arginine residues mutated to alanine to create NLS mutants are marked in red.

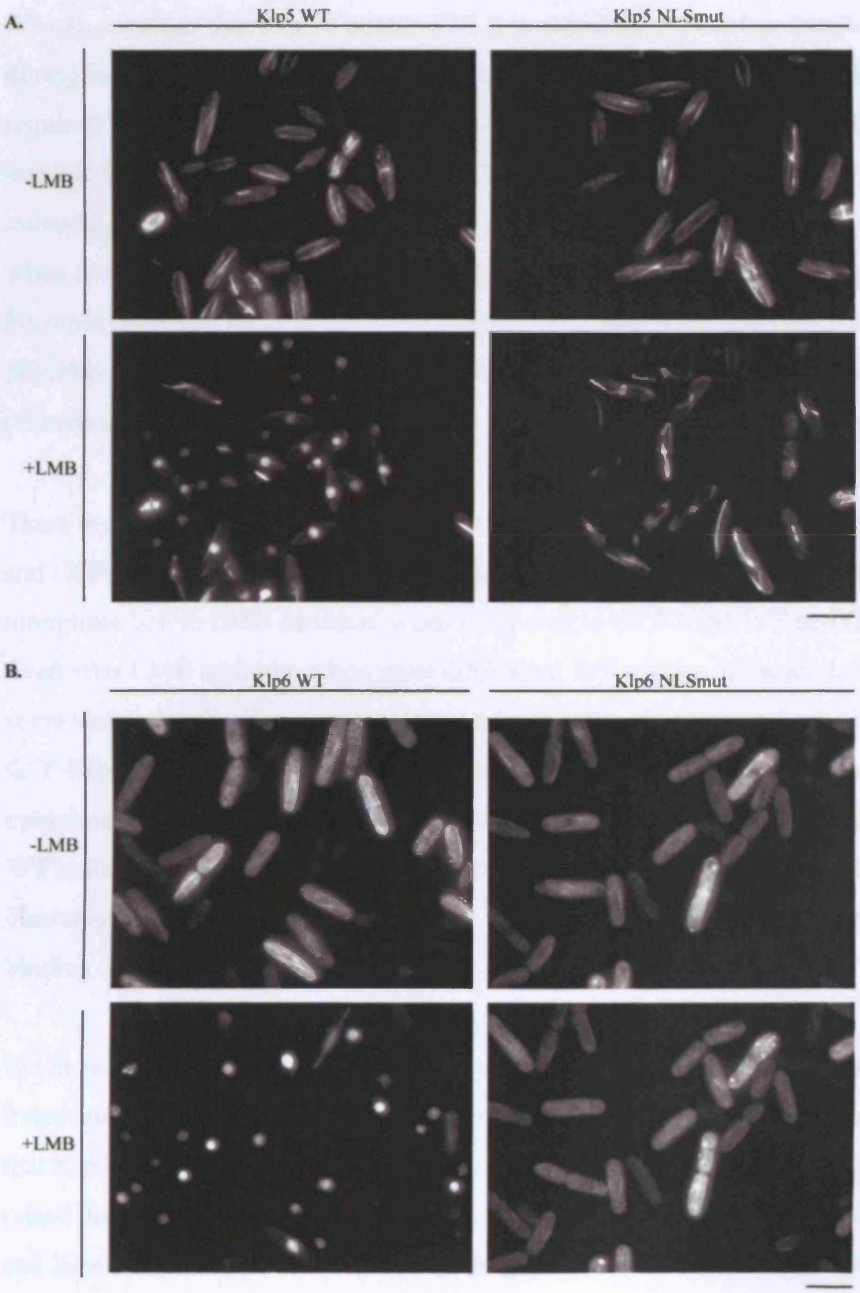

Figure 3.7 Klp5 and Klp6 NLS mutants do not enter the nucleus

Δklp5Δklp6 cells were transformed with pREP41-eGFP plasmids containing either Klp5 WT, Klp5 NLSmut, Klp6 WT or Klp6 NLSmut. Images shown are before LMB addition (-LMB), and the same field of cells 60min after LMB addition (+LMB). Scale bar = 10μm

We can conclude that Klp5's putative NLS is necessary for nuclear localisation of Klp5 during interphase and mitosis in the absence of LMB. Surprisingly, this NLS activity is not required for localisation of Klp5 to the mitotic spindle in the presence of LMB. It is possible that Klp5 contains an additional NLS with weak activity. When the major, strong NLS is mutated, the weak NLS activity could be outweighed by strong NES activity. However, when nuclear export is inhibited by LMB, nuclear localisation of GFP-Klp5-NLSmut becomes apparent. As both Klp5 and Klp6 contain functional classical NLSs, they are most probably targets of one, or both, of the importin-α proteins in fission yeast, Imp1 and Cut15 (Umeda *et al.*, 2005).

There is another interesting observation to be made from Figure 3.7. Both GFP-Klp5 WT and GFP-Klp5-NLSmut show very strong localisation to cytoplasmic microtubules during interphase before LMB addition, when compared to GFP-Klp6 WT and GFP-Klp6-NLS. Even after LMB addition, when most GFP-Klp5 WT resides in the nucleus, there is still some visible localisation to cytoplasmic microtubules. In contrast, both GFP-Klp6 WT and GFP-Klp6-NLSmut show only faint localisation to cytoplasmic microtubules, and diffuse cytoplasmic staining before addition of LMB. Sixty minutes after LMB addition, GFP-Klp6 WT is found entirely in the nucleus; no localisation to cytoplasmic microtubules is visible. This raises the interesting possibility that Klp5 and Klp6 may have different microtubule-binding affinities.

We have established that Klp5 and Klp6 are actively transported into the nucleus independently of each other, that they are both targets of Crm1-mediated nuclear export, and that Klp5 and Klp6 require each other for nuclear retention during mitosis. We have also raised the possibility that the nuclear import of Klp5 is cell-cycle regulated, and that Klp5 and Klp6 differ in their microtubule-binding affinities. These questions are further addressed in the following sections.

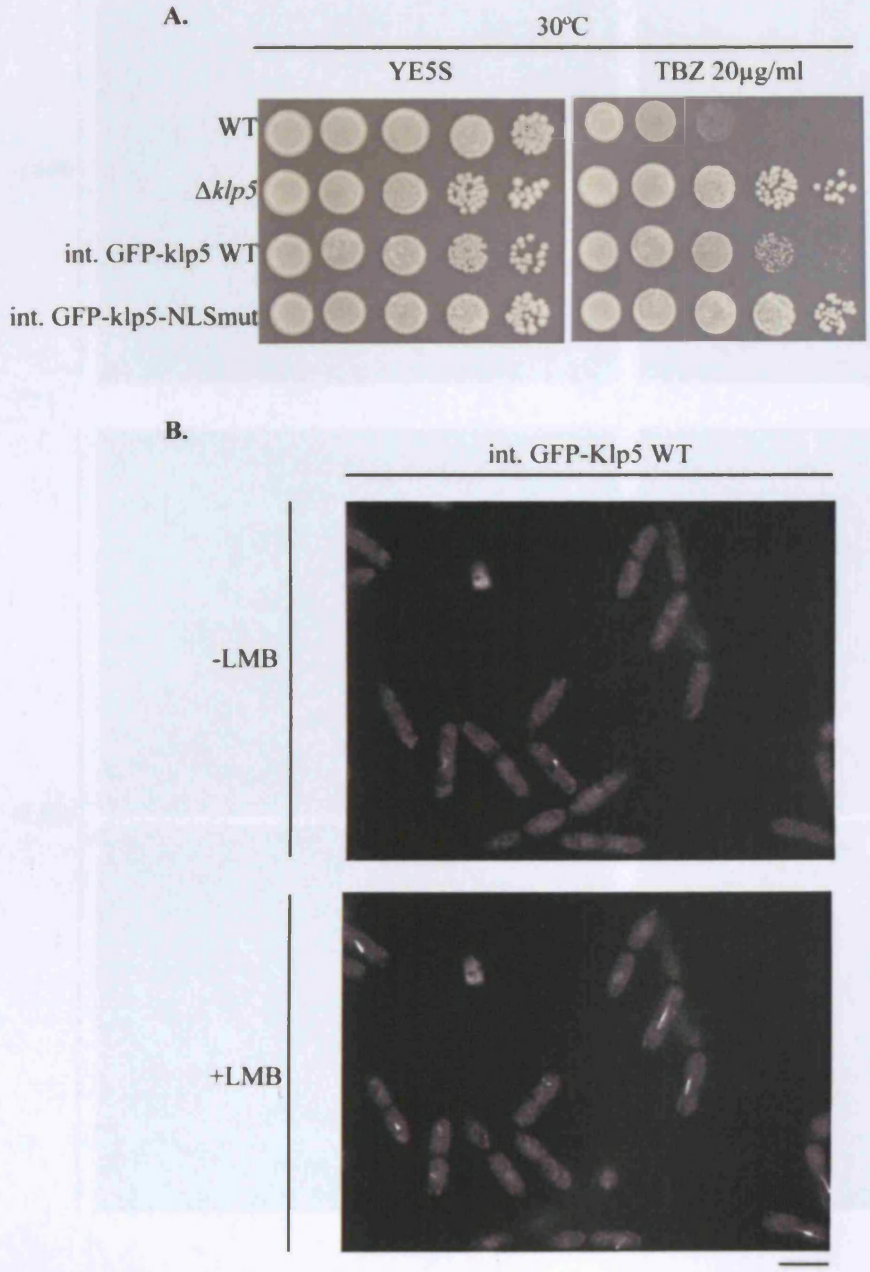

Figure 3.8 Characterisation of GFP-Klp5 strains expressed from genomic locus

A. Dilution assay showing increased TBZ resistance of integrated GFP-Klp5-NLSmut compared to GFP-Klp5 WT. Ten-fold serial dilutions were spotted onto YE5S plates, with additions as shown. Plates were incubated for three days at 30°C. **B.** Images of GFP-Klp5 WT integrated at the genomic locus were taken before LMB addition (-LMB), and 60min after LMB addition (+LMB). Scale bar = 10µm.

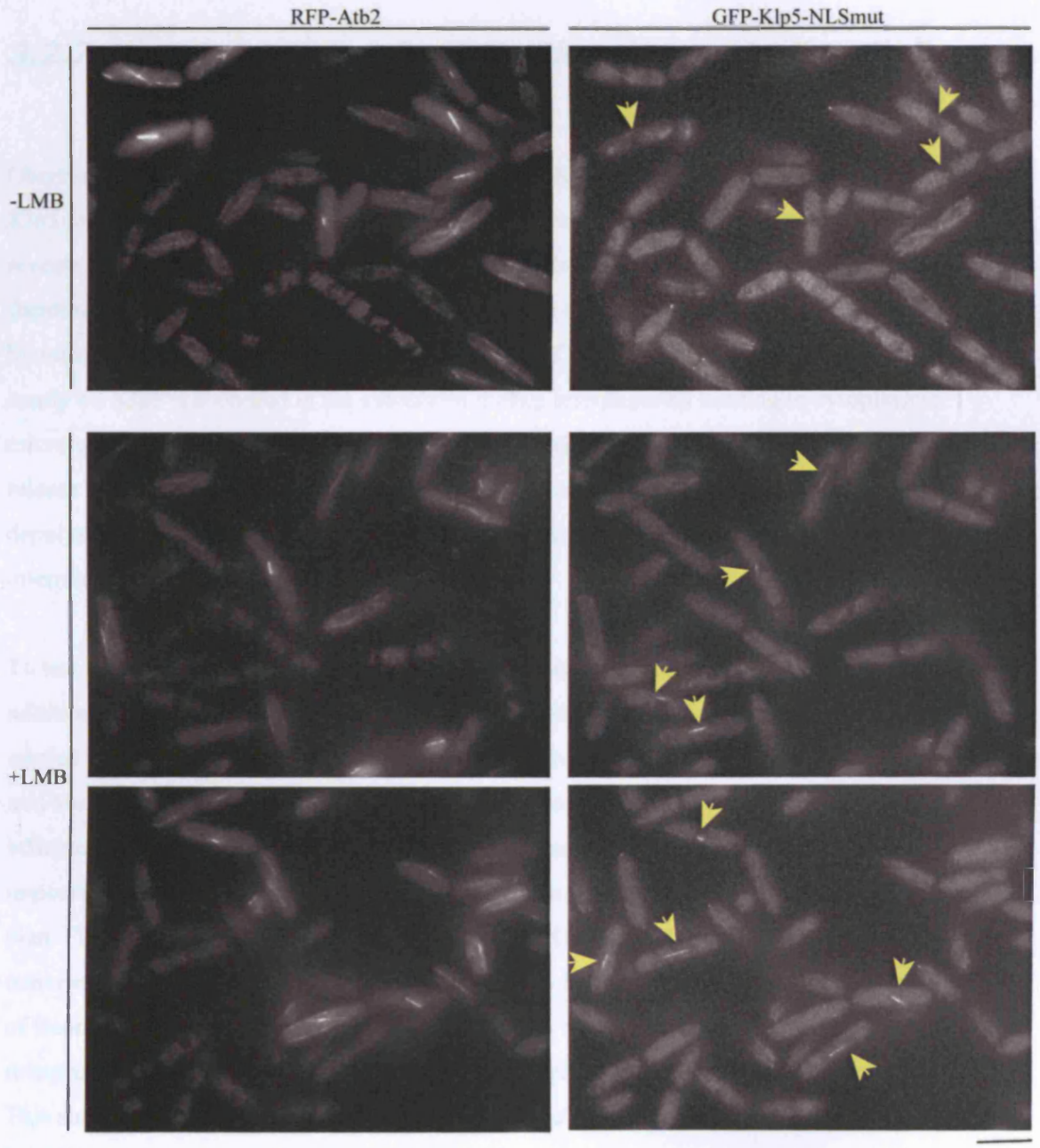

Figure 3.9 GFP-Klp5-NLSmut integrated at the genomic locus is excluded from the nucleus in the absence of LMB

Images of GFP-Klp5-NLSmut and RFP-Atb2 (tubulin) were taken before LMB addition (-LMB), and 60min after LMB addition (+LMB). Each panel shows a different field of cells. Yellow arrowheads indicate mitotic cells. Scale bar = 10μm.

3.2.7 Microtubule depolymerisation does not alter Klp5 subcellular localisation

Observations of overexpressed GFP-Klp5 and GFP-Klp6 (see previous section) show that Klp5 may have a higher affinity for microtubules than Klp6. Experiments using LMB also revealed that very little Klp5-GFP is imported into the nucleus during interphase. We therefore hypothesised that this cell-cycle regulation of subcellular localisation was achieved by microtubule 'anchoring'. Perhaps the affinity of Klp5 for microtubules is so high, that nearly all Klp5 is anchored in the cytoplasm during interphase by binding to cytoplasmic microtubules. At the onset of mitosis, cytoplasmic microtubules disappear, and this could release Klp5 for transport into the nucleus. If this were the case, we reasoned that artificial depolymerisation of cytoplasmic microtubules would cause Klp5-GFP to enter the nuclei of interphase cells.

To test this possibility, depolymerisation of cytoplasmic microtubules was induced by addition of the drug methyl 2-benzimidazolecarbamate (MBC). Trial experiments were first carried out to establish the best conditions for microtubule depolymerisation (see Materials and Methods), using cells containing RFP-Atb2 to confirm that microtubules had been efficiently depolymerised. After microtubule depolymerisation, the efficiency of nuclear import of Klp5-GFP was assessed by adding LMB to inhibit nuclear export (see experiment plan, Figure 3.10 **A.**). The nuclear accumulation of Klp5-GFP after both MBC and LMB treatment was compared with the accumulation after LMB treatment only. The line profiles of fluorescence intensity in Figure 3.10 **B.** show that nuclear accumulation of Klp5-GFP in interphase cells is not increased when microtubules are depolymerised by MBC treatment. This shows that the cell-cycle dependent nuclear localisation of Klp5-GFP is not achieved by microtubule anchoring in the cytoplasm during interphase.

3.2.8 Klp5 subcellular localisation may be regulated by CDK (cyclin-dependent kinase) phosphorylation

Closer inspection of the Klp5 amino acid sequence revealed that there are two consensus Cyclin Dependent Kinase (CDK) sites in very close proximity to the NLS. This raised the interesting possibility that the observed cell-cycle dependent subcellular localisation of Klp5 could be regulated by phosphorylation of these sites. Phosphorylation of these sites by CDK at the onset of mitosis might enhance nuclear import specifically during mitosis by facilitating recognition of the NLS by importin-α. To test this possibility, the

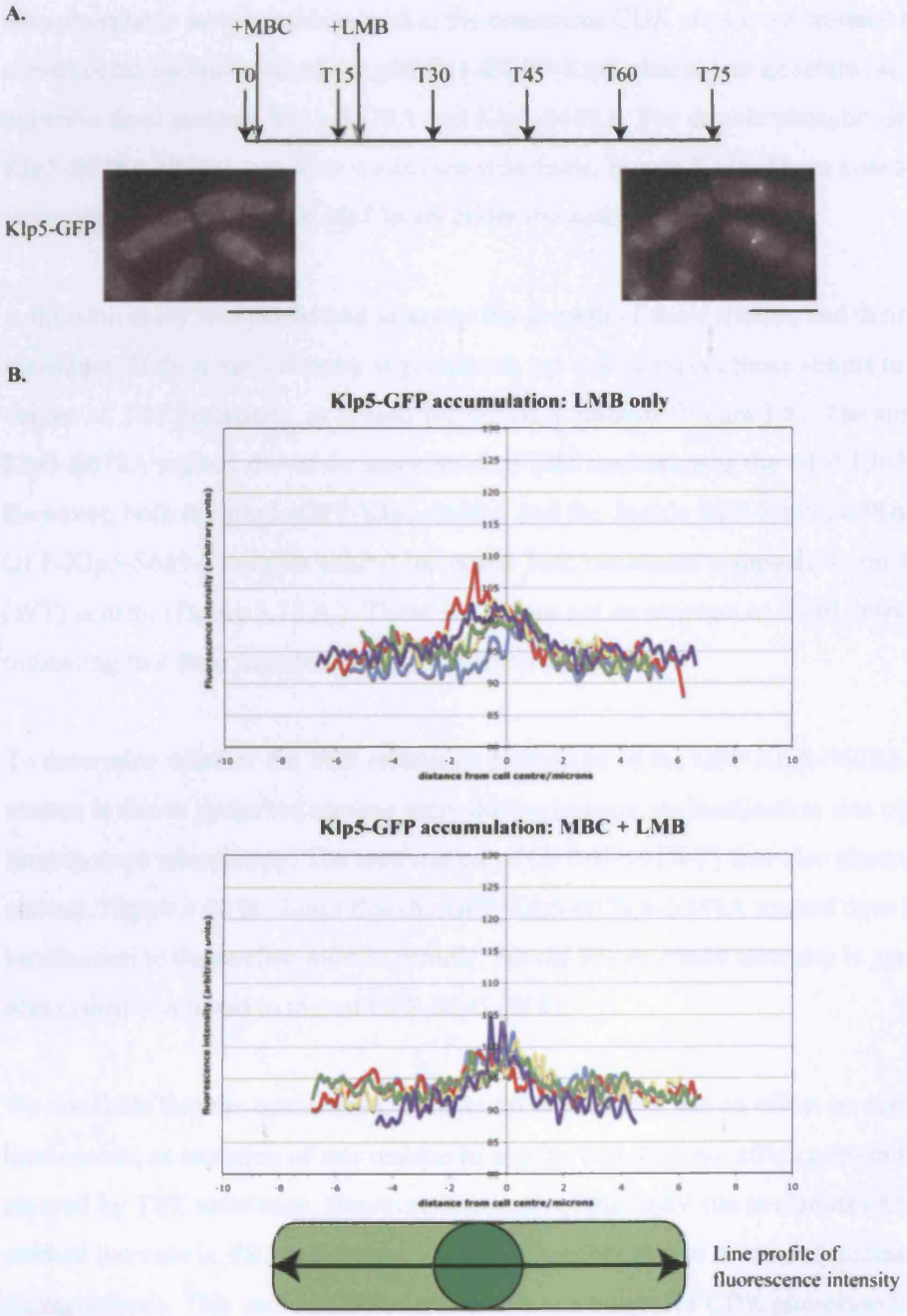

Figure 3.10 Depolymerisation of microtubules does not increase nuclear accumulation of Klp5-GFP

A. Experiment plan. 50μg/ml of MBC was added immediately after first image was taken. 50ng/ml of LMB was added 15mins after MBC addition. Images shown taken at T0 and T75. Timepoints (T) refer to minutes. Scale bar = 10μm. **B.** Line profiles of fluorescence intensity showing nuclear accumulation of Klp5-GFP 60min after LMB addition (T75 of experiment plan) in the presence (lower graph) or absence (upper graph) of MBC to depolymerise MTs. Line profiles of five individual cells shown in each graph.

phosphorylable serine residues within the consensus CDK sites were mutated to alanine by site-directed mutagenesis of the pREP41-EGFP-Klp5 plasmid, to generate the single phospho-dead mutants Klp5-S678A and Klp5-S689A. The double phospho-dead mutant Klp5-S678A-S689A was also made (see schematic, Figure 3.11). These constructs were then integrated into the genomic *klp5* locus under the native promoter.

A dilution assay was performed to assess the growth of these strains, and their TBZ resistance. If their nuclear entry is perturbed, we would expect these strains to exhibit some degree of TBZ resistance, as is seen for the NLS mutants (Figure 3.8). The single GFP-Klp5-S678A mutant shows the same level of TBZ resistance as the GFP-Klp5 (WT) control. However, both the single GFP-Klp5-S689A and the double GFP-Klp5-S678A GFP-Klp5-S689A mutants exhibit increased TBZ resistance compared to the GFP-Klp5 (WT) control (Figure 3.12 **A.**). These strains are not as resistant as a full deletion of *klp5*, indicating that their function is not completely abolished.

To determine whether the TBZ resistance phenotype of the GFP-Klp5-S678A-S689A mutant is due to perturbed nuclear entry during mitosis, its localisation was observed by fluorescence microscopy. The localisation of GFP-Klp5 (WT) was also observed as a control. Figure 3.12 **B.** shows that the GFP-Klp5-S678A-S689A mutant does show localisation to the nuclear mitotic spindle, but the fluorescence intensity is greatly diminished compared to that of GFP-Klp5 (WT).

We conclude that the consensus CDK site S678 probably has no effect on nuclear localisation, as mutation of this residue to alanine (A) does not affect protein function as assayed by TBZ resistance. However, mutation of the S689 site to alanine (A) causes a marked increase in TBZ resistance, which is probably due to decreased nuclear localisation during mitosis. This could be because this site is a target for CDK phosphorylation, which upregulates nuclear import during mitosis. Alternatively, it may be that reduced nuclear localisation is observed simply because mutation of the S678 residue directly interferes with the function of the NLS.

To confirm that CDK phosphorylation plays a role in the cell-cycle specific nuclear localisation of Klp5, it would be necessary to demonstrate that the S689 residue is actually phosphorylated by CDK. If a slower-migrating, phosphorylated form of Klp5 was visible by Western, and this was abolished in the S>A mutant, it would provide convincing evidence. However, such a bandshift has not been observable using cell extracts under our experimental conditions.

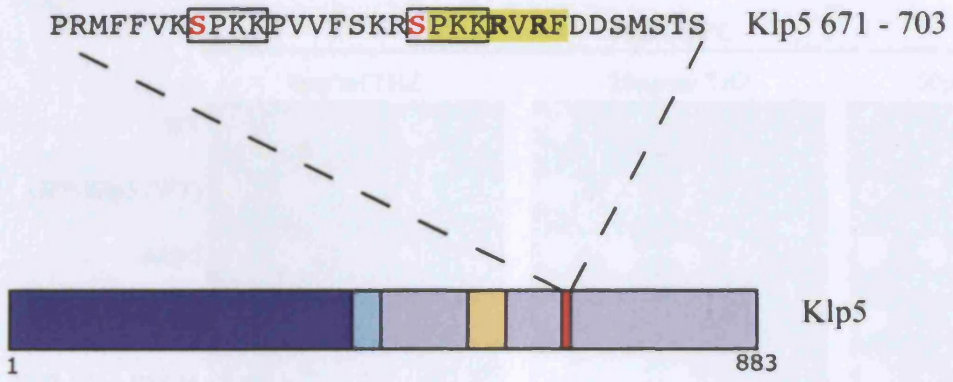

Figure 3.11 Consensus CDK sites close to Klp5 NLS

Amino acid sequence of Klp5 NLS highlighted in yellow (as before). Consensus CDK sites outlined in black. Serine residues mutated to make phospho-dead mutants are marked in red.

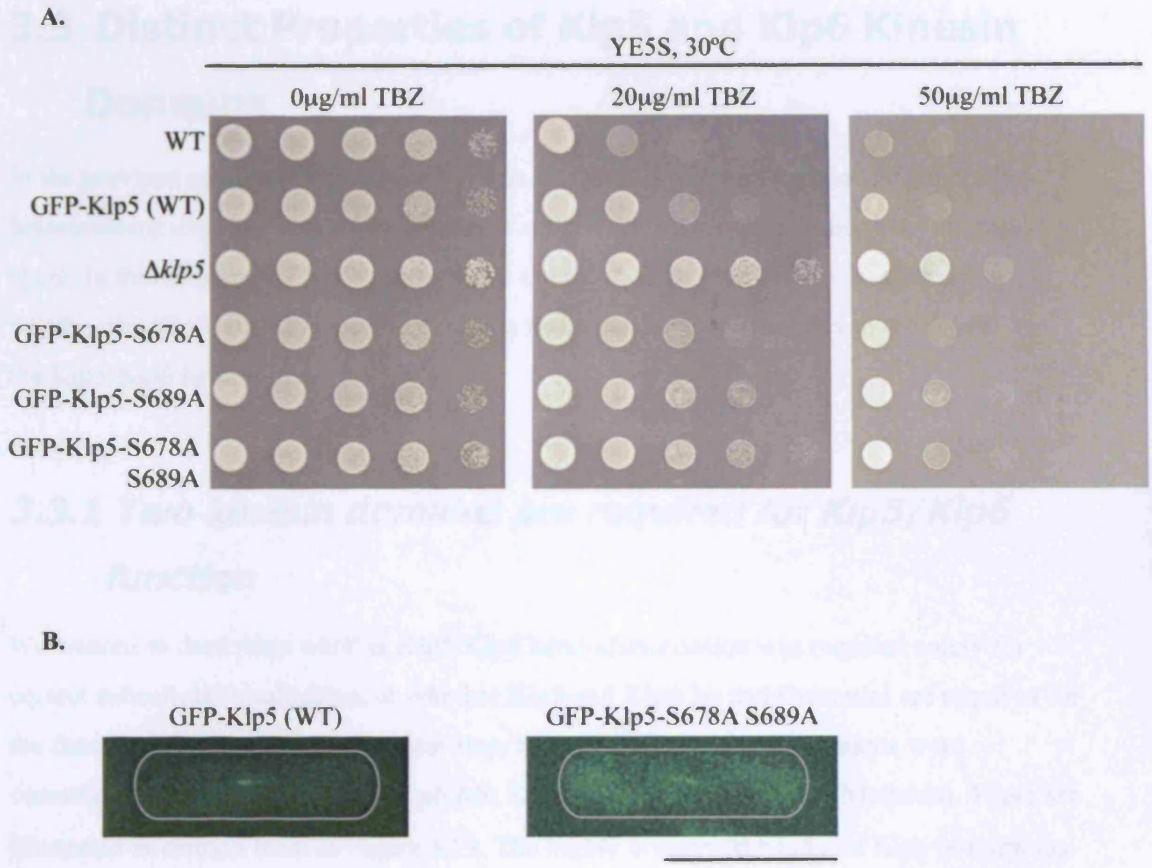

Figure 3.12 Klp5 S>A putative CDK phosphomutants show partial loss of function phenotype

A. Dilution assay of single and double S>A mutants, S678A and S689A, and the double mutant S678A S689A, as described in text and Figure 3.11. Ten-fold serial dilutions were spotted onto YE5S plates, with additions as shown. Plates were incubated for two days at 30°C. **B.** Fluorescence microscopy still images showing localisation of either GFP-Klp5 (WT) or GFP-Klp5-S678A S689A in mitotic cells. Cell outlines marked. Scale bar = 10μm.

3.3 Distinct Properties of Klp5 and Klp6 Kinesin Domains

In the previous section of this chapter, it was established that one function of Klp5/Klp6 heterodimerisation is to ensure their correct subcellular distribution throughout the cell-cycle. In this section, we further investigate the role of heterodimerisation, addressing whether the Klp5 and Klp6 kinesin domains make distinct contributions to the function of the Klp5/Klp6 heterodimer.

3.3.1 Two kinesin domains are required for Klp5/Klp6 function

We wanted to determine whether Klp5/Klp6 heterodimerisation was required solely for correct subcellular localisation, or whether Klp5 and Klp6 N- and C-termini are required for the function of the complex. As a first step, four different truncation mutants were constructed: Klp5 ΔN, Klp5 ΔC, Klp6 ΔN, Klp6 ΔC (see Materials and Methods). These are illustrated in cartoon form in Figure 3.13. The highly conserved Klp5 and Klp6 N-terminus contains the kinesin domain (dark blue), whereas the highly divergent C-terminus contains the identified NLS (red) (section 3.2.6) and an additional conserved region of unknown function (yellow). All truncations contain the coiled-coil domain (light blue) so that they are able to dimerise with their full-length partner Klp molecule. They were designed with the hope that they would still be able to localise to the nucleus. This would allow us to address the necessity of each domain independently of the effect of heterodimerisation on nuclear localisation.

Once the truncations were made, their effect on Klp5/6 activity was assayed for in two different ways: 1) growth on media containing the microtubule depolymerising drug, TBZ, because loss of Klp function causes TBZ resistance; and 2) by assessing viability with *Δalp14;* deletion of *klp5* or *klp6* is synthetic lethal with deletion of *alp14* (Garcia *et al.*, 2002b). A dilution assay was performed to test for TBZ resistance. Figure 3.14 **A.** shows that the *klp5 ΔN* and *klp6 ΔN* strains are as resistant to TBZ as full deletions of *klp5* or *klp6*, indicating loss of Klp function. Conversely, the *klp5 ΔC* or *klp6 ΔC* constructs show no resistance to TBZ; in fact, the *klp5 ΔC* strain possibly shows slight TBZ sensitivity compared to WT. The test for synthetic lethality yielded similar results; Table 3.1 shows that both ΔN strains are synthetic lethal with *Δalp14*, as are full deletions of *klp5* or *klp6*. However, both ΔC strains are viable with *Δalp14*.

The apparent functionality of the ΔC constructs is rather surprising, as the C-termini contain the NLSs, and mutation of just two residues within the Klp5 or the Klp6 NLS causes TBZ resistance (see section 3.2.6). It could be that the presence of just one NLS within the Klp5/6 heterodimer is sufficient for nuclear import of both Klp5 and Klp6; or, if Klp5 and Klp6 enter the nucleus independently, the ΔC truncation mutants may be small enough to enter the nucleus by passive diffusion. Full-length Klp5 and Klp6 have masses of 99kDa and 87.7kDa respectively, and the mass of the ΔC truncations will be approximately half that of the full-length proteins. Molecules with a mass of ~60kDa or less are predicted to be able to enter the nucleus by diffusion through nuclear pores, so it seems possible that Klp5 ΔC and Klp6 ΔC are able to enter the nucleus in this way, although when tagged with GFP (~27kDa) they might be too big. To enter the nucleus passively would certainly require that they enter independently, as a heterodimeric Klp5 ΔC/Klp6 ΔC would certainly be too large; independent nuclear entry is consistent with the results described in section 3.2.2.

The dilution assay gives a preliminary indication that deletion of one Klp C-terminus does not seriously impair Klp function, i.e. perhaps just one C-terminus is sufficient for function. To test whether any C-termini are required for function of Klp5/Klp6, the double C-terminal deletion mutant, *klp5 ΔC klp6 ΔC* was constructed. Figure 3.14 **B.** compares the growth and TBZ resistance of this strain to the single ΔC mutants, full *klp* deletions, and WT. The double ΔC mutant also fails to exhibit a TBZ resistant phenotype, indicating that both C-termini are dispensable for Klp function. This also shows that in truncated mutants, neither C-terminal NLS is required for function of the Klp heterodimer, although full-length Klp5 and Klp6 both require their C-terminal NLSs. Again, this is consistent with the notion that the truncation mutants may enter the nucleus independently by passive diffusion.

The dilution assay in Figure 3.14 **A.** indicates that loss of just one Klp N-terminus abrogates function as assessed by TBZ resistance. One possible explanation for this was that the ΔN constructs and their corresponding full-length partner Klp molecules were unable to localise to the nucleus, as is the case for full deletions of both Klp5 and Klp6 (section 3.2.1). To test this possibility, Klp5 ΔN and Klp6 ΔN were C-terminally tagged with GFP and their localisation observed. Figure 3.15 i) and iii) shows that both of these truncation constructs are able to localise to the nuclear mitotic spindle, although the localisation of Klp5 ΔN-GFP is weak (i). To see whether Klp5 ΔN is sufficient for localising full-length Klp6 to the nuclear mitotic spindle, Klp6-GFP localisation was observed in the *klp5 ΔN* strain (ii); the reciprocal experiment was also carried out i.e. Klp5-GFP localisation was observed in the *klp6 ΔN* strain (iv). In both cases, the full-length protein localises to the nuclear mitotic spindle.

These results demonstrate that the Klp5/6 heterodimer cannot function if either the Klp5 or the Klp6 kinesin domain is deleted, and that this is not due to mislocalisation of the Klp proteins during mitosis. Conversely, neither C-terminal domain is required, presumably because the truncated ΔC molecules are probably small enough to enter the nucleus by diffusion. Alternatively, under these circumstances, sequences located in the remaining N-terminal regions might function as a second NLS.

3.3.2 Klp5 N homodimer and Klp6 N homodimer have different phenotypes

The results in the previous section show that a one-headed Klp5/Klp6 heterodimer is non-functional, demonstrating that two kinesin domains are required. We next investigated whether both Klp5 and Klp6 kinesin domains are required, or whether homodimerisation of either the Klp5 or the Klp6 kinesin domains would be sufficient for function. To do this, the Klp6 kinesin domain was deleted and replaced with the Klp5 kinesin domain to create a chimeric Klp5N/Klp6C molecule. This molecule retains the Klp6 coiled-coil domain so that it should still be able to dimerise with the WT Klp5 molecule. This heterodimer consisting of WT Klp5 and the Klp5N/Klp6C chimera is homodimeric for the Klp5 N-terminus containing the Klp5 kinesin domain, and is thus referred to as the Klp5 N homodimer. The Klp6 N homodimer was constructed in a similar manner (see Figure 3.16 **A.** and Materials and Methods). The growth and TBZ resistance of these strains was tested by a dilution assay, shown in Figure 3.16 **B.** Intriguingly, the Klp5 homodimer and the Klp6 homodimer exhibit very different phenotypes. The Klp5 homodimer strain is extremely sick; it grows very slowly and cells appear dark pink on the Phloxine B plate. It is is also TBZ resistant. This striking phenotype is not due to the loss of the Klp6 N-terminus, as the *klp6 ΔN* strain, included here as a control, exhibits normal growth, like a complete deletion of *klp6* (*Δklp6*). In contrast, the phenotype of the Klp6 homodimer is similar to the *klp* deletion phenotype; it exhibits normal growth and is highly resistant to TBZ.

To further characterise the phenotype of the Klp5 homodimer, another dilution assay was carried out, at different temperatures, and with additional controls included for comparison (Figure 3.17 **A.**). This demonstrates that the slow growth phenotype of the Klp5 homodimer is definitely due to the presence of two Klp5 N-termini; it is neither due to fusing the Klp6 C-terminus to the Klp5 N-terminus (Klp5N/Klp6C *Δklp5* strain), nor to deletion of the Klp 6 N-terminus (*klp6 ΔN* strain). From this we also infer that Klp5 and the chimeric Klp5N/Klp6C molecule are dimerising. The Klp5 homodimer strain also exhibits resistance to TBZ (as shown before) and to low temperature. This is difficult to distinguish because of the slow growth phenotype, but the difference in growth on YE5S compared with growth on

A.

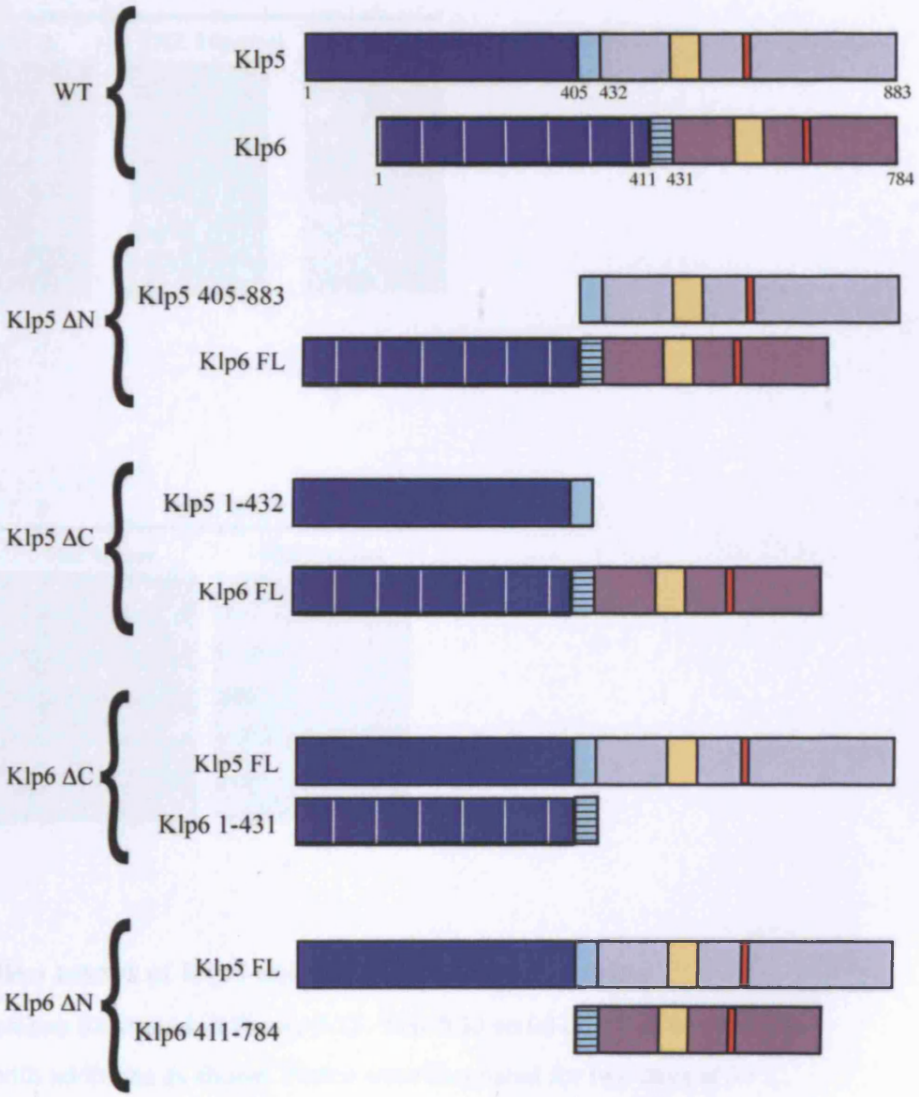

Figure 3.13 Cartoon illustrating Klp5 and Klp6 ΔN and ΔC

Cartoons of WT, Klp5 ΔN, Klp5 ΔC, Klp6 ΔN, Klp6 ΔC. The full-length (FL) partner Klp molecule is shown so the entire Klp5/6 heterodimer is shown for each strain.

A.

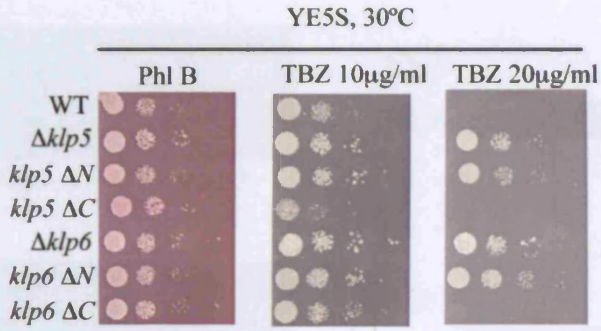

B.

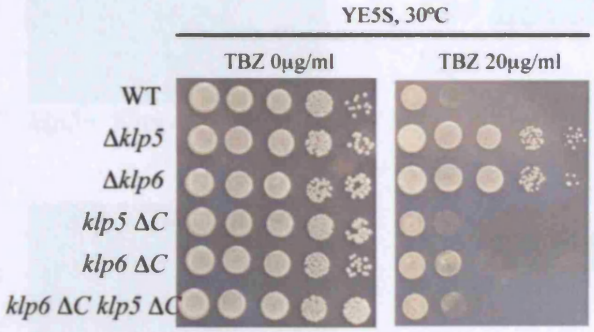

Figure 3.14 Dilution assays of Klp5 and Klp6 ΔN and ΔC strains

Dilution assays on strains illustrated in Figure 3.13. Ten-fold serial dilutions were spotted onto YE5S plates, with additions as shown. Plates were incubated for two days at 30°C.

	Δalp14
WT	V
Δklp5	SL
klp5 ΔN	SL
klp5 ΔC	V
Δklp6	SL
klp6 ΔN	SL
klp6 ΔC	V

Table 3.1 Synthetic lethality of Klp5 and Klp6 ΔN strains with *Δalp14*

V = viable. SL = synthetic lethal.

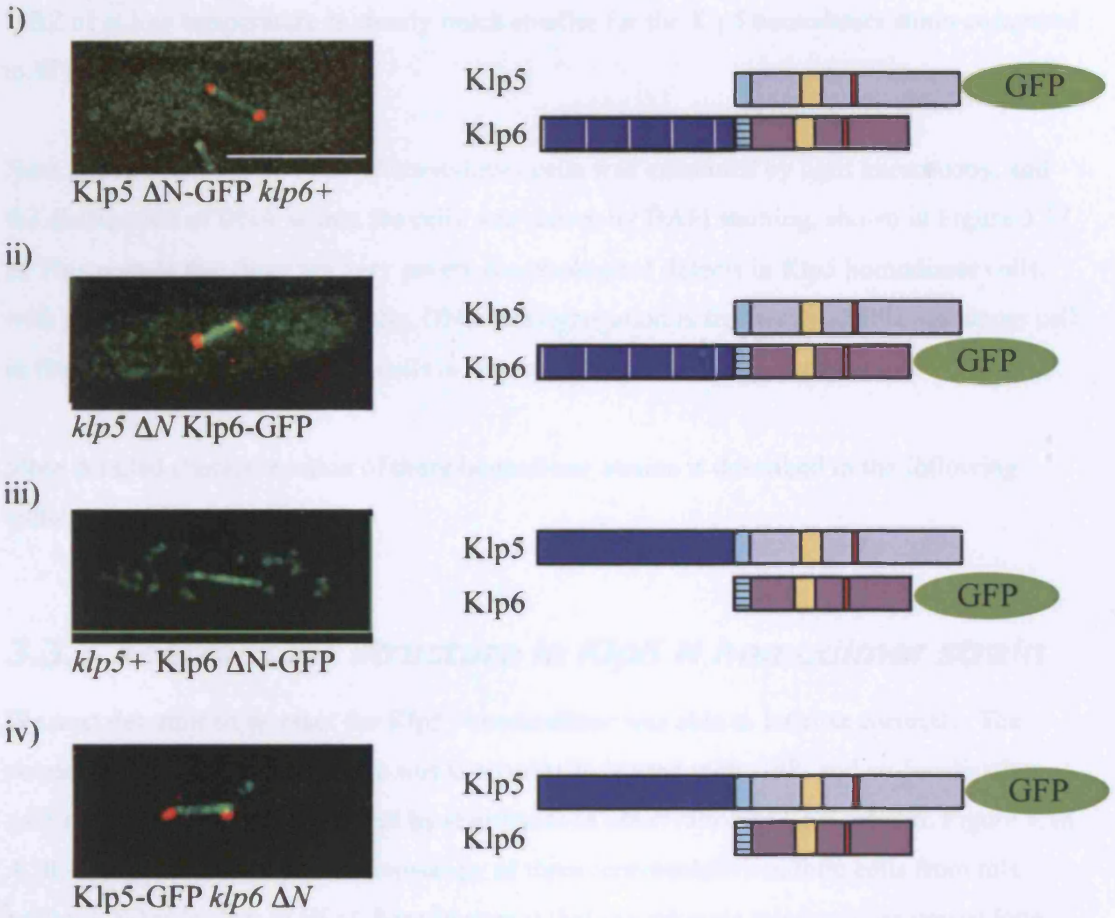

Figure 3.15 Klp5 and Klp6 ΔN localise to the mitotic spindle, and are also sufficient for localisation of the full-length partner Klp

Klp5 ΔN (i) or Klp6 ΔN (iii) were tagged with GFP and mitotic localisation was observed. The localisation of full-length Klp6-GFP (ii) was observed in the *klp5 ΔN* strain, and the localisation of full-length Klp5-GFP (iv) was observed in the *klp6 ΔN* strain. Sad1-dsRED was used as a marker for the SPBs. Cartoons (on right) of Klp5 and Klp6 correspond to those in Figure 3.13, and illustrate which molecule is tagged with GFP in each case. Scale bar = 10μm.

TBZ or at low temperature is clearly much smaller for the Klp5 homodimer strain compared to WT.

Next, the morphology of Klp5 N homodimer cells was examined by light microscopy, and the distribution of DNA within the cells was shown by DAPI staining, shown in Figure 3.17 **B.** This reveals that there are very severe morphological defects in Klp5 homodimer cells, with many long and branched cells. DNA missegregation is frequently visible e.g. upper cell in first panel; the DNA in many cells is dispersed and completely disorganised.

More detailed characterisation of these homodimer strains is described in the following sections.

3.3.3 Aberrant MT structure in Klp5 N homodimer strain

We next determined whether the Klp5 N homodimer was able to localise correctly. The chimeric Klp5N/Klp6C molecule was C-terminally tagged with GFP, and co-localisation with microtubules was determined by simultaneous observation of RFP-tubulin. Figure 3.18 **A, B,** and **C.** show time-lapse microscopy of three representative mitotic cells from this analysis. What is clear in all of these images is that cytoplasmic microtubules persist long into mitosis, and that their depolymerisation is extremely slow. In **A.** chimeric Klp5N/Klp6C-GFP does not localise to the spindle (visualised by RFP-tubulin) during early mitosis, but shows very strong localisation to the long, straight cytoplasmic microtubules that are still present. As mitosis progresses, these microtubules break down very slowly, and Klp5N/Klp6C-GFP gradually accumulates on the mitotic spindle (~12min). **B.** and **C.** show the same phenotype, although filming of these cells started later in mitosis. In the cell shown in **C.**, two long, stable cytoplasmic microtubules are still visible at the stage of mitotic spindle breakdown.

Cytoplasmic microtubules usually disappear at the onset of mitosis because the growth of new microtubules is inhibited (Sagolla *et al.*, 2003). Remaining cytoplasmic microtubules complete their normal cycle of growth and catastrophe, meaning that they disappear quickly because they are dynamic structures. The time-lapse images in Figure 3.18 **A.** – **C.** do not show nucleation of new cytoplasmic microtubules during interphase; rather, existing microtubules are extremely slow to depolymerise. This suggests that microtubule dynamics are severely perturbed in this strain, namely catastrophe frequency and/or depolymerisation rate. The mitotic spindle appears to elongate normally in this strain (clearly visible in Figure 3.18 **A. and B.**), indicating that microtubule growth rate may not be affected.

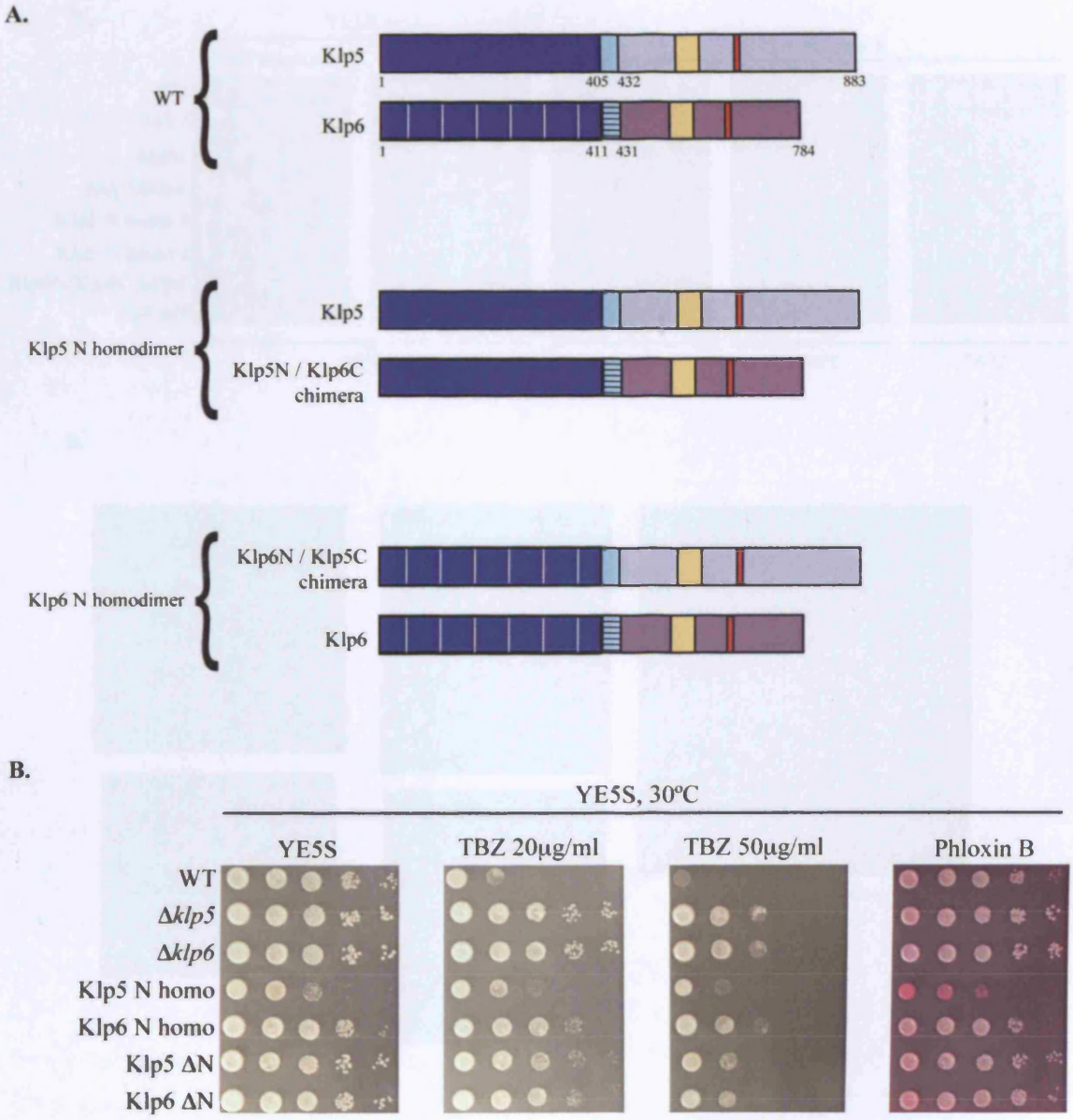

Figure 3.16 Klp5 N homodimer and Klp6 N homodimer

A. Cartoons showing domain structure of WT Klp5/Klp6 heterodimer, Klp5 N homodimer, and Klp6 N homodimer. **B.** Dilution assay showing growth and TBZ resistance of homodimer strains, with various controls. Ten-fold serial dilutions were spotted onto YE5S plates, with additions as shown. Plates were incubated for two days at 30°C.

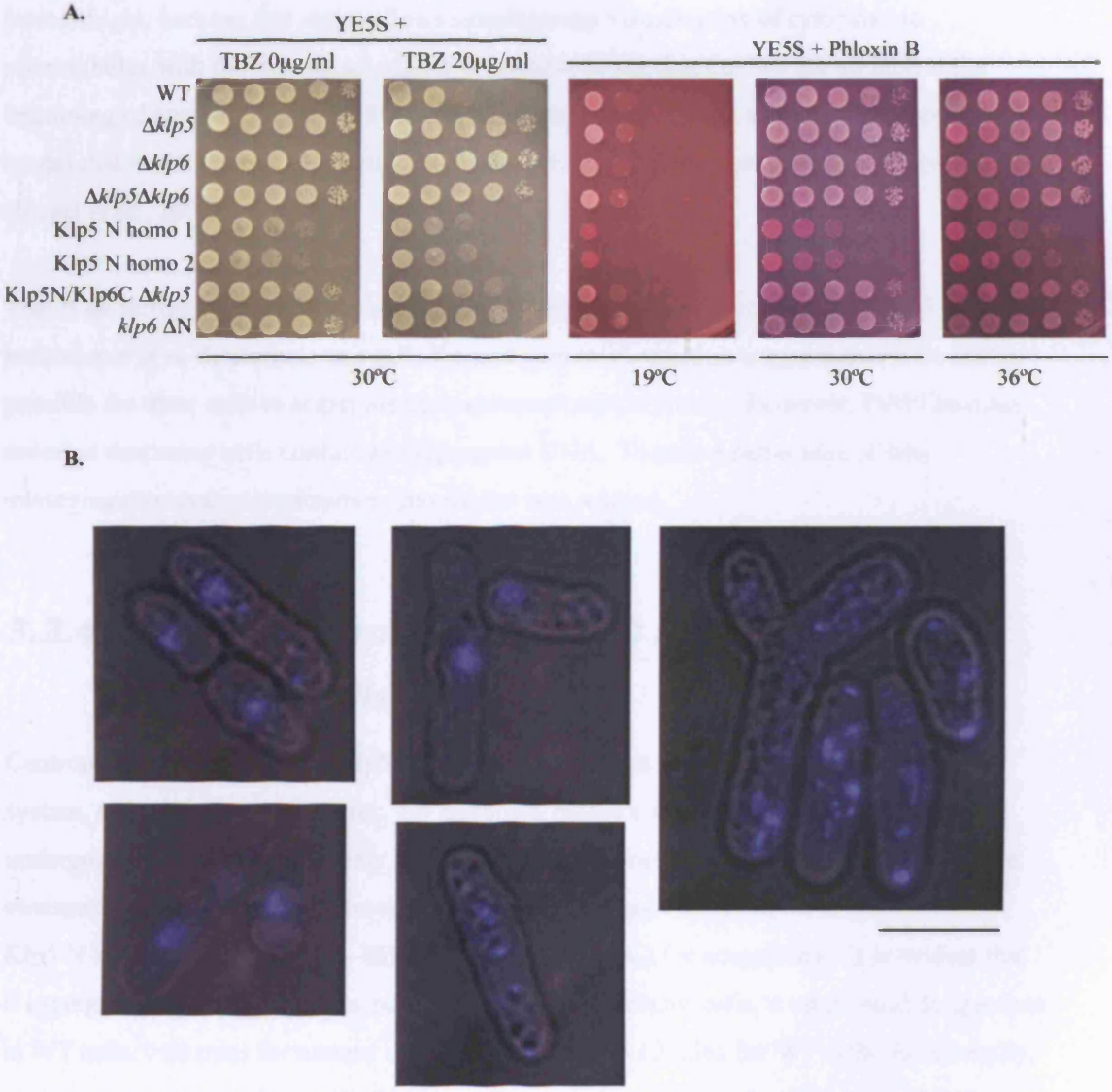

Figure 3.17 Characterisation of Klp5 homodimer phenotype

A. Dilution assay showing growth and TBZ resistance of Klp5 homodimer, with additional controls for comparison. Ten-fold serial dilutions were spotted onto YE5S plates, with additions as shown. Plates were incubated for two days at the indicated temperatures. **B.** Cell morphology and DNA distribution, as revealed by DAPI staining, in Klp5 homodimer cells. Scale bar = 10μm.

Interestingly, because this strain allows simultaneous visualisation of cytoplasmic microtubules with the mitotic spindle, it is possible to see that the two are aligned at the beginning of mitosis (Figure 3.18 **A.** and three other samples, not shown). This supports the model that initial spindle orientation is dictated by the alignment of interphase microtubules (Vogel *et al.*, 2007).

This is an intriguing phenotype, but it does not explain why the presence of a Klp5 N homodimer is so deleterious to a cell. Normal spindle elongation suggests that it would be possible for these cells to segregate their chromosomes correctly. However, DAPI staining revealed that many cells contain missegregated DNA. To gain a better idea of why missegregation occurs, centromere movement was studied.

3.3.4 Aberrant centromere and SPB movement in Klp5 homodimer cells

Centromere movement in the Klp5 homodimer strain was studied using the *cen2*-GFP system, as in the previous chapter. For unknown reasons, the population of cells clearly undergoing mitosis was extremely low in this strain, so only three good quality films were obtained. Figure 3.19 shows kymographs of *cen2*-GFP movement in these three films of Klp5 N homodimer cells **B. i) – iii)**, and in a WT cell **(A.)** for comparison. It is evident that if segregation of *cen2*-GFP does occur in Klp5 N homodimer cells, it takes much longer than in WT cells; >60 mins for mutant cells compared with <10 mins for WT cells. Additionally, centromere movement in the Klp5 N homodimer strain is extremely abnormal, exhibiting phenotypes quite distinct from those visualised in a *Δklp6* mutant (see previous chapter). Cell **i)** in Figure 3.19 **B.** seems to show fairly normal congression, and one *cen2*-GFP focus segregates to a pole. The other appears to segregate, but then continues to move well beyond its destination SPB, while the SPBs simultaneously appear to move slightly closer together. Eventually the 'lost' *cen2*-GFP moves back towards the SPB. The kymograph gives the impression that it may have finally reached its destination SPB; however, a still image taken at 60 mins (Figure 3.19 **C.**) shows that the 'lost' *cen2*-GFP lies well outside the horizontal spindle axis, so correct chromosome segregation has not been achieved at this stage. One possibility is that the lost *cen2*-GFP represents a kinetochore that is unattached to spindle microtubules. However, if that is the case, it is difficult to explain its continual directed movement, first in one direction, then in the opposite direction. It is possible that this kinetochore became detached from the spindle microtubule in the middle of anaphase A, and either reattached later, or was subjected to non-spindle forces that caused directed movement e.g. polar ejection force.

A.

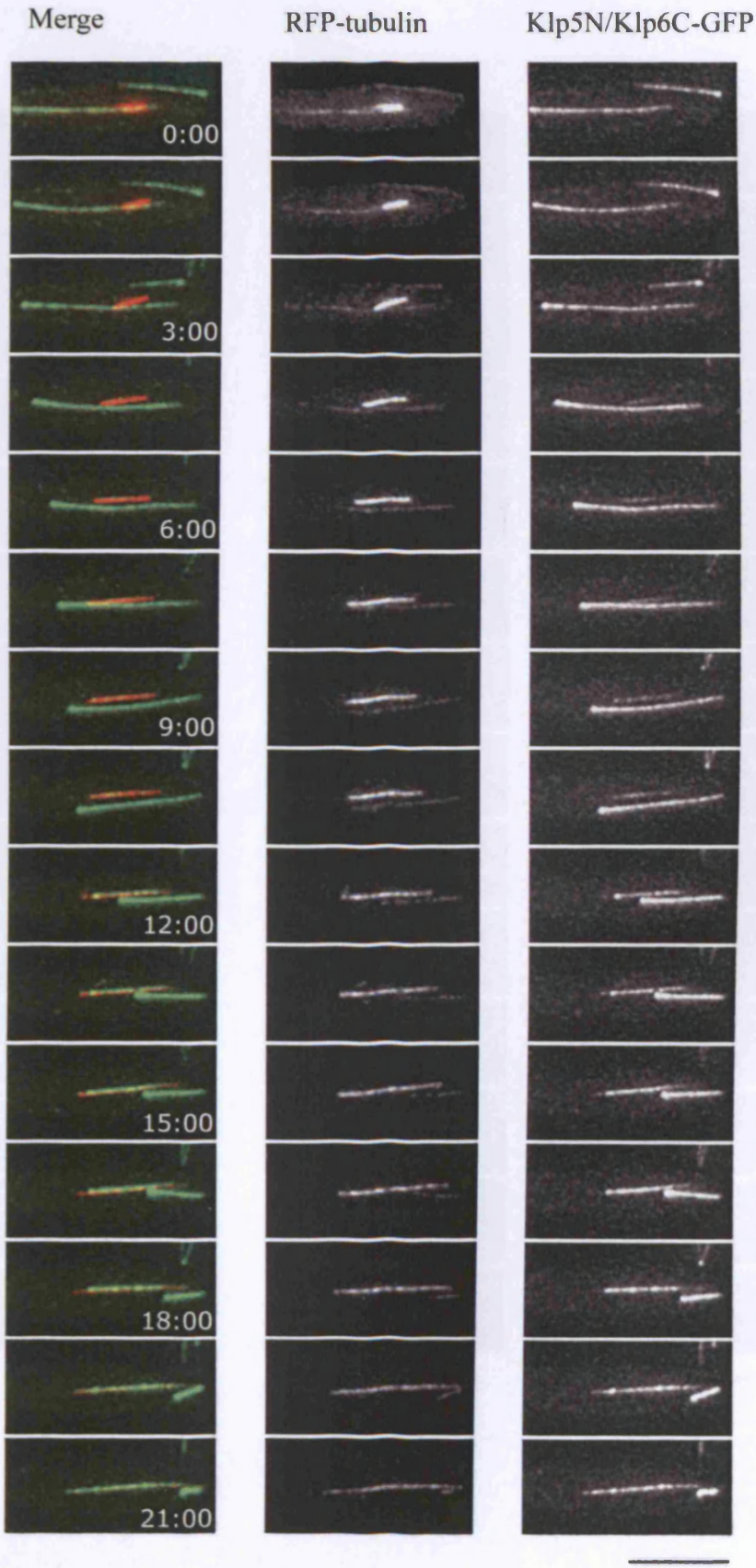
Merge
RFP-tubulin
Klp5N/Klp6C-GFP
0:00
3:00
6:00
9:00
12:00
15:00
18:00
21:00

B.

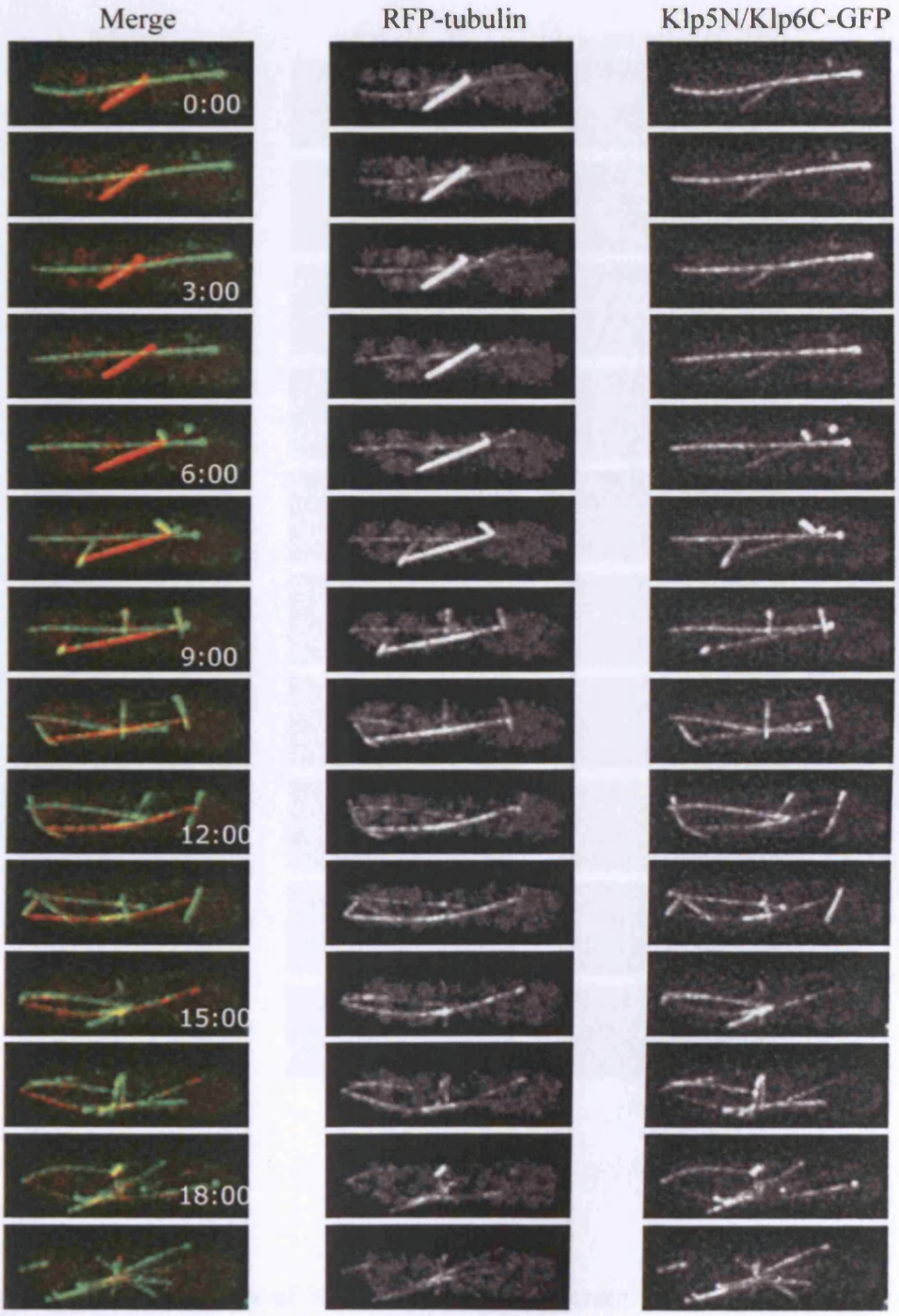
Merge
RFP-tubulin
Klp5N/Klp6C-GFP
0:00
3:00
6:00
9:00
12:00
15:00
18:00

C.

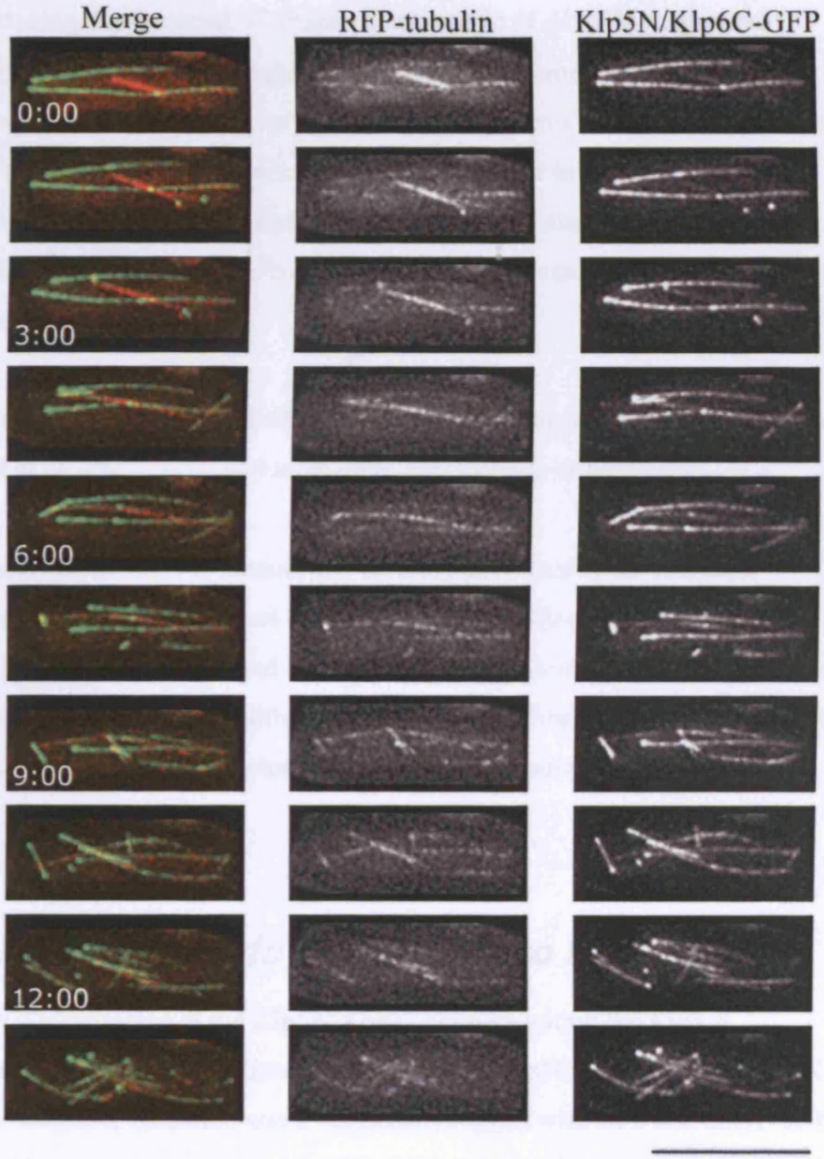

Figure 3.18 Time-lapse microscopy of Klp5 N homodimer strain

A, B, C. Three different time-lapse movies of Klp5N/Klp6C-GFP and RFP-Atb2 (tubulin). Images were acquired every 1:30 mins. Time shown in minutes. Scale bar = 10μm.

Cell **ii)** also shows unusual centromere and SPB movement. Initially, it looks as if monopolar segregation of the *cen2*-GFP signals has occurred, and the SPBs separate at a constant rate, producing the 'inverted V' shape characteristic of *Δklp6* kymographs. However, the SPBs then move closer together, and then the centromeres segregate to opposite poles. Poleward movement is very slow, and centromeres had still not reached their destination SPBs by 60 minutes after start of filming. Again, the initial monopolar segregation would suggest a defect in microtubule-kinetochore attachment. The slow poleward movement could be explained by the very slow depolymerisation rate observed in Klp5 N homodimer cells.

Cell **iii)** exhibits monopolar segregation of the *cen2*-GFP foci, which is usually interpreted as being the result of incorrect, syntelic kinetochore-microtubule attachments.

These analyses confirm that Klp5 N homodimer cells are defective in chromosome segregation. However, the phenotypes are so varied that it is difficult to pin down a single defect in sister chromatid segregation and the nature of the MT-kinetochore attachments. Nonetheless, we envisage that hyperstabilisation of MTs (including spindles) prevents the establishment of stable bipolar MT-kinetochore attachments, leading to chromosome segregation defects.

3.3.5 *Klp6 homodimers do not localise to the nucleus*

Having analysed the localisation of the Klp5N/Klp6C chimera within the Klp5 N homodimer, we next observed the localisation of the Klp6N/Klp5C chimera within the Klp6 N homodimer. The chimeric molecule was C-terminally tagged with GFP and observed by fluorescence microscopy in conjunction with RFP-Atb2 (tubulin) to visualise microtubules. Figure 3.20 **A.** shows representative mitotic and interphase cells. There is no visible localisation of Klp6N/Klp5C-GFP to the mitotic spindle, and localisation along the interphase microtubules is very weak; instead, the chimeric molecule appears to concentrate in one or two bright foci on the microtubules.

The lack of nuclear mitotic localisation is similar to that seen in a single *klp* deletion background, and is consistent with the TBZ resistance observed for the Klp6 N homodimer strain. It was observed in section 3.2.6 that the localisation of GFP-Klp6 to cytoplasmic microtubules is much weaker than that of GFP-Klp5. As the microtubule binding sites are located within the kinesin domain, it may be that a kinesin dimer consisting of two Klp6 kinesin domains has only a very weak affinity for microtubules. An additional explanation could be that the balance of NLS vs. NES activity is upset, resulting in decreased nuclear

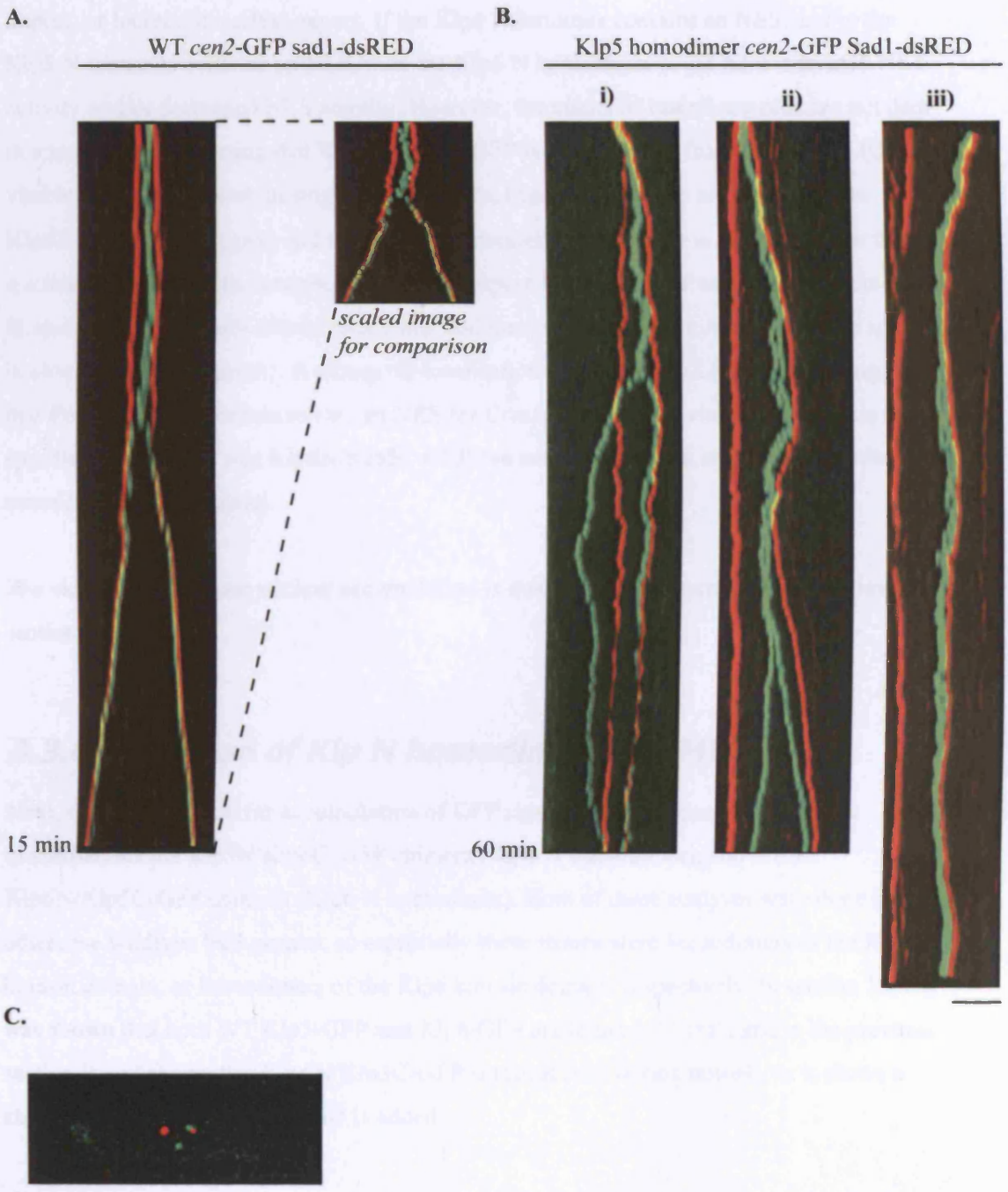

Figure 3.19 Kymographs of *cen2*-GFP movement in WT and Klp5 homodimer cells

Kymographs of *cen2*-GFP movement in individual **A.** WT or **B.** Klp5 homodimer cells. Sad1-dsRED marks the SPBs. Time-lapse images were taken every 30secs, deconvolved and projected, then kymographs were generated. WT image is shown full-size, and scaled for time for direct comparison with Klp5 homodimer kymographs. **C.** Still image taken at 60min from **B. i)**, showing *cen2*-GFP signal outside of spindle axis. Scale bar = 5μm.

import, or increased nuclear export. If the Klp6 N-terminus contains an NES, and/or the Klp5 N-terminus contains an NLS, then the Klp6 N homodimer could have increased NES activity and/or decreased NLS activity. However, the nuclei of interphase cells are not dark in appearance, suggesting that Klp6N/Klp5C-GFP is not excluded from the nucleus (Cf. visible nuclear exclusion in single *Δklp* mutants, Figure 3.1). To try and visualise the Klp6N/Klp5C-GFP signal, and to determine whether this molecule is unable to enter the nucleus, or unable to be retained, the nuclear export inhibitor LMB was added. Figure 3.20 **B.** shows a field of cells 60min after LMB addition; weak localisation to the mitotic spindle is observed (yellow arrow). A change in localisation in response to LMB strongly suggests that this chimeric molecule retains an NES for Crm1 binding. The visible localisation to the spindle demonstrates that Klp6N/Klp5C-GFP can enter the nucleus, and that it does have some MT binding activity.

The extent of interphase nuclear accumulation is quantified and described in the following section.

3.3.6 Response of Klp N homodimers to LMB

Next, the extent of nuclear accumulation of GFP signal in the presence of LMB was quantified for the Klp5N/Klp6C-GFP chimera (Klp5 N homodimer), and for the Klp6N/Klp5C-GFP chimera (Klp6 N homodimer). Both of these analyses were done in an otherwise wildtype background, so essentially these strains were homodimers of the Klp5 kinesin domain, or homodimers of the Klp6 kinesin domain, respectively. In section 3.2.2 it was shown that both WT Klp5-GFP and Klp6-GFP are targets of Crm1, and in the previous section it was shown that Klp6N/Klp5C-GFP is too, at least during mitosis, as it shows a change in localisation when LMB is added.

Quantification of fluorescence intensity was performed as before: 60 minutes after LMB addition, images of the cells were captured by fluorescence microscopy, and then line profiles were constructed to show the distribution of fluorescence intensity along the longitudinal axis of the cell. Results for Klp6N/Klp5C-GFP are shown in Figure 3.21 **B.**, with the results for WT Klp5-GFP (**A.**) shown again for comparison. Klp6N/Klp5C-GFP does not appear to accumulate in interphase cells at all in response to LMB, although it was established in the previous section that this molecule is a target of Crm1, at least in mitosis. WT Klp5-GFP only shows modest levels of nuclear accumulation in interphase cells, so this effect is probably due to elements in the Klp5 C-terminus, as this region is common to both the Klp5-GFP and the Klp6N/Klp5C-GFP molecules. As suggested previously, it may be that the Klp5 NLS is down-regulated in some way during interphase. Although nuclear

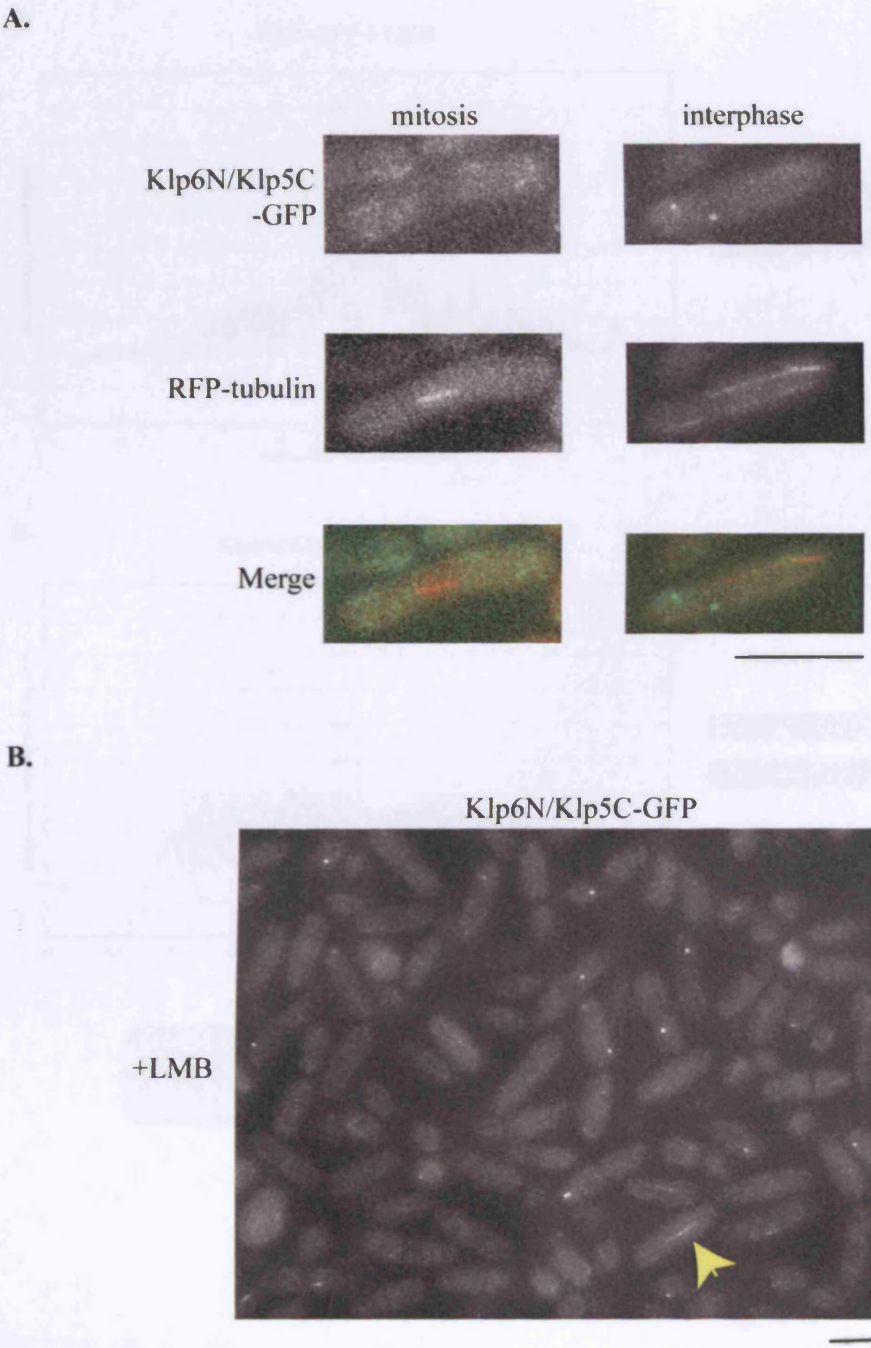

Figure 3.20 Localisation of Klp6N/Klp5C-GFP

A. Before and **B.** after LMB addition. **A.** Fluorescence microscopy of the Klp6 N homodimer strain. Klp6N/Klp5C-GFP was visualised in conjunction with RFP-Atb2 (tubulin). Representative mitotic and interphase cells are shown. **B.** Field of cells 60min after LMB addition. Yellow arrow shows localisation of Klp6N/Klp5C-GFP to mitotic spindle. Scale bars = 10μm.

A.

Klp5-GFP + LMB

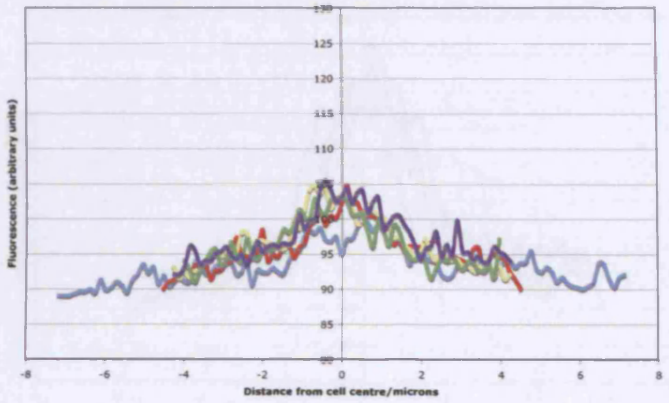

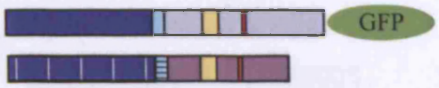

B.

Klp6N/Klp5C-GFP + LMB

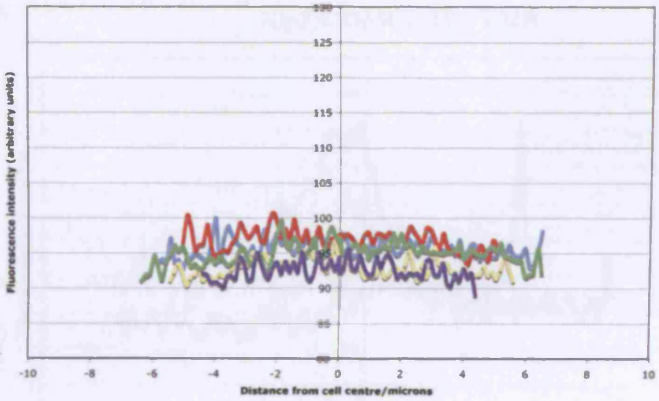

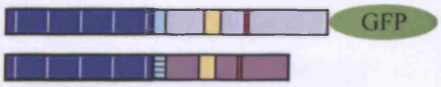

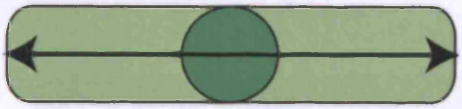

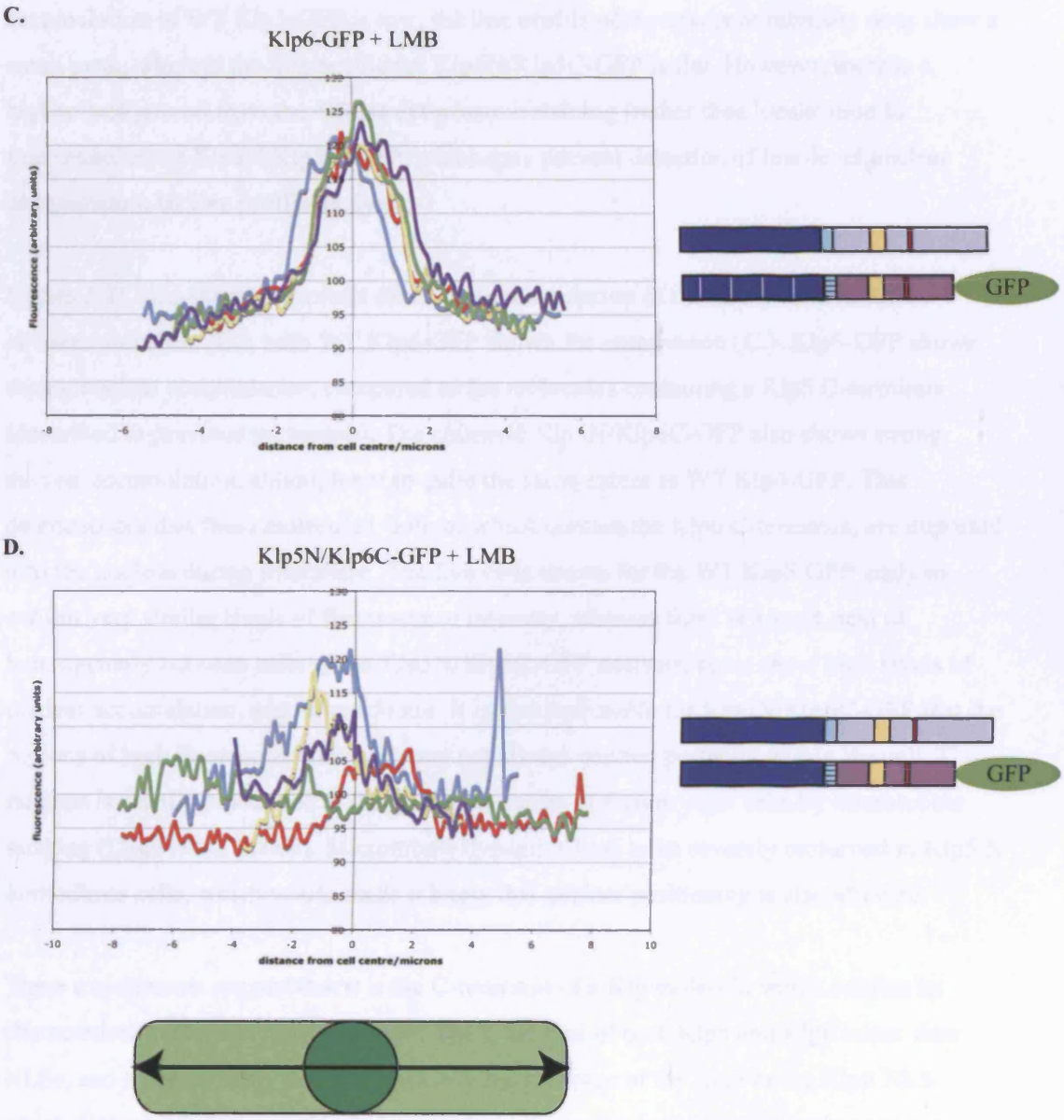

Figure 3.21 Response of Klp N homodimers to LMB

Line profiles of fluorescence intensity showing GFP nuclear accumulation in interphase cells 60min after LMB addition. A cartoon of each construct is shown next to the corresponding graph. A line was drawn along the longitudinal axis of each cell (n=5 for each strain) and the fluorescence intensity calculated using ImageJ software.

accumulation of WT Klp5-GFP is low, the line profile of fluorescence intensity does show a small peak, whereas the line profile for Klp6N/Klp5C-GFP is flat. However, there is a higher background from the diffuse cytoplasmic staining (rather than localisation to microtubules) of Klp6N/Klp5C-GFP, which may prevent detection of low-level nuclear accumulation by line profile analysis.

Figure 3.21 also shows the extent of nuclear accumulation of the Klp5N/Klp6C-GFP chimera molecule (**D.**), with WT Klp6-GFP shown for comparison (**C.**). Klp6-GFP shows strong nuclear accumulation, compared to the molecules containing a Klp5 C-terminus (described in previous paragraph). The chimeric Klp5N/Klp6C-GFP also shows strong nuclear accumulation, although not to quite the same extent as WT Klp6-GFP. This demonstrates that these molecules, both of which contain the Klp6 C-terminus, are imported into the nucleus during interphase. The five cells shown for the WT Klp6-GFP analysis exhibit very similar levels of fluorescence intensity, whereas there is a great deal of heterogeneity between cells in the Klp5N/Klp6C-GFP analysis; some show high levels of nuclear accumulation, and others do not. It is also noticeable for Klp5N/Klp6C-GFP that the regions of high fluorescence intensity are not always centred perfectly within the cell. The nucleus is usually positioned at the geometric centre of fission yeast cells by microtubule pushing (Daga *et al.*, 2006b). Microtubule dynamics look to be severely perturbed in Klp5 N homodimer cells, which would make it likely that nuclear positioning is also affected.

These experiments suggest that it is the C-terminus of a Klp molecule which confers its characteristic pattern of nuclear import. The C-termini of both Klp5 and Klp6 house their NLSs, and it seems likely that it is primarily the presence of the Klp5 or the Klp6 NLS which dictates whether a molecule is imported into the nucleus during interphase or not.

3.3.7 Klp mutants have altered MT dynamics

The images in Figure 3.18 show that cytoplasmic microtubules disappear very slowly in the Klp5 N homodimer strain, suggesting that microtubule dynamics are perturbed. To investigate this further, rates of microtubule growth and shrinkage and catastrophe frequency were measured in WT, *Δklp5, Δklp6,* Klp5 N homodimer and Klp6 N homodimer strains. To visualise microtubules in each of these strains, P3-GFP-Atb2 was introduced at the genomic *atb2* locus. P3 contains the strong *nmt1* promoter, which is induced in the absence of thiamine. Overexpression of tubulin is highly deleterious to cells, so cultures were grown in +thiamine conditions. Microtubule growth and shrinkage rates were calculated by taking time-lapse movies of cells expressing GFP-Atb2, and then constructing kymographs from single anti-parallel microtubule bundles (illustrated in Figure 3.22 **C.**). The slopes of

growing or shrinking microtubules were measured to give growth and shrinkage rates. The number of catastrophes for a single MT bundle was also observed. Only cytoplasmic microtubules were analysed, as it has been established that Klp molecules fail to localise to the spindle in *Δklp5, Δklp6* and Klp6 N homodimer strains.

Figure 3.22 **A.** shows microtubule growth (blue bars) and shrinkage (red bars) rates for the five strains analysed. The average rate of MT growth in WT cells was 3.27μm/min, similar to previously published rates of 3.18μm/min reported by Sagolla *et al.* (2003) and 3.0μm/min reported by Busch and Brunner (2004), but lower than the rate of 6.36μm/min reported by Grallert *et al.* (2006). This rate was similar in the various Klp mutant strains analysed too, indicating that Klp5 and Klp6 do not influence MT growth in interphase. The average rate of MT shrinkage in WT cells was 8.12μm/min, which is much less than the rate of 16.99μm/min reported by Sagolla *et al.* (2003), but consistent with the rate of 8.5μm/min reported by Busch and Brunner (2004), and not too dissimilar from the rate of 12.0μm/min reported by Grallert *et al.* (2006). Although different groups report different rates of microtubule growth and shrinkage, a comparison between our WT rate and the Klp mutant rates is still valid. The shrinkage rates are significantly reduced in the *Δklp5, Δklp6* and Klp6 N homodimer strains to 6.13μm/min, 5.90μm/min and 6.20μm/min, respectively. Intriguingly, the shrinkage rate is reduced to an even greater extent in the Klp5 N homodimer strain, to 3.60μm/min.

Figure 3.22 **B.** shows the frequency of catastrophes per MT bundle (i.e. half of one anti-parallel bundle as shown in **C.**). In wildtype cells the catastrophe frequency is more than 0.9/min; this is drastically reduced to less than 0.3/min in all the different Klp mutants, and to less than 0.2/min in the Klp5 N homodimer strain. We note that our WT catastrophe rate is much greater than the 0.33/min reported by Busch and Brunner (2004). Again, the reason for this is unclear, but it does not invalidate comparison between our WT and Klp mutant frequencies.

Observation of long microtubules and resistance to cold-shock and microtubule-destabilizing drugs had previously indicated that *Δklp* mutant cells have hyperstable microtubules. Now these analyses show that microtubules are stabilised in Klp mutants because both the microtubule shrinkage rate and the catastrophe frequency is reduced. Interestingly, microtubules are even more stabilised in the Klp5 N homodimer strain.

A.

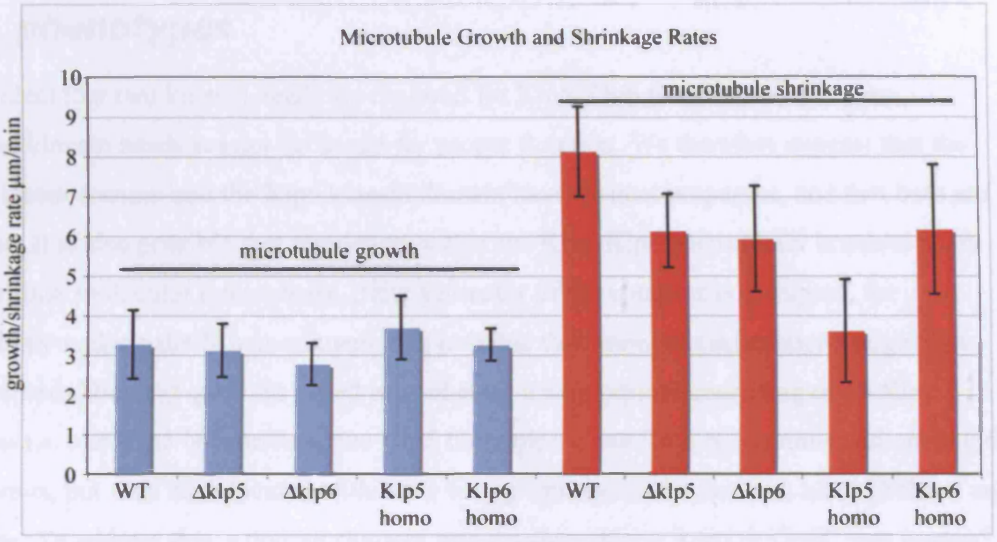

B.

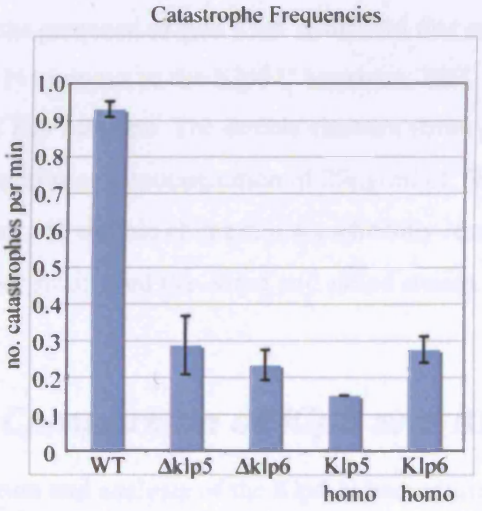

C.

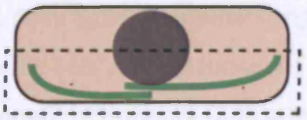

Figure 3.22 Measurements of Microtubule Dynamics

Microtubule dynamics were measured by kymographic analysis of anti-parallel MT bundles, as depicted in cartoon (**C.**). **A.** Rates of microtubule growth (blue bars) and shrinkage (red bars) were compared in WT, *Δklp5*, *Δklp6*, Klp5 N homodimer and Klp6 N homodimer strains. **B.** Catastrophe frequencies (number of catastrophes per MT bundle per minute) were calculated for the same strains as in **A.** $n = 5$. Error bars show standard deviation.

3.3.8 Double chimera partially rescues Klp N homodimer phenotypes

It is evident that two kinesin heads are required for Klp5/Klp6 function, but that two identical kinesin heads are not sufficient for proper function. We therefore suggest that the Klp5 kinesin domain and the Klp6 kinesin domain have distinct properties, and that both are required. It is also possible that regulation within the Klp5/Klp6 heterodimer is achieved by intra- or intermolecular interactions. If the geometry of the complex is disrupted, for example by making the N homodimers, it is possible that important interactions might also be disrupted. The next question posed was whether a heterodimer consisting of all Klp domains i.e. one Klp5 N-terminus, one Klp5 C-terminus, one Klp6 N-terminus and one Klp6 C-terminus, but with each located within the wrong intramolecular context, would behave as wildtype. To address this, a double chimera was constructed, i.e. Klp5N/Klp6C was crossed to Klp6N/Klp5C. The viability and TBZ resistance of this strain was initially tested by a dilution assay, shown in Figure 3.23. The growth defect of the Klp5 N homodimer is rescued by expression of the chimeric Klp6N/Klp5C instead of WT Klp5, once again demonstrating that it is the presence of two Klp5 N-termini that is detrimental to the cell, not the fusing of the Klp5 N terminus to the Klp6 C terminus. TBZ resistance is a good preliminary indicator of loss of Klp function. The double chimera strain grows as well as the *Δklp5* or a *Δklp6* deletion strains at a concentration of 20μg/ml of TBZ. However, at the higher concentration of 50μg/ml, the double chimera is significantly less resistant to TBZ than both the Klp6 N homodimer strain, and the *Δklp5* and *Δklp6* strains.

3.3.9 Comparison of Klp5 and Klp6 protein sequences

Construction and analysis of the Klp5 N homodimer and Klp6 N homodimer strains revealed that the Klp5 and Klp6 kinesin domains must make distinct contributions to the function of the Klp5/Klp6 heterodimer. To try and understand the reasons for the drastic differences observed between the two N homodimer strains, alignments were made of kinesin domain protein sequences for Klp5, Klp6 and Kip3 (the budding yeast Kinesin-8 member), shown in Figure 3.24. These three Kinesin-8 proteins show a very high level of sequence conservation in their kinesin domains. Klp5 and Klp6 also share identity in the ~100 amino acids N-terminal to the start of the kinesin domain. Identity is shared with Kip3 in this region too, although the Kip3 sequence contains two inserts of 28 and ~10 amino acids not present in Klp5 or Klp6.

The Klp5 N homodimer appears to have a very high affinity for MTs, whereas the Klp6 N homodimer appears to have a low affinity. One possible reason for this is that the Klp5 and

Klp6 kinesin domains differ in their ability to bind and hydrolyse ATP. However, inspection of the P-loop, Switch I and Switch II motifs that together make up the kinesin nucleotide binding pocket revealed that they are perfectly conserved in both Klp5 and Klp6. This makes it seem unlikely that they would differ significantly in their ability to bind or hydrolyse ATP.

Another possible reason for the differences observed between Klp5 and Klp6 N homodimers is that there are differences in the regions that contact microtubules. Klp5 and Klp6 kinesin domains do not contain the highly conserved KVD, KEC, or positively charged necks of the Kinesin-13 family that are involved in MT binding. Likewise, the K-loop insert in loop L12 that is involved in MT binding in the KIF1 family of monomeric kinesins is not conserved in Klp5 and Klp6. A number of positively charged residues within loop L8 were found to be important for the association of Kinesin-1 with the microtubule (Woehlke *et al.*, 1997). The sequence of the L8 region is not very highly conserved between Kinesin-1 and Klp5 or Klp6 (29% identity and 46% homology between Kinesin-1 and Klp5), but there are a number of positively charged lysine (K) or arginine (R) residues within the Klp5, Klp6 and Kip3 sequences that could contribute to electrostatic interactions with the microtubule (circled residues in Figure 3.24). Interestingly, Klp5 contains four positively charged residues within this region, whereas Klp6 contains only two. Kip3, which functions as a homodimer, contains three positively charged residues within the same region. We hypothesise that the Klp5 kinesin domain has a higher affinity for microtubules than the Klp6 kinesin domain, because the Klp5 L8 region contains more positively charged residues that could contribute to microtubule binding. It would be of great interest to test this hypothesis by mutating the L8 positively charged residues in Klp5 and Klp6 to see whether their affinity for microtubules is altered.

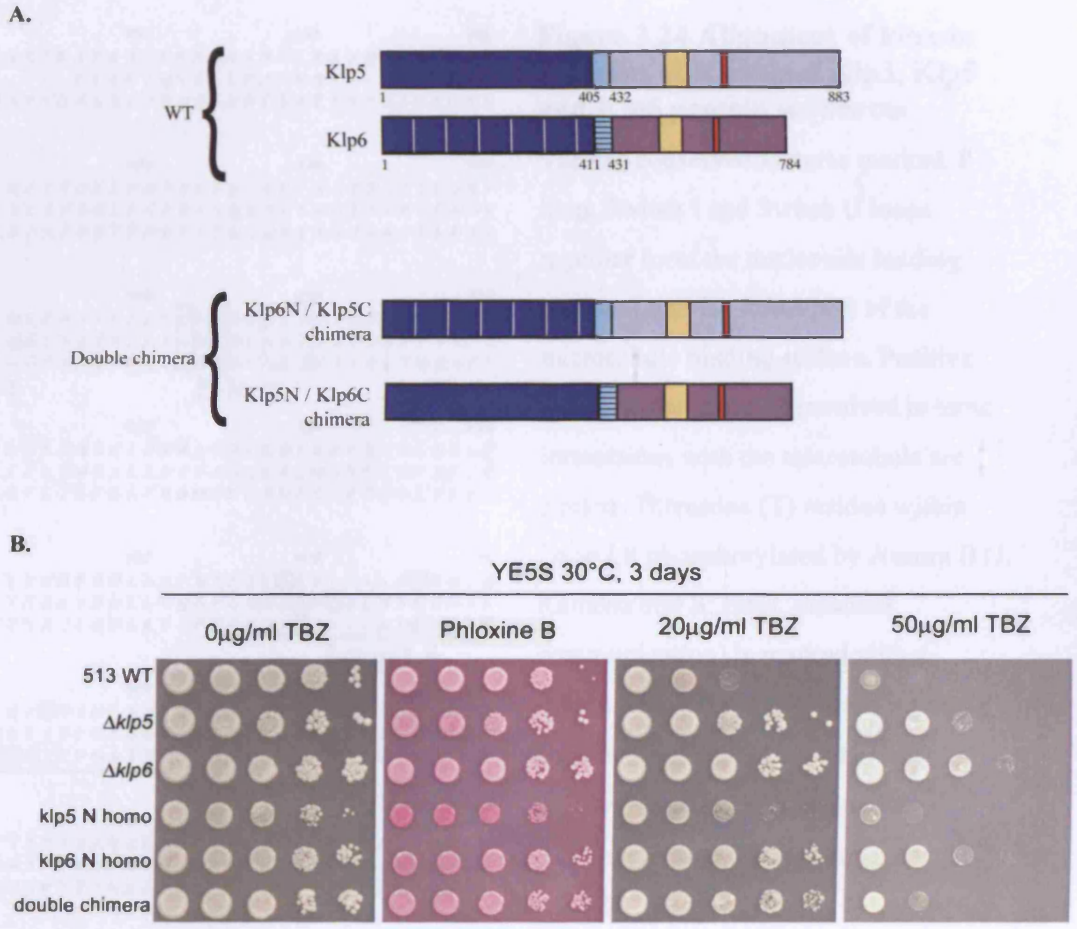

Figure 3.23 Klp Double Chimera Strain

A. Cartoons showing domain structure of the Klp5/6 double chimera. The chimera was constructed by crossing Klp5N/Klp6C to Klp6N/Klp5C. **B.** Dilution assay showing growth and TBZ resistance of double chimera strain compared to WT, *Δklp* mutants and N homodimer strains. Ten fold dilutions of each strain were spotted onto YE5S plates, with additions as shown. Plates were incubated for three days at 30°C.

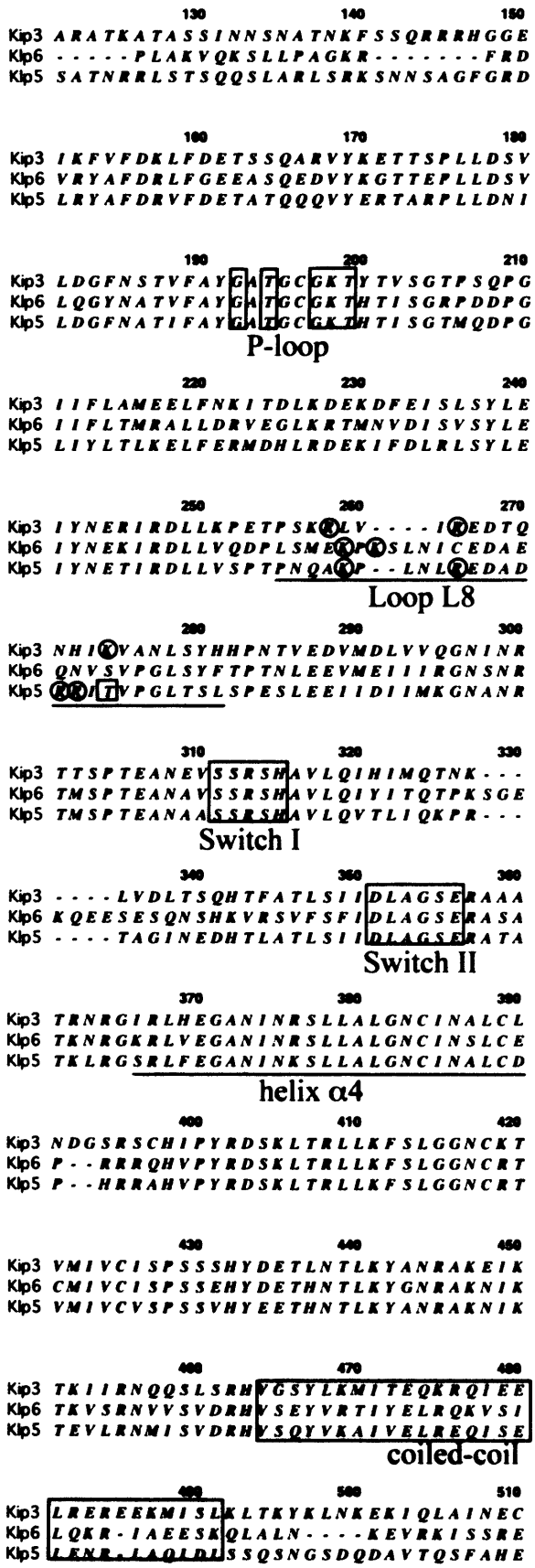

Figure 3.24 Alignment of kinesin domains of Kinesin-8 Kip3, Klp5 and Klp6 protein sequences

Various conserved features marked. P-loop, Switch I and Switch II loops together form the nucleotide binding pocket. Loop L8 forms part of the microtubule binding surface. Positive residues that could be involved in ionic interactions with the microtubule are circled. Threonine (T) residue within Loop L8 phosphorylated by Aurora B (J. Kamenz and S. Hauf, personal communication) is marked with a square. Helix α4 is important for energy transduction, and involved in MT depolymerisation in Kinesin-13s. Alignment done using MacVector v.9.5.2

3.4 Summary

The data presented in this chapter reveal that Klp5/Klp6 heterodimerisation is essential for function. The first section of this chapter dealt with the significance of heterodimerisation in relation to subcellular localisation, while the second section aimed to address whether heterodimerisation was also significant because Klp5 and Klp6 make different contributions to the complex.

It was found that Klp5-GFP fails to localise to the nucleus in *Δklp6* cells, and similarly, Klp6-GFP cannot localise to the nucleus in *Δklp5* cells. LMB inhibits nuclear export of Klp5-GFP and Klp6-GFP, showing that they are both targets of the exportin-1 Crm1. By inhibiting nuclear export using LMB, it was shown that Klp5-GFP or Klp6-GFP are able to enter the nucleus in the absence of the partner Klp molecule, but are not retained. It was also revealed that Klp6 must shuttle between the nucleus in both interphase and mitosis, as it accumulates strongly in interphase nuclei after LMB. Conversely, Klp5-GFP does not accumulate strongly in interphase nuclei, suggesting that its nuclear import may be cell-cycle regulated in some way.

Results from immunoprecipitation experiments comparing Klp5 WT with a coiled-coil mutant of Klp5 suggest that the Klp5 coiled-coil is required for heterodimerisation with Klp6. However, there were problems with GFP-Klp5 detection in whole cell extracts by Western blotting. Deletion of the Klp6 coiled-coil showed that this region does not contain an NES, but that it is required for proper nuclear localisation of both Klp6 and Klp5.

It was found that Klp5 and Klp6 both contain an NLS in their C-termini, within a region that is highly conserved between the two proteins. Two consensus CDK phosphorylation sites lie in very close proximity to the Klp5 NLS. Mutation of S689 reduced, but did not completely abolish, nuclear localisation of Klp5, raising the possibility that Klp5 nuclear entry is regulated by CDK activity. It seems unlikely that Klp5 is anchored in the cytoplasm by microtubules during interphase to prevent it entering the nucleus, as depolymerisation of microtubules did not increase the extent of Klp5 nuclear accumulation in response to LMB.

By making deletions of Klp5 or Klp6 N- or C-termini, it was established that two N-termini (containing the kinesin domains) are necessary for Klp5/Klp6 function, whereas both C-termini are dispensable. The necessity of two kinesin domains was independent of nuclear localisation, as the ΔN constructs localise to the nucleus.

It was next established that two identical kinesin domains are also insufficient for correct Klp function. The Klp5 N homodimer strain shows severe growth, morphology and chromosome segregation defects. The Klp6 N homodimer does not localise to the nuclear mitotic spindle, although addition of LMB shows that it is able to enter the nucleus during mitosis. We speculate that the differences between the Klp5 and Klp6 N homodimers could be accounted for by different microtubule-binding strengths of the two different kinesin domains. Comparison of the Klp5 and Klp6 protein sequences revealed that Klp5 contains more positively charged residues within loop L8, a region of the kinesin domain known to directly contact MTs.

Construction of the double chimera (Klp5N/Klp6C, Klp6N/Klp5C) restored cell viability, compared to the Klp5 N homodimer; however, it did not restore WT Klp activity, as the strain exhibits TBZ resistance.

3.5 Discussion

In this chapter we show that Klp5 and Klp6 are inter-dependent for their localisation to the nucleus, and therefore for their localisation to the nuclear mitotic spindle. Both proteins are able to enter the nucleus independently, but in the absence of their partner Klp, nuclear export activity exceeds nuclear import activity, resulting in cytoplasmic localisation. The sensitivity of both Klp5 and Klp6 to LMB shows that they are targets of Crm1-mediated export; however, the leucine-rich NESs associated with Crm1 export have not been identified in Klp5 or Klp6 in this study.

Klp5 and Klp6 each contain only one coiled-coil region. Kinesin-1, and other kinesins, dimerise via their coiled-coils, so this seemed the most obvious site for Klp5/Klp6 heterodimerisation. Consistent with this supposition, an immunoprecipitation experiment revealed that mutation of the Klp5 coiled-coil domain greatly reduced its binding to Klp6. An attractive model to explain the necessity of heterodimerisation for nuclear retention is one of intermolecular NES masking i.e. that the physical association of Klp5 and Klp6 makes their NESs inaccessible to exportins, so that they cannot be transported out of the nucleus. Deletion of the Klp6 coiled-coil (Klp6 ΔCC) showed that this region does not contain an NES, because the Klp6 ΔCC molecule did not show increased localisation to the nucleus, as would be expected for an NES mutant; instead it showed reduced localisation to the nucleus. Interestingly, the nuclear localisation of Klp5 was also reduced in the Klp6 ΔCC mutant. This is consistent with the idea that Klp5 and Klp6 physically associate via their coiled-coil domains, and that this physical association is required for prevention of premature nuclear export during mitosis. Although the Klp6 NES does not reside within the

interaction domain, NES masking is still a mechanistic possibility; perhaps Klp5 and Klp6 also interact at regions outside of the coiled-coil to occlude each others' NESs, or perhaps the association via their coiled-coils induces a conformational change in each protein such that the NES is buried in some way (i.e. intramolecular masking induced by an intermolecular protein-protein interaction).

It is also possible that the combined action of both Klp5 and Klp6 NLSs together is sufficient to localise them to the nucleus, whereas just one NLS is not sufficient. However, we think that this possibility is unlikely. We show that both Klp5 and Klp6 are targets of Crm1-mediated export, and that export activity exceeds import activity for both of the Klp monomers. It therefore seems that if the individual nuclear import and export activities of Klp5 and Klp6 were simply added together in the context of the heterodimer, export activity would still exceed import activity. For this reason we favour a model of NLS and NES regulation.

Classical, canonical NLSs were identified in the C-termini of Klp5 and Klp6, so both are probably targets of one or both of the fission yeast importin-α proteins Imp1 and Cut15 (Umeda *et al.*, 2005). The association and dissociation of importin-α and -β from their cargo is regulated by Ran associated with either GTP or GDP. It was recently shown that fission yeast Alp7/TACC is a target of the Ran-GTPase machinery and this is required for spindle formation, analogous to Ran-dependent spindle assembly in higher eukaryotes (Sato and Toda, 2007). In this study we propose that Klp5 and Klp6 are additional mitotic targets of importins in fission yeast, and are required for proper formation of the mitotic spindle and for regulation of kinetochore-MT attachments.

It seems likely that the NESs of Klp5 and Klp6 are also located in the C-termini of the proteins. We have established that the NLSs reside in the C-terminus, and we have also shown that ΔN Klp mutants are able to localise to the nucleus, but do not show excessive nuclear accumulation. ΔC Klp mutants do not show a loss of Klp function phenotype, so we presume that they too are able to localise to the nucleus. If the NESs were located in the N-termini of the Klp molecules, it would be expected that ΔN molecules would show nuclear accumulation (as NLS activity would exceed NES activity), and that ΔC molecules would show nuclear exclusion (as NES activity would exceed NLS activity). As this does not happen, we propose that Klp5 and Klp6 contain no / negligible NLS and NES activity in their N-termini, and that the ΔC molecules are free to diffuse into and out of the nucleus. The ΔN molecules are proposed to contain both NLS and NES activity and can therefore be actively transported into and out of the nucleus. This model would predict that the ΔN

molecules would respond to LMB treatment, whereas the ΔC molecules should not, which could be easily tested.

The nuclear import of Klp6 seems to be straightforward and easy to define. Mutation of the Klp6 NLS completely abolishes entry of Klp6 in both interphase and mitosis, and addition of LMB causes nuclear accumulation in interphase cells, and restores localisation to the nuclear spindle during mitosis in *Δklp5* cells. These results indicate that the identified NLS is probably the sole NLS in this molecule, and that it is constitutively active throughout the cell cycle: Klp6 localises to the nucleus during mitosis, and nuclear accumulation in response to LMB indicates that Klp6 must be constantly shuttling between the nucleus and the cytoplasm during interphase. In contrast, nuclear import of Klp5 seems more complex. Mutation of the Klp5 NLS abolishes entry of Klp5 in both interphase and mitosis. However, some low-level NLS activity must remain, as addition of LMB results in the localisation of some Klp5 to the mitotic spindle. It is possible that Klp5 contains an additional, very weak NLS, whose activity in the NLS mutant in the absence of LMB is exceeded by the NES activity. Although we cannot find a classical NLS in the Klp5 N-terminus, a non-classical, uncharacterised motif could exist. Alternatively, perhaps low levels of Klp5 enter the nucleus by another means, for example by association with another protein such as tubulin.

Another interesting feature of Klp5 nuclear import is that it appears to be co-ordinated with the cell cycle; unlike Klp6, it does not seem to shuttle between the nucleus and the cytoplasm during interphase, as addition of LMB causes only very low levels of Klp5 nuclear accumulation in interphase cells. This behaviour is not due to cytoplasmic anchoring of Klp5 by interphase microtubules, as depolymerisation of microtubules does not cause any increase in the amount of Klp5 entering the nucleus in interphase. An interesting possibility is that Klp5's NLS could be regulated by CDK phosphorylation, which would be an elegant mechanism to control its activity in a cell-cycle dependent manner. An S>A mutation (phospho-dead) of one of the CDK consensus sites overlapping the Klp5 NLS resulted in decreased localisation to the nuclear spindle, and increased TBZ resistance. This suggests that CDK phosphorylation during mitosis might function to enhance importin binding to the Klp5 NLS and therefore increase its import into the nucleus. It would be interesting to pursue this possibility further, for example by demonstrating that CDK (Cdc2) can phosphorylate this site in Klp5.

Alternatively, Klp5's NLS might be regulated by intramolecular inhibition. In Kinesin-1, the tail domain can fold back to associate with the head domain, which partially inhibits kinesin's ATPase activity (Stock *et al.*, 1999) (Coy *et al.*, 1999) (Friedman and Vale, 1999). Similarly, the C-terminus of MCAK inhibits the kinesin domain's ability to hydrolyse ATP;

a C-terminus truncated form of MCAK depolymerises MTs faster and binds microtubules with higher affinity (Moore and Wordeman, 2004b). Deletion of Klp5/Klp6 (and therefore abolition of their MT depolymerising activity) results in long microtubules and increased TBZ resistance. If the MT depolymerising activity of Klp5/Klp6 were increased, we would expect microtubules to be shorter, and cells to show increased sensitivity to TBZ. Interestingly, the Klp5 ΔC mutant is slightly more sensitive to TBZ than WT, and considerably more sensitive than the Klp6 ΔC mutant. Perhaps the Klp5 tail folds back to inhibit depolymerisation activity of Klp5 or Klp5/Klp6, and such an intramolecular association could also inhibit the Klp5 NLS. Another possibility is that Klp5 phosphorylation at the onset of mitosis could disrupt the intramolecular interaction, causing the molecule to unfold, revealing the NLS and fully activating Klp5's depolymerisation activity.

The different responses of Klp5 and Klp6 to LMB during interphase suggest that, at least during interphase, they enter the nucleus independently of each other. If the NLS of Klp5 is regulated so that Klp5 only enters the nucleus during mitosis, then this also indirectly regulates the localisation of Klp6 in a cell-cycle dependent manner. We showed that Klp6 cannot be retained in the nucleus in the absence of Klp5 (and vice-versa). This would mean that although Klp6 enters the nucleus during interphase, because Klp5 is not present in the nucleus then, Klp6 would not be able to remain in the nucleus and would be immediately exported out to the cytoplasm. This model is illustrated in Figure 3.25.

Having established that Klp5/Klp6 heterodimerisation was necessary for correct localisation of the proteins during mitosis, we then went on to find that two kinesin domains are required for Klp5/Klp6 function, and that the Klp5 and the Klp6 kinesin domains contribute distinct properties to the overall function of the heterodimeric molecule.

Deletion of either the Klp5 or the Klp6 kinesin domain caused strong TBZ resistance, and was synthetic lethal with *Δalp14*, indicating that Klp function had been completely lost. This observation, like that in the previous chapter that just one head (Klp5) defective in ATPase activity abrogates Klp function, is surprising when compared to some published studies. If heterodimers of Kinesin-1 are constructed with one mutant head that hydrolyzes ATP slowly, the molecule is still able to move along the microtubule (Kaseda *et al.*, 2003). MCAK depolymerises MTs more efficiently in its WT dimeric form, but the minimal domain, which is monomeric, still has depolymerising activity (Hertzer *et al.*, 2006). It has not been shown whether the naturally occurring Kinesin-2 Kif3A/Kif3B heterodimer retains any function in monomeric form. In contrast to some other kinesins, it appears that dimerisation is absolutely essential for function of Klp5 and Klp6. Confirmation of

localisation of ΔN Klp mutants to the nuclear mitotic spindle demonstrated that it is not simply nuclear localisation that dimerisation is required for.

Construction of chimeric Klp proteins to create molecules that were homodimeric for the Klp5 or the Klp6 kinesin domain revealed why the presence of two kinesin domains is necessary. The phenotypes of Klp5 N and Klp6 N homodimers are very different, indicating that the two kinesin domains present within the WT Klp5/Klp6 heterodimer may contribute distinct properties to the overall function of the molecule. Loss of either of these different kinesin domains renders the molecule non-functional. GFP-Klp5 overexpressed from a plasmid shows more localisation to cytoplasmic MTs than GFP-Klp6, even in the presence of LMB. Additionally, visualisation of the Klp5 N homodimer revealed very strong MT localisation, whereas the Klp6 N homodimer exhibited weak or no MT localisation. These observations suggested that Klp5 might have a higher affinity for MTs than Klp6. A comparison of Klp5 and Klp6 protein sequences revealed that Klp5 contains more positively charged residues (thought to interact with tubulin) within the microtubule-interacting loop L8 region. It is also interesting to note that Aurora B phosphorylates Klp5 at a site adjacent to two of the positively charged L8 residues (J. Kamenz and S. Hauf, personal communication). Addition of a negatively charged phosphate group at this position would presumably reduce Klp5's affinity for MTs, allowing Aurora B to regulate Klp5 MT binding.

It would be of enormous interest to carry out biochemical studies on Klp5 and Klp6, to compare the activities of homodimers and heterodimers. Data from Rob Cross' group indicates that Klp5 N+CC and Klp6 N+CC constructs (which are presumably monomeric) have very different motilities in *in vitro* gliding assays: Klp6 drove MT sliding at 124 ± 34nm/s, whereas Klp5 drove sliding at a velocity of just 14 ± 4 nm/s. A combination of both Klp5 and Klp6 constructs drove sliding at 17 ± 4nm/s (M. Erent, personal communication). This may be consistent with the idea that Klp5 and Klp6 differ in their MT binding abilities. If Klp5 binds MTs very tightly, it would be expected that it moves slowly along the MTs. Perhaps Klp6 is able to promote detachment of Klp5 from the MT. Conversely, Klp6 might be a fast motor, but falls off MTs too easily because it only possesses a weak affinity for MTs. In this way, a balance of Klp5 and Klp6 activities is required for proper Klp function. It would be particularly interesting to compare MT binding affinities of Klp5 and Klp6. An attempt was made to carry out a MT-binding assay during our study, but unfortunately there was not sufficient time to optimise the experiment. It is difficult to speculate at this time whether Klp5 and Klp6 make different contributions to MT depolymerisation, although both proteins are required.

Our study of MT dynamics in interphase fission yeast cells revealed that Klp5 and Klp6 make significant contributions to the frequency of MT catastrophe, and the rate of MT shrinkage. In the Klp5 N homodimer, the rates of catastrophe and MT shrinkage were reduced to even lower levels than those seen in *Δklp5* or *Δklp6* deletion mutants; the difference in shrinkage rate was the most marked. If the Klp5 N homodimer binds to MTs too tightly, perhaps this stabilises the straight, stable conformation of the tubulin protofilaments, so that dissociation of tubulin subunits only occurs very slowly. In contrast, MT dynamics in the Klp6 N homodimer strain are very similar to those in the *Δklp5* or *Δklp6* deletion mutants. If the Klp6 N homodimer is unable to bind to MTs very well, then it would not be able to influence MT dynamics, which explains why its phenotype is similar to that of a deletion mutant. Although we were unable to address the effect of Klp6 N homodimerisation on chromosome segregation, by extrapolation from results obtained from studying interphase MT dynamics, we predict that chromosome congression and segregation in the Klp6 homodimer would look very similar to a *klp* deletion.

It is clear that chromosome segregation is severely perturbed in the Klp5 N homodimer, which is unsurprising considering the extent of MT stabilisation in this mutant. However, microscopic analysis revealed that during early to mid-mitosis, very little Klp5 N homodimer is localised to the mitotic spindle; instead, the majority seems to be associated with the slowly depolymerising microtubules in the cytoplasm. This observation suggests that cytoplasmic microtubules might play a role in anchoring Klp5, i.e. sequestering it away from the nucleus. However, if no Klp5 N homodimer was entering the nucleus until later in mitosis, we would expect chromosome attachment and the resultant segregation to proceed in a manner similar to that seen in a *Δklp* mutant; but this is not what is observed. The severe defects in chromosome segregation that occur in the Klp5 N homodimer strain suggest that the molecule must enter the nucleus earlier in mitosis. The Klp5 N homodimer appears to render MTs extremely stable, and hyperstabilisation of kinetochore-MTs could explain the severe defects that are observed. Addition of LMB to the Klp5 homodimer strain showed that the Klp5N/Klp6C chimera was able to accumulate in the nucleus to reasonably high levels during interphase, and certainly to levels exceeding the accumulation of native Klp5 in a WT strain. During interphase, cytoplasmic MTs are present, but they obviously did not prevent Klp5N/Klp6C from entering the nucleus, arguing against the cytoplasmic MT sequestration model. Depolymerisation of interphase cytoplasmic MTs did not increase nuclear entry of WT Klp5, which also argues against MT sequestration. It was not possible to address whether depolymerisation of the left-over cytoplasmic MTs in mitosis in the Klp5 N homodimer increased nuclear localisation, because MTs in this strain could not be completely depolymerised under our experimental conditions. Regarding the presence or absence of the Klp5 N homodimer in the nucleus in early mitosis (the critical point at which

MT-kinetochore attachments are formed), it is possible that some homodimer is present, but is not easily visualised. Because the fluorescent signal from the cytoplasmic MTs is extremely strong, a weaker signal elsewhere in the cell could well be obscured because of the way the DeltaVision microscope software adjusts for contrast. It would be interesting to investigate by FRAP whether prometaphase and metaphase spindles are hyperstabilised in the Klp5 N homodimer strain.

Results from LMB experiments with the Klp5N/Klp6C (Klp5 N homodimer) and Klp6N/Klp5C (Klp6 N homodimer) chimera molecules support our argument that nuclear import is regulated by the C-terminal NLS, rather than by strength of MT binding. We propose that 1) the Klp5 NLS is cell-cycle regulated, such that its strength is upregulated during mitosis, whereas the Klp6 NLS is constitutively active; and 2) that the Klp5 kinesin domain has a greater affinity for MTs than the Klp6 kinesin domain. If the C-termini (including the identified NLSs) are the major factors determining nuclear entry of a Klp molecule, rather than the N-termini, via MT-binding, then we would expect that the Klp5N/Klp6C chimera would show constitutive nuclear import, and that the Klp6N/Klp5C chimera would show mitosis-specific nuclear import. This is exactly what was observed (Figure 3.21). We also speculated whether an additional, weak NLS might reside within the Klp5 N-terminus, which allows some nuclear accumulation of Klp5 when nuclear export is inhibited by LMB. Interestingly, the Klp6N/Klp5C chimera shows absolutely no nuclear accumulation during interphase upon LMB addition, suggesting that the combination of the Klp6 N-terminus (no weak NLS activity) with the Klp5 C-terminus (no interphase NLS activity) is completely unable to enter the nucleus during interphase.

However, it is rather puzzling that Klp6N/Klp5C does not localise to the nucleus during mitosis, unless LMB is added. Even with LMB, its localisation to the mitotic spindle looks rather weak. Localisation to cytoplasmic microtubules is not visible. Although we postulate that the Klp6 N-terminus may have weaker MT-binding activity than the Klp5 N-terminus, it is known that Klp6 WT is able to bind MTs in both *Δklp5* and *klp5 ΔN* strains, so this factor alone could not account for the lack of localisation of Klp6N/Klp5C. The possibility of Klp5 intramolecular regulation was mentioned earlier. Perhaps in the Klp6N/Klp5C chimera, the Klp5 C-terminus folds back to regulate the Klp6 N-terminus, and that, unlike in WT Klp5, this interaction cannot be disrupted during mitosis. This could result in permanent inactivation of both the Klp5 NLS, and the Klp6 kinesin domain, resulting in no nuclear localisation and drastically reduced MT binding. Additionally, perhaps a Klp5 N homodimer is so harmful to a cell because one of the N-termini cannot be appropriately regulated (i.e. within the Klp5N/Klp6C chimera). If there is indeed intramolecular regulation of Klp molecules, it would be interesting to construct ΔC homodimers to examine the phenotype of

Klp5 or Klp6 kinesin domain homodimerisation in the absence of complications caused by interactions with regulatory C-terminal tails. Alternatively, full-length homodimers could be constructed e.g. by expressing a Klp5 construct that contains the Klp6 coiled-coil domain from the *klp6* locus, so that it would dimerise with WT Klp5 expressed from the *klp5* locus.

Additional evidence favouring a model where intramolecular regulation contributes to the function of the Klp complex comes from the double chimera strain. The double chimera, unlike the Klp5 homodimer, is not harmful to the cell; however, neither is it fully functional, as it is TBZ resistant. Preliminary results show that Klp5N/Klp6C and Klp6N/Klp5C in the context of the double chimera are unable to enter the nucleus, demonstrating that the geometry of the complex is important, in addition to a requirement for both Klp5 and Klp6 kinesin domains.

Another aspect of this work that is currently unclear is whether Klp5 and Klp6 always associate with one another as a heterodimer. Our work shows that they are able to enter the nucleus in the absence of one another, although unable to be retained. This does not demonstrate that they enter the nucleus independently in a WT situation; however, the difference in the nuclear accumulation of Klp5-GFP and Klp6-GFP in WT interphase cells upon LMB addition does suggest that at least some of the Klp population is not heterodimerised during interphase. Conversely, other lines of evidence suggest that Klp5 and Klp6 probably do heterodimerise during interphase, for example the identical phenotypes of *Δklp5* and *Δklp6* cells, and the non-additivity of the double mutant. The appearance of long, curved interphase MTs in all three of these mutants suggests Klp5 and Klp6 do act together in the same complex during interphase. It is possible that Klp5 and Klp6 associate in the cytoplasm, dissociate for transport into the nucleus, then reassociate for nuclear retention and function.

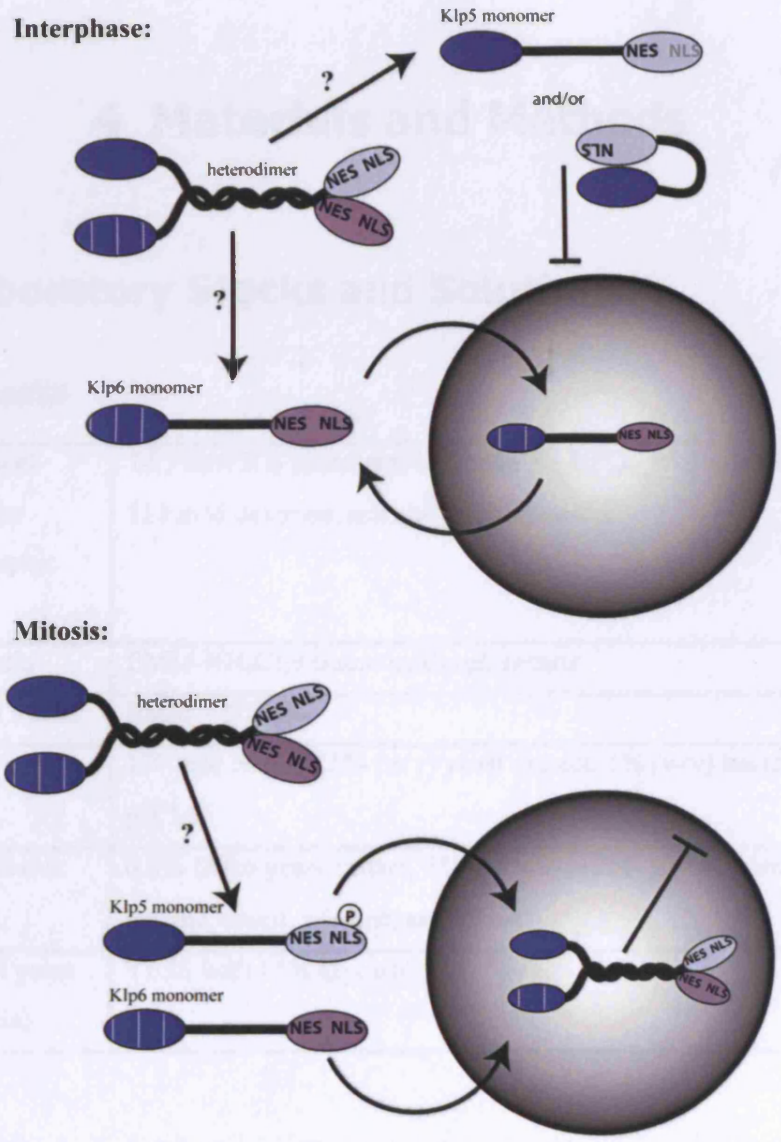

Figure 3.25 Model for cell-cycle dependent regulation of Klp5/Klp6 nuclear transport

Klp5 and Klp6 function as heterodimers in the cytoplasm and the nucleus, but are transported into the nucleus as monomers. During interphase, Klp5 is unable to enter the nucleus, perhaps because its NLS is not phosphorylated, or because an intramolecular interaction masks the NLS. Klp6 enters the nucleus, but is rapidly exported in the absence of Klp5 because its NES is exposed. During mitosis, Klp5's NLS is activated by CDK phosphorylation, and/or by relief of intramolecular inhibition. Both Klp5 and Klp6 enter the nucleus, where they dimerise, thereby masking their NESs and preventing premature nuclear export.

4 Materials and Methods

4.1 Laboratory Stocks and Solutions

4.1.1 Media

EMM (Minimal media used for proto/auxotrophic selection)	14.7 mM KH phthalate, 15.5 mM Na_2HPO_4, 93.5 mM NH_4Cl, 111 mM dextrose, salt and vitamin stocks.
DV clear media	EMM-NH_4Cl_2+amino acids+glutamate
N_2 starvation media	EMM – NH_4Cl_2
L Broth (for bacteria)	170 mM NaCl, 0.5% (w/v) yeast extract, 1% (w/v) bacto-tryptone, pH 7.0.
YE5S (rich fission yeast media)	0.5% Difco yeast extract, 3% dextrose +250 μg/ml, histidine, leucine, uracil, adenine, and lysine.
YFM (fission yeast freezing media)	YE5S with 15% glycerol

4.1.2 Molecular Biology Reagents

TBE	0.02M Tris borate, 0.4 mM Na_2EDTA
TAE	0.08M Tris acetate, 2 mM Na_2EDTA
TE	10 mM Tris-HCl, pH 7.5, 1mM EDTA.
6X loading buffer (DNA agarose gel)	30% glycerol, 150mM EDTA, pH 8.0, 0.3% bromophenol blue, 0.3% xylene cyanol.
SCE	1M sorbitol, 0.1M sodium citrate, pH7.0, 60mM EDTA
SCE/ME/Zymolase	SCE, plus 8μl/ml 2-mercaptoethanol, 2mg/ml zymolase T-20 200μl aliquots kept at -20°C
SDS solution	100mM Tris/HCl, pH 9.0, 50mM EDTA, 2% SDS
Breaking buffer	2% Triton X-100, 1% SDS, 100mM NaCl, 10mM Tris-HCl pH 8.0, 1mM Na_2EDTA pH8.0
LiOAc/TE	100mM lithium acetate/acetic acid, pH7.5, 10mM Tris-HCl, 0.1mM EDTA, pH7.5

4.1.3 Biochemistry Reagents

HB Buffer	25mM MOPS, pH 7.2, 60mM β-glycerophosphate, 15mM $MgCl_2$, 15mM EGTA, 0.1mM sodium orthovanadate, 1% Triton X-100.
HB+ Buffer (made immediately before use)	HB buffer as above, plus 1X protease inhibitor cocktail (containing 20μg/ml leupeptin, 20μg/ml aprotinin, 20μg/ml pepstatin A), 15mM P-nitrophenyl-phosphate (PNPP), 1mM dithiothreitol (DTT), 1mM phenyl-methyl-sulfonyl-fluoride (PMSF).
Urea buffer	8M urea, 200mM NaCl, 100mM Tris-HCl pH 7.5, 0.2% SDS, 1mM PMSF
5X loading buffer (SDS-PAGE)	60 mM Tris-HCl (pH 6.8), 25% Glycerol, 2% SDS, 14.4 mM 2-mercaptoethanol, 1% bromophenol blue.
SDS-PAGE buffer	1X NuPAGE® MOPS Running Buffer
Transfer Buffer	39 mM glycine, 48 mM Tris base, 0.037% SDS, 20% methanol.
PBS	170mM sodium chloride, 3mM KCl, 10mM Na_2HPO_4, 2mM KH_2PO_4.
PBS-T	As above, plus 0.1% Tween-20

4.1.4 Commercial Kits

TaKaRa LA Taq™ – Polymerase chain reaction (PCR) kit

TaKaRa Z Taq™ – Polymerase chain reaction (PCR) kit

GENECLEAN®II Kit (Q BIOgene) – for purification of DNA fragments

QuikChange® II (Stratagene) – for site-directed mutagenesis of plasmids

4.2 Fission Yeast Culture

4.2.1 Strain growth and maintenance

Fission yeast strains were frozen and stored, revived, grown and maintained according to well-described methods (Moreno *et al.*, 1991). *S. pombe* cells were grown either in liquid culture media or on agar plates containing 1.6% agar. The recipes for different media types are listed above in section 4.1.1. Stocks of yeast strains were stored in YFM media at -70°C. Selective media plates were made by adding various drugs to bottles of cooled molten agar medium, as detailed in the table below:

G418	YE5S + 100μg/ml Geneticine (G418)
Phloxine B	YE5S + 5mg/L Phloxin B (Sigma # P4030)
Hygromycin B	YE5S + 300μg/ml hygromycin B (Hph, Roche)
clonNAT	YE5S + 100μg/ml nourseothricin (clonNAT, Werner Bio-agents)
5-FOA	YE5S + 1mg/ml fluoroorotic acid

4.2.2 Dilution assays

Freshly streaked cells were diluted in 100μl of water, then 2 μl of this suspension was added to 10ml of isoton (Beckman Coulter). After sonication, cells were counted on a Sysmex Microcell counter F-800 on the white blood cell channel. 2 x 10^6 cells were suspended in 100μl of water, then 10-fold dilutions of this cell suspension were made, and 2.5μl or 5μl of each dilution was spotted onto YE5S plates containing the appropriate drug, or none. Unless otherwise indicated, plates were incubated at 30°C and photographed after 2 or 3 days of growth.

4.2.3 Synchronisation of cultures

A hydroxyurea (HU) block-and-release protocol was used to enrich for the number of mitotic cells in a culture. HU blocks cells in S-phase by stalling DNA replication. Freshly-made HU was added to exponentially-growing cultures (2 x 10^6 cells/ml) at a concentration of 11mM. The cultures were incubated at 26°C for 4 hrs, then filtered, washed with 3 volumes of HU-free media and resuspended in HU-free media. Mitosis occurred approximately 90mins following release from the arrest.

4.2.4 Random spore analysis

Many strains were generated in this study by crossing two existing strains together. An h^+ and an h^- strain of different genotypes were mixed together on EMM plates lacking nitrogen to induce conjugation and sporulation. Once ascii were visible under the microscope (2-3 days), a toothpick of ascii/cells was suspended in 100µl of 0.5% helicase for 1-5 hours to break down the ascus wall. 43µl of ethanol was added to kill any remaining cells so that only spores remain. The ascii/cells were then pelleted, suspended in 1ml of water, and between 0.5µl and 20µl was plated onto YE5S plates to grow for several days before replica plating onto different selection media to determine the genotype of each colony.

4.3 Polymerase Chain Reaction (PCR)

All PCRs were performed on a Peltier Thermal Cycler-200 or DNA Engine.

4.3.1 Standard PCR

Reaction mix:

	Vol/µl
10x LA Taq buffer (incl. $MgCl_2$)	3.5
dNTP mix (2.5mM of each)	2.8
Template DNA (~100ng/µl)	1
Fwd primer (10µM)	1
Rev primer (10µM)	1
water	23.7
LA Taq	1
TOTAL	35µl

PCR program:

Temp	Time/min	
95°	3:00	
95°	0:30	30 cycles
54°	0:30	
72°	2:30*	
72°	7:00	
4°	∞	

(* ~1:00min allowed per 1kB to be amplified)

4.3.2 Long oligo PCR

Reaction mix:

	Vol/µl
10x LA Taq buffer (incl. $MgCl_2$)	5
$MgCl_2$ (25mM)	5
dNTP mix (2.5mM of each)	16
Template DNA (~100ng/µl)	1
Fwd primer (10µM)	5
Rev primer (10µM)	5
water	12
LA Taq	1
TOTAL	50µl

PCR program:

Temp	Time/min	
95°	3:00	
95°	1:00	5 cycles
48°	2:00	
74°	4:00	
95°	1:00	35 cycles
52°	2:00	
74°	2:00	
74°	10:00	
4°	∞	

4.3.3 Colony PCR

A small amount of cells was suspended in 12µl of freshly prepared 40mM NaOH, 0.01% sarcosyl. Samples were heated to 95° for 15 minutes, then briefly centrifuged and the supernatant used in the PCR reaction mix.

Reaction mix:

	Vol/µl
10x Z-Taq buffer	2
dNTP mix (2.5mM of each)	1.6
Sample sup	1.5
Fwd primer (10µM)	0.4
Rev primer (10µM)	0.4
water	13.9
Z-Taq	1
TOTAL	20µl

PCR program:

Temp	Time/min	
95°	5:00	
98°	0:05	
55°	0:10	40 cycles
72°	0:30	
72°	13:00	
4°	∞	

5µl of each reaction was visualised on a 0.8% agarose gel containing ethidium bromide.

4.4 Molecular Biology

4.4.1 Ethanol precipitation of PCR products

PCR products were precipitated by adding 1/5 volume 5M NaCl and 3x volume cold ethanol. The reactions were kept at -80°C for >10 minutes, then centrifuged at 13000 rpm for 15 minutes. The pellets were rinsed with 70% ethanol and air-dried for ~20 minutes, then dissolved in 10µl of water. 0.5µl of precipitated DNA was visualised on a 0.8% agarose gel containing ethidium bromide.

4.4.2 Genomic DNA preparation

Both of the following methods were used in this study.

1) A toothpick of cells was suspended in 200µl of SCE/ME/Zymolyase and incubated for 45mins at 37°C on a shaking thermomixer. 200µl of SDS-solution was added, and samples were heated at 65°C for 5mins. Then 200µl of 5M KOAc was added before centrifuging at 13000rpm for 10mins. 350µl of supernatant was transferred to a fresh tube and 800µl of ethanol added. Tubes were centrifuged at 6000rpm, and the resulting pellet rinsed with 70% ethanol, air-dried at 37°C for 20mins, then dissolved in 200µl of water.

2) A 5 ml culture was grown overnight to saturation. Cells were harvested, washed in 500µl water, then re-suspended in 200µl breaking buffer. 200µl of phenol:chloroform:isoamyl alcohol was added along with 0.3g of acid washed beads and the mixture vortexed using the Bio101 Fastprep FP120 cell disruptor (Anachem). 3 spins of 25secs at setting 5.5 were used; samples were chilled on ice between each spin. 200µl TE (pH 8.0) was then added and the mixture centrifuged for 5 mins. The top aqueous layer was then carefully transferred to a fresh eppendorf, 1ml EtOH was added and the mixture was incubated at room temperature for 5 mins. The genomic DNA was pelleted by centrifuging

for 2 mins, washed with 500µl of 70% EtOH, and then air-dried at room temperature. The pellet was resuspended in 20µl TE.

4.4.3 Yeast transformation (PCR product)

Based on method of Keeney and Boeke (1994).
~1 x 10^8 mid-log phase cells were harvested, washed in water, then resuspended in 100µl of lithium acetate in TE. Ethanol-precipitated DNA ws dissolved in 10µl water and then 3µl salmon sperm carrier DNA (10µg/ml, Stratagene) was added. 100µl of cells in LiOAc/TE were added to the DNA and rotated at room temp for 10 minutes. 260µl of 40% PEG in LiOAc/TE was then added and mixed by gentle pipetting. Tubes were rotated at room temp for ~1-2 hours. 43µl DMSO was added and cells heat-shocked at 42°C for 5 minutes. Cells were then spun down, washed in water, and resuspended in 100µl water. They were divided between two YE5S plates and incubated overnight at 30°C. They were subsequently replica plated onto the relevant selective medium.

To increase transformation efficiency, an additional recovery step was added. After heat shock, cells were spun down, washed once in pre-warmed YE5S, then resuspended in 200µl pre-warmed YE5S. They were incubated with rotation at 30°C for 90 minutes before being plated onto YE5S plates as above.

4.4.4 Yeast transformation (plasmid)

~1 x 10^7 mid-log phase cells were harvested, washed in water, then resuspended in 120µl of lithium acetate in TE. The cells were incubated with shaking at 26°C for one hour. 20µl of this cell suspension was added to 1µl of plasmid DNA and 2µl of carrier DNA. 50µl of 40% PEG in LiOAc/TE was then added and this mixture was incubated for a further hour at 26°C. Cells were heat shocked at 42°C for 5 minutes, spun down, washed and resuspended in sterile water and plated onto two EMM-Leu plates with thiamine added if required. Plates were incubated at 30°C until colonies appeared.

4.4.5 Gene tagging and deletion

A one-step PCR-based method was used to tag or delete genes at their endogenous loci (Bahler *et al.*, 1998). Oligonucleotides were designed with ~80bp of homology to flanking sequences of the insertion site at the endogenous locus, and 20bp of homology to the PCR template plasmids. All templates for PCR were based on the pFA6a plasmid, and contained one of the following selective markers: *kanR, ura4+, nat, hph* (Sato *et al.*, 2005). Genes

were deleted by a selective marker only; additionally some genes in this study were C-terminally tagged with GFP plus a selective marker, e.g. GFP-*kanR*. PCR products for deletion or tagging were transformed into the appropriate strain as described above, and transformants were selected on the appropriate selective medium (described in section 4.2.1). Successful transformation was confirmed either by colony PCR, or by visualisation of the GFP signal by fluorescence microscopy.

4.4.6 Site-directed mutagenesis

Site-directed mutants of klp5 and klp6 were generated using the Stratagene QuikChange® II kit according to the manufacturer's protocol. The plasmids pREP41-EGFP-klp5 or pREP41-EGFP-klp6 (kind gift from Eric Chang, Houston, Texas) were used as templates. Mutated plasmids were sequenced, then transformed into yeast. To create site-directed mutants integrated at the genomic locus, the mutated klp5 or klp6 sequence (with or without GFP) was amplified by PCR and transformed into either a klp5::ura4+ or klp6::ura4+ strain; transformants were selected for on plates containing 5-FOA and checked by colony PCR.

4.4.7 Domain deletions and chimeras

N-terminal Deletions (ΔN):

N-terminal deletions were constructed so that the truncated protein was expressed under the native *klp5* or *klp6* promoter. This was achieved in the following way:
The entire *klp5* or *klp6* gene was replaced by *ura4+*. The C-terminus (coiled-coil to end) of *klp5* or *klp6* was amplified by PCR using genomic DNA as a template, and oligos as listed in section 4.7.2. The PCR product was integrated into the *klp5* or *klp6* locus, and transformants were selected by negative selection of the *ura4+* marker by replica plating onto YE5S plates containing 5-FOA. 200μl of Phloxin B was added to plates to aid visualisation of transformants against background growth. Constructs were checked by colony PCR.

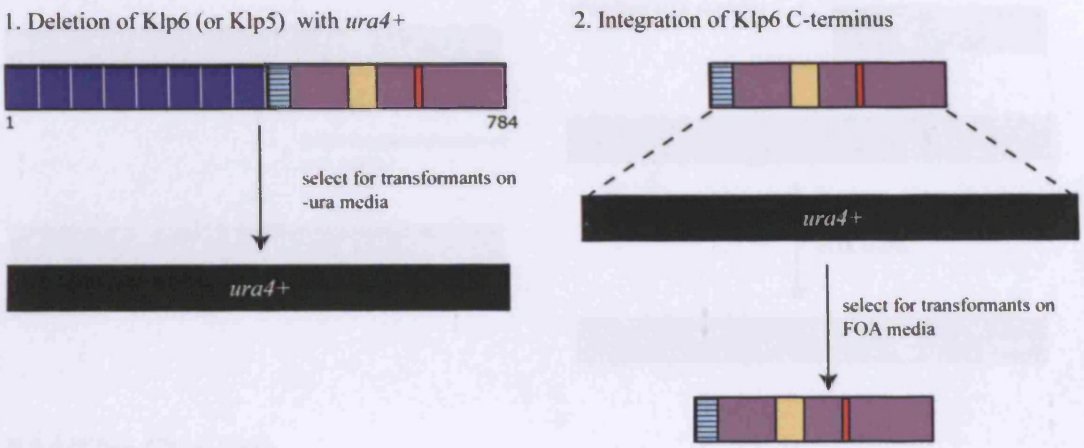

C-terminal Deletions (ΔC):

C-terminal deletions were generated simply by replacing the *klp5* or *klp6* C-terminus (from after the coiled-coil domain) with the *ura4+* marker. Constructs were checked by colony PCR.

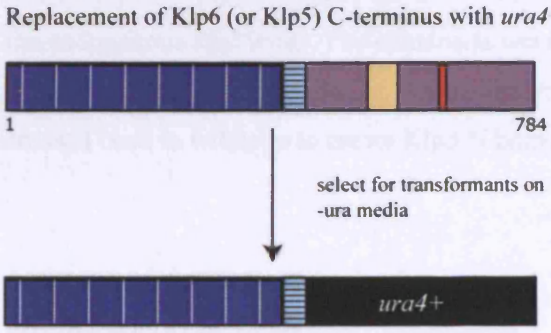

Coiled-coil Deletions (ΔCC):

A coiled-coil deletion was created at the endogenous locus by using the ΔC construct described above. The C-terminus (not including the coiled-coil) was amplified by PCR using genomic DNA as a template. This was then integrated into the endogenous locus, such that the coiled-coil was deleted (see diagram). Selection for transformants was on media containing 5-FOA, as before. Constructs were checked by colony PCR.

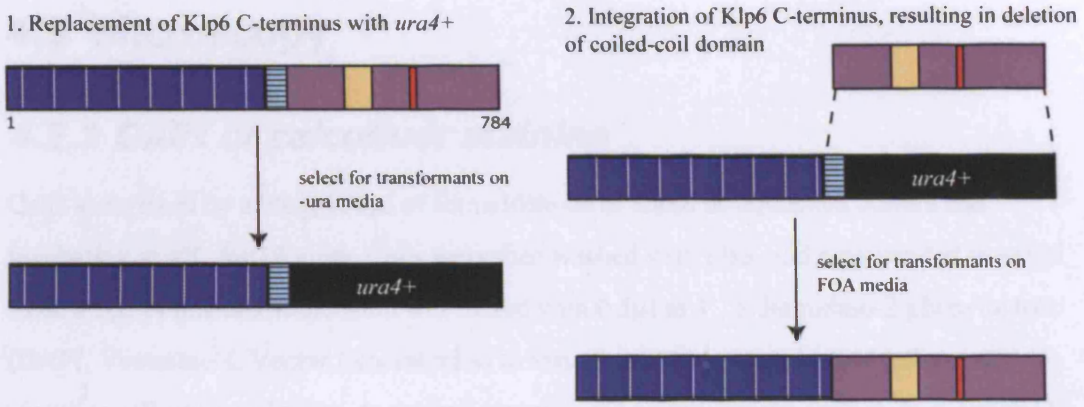

Klp5/Klp6 Chimeras:

Chimeric molecules were also generated by a two-step process. Firstly, the region coding for the N-terminus of one of the Klp molecules e.g. *klp6* was replaced with *ura4+*. The gene sequence coding for the N-terminus of the other Klp molecule, i.e. Klp5, was then integrated into the *ura4+* and transformants selected on 5-FOA plates. This second step e.g. integration of *klp5 N* into the *klp6* locus was carried out in a strain deleted for the other *klp,* i.e. *Δklp5* in this example, to prevent homologous recombination of the Klp5 N-terminus PCR product at the endogenous *klp5* locus. The constructs were checked by colony PCR and by sequencing across the Klp5/Klp6 boundaries. Once chimera strains had been generated, they were crossed back to wildtype to create Klp5 N homodimer and Klp6 N homodimer strains.

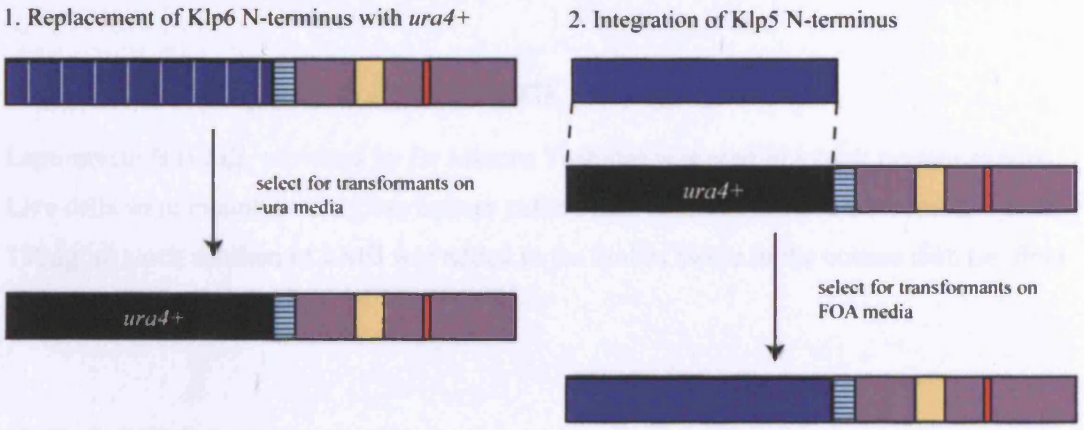

4.5 Microscopy

4.5.1 DAPI or calcofluor staining

Cells were fixed by adding 150µl of formaldehyde to 850µl of liquid cell culture and incubating at 4°C for 10 mins. Cells were then washed with PBS, and resuspended in ~10µl PBS. 0.5µl of this cell suspension was mixed with 0.5µl of 4', 6-diamidino-2-phenylindole (DAPI, Vectashield, Vector Laboratories) to visualise DNA, or 0.5µl of calcofluor, to visualise cell walls and septa. A coverslip was placed on top and the cells were examined by fluorescence microscopy.

4.5.2 Live cell analysis

For live cell analysis, 100µl of a log-phase culture was mounted on a glass bottom culture dish (MatTek) coated with lectin, and 2-3ml of minimal media $-NH_4Cl_2$ supplemented with glutamate and amino acids was added. Cells were observed with an Olympus IX-70 inverted fluorescence microscope equipped with a Roper CoolSNAP HQ (Photometrix, Tucson, AZ) charge-coupled device (CCD) camera and an Olympus UPlanSApo x100/1.40 NA oil objective lens. Images were collected using DeltaVision software (Applied Precision, Issaquah, WA). 10-12 *Z*-sections (0.3 µm apart) were acquired and subsequently deconvolved and projected to two-dimensional images using SoftWoRx software (Applied Precision). Observation was carried out at room temperature (22°C).

4.5.3 Leptomycin B treatment

Leptomycin B (LMB, provided by Dr Minoru Yoshida) was used to inhibit nuclear export. Live cells were mounted on a glass bottom culture dish (MatTek) coated with lectin. 1µl of 100µg/ml stock solution of LMB was added to the 2ml of media in the culture dish (ie. final concentration of 50ng/ml.)

4.5.4 MBC treatment

Carbendazim (MBC/CBZ, Sigma Aldrich) was used to depolymerise microtubules in liquid culture. 30µl of 5mg/ml stock was added to 970µl of media in an eppendorf, mixed well, and centrifuged at 13 000rpm for 5 min to prevent crystal formation. This prepared media was then carefully pipetted in a culture dish already containing cells and 2ml of media. This gave a final concentration of MBC/CBZ of 50µg/ml.

4.5.5 Fluorescence intensity line profiling

To assess nuclear accumulation of Klp5-GFP or Klp6-GFP, projections were made of images taken 60 minutes after addition of LMB. These were imported into ImageJ software (v.1.37, NIH) for line-scan analysis. Lines were drawn from one end of a cell to the other, along the longitudinal axis, and fluorescence intensity across each line was measured using the plot profile function. Fluorescence data was exported in numerical format and graphs drawn using Microsoft Excel.

4.5.6 Constructing kymographs

Kymographs were generated using DeltaVision software. Time-lapse images were taken, deconvolved and projected as described above. The images were rotated to orient the microtubule / spindle of interest along the horizontal axis, and cropped closely around the region of interest. The time-lapse images were converted to a 3D stack by exchanging the values for *Z* and *T* (time). This stack was rotated 180° around *x* to align the time points in a vertical stack.

4.6 Biochemistry

4.6.1 Whole cell extracts

Cell extracts were prepared using either HB or urea buffer. A total of ~1 x 10^8 log-phase cells were harvested, washed in water and transferred to a screw-top tube. Cells were resuspended in either 50µl of HB+ buffer or 200µl of urea buffer and ~0.3g of acid-washed glass beads (one PCR-tube full) were added. Cells were broken using a Bio101 Fastprep FP120 cell disruptor (Anachem). 3 spins of 25secs at setting 5.5 were used; samples were chilled on ice between each spin. The base of each tube was pierced with a needle, so that the extracts could be spun into clean eppendorfs (5000rpm for 1min). The soluble extracts were cleared by spinning at 13000 rpm for 10mins. Protein concentration of HB extracts was determined using a Bradford Assay (BioRad). Protein concentration of urea extracts was determined with a NanoDrop® ND-1000 UV-Vis Spectrophotometer. Extracts were boiled in sample buffer for 10mins, then analysed by SDS-PAGE. 200µg of protein was loaded per lane.

4.6.2 Immunoprecipitation

Strains transformed with the pREP41-GFP plasmid (with various inserts) were grown overnight to log-phase in EMM-Leucine without thiamine, to induce expression from the *nmt41* promoter. Extracts were prepared using HB buffer (see above). 20mg of extract was used per sample. 3µl of polyclonal rabbit α-GFP (Invitrogen Molecular Probes) was added and samples were rotated at 4°C for 2hrs. Protein A Sepharose CL-4B (Pharmacia) beads were allowed to swell in HB buffer, then washed three times in HB buffer. A 10% suspension was made, then 100µl of this suspension was added to each tube (i.e. ~10µl packed volume beads per sample). Samples were rotated for another 2hrs at 4°C. Beads were washed five times with 500µl of HB buffer, aspirating the supernatant each time. SDS PAGE buffer was then added to the beads and these samples were boiled for 10mins. All of this eluate was loaded onto a gel (or divided between two gels) for SDS-PAGE.

4.6.3 Western blot analysis

Protein were analyzed by SDS-PAGE using Invitrogen NuPAGE® Bis-Tris Pre-Cast Gels according to the manufacturer's instructions. For Western blots, proteins were transferred onto Immobilon™-P (Millipore) membrane, again using the Invitrogen NuPAGE® system according to instructions. Membranes were blocked in 5% milk/PBS-T for 1hr at room temperature. Primary antibodies used in this study were either monoclonal mouse α-GFP (Boeringer clone 7.1&13.1), or monoclonal mouse α-HA 16B12 (BabCO, MMS-101R), diluted to 1:1000 in 5% milk/PBS-T. Membranes were incubated with primary antibody in heat-sealed cellophane packets at 4°C overnight. They were then washed for 10mins with PBS-T three times. Bound antibodies were detected using horseradish peroxidase-conjugated goat α-mouse IgG (BioRad); membranes were then washed another three times, and then proteins were visualised using chemiluminescence (ECL, Amersham).

4.7 Oligonucleotides

4.7.1 Short Oligos

klp5-G149E-seq: GGCCGTGATCTTCGTTATGC

klp5-G297A-seq: CCGACAGAAGCTAACGCTGCTTCATCTCG

Klp5-Pmut-chk: GTCCAGTCCCAAAAGTTCCTG

Klp5 5'UTR chk fwd: GTTGTTTGCGAGTGCCCTTC

Klp6 5'UTR chk fwd: CAAGCTTCCCATACTTGTGTTC

Klp5 N chk fwd: GTCAAGACAGTCGTCCATTACCG

Klp6 N chk fwd: GAAAGAAGGGTCTTCAATTTCCG

Klp5 B4 CC chk fwd: CCGAAGTGTTAAGGAACATGATCAG

Klp6 B4 CC chk fwd: GGTTTCGAGAAACGTGGTGAGCGTAG

Klp5 CC chk fwd: GCAATCGTTGAGTTACGTGAGC

Klp6 CC chk fwd: GGATTGCTGAAGAGTCTAAGC

Klp5 post-CC chk rev: GTTACAGCGTCCTGATCAGAACC

Klp6 post-CC chk rev: CTCGAGAAGAAATTTTTCGTACCTCC

Klp6 chk rev (3' UTR): GTGAAAACCGATCTCGTTGG

Klp5-chk-rev(3' UTR): GTCTGCCACCTCCAATGTAC

Klp5 CC chk rev: GCTCACGTAACTCAACGATTGC

Klp6 CC chk rev: GCTTAGACTCTTCAGCAATCC

Klp5-RARA-seq: CGTGATAGAGTTCATAGTTTTCCC

Klp6-RARA-seq: GGAAAAGCACCTCTATTATCAATG

Klp5-CC-seq: CTCCGTCTTCTGTTCATTACGAAG

Klp6-CC-seq: GGCAATCGAGCCAAAAACATCAAAACG

Klp6 P-loop-seq-fwd: GCCTCACAGGAGGATGTTTACAAGGG

Klp6 SwitchII-seq-fwd: CGTCACGCTCGCATGCCGTTTTACAG

4.7.2 Long Oligos

Klp5 tagging (C-terminus):

Klp5-tag-fwd

CTACTCTTCATCTTTCAAATCCAGCTAACATTATTAGGAAATCTTTAAGCATGGC
TGAAAACGAAGAAGAGAAAGCCACCCGGATCCCCGGGTTAATTAA

Klp5-tag-rev

ACATATATGTACGCTTGTATTTGATAGTGCATTACGAACGAATTGTGCAAGTTTA
CTAAGAGAATTTTAGGGTTTATAAAGAATTCGAGCTCGTTTAAAC

Klp6 tagging (C-terminus):

Klp6-tag-fwd

TGAAACAACCAGTACGCCGTATATCGCTTGTTTCACAACCTTTACAAAAAACTG
GCGGGACTGAGAATACTCCTAATGCTCGGATCCCCGGGTTAATTAA

Klp6-tag-rev

ATATGTCAAACAGTGTCTAAAGGGGAATGCAAAAAAATGATGAAATGCTAAAT
CATAAGTAGCTTAAAAATGAAAATGAAGAATTCGAGCTCGTTTAAAC

Klp5 genomic integration from pREP41 plasmid:

Klp5-rigGFP(N)-fw

GGTTATTGGAATTGTTGTTTGCGAGTGCCCTTCTTTTCATCTGTTTTGGATGATTG
CTTGCATGGAAATTTTGCTTTTCAATGAGTAAAGGAGAAGAACTTTTC

Klp5-rigGFP(N)-rev

ATCAAGCTTATCCGTTTTTTTTTTTTAAATATACCCAACAGGATATTTAGAGGAT
TCGTATTTGAATATACGGACCTTTATTAGGTGGCTTTCTCTTCTTCG

Klp5-rigGFP-fw:

GGTTATTGGAATTGTTGTTTGCGAGTGCCCTTCTTTTCATCTGTTTTGGATGATTC
TTGCATGGAAATTTTGCTTTTCAATGTCAAGACAGTCGTCCAT

Klp5-rigGFP-rev:

ATCAAGCTTATCCGTTTTTTTTTTTTAAATATACCCAACAGGATATTTAGAGGAT
TCGTATTTGAATATACGGACCTTTATTTGTATAGTTCATCCATGC

Klp6 genomic integration from pREP41 plasmid:

Klp6-rigGFP(N)-fwd

CCCATACTTGTGTTCTTCTTAATAGCTTCACACAACTAAAACAAATTCATTCCTA
GAATCAGTATTACGATACTGCTATGAGTAAAGGAGAAGAACTTTTC

Klp6-rigGFP(N)-rev

CGGTTTCGAATCTTTATTCTTTATTTCAACAGGAGGTACGGAACTAGTAGTGGGA
ACTTCACTAAATCGAACTCGTTTCTTCAAAGGCTTCTTTAGAACTCG

Klp6-rigGFP-fwd

GCTTCCCATACTTGTGTTCTTCTTAATAGCTTCACACAACTAAAACAAATTCATT
CCTAGAATCAGTATTACGATACTGCTATGAAAGAAGGGTCTTCAATTTC

Klp5 C-term deletion:

Klp5-Cdelura-fwd:

GCCAATATGTAAAAGCAATCGTTGAGTTACGTGAGCAAATTTCAGAGTTGGAGA
ATCGTCTCGCACAGATCGATTTGTCACTACAAATCCCACTGGCTATATGT

Klp5-Cdelura-rev:

ATCAAGCTTATCCGTTTTTTTTTTTTAAATATACCCAACAGGATATTTAGAGGAT
TCGTATTTGAATATACGGACCTTTATTCTTATTCAATGTCAATCCA

Klp5 N-term deletion:

Klp5-Csubcl-fwd:

TATTGGAATTGTTGTTTGCGAGTGCCCTTCTTTTCATCTGTTTTGGATGATTGCTT
GCATGGAAATTTTGCTTTTCAATG GTAAGCCAATATGTAAAAGC

Klp5-Csubcl-rev:

ATCAAGCTTATCCGTTTTTTTTTTTTAAATATACCCAACAGGATATTTAGAGGAT
TCGTATTTGAATATACGGACCTTTAGGTGGCTTTCTCTTCTTCGT

Klp5 C-term deletion:

Klp6-Cdelura-fwd:

GTGAATATGTACGCACCATTTACGAATTACGACAAAAGGTTAGCATACTTCAAA
AGAGGATTGCTGAAGAGTCTAAGCAACTACAAATCCCACTGGCTATATGT

Klp6-Cdelura-rev:

CCAATGAGGAGTTGATGTTGTCCTTCCAAAAAAAATTATACCAACTATTTGAGT
GAAAACCGATCTCGTTGGTTTCTTCATTCTTATTCAATGTCAATCCA

Klp6 N-term deletion:

Klp6-Csubcl-fwd:

CCCATACTTGTGTTCTTCTTAATAGCTTCACACAACTAAAACAAATTCATTCCTA
GAATCAGTATTACGATACTGCTATGATTTACGAATTACGACAAAA

Klp6-Csubcl-rev:

CCAATGAGGAGTTGATGTTGTCCTTCCAAAAAAAATTATACCAACTATTTGAGT
GAAAACCGATCTCGTTGGTTTCTTCAAGCATTAGGAGTATTCTCAG

Klp6 N-term deletion: (for creation of chimera or coiled-coil deletion)

Klp5-Ndel-Ura4-fwd

GGTTATTGGAATTGTTGTTTGCGAGTGCCCTTCTTTTCATCTGTTTTGGATGATTG
CTTGCATGGAAATTTTGCTTTTCACGCCAGGGTTTTCCCAGTCACGAC

Klp5-Ndel-Ura4-rev

CAAATCGATCTGTGCGAGACGATTCTCCAACTCTGAAATTTGCTCACGTAACTCA
ACGATTGCTTTTACATATTGGCTTACAGCGGATAACAATTTCACACAGGA

Integration of Klp6 N-term into Klp5 N-term:

Klp6N-int-Klp5-fwd

GGTTATTGGAATTGTTGTTTGCGAGTGCCCTTCTTTTCATCTGTTTTGGATGATTG
CTTGCATGGAAATTTTGCTTTTCAATGAAAGAAGGGTCTTCAATTTCC

Klp6N-int-Klp5-rev

CAAATCGATCTGTGCGAGACGATTCTCCAACTCTGAAATTTGCTCACGTAACTCA
ACGATTGCTTTTACATATTGGCTTACGGTGCGTACATATTCACTTACATG

Klp6 N-term deletion: (for creation of chimera or coiled-coil deletion)

Klp6-Ndel-Ura4-fwd

CTTCCCATACTTGTGTTCTTCTTAATAGCTTCACACAACTAAAACAAATTCATTC
CTAGAATCAGTATTACGATACTGCTCGCCAGGGTTTTCCCAGTCACGAC

Klp6-Ndel-Ura4-rev

CTCCTTATTTAAAGCCAATTGCTTAGACTCTTCAGCAATCCTCTTTTGAAGTATG
CTAACCTTTTGTCGTAATTCGTAAATAGCGGATAACAATTTCACACAGGA

Klp6-Ndel-Ura4-rev(new)

GCTTAGACTCTTCAGCAATCCTCTTTTGAAGTATGCTAACCTTTTGTCGTAATTC
GTAAATGGTGCGTACATATTCACTAGCGGATAACAATTTCACACAGGA

Integration of Klp5 N-term into Klp6 N-term:

Klp5N-int-Klp6-fwd

CTTCCCATACTTGTGTTCTTCTTAATAGCTTCACACAACTAAAACAAATTCATTC
CTAGAATCAGTATTACGATACTGCTATGTCAAGACAGTCGTCCATTACC

Klp5N-int-Klp6-rev

CTCCTTATTTAAAGCCAATTGCTTAGACTCTTCAGCAATCCTCTTTTGAAGTATG
CTAACCTTTTGTCGTAATTCGTAAATATGTCGATCTACACTGATCATG

Klp5 Coiled-coil deletion:

Klp5N-int-Klp5-CCdel-fwd

GGTTATTGGAATTGTTGTTTGCGAGTGCCCTTCTTTTCATCTGTTTTGGATGATTG
CTTGCATGGAAATTTTGCTTTTCAATGTCAAGACAGTCGTCCATTAC

Klp5N-int-Klp5-CCdel-rev

CGCAATAAATTTCTGGCTTCTGCAAGCTTCGATTCATGAGCAAAAGATTGAGTT
ACAGCGTCCTGATCAGAACCATTTGATTGCGATGAACTGATCATGTTCCTTAACA
C

Klp5-N+CCdel-Ura4-rev

CGCAATAAATTTCTGGCTTCTGCAAGCTTCGATTCATGAGCAAAAGATTGAGTT
ACAGCGTCCTGATCAGAACCATTTGATTGCGATGAAGCGGATAACAATTTCACA
CAGGA

Klp6 Coiled-coil deletion

Klp6N-int-Klp6-CCdel-fwd

CATACTTGTGTTCTTCTTAATAGCTTCACACAACTAAAACAAATTCATTCCTAGA
ATCAGTATTACGATACTGCTATGAAAGAAGGGTCTTCAATTTCCG

Klp6N-int-Klp6-CCdel-fwd

GAGTTTTTGAGCATGCTTCTAGCATCTAACATTTTAATTTCTCGAGAAGAAATTT
TTCGTACCTCCTTATTTAAAGCCAAATCTACGCTCACCACGTTTCTCG

4.7.3 Site-Directed Mutagenesis Oligos

Klp5 R693A R695A: (NLS mutant)

Klp5-RARA-Fwd

CGTTCTCCAAAAAAGGCGGTTGCTTTCGACGATTCAATGTCTACGTC

Klp5-RARA-Rev

GACGTAGACATTGAATCGTCGAAAGCAACCGCCTTTTTTGGAGAACG

Klp6 R673A R675A: (NLS mutant)

Klp6-RARA-Fwd
GAAGCCTTTGAAGAAAGCAGTTGCATTTAGTGAAGTTCCCACTACTAGTTC

Klp6-RARA-Rev
GAACTAGTAGTGGGAACTTCACTAAATGCAACTGCTTTCTTCAAAGGCTTC

Klp5 Phosphomutants: (CDK sites)

Klp5 S678A fwd
GCCTCGAATGTTTTTCGTGAAGGCTCCAAAAAAACCAGTTG

Klp5 S678A rev
CAACTGGTTTTTTTGGAGCCTTCACGAAAAACATTCGAGGC

Klp5 S689A fwd
CCAGTTGTATTTTCAAAACGTGCTCCAAAAAAGAGGGTTCGTTTCG

Klp5 S689A rev
CGAAACGAACCCTCTTTTTTGGAGCACGTTTTGAAAATACAACTGG

Klp5 L415R I419R: (coiled-coil mutant)

Klp5-CCmut fwd
GCAATCGTTGAGCGACGTGAGCGTCGTTCAGAGTTGGAGAATCG

Klp5-CCmut rev CGATTCTCCAACTCTGAACGTTGCTCACGTCGCTCAACGATTGC

Klp5 Rigor Mutants:

klp5-T151N fwd
GGAGCAACTGGATGTGGTAAAAATCACACCATTAGTGGAAC

klp5-T151N rev
GTTCCACTAATGGTGTGATTTTTACCACATCCAGTTGCTCC

klp5-G297A fwd

CAATTATTGACTTGGCTGCCTCAGAACGTGCAACAGCTACC

klp5-G297A rev

GGTAGCTGTTGCACGTTCTGAGGCAGCCAAGTCAATAATTG

klp5-E299A fwd

CTTGGCTGGCTCAGCACGTGCAACAGCTAC

klp5-E299A rev

GTAGCTGTTGCACGTGCTGAGCCAGCCAAG

4.8 Fission Yeast Strains

4.8.1 Fission yeast nomenclature

cis-elements such as gene names are italicized, e.g. *klp5*. Mutant alleles are referred to by the number given after the gene name, e.g. *leu1, cut9-665*. Within the text of this thesis, a gene deletion is denoted by using a 'Δ' before the gene name, e.g. *Δklp5*. Deletions of various domains are denoted in a similar way, e.g. ΔN (deletion of N-terminus), ΔCC (deletion of coiled-coil). Protein products are written in Roman type (i.e. non-italicized), with the first letter capitalized e.g. Klp5. Tagged gene products are written with the name of the tag preceding the protein name if the protein is N-terminally tagged, e.g. RFP-tubulin, or with the tag after the protein name if the protein is C-terminally tagged, e.g. Klp5-GFP.

In the genotypes given in the strain list below, the deletion of a gene by a specific marker is described by giving the gene name, followed by '::' (to mean 'replaced by'), followed by the marker, e.g. *klp5::kanR*. This convention is also used to denote insertion of a partial gene sequence into the *ura4*$^+$ marker, e.g. *klp6::ura4+::klp6 (AA 411-784)* means that the sequence coding for amino acids 411-784 of Klp6 was inserted into the *klp6* locus, which had previously been deleted by the *ura4*$^+$ marker.

4.8.2 Strain List

Name	Genotype	Source
513	*h$^-$ leu1 ura4*	Lab stock
108-3D	*h$^+$ leu1 ura4 his2*	Lab stock

AR031	*h⁺ leu1 his2 ura4 klp5-GFP-kanR sad1-dsRED-LEU2*	This study
AR044	*h⁻ leu1 klp5-GFP-kanR sad1-dsRED-LEU2*	This study
AR251	*h⁻ leu1 ura4 klp5-2mRFP-kanR klp6-GFP-kan*	This study
AR065	*h⁻ leu1 ura4 klp5-GFP-kanR pREP3(RFP-atb2 LEU2)*	This study
AR085	*h⁻ leu1 ura4 klp6-GFP-kanR pREP3(RFP-atb2 LEU2)*	This study
MS1630	*h⁻ leu1 ura4 GFP-atb2-kanR cut12-CFP-natR mis6-2mRFP-hphR*	Lab stock
AR320	*h⁻ leu1 ura4 his2? his7? ade6-m216?GFP-atb2-kanR cut12-CFP-natR mis6-2mRFP-hphR klp5::ura4*	This study
AR030	*h? leu1 his2? klp6::kanR his7+::lacI-GFP ura4? cen2::Kan-ura4+-lacOp sad1-dsRed::LEU2*	This study
KZ85	*h⁻ leu1 his7+::lacI-GFP ura4? cen2::Kan-ura4+-lacOp sad1-dsRed::LEU2*	Lab stock
NK027	*h⁻ klp5::kanR leu1 ura4*	Lab stock
NK113	*h⁺ mad3::ura4+ leu1 ura4 his2*	Lab stock
AE249	*h⁻ mad1::ura4+ leu1 ura4*	Dr Matsumoto
NK028-6A	*h⁻ leu1ura4his2/7 -mad2::ura4*	Lab stock
NK117	*h⁻ bub3::ura4+ leu1 ura4*	Lab stock
SS560	*h⁻ mph1::ura4+ leu1 ura4 ade6-m216*	Dr Sazer
393	*h⁻ leu1-32 ura4DS/E his1-102 ade6-216 bub1::ura4*	Dr Javerzat
AR014	*h⁺ klp5::kanR mad1::ura4+ leu1 ura4 his2*	This study
NK029-1B	*h⁻ leu1 ura4 kanR-klp5::KanR -mad2::ura4*	Lab stock
AR008	*h⁻ klp5::kanR mad3::ura4+ leu1ura4*	This study
AR020	*h⁻ klp5::kanR bub1::ura4+ leu1 ura4 ade?*	This study
AR012	*h⁺ klp5::kanR bub3::ura4+ leu1 ura4 his2*	This study
AR010	*h⁻ klp5::kanR mph1::ura4+ leu1ura4 ade6-m216*	This study
AR079	*h⁺ leu1 ura4 ade6-216 klp6::hygR bub1::ura4+ his7⁺::lacI-GFP cen2::Kan-ura4+-lacOp sad1-dsRed::LEU2*	This study
AR055	*h⁻ ura4? mad2::nat klp6::hygR his7+::lacI-GFP cen2::Kan-ura4+-lacOp sad1-dsRed::LEU2*	This study
PN4347	*h⁻ leu1-32 ura4-D18 bub1::bub1-K762R-GFP-kanR*	Dr Yamaguchi

PN4157	*h⁻ leu1 ura4 ade6-704 bub1::bub1-KD-del-GFP-kanR*	Dr Yamaguchi
PN4464	*h⁻ leu1-32 ura4-D18 bub1::bub1-P*-GFP-kanR*	Dr Yamaguchi
AR136	*h⁺ leu1 ura4 his7 klp5::ura4+ bub1-K762R-GFP-kan*	This study
AR138	*h⁻ leu1 ura4 klp5::ura4+ bub1-KD-del-GFP-kan*	This study
AR134	*h⁻ leu1 ura4 klp5::ura4+ bub1-P*-GFP-kan*	This study
AR428	*h⁺ leu1 ura4 his2 cut9-665 GFP-atb2-kanR mis6-2mRFP-hph*	This study
AR440	*h⁺ leu1 ura4 his2 cut9-665 GFP-atb2-kanR mis6-2mRFP-hph klp5::nat*	This study
AR017	*h⁻ klp5::ura4+ leu1 ura4*	This study
NK028-5A	*h⁻ leu1 ura4 his2/7 klp6::ura4+*	Lab stock
AR197	*h⁻ leu1 ura4 klp5::ura4+::GFP-klp5*	This study
AR198	*h⁻ leu1 ura4 klp5::ura4+::GFP-klp5-T151N*	This study
AR200	*h⁻ leu1 ura4 klp5::ura4+::GFP-klp5-G297A*	This study
AR202	*h⁻ leu1 ura4 klp5::ura4+::GFP-klp5-E299A*	This study
AR219	*h⁻ leu1 ura4 klp5::ura4+::GFP-klp5 pREP3(RFP-atb2 LEU2)*	This study
AR220	*h⁻ leu1 ura4 klp5::ura4+::GFP-klp5-T151N pREP3(RFP-atb2 LEU2)*	This study
AR221	*h⁻ leu1 ura4 klp5::ura4+::GFP-klp5-G297A pREP3(RFP-atb2 LEU2)*	This study
AR222	*h⁻ leu1 ura4 klp5::ura4+::GFP-klp5-E299A pREP3(RFP-atb2 LEU2)*	This study
AR346	*h⁺ leu1 ura4 his2 his7? klp5::ura4+::klp5-T151N GFP-atb2-kanR cut12-CFP-natR mis6-2mRFP-hphR*	This study
AR066	*h⁻ leu1 ura4 Klp5-GFP-kanR klp6::ura4 pREP3(RFP-atb2 LEU2)*	This study
AR067	*h⁺ leu1ura4 ade6-m216 Klp5::ura4 Klp6-GFP-kanR pREP3(RFP-atb2 LEU2)*	This study
AR236	*h⁻ leu1ura4 Klp6-3HA-kanR pREP41(GFP-klp5 LEU2)*	This study
AR237	*h⁻ leu1ura4 Klp6-3HA-kanR pREP41(GFP-klp- CCmut LEU2)*	This study
MA108	*h⁻ leu1 ura4 Klp6-HA-kanR*	Lab stock
AR161	*h⁺ leu1 ura4 his2 pREP41(GFP-klp5 LEU2)*	This study
AR294	*h⁻ klp5::ura4+::GFP-klp5-CCmut leu1 ura4*	This study

AR293	*h⁻ leu1 ura4 klp6 N::ura4+::klp6 N (CC deletion aa 402 - 431)*	This study
AR300	*h⁻ leu1 ura4 klp6 N::ura4+::klp6 N (CC deletion aa 402 - 431)-GFP-kanR*	This study
AR304	*h? leu1 ura4 klp5-GFP-kanR sad1-dsRED-LEU2 klp6 N::ura4+::klp6 N (CC deletion aa 402 - 431)-GFP-kan*	This study
AR214	*h⁻ leu1 ura4 klp5::ura4+ klp6::hph pREP41(GFP-klp5 LEU2)*	This study
AR216	*h⁻ leu1 ura4 klp5::ura4+ klp6::hph pREP41(GFP-klp5-R693A-R695A LEU2)*	This study
AR217	*h⁻ leu1 ura4 klp5::ura4+ klp6::hph pREP41(GFP-klp6-R673A-R675A LEU2)*	This study
AR218	*h⁻ leu1 ura4 klp5::ura4+ klp6::hph pREP41(GFP-klp6 LEU2)*	This study
AR197	*h⁻ leu1 ura4 klp5::ura4+::GFP-klp5*	This study
AR375	*h⁻ leu1 ura4 klp5::ura4+::GFP-klp5-R693A-R695A*	This study
AR297	*h⁻ klp5::ura4+::GFP-klp5-S678A leu1 ura4*	This study
AR298	*h⁻ klp5::ura4+::GFP-klp5-S689A leu1 ura4*	This study
AR299	*h⁻ klp5::ura4+::GFP-klp5-S678A-S689A leu1 ura4*	This study
AR107	*h⁺ leu1 ura4 his7 ade6-m216 Klp5::ura4::klp5 (AA 405-883)*	This study
AR393	*h⁺ leu1 ura4 his7 ade6-m216 Klp5::ura4::klp5 (AA 405-883)-GFP-kanR*	This study
AR409	*h⁻ leu1 ura4 ade6-m216? Klp5::ura4::klp5 (AA 405-883)-GFP-kanR sad1-dsRED-nat*	This study
AR157	*h⁻ leu1 ura4 klp6-GFP-kanR Klp5::ura4::klp5 (AA 405-883) sad1-dsRED-LEU2*	This study
AR101	*h⁻ leu1 ura4 his2/7 klp6::ura4+::klp6 (AA 411-784)*	This study
AR167	*h⁻ leu1 ura4 his2/7 klp6::ura4+::klp6 (AA 411-784)-GFP-kanR*	This study
AR112	*h⁺ leu1 ura4 his 2/7 klp5-GFP-kanR klp6::ura4+::klp6(aa 411-784) sad1-dsRED*	This study
AR118	*h⁻ leu1 ura4 klp5 C::ura4+ (AA 1-432 remaining)*	This study
AR128	*h⁺ leu1 ura4 his7 alp14::kanR klp5 C::ura4+*	This study
AR204	*h⁻ leu1 ura4 klp5 C::ura4+ (AA 1-432 remaining) klp6 C::ura4+ (AA 1-431 remaining)*	This study

AR119	*h⁻ leu1 ura4 klp6 C::ura4+ (AA 1-431 remaining)*	This study
AR130	*h⁺ leu1 ura4 his7 alp14::kanR klp6 C::ura4+*	This study
AR257	*h⁺ leu1 ura4 his2 klp5::kanR klp6 N::ura4+ (AA 411 onwards remaining)*	This study
AR354	*h⁺ leu1 ura4 his2 klp5::kanR klp6 N::ura4+ (AA 411 onwards remaining):: klp5 N (AA 1-404)*	This study
AR374	*h⁺ leu1 ura4 his2 klp6 N::ura4+ (AA 411 onwards remaining):: klp5 N (AA 1-404)*	This study
AR399	*h⁻ leu1 ura4 klp6 N::ura4+ (AA 411 onwards remaining):: klp5 N (AA 1-404)-GFP-nat*	This study
AR400	*h⁻ leu1 ura4 klp5 N::ura4+ (AA 405 onwards remaining):: klp6 N (AA 1-410) klp6::ura*	This study
AR402	*h⁻ leu1 ura4 klp5 N::ura4+ (AA 405 onwards remaining):: klp6 N (AA 1-410)*	This study
AR404	*h⁻ leu1 ura4 klp5 N::ura4+ (AA 405 onwards remaining):: klp6 N (AA 1-410) klp6::hph*	This study
AR445	*h⁺ leu1 ura4 his2 klp5 N::ura4+ (AA 405 onwards remaining):: klp6 N (AA 1-403)-GFP-nat*	This study
AR446	*h⁺ leu1 ura4 his2 klp5 N::ura4+ (AA 405 onwards remaining):: klp6 N (AA 1-410) klp6 N::ura4+ (AA 411 onwards remaining):: klp5 N (AA 1-404)*	This study
AR449	*h⁻ leu1 ura4 nmtP3-GFP-atb2-kanR klp6 N::ura4+ (AA 411 onwards remaining):: klp5 N (AA 1-404)*	This study
AR450	*h⁻ leu1 ura4 nmtP3-GFP-atb2-kanR klp5 N::ura4+ (AA 405 onwards remaining):: klp6 N (AA 1-403)*	This study
AR287	*h⁻ leu1 ura4 nmtP3-GFP-atb2-kanR klp5::ura4+*	This study
AR289	*h⁻ leu1 ura4 nmtP3-GFP-atb2-kanR klp6::ura4+*	This study
MA201	*h⁻ leu1ura4 nmtP3-GFP-atb2-kanR*	This study
AR448	*h⁻ leu1 ura4 ade6-216 bub1::ura4+ his7+::lacI-GFP cen2::Kan-ura4+-lacOp sad1-dsRed::LEU2*	This study
KZ147	*h⁻ leu1 cen2-GFP sad1-dsRED mad2::kanR*	Lab stock

5 Concluding Remarks

This thesis has described the continued characterisation of the fission yeast Kinesin-8 members, Klp5 and Klp6. Our study has shed light on both the role and the regulation of Klp5/Klp6 during mitosis.

Klp5 and Klp6 are clearly required for proper chromosome movements during mitosis. As chromosome movements are dependent on microtubule plus-end dynamics, the defective movements observed in *Δklp* could be (and have been) attributed solely to altered microtubule dynamics. Microtubules are stabilised in *Δklp* cells, but this does not appear to result in reduced chromosome movements or in reduced tension across sister kinetochores. Our results suggest that the predominant phenotype observed in *Δklp* mitotic cells could be due to persistence of defective MT-kinetochore attachments, specifically merotelic attachments, in which one kinetochore is attached to both poles. When cells are competent for the spindle checkpoint, a delay is imposed, allowing time for another, presumably slower-acting, mechanism to correct the erroneous attachments. However, in the absence of a functional checkpoint, anaphase lagging chromosomes are observed in *Δklp* cells, which are the hallmark of uncorrected merotelic attachments. In higher organisms, merotelic attachments can be directly visualised by microscopy; unfortunately yeast cells are too small for this to be possible. We think it probable that Klp5/Klp6 possess MT depolymerising activity that destabilises erroneous merotelic attachments. In this sense, the function of these Kinesin-8 proteins in fission yeast is akin to that of the Kinesin-13s in higher eukaryotes.

Klp5/Klp6 also contribute to the global regulation of MT dynamics, as evidenced by the effect of deletion on length of both cytoplasmic interphase MTs and mitotic spindle MTs. We speculate that spindle elongation in anaphase B may in part be effected by inhibition of Klp5/Klp6 depolymerising activity, possibly by Aurora B phosphorylation in the motor domain of Klp5. This would be an interesting hypothesis to test.

Interestingly, dimerisation appears to be essential for Klp function *in vivo* – constructs that are monomeric for the kinesin domain (ΔN mutants), or have one defective kinesin domain (ATPase mutants) showed phenotypes similar to complete deletion of *klp5* or *klp6*. Furthermore, heterodimerisation is essential for proper Klp function, suggesting that Klp5 and Klp6 must make distinct contributions to the function of the Klp5/Klp6 heterocomplex. A more detailed comparison of Klp5 and Klp6 sequences and/or structures and subsequent

mutational analysis may reveal the regions or residues that are responsible for the differences between them. Such work would be of general interest and relevance to the kinesin field. Additionally, the geometry of the Klp5/Klp6 heterocomplex is important for its function, raising the possibility of inter- and intramolecular regulation of the complex. There was not sufficient time to address this during our study, but it would be an interesting area for future study. The findings regarding the necessity of heterodimerisation must be considered for any future biochemical work to be carried out on Klp5 and Klp6. It is possible that these proteins would be able to function as monomers *in vitro* e.g. as depolymerises and/or motors, but it would certainly be preferable to study dimers.

We have shown that Klp5/Klp6 are regulated at the level of nuclear import and export by their canonical NLSs and by the exportin Crm1. Other components important for spindle assembly are also regulated by Ran, and the activities of many proteins, especially transcription factors, are controlled by regulating their access to the nucleus. It would be good to further define how the cell-cycle dependent nuclear import of Klp5 is achieved, and how heterodimerisation causes nuclear retention. It is important to elucidate such mechanisms, as they could well be conserved in very different types of proteins.

There are a number of specific experiments that, if successfully carried out, could provide answers to outstanding questions raised in this thesis. These are mainly biochemical experiments, which would nicely complement the data obtained from cell and molecular biology techniques that are presented here. Firstly, it would be good to confirm heterodimerisation of Klp5/Klp6 by gel filtration and/or velocity sedimentation. This could also reveal whether monomer and homodimer pools of Klp5 and Klp6 exist. As mentioned previously, we would like to investigate whether Klp5 and Klp6 exhibit different affinities for microtubules, by carrying out a microtubule-binding assay. It will also be important to demonstrate whether Klp5 and Klp6 possess microtubule depolymerising activity, for example by carrying out a sedimentation assay. Additionally, further work is required to show whether Klp5 is phosphorylated at the CDK consensus site overlapping its NLS. This could be determined by mass spectrometry, or by an in vitro phosphorylation assay.

We envisage that the continued study of mitotic regulators such as Klp5 and Klp6 in genetically tractable model organisms like fission yeast will facilitate the discovery and characterisation of similar molecules and mechanisms in human cells. This will enable us to further disseminate the process of cell division and contribute to the discovery of drug targets of the future.

6 References

Adams, R.R., Carmena, M., and Earnshaw, W.C. (2001). Chromosomal passengers and the (aurora) ABCs of mitosis. Trends Cell Biol *11*, 49-54.

Al-Bassam, J., Larsen, N.A., Hyman, A.A., and Harrison, S.C. (2007). Crystal structure of a TOG domain: conserved features of XMAP215/Dis1-family TOG domains and implications for tubulin binding. Structure *15*, 355-362.

Al-Bassam, J., van Breugel, M., Harrison, S.C., and Hyman, A. (2006). Stu2p binds tubulin and undergoes an open-to-closed conformational change. J Cell Biol *172*, 1009-1022.

Alberts, B., Johnson, A., Lewis, J., Raff, M., Roberts, K., and Walter, P. (2002). Molecular Biology of the Cell. Garland Science, New York, USA.

Alexandru, G., Uhlmann, F., Mechtler, K., Poupart, M.A., and Nasmyth, K. (2001). Phosphorylation of the cohesin subunit Scc1 by Polo/Cdc5 kinase regulates sister chromatid separation in yeast. Cell *105*, 459-472.

Allingham, J.S., Sproul, L.R., Rayment, I., and Gilbert, S.P. (2007). Vik1 modulates microtubule-Kar3 interactions through a motor domain that lacks an active site. Cell *128*, 1161-1172.

Amos, L., and Klug, A. (1974). Arrangement of subunits in flagellar microtubules. J Cell Sci *14*, 523-549.

Amos, L.A., and Hirose, K. (2007). A cool look at the structural changes in kinesin motor domains. J Cell Sci *120*, 3919-3927.

Anders, A., Lourenco, P.C., and Sawin, K.E. (2006). Noncore components of the fission yeast gamma-tubulin complex. Mol Biol Cell *17*, 5075-5093.

Andreassen, P.R., Lacroix, F.B., and Margolis, R.L. (1997). Chromosomes with Two Intact Axial Cores Are Induced by G2 Checkpoint Override: Evidence That DNA Decatenation Is not Required to Template the Chromosome Structure. The Journal of Cell Biology *136*, 29-43.

Andrews, P.D., Ovechkina, Y., Morrice, N., Wagenbach, M., Duncan, K., Wordeman, L., and Swedlow, J.R. (2004). Aurora B regulates MCAK at the mitotic centromere. Dev Cell *6*, 253-268.

Asakawa, K., Kume, K., Kanai, M., Goshima, T., Miyahara, K., Dhut, S., Tee, W.W., Hirata, D., and Toda, T. (2006). The V260I mutation in fission yeast alpha-tubulin Atb2 affects microtubule dynamics and EB1-Mal3 localization and activates the Bub1 branch of the spindle checkpoint. Mol Biol Cell *17*, 1421-1435.

Asakawa, K., Toya, M., Sato, M., Kanai, M., Kume, K., Goshima, T., Garcia, M.A., Hirata, D., and Toda, T. (2005). Mal3, the fission yeast EB1 homologue, cooperates with Bub1 spindle checkpoint to prevent monopolar attachment. EMBO Rep *6*, 1194-1200.

Asbury, C.L. (2005). Kinesin: world's tiniest biped. Curr Opin Cell Biol *17*, 89-97.

Bahler, J., Wu, J.Q., Longtine, M.S., Shah, N.G., McKenzie, A., 3rd, Steever, A.B., Wach, A., Philippsen, P., and Pringle, J.R. (1998). Heterologous modules for efficient and versatile PCR-based gene targeting in Schizosaccharomyces pombe. Yeast *14*, 943-951.

Berliner, E., Young, E.C., Anderson, K., Mahtani, H.K., and Gelles, J. (1995). Failure of a single-headed kinesin to track parallel to microtubule protofilaments. Nature *373*, 718-721.

Bernard, P., Hardwick, K., and Javerzat, J.P. (1998). Fission yeast bub1 is a mitotic centromere protein essential for the spindle checkpoint and the preservation of correct ploidy through mitosis. J Cell Biol *143*, 1775-1787.

Bernard, P., Maure, J.F., Partridge, J.F., Genier, S., Javerzat, J.P., and Allshire, R.C. (2001). Requirement of heterochromatin for cohesion at centromeres. Science *294*, 2539-2542.

Booher, R.N., Alfa, C.E., Hyams, J.S., and Beach, D.H. (1989). The fission yeast cdc2/cdc13/suc1 protein kinase: regulation of catalytic activity and nuclear localization. Cell *58*, 485-497.

Boyarchuk, Y., Salic, A., Dasso, M., and Arnaoutov, A. (2007). Bub1 is essential for assembly of the functional inner centromere. J Cell Biol *176*, 919-928.

Browning, H., Hackney, D.D., and Nurse, P. (2003). Targeted movement of cell end factors in fission yeast. Nat Cell Biol *5*, 812-818.

Brunner, D., and Nurse, P. (2000). CLIP170-like tip1p spatially organizes microtubular dynamics in fission yeast. Cell *102*, 695-704.

Busch, K.E., and Brunner, D. (2004). The microtubule plus end-tracking proteins mal3p and tip1p cooperate for cell-end targeting of interphase microtubules. Curr Biol *14*, 548-559.

Carazo-Salas, R.E., Antony, C., and Nurse, P. (2005). The kinesin Klp2 mediates polarization of interphase microtubules in fission yeast. Science *309*, 297-300.

Carazo-Salas, R.E., Gruss, O.J., Mattaj, I.W., and Karsenti, E. (2001). Ran-GTP coordinates regulation of microtubule nucleation and dynamics during mitotic-spindle assembly. Nat Cell Biol *3*, 228-234.

Carazo-Salas, R.E., and Nurse, P. (2006). Self-organization of interphase microtubule arrays in fission yeast. Nat Cell Biol *8*, 1102-1107.

Carroll, C.W., and Straight, A.F. (2006). Centromere formation: from epigenetics to self-assembly. Trends Cell Biol *16*, 70-78.

Cassimeris, L. (2007). Tubulin delivery: polymerization chaperones for microtubule assembly? Dev Cell *13*, 455-456.

Charrasse, S., Coubes, P., Arrancibia, S., and Larroque, C. (1996). Expression of the tumor over-expressed ch-TOG gene in human and baboon brain. Neurosci Lett *212*, 119-122.

Charrasse, S., Mazel, M., Taviaux, S., Berta, P., Chow, T., and Larroque, C. (1995). Characterization of the cDNA and pattern of expression of a new gene over-expressed in human hepatomas and colonic tumors. Eur J Biochem *234*, 406-413.

Charrasse, S., Schroeder, M., Gauthier-Rouviere, C., Ango, F., Cassimeris, L., Gard, D.L., and Larroque, C. (1998). The TOGp protein is a new human microtubule-associated protein homologous to the Xenopus XMAP215. J Cell Sci *111 (Pt 10)*, 1371-1383.

Cheeseman, I.M., Anderson, S., Jwa, M., Green, E.M., Kang, J., Yates, J.R., 3rd, Chan, C.S., Drubin, D.G., and Barnes, G. (2002). Phospho-regulation of kinetochore-microtubule attachments by the Aurora kinase Ipl1p. Cell *111*, 163-172.

Cheeseman, I.M., Chappie, J.S., Wilson-Kubalek, E.M., and Desai, A. (2006). The conserved KMN network constitutes the core microtubule-binding site of the kinetochore. Cell *127*, 983-997.

Ciferri, C., De Luca, J., Monzani, S., Ferrari, K.J., Ristic, D., Wyman, C., Stark, H., Kilmartin, J., Salmon, E.D., and Musacchio, A. (2005). Architecture of the human ndc80-hec1 complex, a critical constituent of the outer kinetochore. J Biol Chem *280*, 29088-29095.

Cimini, D. (2007). Detection and correction of merotelic kinetochore orientation by Aurora B and its partners. Cell Cycle *6*, 1558-1564.

Cimini, D., Cameron, L.A., and Salmon, E.D. (2004). Anaphase spindle mechanics prevent mis-segregation of merotelically oriented chromosomes. Curr Biol *14*, 2149-2155.

Cimini, D., Howell, B., Maddox, P., Khodjakov, A., Degrassi, F., and Salmon, E.D. (2001). Merotelic kinetochore orientation is a major mechanism of aneuploidy in mitotic mammalian tissue cells. J Cell Biol *153*, 517-527.

Cimini, D., Moree, B., Canman, J.C., and Salmon, E.D. (2003). Merotelic kinetochore orientation occurs frequently during early mitosis in mammalian tissue cells and error correction is achieved by two different mechanisms. J Cell Sci *116*, 4213-4225.

Cimini, D., Wan, X., Hirel, C.B., and Salmon, E.D. (2006). Aurora kinase promotes turnover of kinetochore microtubules to reduce chromosome segregation errors. Curr Biol *16*, 1711-1718.

Ciosk, R., Zachariae, W., Michaelis, C., Shevchenko, A., Mann, M., and Nasmyth, K. (1998). An ESP1/PDS1 complex regulates loss of sister chromatid cohesion at the metaphase to anaphase transition in yeast. Cell *93*, 1067-1076.

Cottingham, F.R., and Hoyt, M.A. (1997). Mitotic spindle positioning in Saccharomyces cerevisiae is accomplished by antagonistically acting microtubule motor proteins. J Cell Biol *138*, 1041-1053.

Courtwright, A.M., and He, X. (2002). Dam1 is the right one: phosphoregulation of kinetochore biorientation. Dev Cell *3*, 610-611.

Coy, D.L., Hancock, W.O., Wagenbach, M., and Howard, J. (1999). Kinesin's tail domain is an inhibitory regulator of the motor domain. Nat Cell Biol *1*, 288-292.

D'Angiolella, V., Mari, C., Nocera, D., Rametti, L., and Grieco, D. (2003). The spindle checkpoint requires cyclin-dependent kinase activity. Genes Dev *17*, 2520-2525.

Daga, R.R., Lee, K.G., Bratman, S., Salas-Pino, S., and Chang, F. (2006a). Self-organization of microtubule bundles in anucleate fission yeast cells. Nat Cell Biol *8*, 1108-1113.

Daga, R.R., Yonetani, A., and Chang, F. (2006b). Asymmetric microtubule pushing forces in nuclear centering. Curr Biol *16*, 1544-1550.

David-Pfeuty, T., Erickson, H.P., and Pantaloni, D. (1977). Guanosinetriphosphatase activity of tubulin associated with microtubule assembly. Proc Natl Acad Sci U S A *74*, 5372-5376.

De Antoni, A., Pearson, C.G., Cimini, D., Canman, J.C., Sala, V., Nezi, L., Mapelli, M., Sironi, L., Faretta, M., Salmon, E.D., and Musacchio, A. (2005). The Mad1/Mad2 complex as a template for Mad2 activation in the spindle assembly checkpoint. Curr Biol *15*, 214-225.

de Gramont, A., Ganier, O., and Cohen-Fix, O. (2006). Before and after the spindle assembly checkpoint--an APC/C point of view. Cell Cycle *5*, 2168-2171.

Desai, A., Verma, S., Mitchison, T.J., and Walczak, C.E. (1999). Kin I kinesins are microtubule-destabilizing enzymes. Cell *96*, 69-78.

Ding, D.Q., Yamamoto, A., Haraguchi, T., and Hiraoka, Y. (2004). Dynamics of homologous chromosome pairing during meiotic prophase in fission yeast. Dev Cell *6*, 329-341.

Ding, R., McDonald, K.L., and McIntosh, J.R. (1993). Three-dimensional reconstruction and analysis of mitotic spindles from the yeast, Schizosaccharomyces pombe. J Cell Biol *120*, 141-151.

Ding, R., West, R.R., Morphew, D.M., Oakley, B.R., and McIntosh, J.R. (1997). The spindle pole body of Schizosaccharomyces pombe enters and leaves the nuclear envelope as the cell cycle proceeds. Mol Biol Cell *8*, 1461-1479.

Dong, C., Li, Z., Alvarez, R., Feng, X.-H., and Goldschmidt-Clermont, P.J. (2000). Microtubule Binding to Smads May Regulate TGF[beta] Activity. Molecular Cell *5*, 27-34.

Drummond, D.R., and Cross, R.A. (2000). Dynamics of interphase microtubules in Schizosaccharomyces pombe. Curr Biol *10*, 766-775.

Endow, S.A., and Waligora, K.W. (1998). Determinants of kinesin motor polarity. Science *281*, 1200-1202.

Enquist-Newman, M., Cheeseman, I.M., Van Goor, D., Drubin, D.G., Meluh, P.B., and Barnes, G. (2001). Dad1p, third component of the Duo1p/Dam1p complex involved in kinetochore function and mitotic spindle integrity. Mol Biol Cell *12*, 2601-2613.

Erickson, H.P. (2000). Gamma-tubulin nucleation: template or protofilament? Nat Cell Biol *2*, E93-96.

Evans, L., Mitchison, T., and Kirschner, M. (1985). Influence of the centrosome on the structure of nucleated microtubules. J Cell Biol *100*, 1185-1191.

Fan, J., Griffiths, A.D., Lockhart, A., Cross, R.A., and Amos, L.A. (1996). Microtubule minus ends can be labelled with a phage display antibody specific to alpha-tubulin. J Mol Biol *259*, 325-330.

Fan, J.B., Chikashige, Y., Smith, C.L., Niwa, O., Yanagida, M., and Cantor, C.R. (1989). Construction of a Not I restriction map of the fission yeast Schizosaccharomyces pombe genome. Nucleic Acids Res *17*, 2801-2818.

Fornerod, M., and Ohno, M. (2002). Exportin-mediated nuclear export of proteins and ribonucleoproteins. Results Probl Cell Differ *35*, 67-91.

Fornerod, M., Ohno, M., Yoshida, M., and Mattaj, I.W. (1997). CRM1 is an export receptor for leucine-rich nuclear export signals. Cell *90*, 1051-1060.

Friedman, D.S., and Vale, R.D. (1999). Single-molecule analysis of kinesin motility reveals regulation by the cargo-binding tail domain. Nat Cell Biol *1*, 293-297.

Fujita, A., Vardy, L., Garcia, M.A., and Toda, T. (2002). A fourth component of the fission yeast gamma-tubulin complex, Alp16, is required for cytoplasmic microtubule integrity and becomes indispensable when gamma-tubulin function is compromised. Mol Biol Cell *13*, 2360-2373.

Fukagawa, T., Nogami, M., Yoshikawa, M., Ikeno, M., Okazaki, T., Takami, Y., Nakayama, T., and Oshimura, M. (2004). Dicer is essential for formation of the heterochromatin structure in vertebrate cells. Nat Cell Biol *6*, 784-791.

Fukuda, M., Asano, S., Nakamura, T., Adachi, M., Yoshida, M., Yanagida, M., and Nishida, E. (1997). CRM1 is responsible for intracellular transport mediated by the nuclear export signal. Nature *390*, 308-311.

Funabiki, H., and Murray, A.W. (2000). The Xenopus chromokinesin Xkid is essential for metaphase chromosome alignment and must be degraded to allow anaphase chromosome movement. Cell *102*, 411-424.

Funabiki, H., Yamano, H., Kumada, K., Nagao, K., Hunt, T., and Yanagida, M. (1996). Cut2 proteolysis required for sister-chromatid seperation in fission yeast. Nature *381*, 438-441.

Gachet, Y., Tournier, S., Millar, J.B., and Hyams, J.S. (2001). A MAP kinase-dependent actin checkpoint ensures proper spindle orientation in fission yeast. Nature *412*, 352-355.

Gachet, Y., Tournier, S., Millar, J.B., and Hyams, J.S. (2004). Mechanism controlling perpendicular alignment of the spindle to the axis of cell division in fission yeast. Embo J *23*, 1289-1300.

Gandhi, R., Bonaccorsi, S., Wentworth, D., Doxsey, S., Gatti, M., and Pereira, A. (2004). The Drosophila kinesin-like protein KLP67A is essential for mitotic and male meiotic spindle assembly. Mol Biol Cell *15*, 121-131.

Ganem, N.J., and Compton, D.A. (2004). The KinI kinesin Kif2a is required for bipolar spindle assembly through a functional relationship with MCAK. J Cell Biol *166*, 473-478.

Garcia, M.A., Koonrugsa, N., and Toda, T. (2002a). Two kinesin-like Kin I family proteins in fission yeast regulate the establishment of metaphase and the onset of anaphase A. Curr Biol *12*, 610-621.

Garcia, M.A., Koonrugsa, N., Toda, T., West, R.R., Malmstrom, T., McIntosh, J.R., and Troxell, C.L. (2002b). Spindle-kinetochore attachment requires the combined action of Kin I-like Klp5/6 and Alp14/Dis1-MAPs in fission yeast. Embo J *21*, 6015-6024.

Garcia, M.A., Vardy, L., Koonrugsa, N., and Toda, T. (2001). Fission yeast ch-TOG/XMAP215 homologue Alp14 connects mitotic spindles with the kinetochore and is a component of the Mad2-dependent spindle checkpoint. Embo J *20*, 3389-3401.

Gardner, M.K., Pearson, C.G., Sprague, B.L., Zarzar, T.R., Bloom, K., Salmon, E.D., and Odde, D.J. (2005). Tension-dependent regulation of microtubule dynamics at kinetochores can explain metaphase congression in yeast. Mol Biol Cell *16*, 3764-3775.

Gatt, M.K., Savoian, M.S., Riparbelli, M.G., Massarelli, C., Callaini, G., and Glover, D.M. (2005). Klp67A destabilises pre-anaphase microtubules but subsequently is required to stabilise the central spindle. J Cell Sci *118*, 2671-2682.

Gorbsky, G.J. (1994). Cell cycle progression and chromosome segregation in mammalian cells cultured in the presence of the topoisomerase II inhibitors ICRF-187 [(+)-1,2-bis(3,5-dioxopiperazinyl-1-yl)propane; ADR-529] and ICRF-159 (Razoxane). Cancer Res *54*, 1042-1048.

Gorbsky, G.J. (2004). Mitosis: MCAK under the aura of Aurora B. Curr Biol *14*, R346-348.

Goshima, G., Saitoh, S., and Yanagida, M. (1999). Proper metaphase spindle length is determined by centromere proteins Mis12 and Mis6 required for faithful chromosome segregation. Genes Dev *13*, 1664-1677.

Goshima, G., and Vale, R.D. (2003). The roles of microtubule-based motor proteins in mitosis: comprehensive RNAi analysis in the Drosophila S2 cell line. J Cell Biol *162*, 1003-1016.

Goshima, G., Wollman, R., Stuurman, N., Scholey, J.M., and Vale, R.D. (2005). Length control of the metaphase spindle. Curr Biol *15*, 1979-1988.

Grallert, A., Beuter, C., Craven, R.A., Bagley, S., Wilks, D., Fleig, U., and Hagan, I.M. (2006). S. pombe CLASP needs dynein, not EB1 or CLIP170, to induce microtubule instability and slows polymerization rates at cell tips in a dynein-dependent manner. Genes and Development *20*, 2421-2436.

Gregan, J., Riedel, C.G., Pidoux, A.L., Katou, Y., Rumpf, C., Schleiffer, A., Kearsey, S.E., Shirahige, K., Allshire, R.C., and Nasmyth, K. (2007). The kinetochore proteins Pcs1 and Mde4 and heterochromatin are required to prevent merotelic orientation. Curr Biol *17*, 1190-1200.

Grishchuk, E.L., and McIntosh, J.R. (2006). Microtubule depolymerization can drive poleward chromosome motion in fission yeast. Embo J *25*, 4888-4896.

Guacci, V., Koshland, D., and Strunnikov, A. (1997). A direct link between sister chromatid cohesion and chromosome condensation revealed through the analysis of MCD1 in S. cerevisiae. Cell *91*, 47-57.

Gupta, M.L., Jr., Carvalho, P., Roof, D.M., and Pellman, D. (2006). Plus end-specific depolymerase activity of Kip3, a kinesin-8 protein, explains its role in positioning the yeast mitotic spindle. Nat Cell Biol *8*, 913-923.

Hagan, I., and Yanagida, M. (1992). Kinesin-related cut7 protein associates with mitotic and meiotic spindles in fission yeast. Nature *356*, 74-76.

Hagan, I.M., and Hyams, J.S. (1988). The use of cell division cycle mutants to investigate the control of microtubule distribution in the fission yeast Schizosaccharomyces pombe. J Cell Sci *89 (Pt 3)*, 343-357.

Haller, K., Rambaldi, I., Daniels, E., and Featherstone, M. (2004). Subcellular localization of multiple PREP2 isoforms is regulated by actin, tubulin, and nuclear export. J Biol Chem *279*, 49384-49394.

Hancock, W.O., and Howard, J. (1998). Processivity of the motor protein kinesin requires two heads. J Cell Biol *140*, 1395-1405.

Hartwell, L.H., Culotti, J., Pringle, J.R., and Reid, B.J. (1974). Genetic control of the cell division cycle in yeast. Science *183*, 46-51.

He, X., Rines, D.R., Espelin, C.W., and Sorger, P.K. (2001). Molecular analysis of kinetochore-microtubule attachment in budding yeast. Cell *106*, 195-206.

Helenius, J., Brouhard, G., Kalaidzidis, Y., Diez, S., and Howard, J. (2006). The depolymerizing kinesin MCAK uses lattice diffusion to rapidly target microtubule ends. Nature *441*, 115-119.

Hertzer, K.M., Ems-McClung, S.C., Kline-Smith, S.L., Lipkin, T.G., Gilbert, S.P., and Walczak, C.E. (2006). Full-length dimeric MCAK is a more efficient microtubule depolymerase than minimal domain monomeric MCAK. Mol Biol Cell *17*, 700-710.

Higuchi, T., and Uhlmann, F. (2005). Stabilization of microtubule dynamics at anaphase onset promotes chromosome segregation. Nature *433*, 171-176.

Hirano, T., and Mitchison, T.J. (1994). A heterodimeric coiled-coil protein required for mitotic chromosome condensation in vitro. Cell *79*, 449-458.

Hirose, K., Fan, J., and Amos, L.A. (1995). Re-examination of the polarity of microtubules and sheets decorated with kinesin motor domain. J Mol Biol *251*, 329-333.

Hoog, J.L., Schwartz, C., Noon, A.T., O'Toole, E.T., Mastronarde, D.N., McIntosh, J.R., and Antony, C. (2007). Organization of interphase microtubules in fission yeast analyzed by electron tomography. Dev Cell *12*, 349-361.

Horio, T., Uzawa, S., Jung, M.K., Oakley, B.R., Tanaka, K., and Yanagida, M. (1991). The fission yeast gamma-tubulin is essential for mitosis and is localized at microtubule organizing centers. J Cell Sci *99 (Pt 4)*, 693-700.

Hornig, N.C., Knowles, P.P., McDonald, N.Q., and Uhlmann, F. (2002). The dual mechanism of separase regulation by securin. Curr Biol *12*, 973-982.

Hoyt, M.A., Totis, L., and Roberts, B.T. (1991). S. cerevisiae genes required for cell cycle arrest in response to loss of microtubule function. Cell *66*, 507-517.

Hua, W., Young, E.C., Fleming, M.L., and Gelles, J. (1997). Coupling of kinesin steps to ATP hydrolysis. Nature *388*, 390-393.

Huang, H., Feng, J., Famulski, J., Rattner, J.B., Liu, S.T., Kao, G.D., Muschel, R., Chan, G.K., and Yen, T.J. (2007). Tripin/hSgo2 recruits MCAK to the inner centromere to correct defective kinetochore attachments. J Cell Biol *177*, 413-424.

Huang, T.G., Suhan, J., and Hackney, D.D. (1994). Drosophila kinesin motor domain extending to amino acid position 392 is dimeric when expressed in Escherichia coli. J Biol Chem *269*, 32708.

Hubner, S., Xiao, C.Y., and Jans, D.A. (1997). The protein kinase CK2 site (Ser111/112) enhances recognition of the simian virus 40 large T-antigen nuclear localization sequence by importin. J Biol Chem *272*, 17191-17195.

Hutchins, J.R., Moore, W.J., Hood, F.E., Wilson, J.S., Andrews, P.D., Swedlow, J.R., and Clarke, P.R. (2004). Phosphorylation regulates the dynamic interaction of RCC1 with chromosomes during mitosis. Curr Biol *14*, 1099-1104.

Hyman, A.A., and Sorger, P.K. (1995). Structure and function of kinetochores in budding yeast. Annu Rev Cell Dev Biol *11*, 471-495.

Jones, M.H., Bachant, J.B., Castillo, A.R., Giddings, T.H., Jr., and Winey, M. (1999). Yeast Dam1p is required to maintain spindle integrity during mitosis and interacts with the Mps1p kinase. Mol Biol Cell *10*, 2377-2391.

Jones, M.H., He, X., Giddings, T.H., and Winey, M. (2001). Yeast Dam1p has a role at the kinetochore in assembly of the mitotic spindle. Proc Natl Acad Sci U S A *98*, 13675-13680.

Kaffman, A., Rank, N.M., and O'Shea, E.K. (1998). Phosphorylation regulates association of the transcription factor Pho4 with its import receptor Pse1/Kap121. Genes Dev *12*, 2673-2683.

Kanellopoulou, C., Muljo, S.A., Kung, A.L., Ganesan, S., Drapkin, R., Jenuwein, T., Livingston, D.M., and Rajewsky, K. (2005). Dicer-deficient mouse embryonic stem cells are defective in differentiation and centromeric silencing. Genes Dev *19*, 489-501.

Kang, J., Cheeseman, I.M., Kallstrom, G., Velmurugan, S., Barnes, G., and Chan, C.S. (2001). Functional cooperation of Dam1, Ipl1, and the inner centromere protein (INCENP)-related protein Sli15 during chromosome segregation. J Cell Biol *155*, 763-774.

Kapoor, T.M., and Compton, D.A. (2002). Searching for the middle ground: mechanisms of chromosome alignment during mitosis. J Cell Biol *157*, 551-556.

Kapoor, T.M., Lampson, M.A., Hergert, P., Cameron, L., Cimini, D., Salmon, E.D., McEwen, B.F., and Khodjakov, A. (2006). Chromosomes can congress to the metaphase plate before biorientation. Science *311*, 388-391.

Kaseda, K., Higuchi, H., and Hirose, K. (2003). Alternate fast and slow stepping of a heterodimeric kinesin molecule. Nat Cell Biol *5*, 1079-1082.

Keating, T.J., and Borisy, G.G. (2000). Immunostructural evidence for the template mechanism of microtubule nucleation. Nat Cell Biol *2*, 352-357.

Keeney, J.B., and Boeke, J.D. (1994). Efficient targeted integration at leu1-32 and ura4-294 in Schizosaccharomyces pombe. Genetics *136*, 849-856.

Kerres, A., Jakopec, V., and Fleig, U. (2007). The conserved Spc7 protein is required for spindle integrity and links kinetochore complexes in fission yeast. Mol Biol Cell *18*, 2441-2454.

Kerres, A., Vietmeier-Decker, C., Ortiz, J., Karig, I., Beuter, C., Hegemann, J., Lechner, J., and Fleig, U. (2004). The fission yeast kinetochore component Spc7 associates with the EB1 family member Mal3 and is required for kinetochore-spindle association. Mol Biol Cell *15*, 5255-5267.

Khodjakov, A., La Terra, S., and Chang, F. (2004). Laser microsurgery in fission yeast; role of the mitotic spindle midzone in anaphase B. Curr Biol *14*, 1330-1340.

King, E.M., van der Sar, S.J., and Hardwick, K.G. (2007). Mad3 KEN boxes mediate both Cdc20 and Mad3 turnover, and are critical for the spindle checkpoint. PLoS ONE *2*, e342.

King, J.M., and Nicklas, R.B. (2000). Tension on chromosomes increases the number of kinetochore microtubules but only within limits. J Cell Sci *113 Pt 21*, 3815-3823.

Kirschner, M., and Mitchison, T. (1986). Beyond self-assembly: from microtubules to morphogenesis. Cell *45*, 329-342.

Kitajima, T.S., Hauf, S., Ohsugi, M., Yamamoto, T., and Watanabe, Y. (2005). Human Bub1 defines the persistent cohesion site along the mitotic chromosome by affecting Shugoshin localization. Curr Biol *15*, 353-359.

Kline-Smith, S.L., Khodjakov, A., Hergert, P., and Walczak, C.E. (2004). Depletion of centromeric MCAK leads to chromosome congression and segregation defects due to improper kinetochore attachments. Mol Biol Cell *15*, 1146-1159.

Knowlton, A.L., Lan, W., and Stukenberg, P.T. (2006). Aurora B is enriched at merotelic attachment sites, where it regulates MCAK. Curr Biol *16*, 1705-1710.

La Carbona, S., Le Goff, C., and Le Goff, X. (2006). Fission yeast cytoskeletons and cell polarity factors: connecting at the cortex. Biol Cell *98*, 619-631.

la Cour, T., Kiemer, L., Molgaard, A., Gupta, R., Skriver, K., and Brunak, S. (2004). Analysis and prediction of leucine-rich nuclear export signals. Protein Eng Des Sel *17*, 527-536.

Lampson, M.A., Renduchitala, K., Khodjakov, A., and Kapoor, T.M. (2004). Correcting improper chromosome-spindle attachments during cell division. Nat Cell Biol *6*, 232-237.

Lan, W., Zhang, X., Kline-Smith, S.L., Rosasco, S.E., Barrett-Wilt, G.A., Shabanowitz, J., Hunt, D.F., Walczak, C.E., and Stukenberg, P.T. (2004). Aurora B phosphorylates centromeric MCAK and regulates its localization and microtubule depolymerization activity. Curr Biol *14*, 273-286.

Lansbergen, G., and Akhmanova, A. (2006). Microtubule plus end: a hub of cellular activities. Traffic *7*, 499-507.

Lawrence, C.J., Dawe, R.K., Christie, K.R., Cleveland, D.W., Dawson, S.C., Endow, S.A., Goldstein, L.S., Goodson, H.V., Hirokawa, N., Howard, J., Malmberg, R.L., McIntosh, J.R., Miki, H., Mitchison, T.J., Okada, Y., Reddy, A.S., Saxton, W.M., Schliwa, M., Scholey, J.M., Vale, R.D., Walczak, C.E., and Wordeman, L. (2004). A standardized kinesin nomenclature. J Cell Biol *167*, 19-22.

Lee, D.L., Ivaninskii, S., Burkhard, P., and Hodges, R.S. (2003). Unique stabilizing interactions identified in the two-stranded {alpha}-helical coiled-coil: Crystal structure of a cortexillin I/GCN4 hybrid coiled-coil peptide. Protein Science *12*, 1395-1405.

Levesque, A.A., and Compton, D.A. (2001). The chromokinesin Kid is necessary for chromosome arm orientation and oscillation, but not congression, on mitotic spindles. J Cell Biol *154*, 1135-1146.

Li, R., and Murray, A.W. (1991). Feedback control of mitosis in budding yeast. Cell *66*, 519-531.

Li, Y., Chang, E.C., Garcia, M.A., Koonrugsa, N., Toda, T., West, R.R., Malmstrom, T., McIntosh, J.R., and Troxell, C.L. (2003). Schizosaccharomyces pombe Ras1 effector, Scd1, interacts with Klp5 and Klp6 kinesins to mediate cytokinesis. Genetics *165*, 477-488.

Li, Y., Yu, W., Liang, Y., and Zhu, X. (2007). Kinetochore dynein generates a poleward pulling force to facilitate congression and full chromosome alignment. Cell Res *17*, 701-712.

Liu, X., McLeod, I., Anderson, S., Yates, J.R., 3rd, and He, X. (2005). Molecular analysis of kinetochore architecture in fission yeast. Embo J *24*, 2919-2930.

Logarinho, E., Bousbaa, H., Dias, J.M., Lopes, C., Amorim, I., Antunes-Martins, A., and Sunkel, C.E. (2004). Different spindle checkpoint proteins monitor microtubule attachment and tension at kinetochores in Drosophila cells. J Cell Sci *117*, 1757-1771.

Loiodice, I., Staub, J., Setty, T.G., Nguyen, N.P., Paoletti, A., and Tran, P.T. (2005). Ase1p organizes antiparallel microtubule arrays during interphase and mitosis in fission yeast. Mol Biol Cell *16*, 1756-1768.

Loncarek, J., Kisurina-Evgenieva, O., Vinogradova, T., Hergert, P., La Terra, S., Kapoor, T.M., and Khodjakov, A. (2007). The centromere geometry essential for keeping mitosis error free is controlled by spindle forces. Nature *450*, 745-749.

Losada, A., Hirano, M., and Hirano, T. (1998). Identification of Xenopus SMC protein complexes required for sister chromatid†cohesion. Genes and Development *12*, 1986-1997.

Luo, X., Tang, Z., Xia, G., Wassmann, K., Matsumoto, T., Rizo, J., and Yu, H. (2004). The Mad2 spindle checkpoint protein has two distinct natively folded states. Nat Struct Mol Biol *11*, 338-345.

Lupas, A., Van Dyke, M., and Stock, J. (1991). Predicting coiled coils from protein sequences. Science *252*, 1162-1164.

MacNeal, R.K., and Purich, D.L. (1978). Stoichiometry and role of GTP hydrolysis in bovine neurotubule assembly. J Biol Chem *253*, 4683-4687.

Mallavarapu, A., Sawin, K., and Mitchison, T. (1999). A switch in microtubule dynamics at the onset of anaphase B in the mitotic spindle of Schizosaccharomyces pombe. Curr Biol *9*, 1423-1426.

Maney, T., Hunter, A.W., Wagenbach, M., and Wordeman, L. (1998). Mitotic centromere-associated kinesin is important for anaphase chromosome segregation. J Cell Biol *142*, 787-801.

Maney, T., Wagenbach, M., and Wordeman, L. (2001). Molecular dissection of the microtubule depolymerizing activity of mitotic centromere-associated kinesin. J Biol Chem *276*, 34753-34758.

Manning, A.L., Ganem, N.J., Bakhoum, S.F., Wagenbach, M., Wordeman, L., and Compton, D.A. (2007). The Kinesin-13 Proteins Kif2a, Kif2b, and Kif2c/MCAK Have Distinct Roles during Mitosis in Human Cells. Molecular Biology of the Cell *18*, 2970-2979.

Mayr, M.I., Hummer, S., Bormann, J., Gruner, T., Adio, S., Woehlke, G., and Mayer, T.U. (2007). The human kinesin Kif18A is a motile microtubule depolymerase essential for chromosome congression. Curr Biol *17*, 488-498.

McAinsh, A.D., Tytell, J.D., and Sorger, P.K. (2003). Structure, function, and regulation of budding yeast kinetochores. Annu Rev Cell Dev Biol *19*, 519-539.

McCollum, D. (2004). Cytokinesis: the central spindle takes center stage. Curr Biol *14*, R953-955.

McCully, E.K., and Robinow, C.F. (1971). Mitosis in the fission yeast Schizosaccharomyces pombe: a comparative study with light and electron microscopy. J Cell Sci *9*, 475-507.

McLachlan, A.D., and Stewart, M. (1975). Tropomyosin coiled-coil interactions: evidence for an unstaggered structure. J Mol Biol *98*, 293-304.

McNally, F.J., and Vale, R.D. (1993). Identification of katanin, an ATPase that severs and disassembles stable microtubules. Cell *75*, 419-429.

Melki, R., Carlier, M.F., Pantaloni, D., and Timasheff, S.N. (1989). Cold depolymerization of microtubules to double rings: geometric stabilization of assemblies. Biochemistry *28*, 9143-9152.

Meraldi, P., McAinsh, A.D., Rheinbay, E., and Sorger, P.K. (2006). Phylogenetic and structural analysis of centromeric DNA and kinetochore proteins. Genome Biol *7*, R23.

Meraldi, P., and Sorger, P.K. (2005). A dual role for Bub1 in the spindle checkpoint and chromosome congression. Embo J *24*, 1621-1633.

Michaelis, C., Ciosk, R., and Nasmyth, K. (1997). Cohesins: chromosomal proteins that prevent premature separation of sister chromatids. Cell *91*, 35-45.

Miki, H., Okada, Y., and Hirokawa, N. (2005). Analysis of the kinesin superfamily: insights into structure and function. Trends Cell Biol *15*, 467-476.

Mitchison, T., and Kirschner, M. (1984). Dynamic instability of microtubule growth. Nature *312*, 237-242.

Mitchison, T.J. (1993). Localization of an exchangeable GTP binding site at the plus end of microtubules. Science *261*, 1044-1047.

Moore, A., and Wordeman, L. (2004a). C-terminus of mitotic centromere-associated kinesin (MCAK) inhibits its lattice-stimulated ATPase activity. Biochem J *383*, 227-235.

Moore, A., and Wordeman, L. (2004b). The mechanism, function and regulation of depolymerizing kinesins during mitosis. Trends Cell Biol *14*, 537-546.

Moore, W., Zhang, C., and Clarke, P.R. (2002). Targeting of RCC1 to chromosomes is required for proper mitotic spindle assembly in human cells. Curr Biol *12*, 1442-1447.

Moores, C.A., Cooper, J., Wagenbach, M., Ovechkina, Y., Wordeman, L., and Milligan, R.A. (2006). The role of the kinesin-13 neck in microtubule depolymerization. Cell Cycle *5*, 1812-1815.

Moores, C.A., Hekmat-Nejad, M., Sakowicz, R., and Milligan, R.A. (2003). Regulation of KinI kinesin ATPase activity by binding to the microtubule lattice. J Cell Biol *163*, 963-971.

Moores, C.A., and Milligan, R.A. (2006). Lucky 13-microtubule depolymerisation by kinesin-13 motors. J Cell Sci *119*, 3905-3913.

Moores, C.A., Perderiset, M., Francis, F., Chelly, J., Houdusse, A., and Milligan, R.A. (2004). Mechanism of microtubule stabilization by doublecortin. Mol Cell *14*, 833-839.

Moores, C.A., Yu, M., Guo, J., Beraud, C., Sakowicz, R., and Milligan, R.A. (2002). A mechanism for microtubule depolymerization by KinI kinesins. Mol Cell *9*, 903-909.

Moreno, S., Hayles, J., and Nurse, P. (1989). Regulation of p34cdc2 protein kinase during mitosis. Cell *58*, 361-372.

Moreno, S., Klar, A., and Nurse, P. (1991). Molecular genetic analysis of fission yeast Schizosaccharomyces pombe. Methods Enzymol *194*, 795-823.

Moreno, S., and Nurse, P. (1994). Regulation of progression through the G1 phase of the cell cycle by the rum1+ gene. Nature *367*, 236-242.

Moritz, M., Braunfeld, M.B., Guenebaut, V., Heuser, J., and Agard, D.A. (2000). Structure of the gamma-tubulin ring complex: a template for microtubule nucleation. Nat Cell Biol *2*, 365-370.

Morris, C.A., and Moazed, D. (2007). Centromere assembly and propagation. Cell *128*, 647-650.

Morrison, E.E., Wardleworth, B.N., Askham, J.M., Markham, A.F., and Meredith, D.M. (1998). EB1, a protein which interacts with the APC tumour suppressor, is associated with the microtubule cytoskeleton throughout the cell cycle. Oncogene *17*, 3471-3477.

Musacchio, A., and Salmon, E.D. (2007). The spindle-assembly checkpoint in space and time. Nat Rev Mol Cell Biol *8*, 379-393.

Mythreye, K., and Bloom, K.S. (2003). Differential kinetochore protein requirements for establishment versus propagation of centromere activity in Saccharomyces cerevisiae. J Cell Biol *160*, 833-843.

Nabeshima, K., Kurooka, H., Takeuchi, M., Kinoshita, K., Nakaseko, Y., and Yanagida, M. (1995). p93dis1, which is required for sister chromatid separation, is a novel microtubule and spindle pole body-associating protein phosphorylated at the Cdc2 target sites. Genes Dev *9*, 1572-1585.

Nabeshima, K., Nakagawa, T., Straight, A.F., Murray, A., Chikashige, Y., Yamashita, Y.M., Hiraoka, Y., and Yanagida, M. (1998). Dynamics of centromeres during metaphase-anaphase transition in fission yeast: Dis1 is implicated in force balance in metaphase bipolar spindle. Mol Biol Cell *9*, 3211-3225.

Nakaseko, Y., Goshima, G., Morishita, J., and Yanagida, M. (2001). M phase-specific kinetochore proteins in fission yeast: microtubule-associating Dis1 and Mtc1 display rapid separation and segregation during anaphase. Curr Biol *11*, 537-549.

Nakaseko, Y., Nabeshima, K., Kinoshita, K., and Yanagida, M. (1996). Dissection of fission yeast microtubule associating protein p93Dis1: regions implicated in regulated localization and microtubule interaction. Genes Cells *1*, 633-644.

Nasmyth, K., and Haering, C.H. (2005). The structure and function of SMC and kleisin complexes. Annu Rev Biochem *74*, 595-648.

Noji, H., Yasuda, R., Yoshida, M., and Kinosita, K., Jr. (1997). Direct observation of the rotation of F1-ATPase. Nature *386*, 299-302.

Nonaka, N., Kitajima, T., Yokobayashi, S., Xiao, G., Yamamoto, M., Grewal, S.I., and Watanabe, Y. (2002). Recruitment of cohesin to heterochromatic regions by Swi6/HP1 in fission yeast. Nat Cell Biol *4*, 89-93.

Nurse, P., and Bissett, Y. (1981). Gene required in G1 for commitment to cell cycle and in G2 for control of mitosis in fission yeast.

Nurse, P., and Thuriaux, P. (1977). Controls over the timing of DNA replication during the cell cycle of fission yeast. Exp Cell Res *107*.

O'Connell, C.B., and Khodjakov, A.L. (2007). Cooperative mechanisms of mitotic spindle formation. J Cell Sci *120*, 1717-1722.

O'Shea, E.K., Lumb, K.J., and Kim, P.S. (1993). Peptide 'Velcro': design of a heterodimeric coiled coil. Curr Biol *3*, 658-667.

Ohkura, H., Adachi, Y., Kinoshita, N., Niwa, O., Toda, T., and Yanagida, M. (1988). Cold-sensitive and caffeine-supersensitive mutants of the Schizosaccharomyces pombe dis genes implicated in sister chromatid separation during mitosis. Embo J *7*, 1465-1473.

Ohtsubo, M., Okazaki, H., and Nishimoto, T. (1989). The RCC1 protein, a regulator for the onset of chromosome condensation locates in the nucleus and binds to DNA. J Cell Biol *109*, 1389-1397.

Okada, M., Cheeseman, I.M., Hori, T., Okawa, K., McLeod, I.X., Yates, J.R., 3rd, Desai, A., and Fukagawa, T. (2006). The CENP-H-I complex is required for the efficient incorporation of newly synthesized CENP-A into centromeres. Nat Cell Biol *8*, 446-457.

Oliferenko, S., and Balasubramanian, M.K. (2002). Astral microtubules monitor metaphase spindle alignment in fission yeast. Nat Cell Biol *4*, 816-820.

Ossareh-Nazari, B., Bachelerie, F., and Dargemont, C. (1997). Evidence for a role of CRM1 in signal-mediated nuclear protein export. Science *278*, 141-144.

Ostergren, G. (1951). The mechanism of co-orientation in bivalents and multivalents. Hereditas *37*, 85-156.

Ovechkina, Y., Wagenbach, M., and Wordeman, L. (2002). K-loop insertion restores microtubule depolymerizing activity of a "neckless" MCAK mutant. J Cell Biol *159*, 557-562.

Parry, D.A. (1982). Coiled-coils in alpha-helix-containing proteins: analysis of the residue types within the heptad repeat and the use of these data in the prediction of coiled-coils in other proteins. Biosci Rep *2*, 1017-1024.

Pidoux, A.L., and Allshire, R.C. (2005). The role of heterochromatin in centromere function. Philos Trans R Soc Lond B Biol Sci *360*, 569-579.

Pidoux, A.L., Uzawa, S., Perry, P.E., Cande, W.Z., and Allshire, R.C. (2000). Live analysis of lagging chromosomes during anaphase and their effect on spindle elongation rate in fission yeast. J Cell Sci *113 Pt 23*, 4177-4191.

Pinsky, B.A., Kung, C., Shokat, K.M., and Biggins, S. (2006). The Ipl1-Aurora protein kinase activates the spindle checkpoint by creating unattached kinetochores. Nat Cell Biol *8*, 78-83.

Pockwinse, S.M., Rajgopal, A., Young, D.W., Mujeeb, K.A., Nickerson, J., Javed, A., Redick, S., Lian, J.B., van Wijnen, A.J., Stein, J.L., Stein, G.S., and Doxsey, S.J. (2006). Microtubule-dependent nuclear-cytoplasmic shuttling of Runx2. J Cell Physiol *206*, 354-362.

Pollard, T.D., Earnshaw, W.C. (2004). Cell Biology. Saunders (Elsevier), Pennsylvania, USA.

Poon, I.K., and Jans, D.A. (2005). Regulation of nuclear transport: central role in development and transformation? Traffic *6*, 173-186.

Potapova, T.A., Daum, J.R., Pittman, B.D., Hudson, J.R., Jones, T.N., Satinover, D.L., Stukenberg, P.T., and Gorbsky, G.J. (2006). The reversibility of mitotic exit in vertebrate cells. Nature *440*, 954-958.

Rajagopalan, S., Bimbo, A., Balasubramanian, M.K., and Oliferenko, S. (2004). A potential tension-sensing mechanism that ensures timely anaphase onset upon metaphase spindle orientation. Curr Biol *14*, 69-74.

Raynaud-Messina, B., and Merdes, A. (2007). Gamma-tubulin complexes and microtubule organization. Curr Opin Cell Biol *19*, 24-30.

Reinhart, B.J., and Bartel, D.P. (2002). Small RNAs correspond to centromere heterochromatic repeats. Science *297*, 1831.

Rieder, C.L., and Salmon, E.D. (1994). Motile kinetochores and polar ejection forces dictate chromosome position on the vertebrate mitotic spindle. J Cell Biol *124*, 223-233.

Ris, H., and Witt, P.L. (1981). Structure of the mammalian kinetochore. Chromosoma *82*, 153-170.

Rischitor, P.E., Konzack, S., Fischer, R., Li, Y., Chang, E.C., Garcia, M.A., Koonrugsa, N., Toda, T., West, R.R., Malmstrom, T., McIntosh, J.R., and Troxell, C.L. (2004). The Kip3-like kinesin KipB moves along microtubules and determines spindle position during synchronized mitoses in Aspergillus nidulans hyphae. Eukaryot Cell *3*, 632-645.

Rivera, T., and Losada, A. (2006). Shugoshin and PP2A, shared duties at the centromere. Bioessays *28*, 775-779.

Riviere, Y., Blank, V., Kourilsky, P., and Israel, A. (1991). Processing of the precursor of NF-kappa B by the HIV-1 protease during acute infection. Nature *350*, 625-626.

Rogers, G.C., Rogers, S.L., Schwimmer, T.A., Ems-McClung, S.C., Walczak, C.E., Vale, R.D., Scholey, J.M., and Sharp, D.J. (2004). Two mitotic kinesins cooperate to drive sister chromatid separation during anaphase. Nature *427*, 364-370.

Rogers, S.L., Rogers, G.C., Sharp, D.J., and Vale, R.D. (2002). Drosophila EB1 is important for proper assembly, dynamics, and positioning of the mitotic spindle. J Cell Biol *158*, 873-884.

Ruchaud, S., Carmena, M., and Earnshaw, W.C. (2007). Chromosomal passengers: conducting cell division. Nat Rev Mol Cell Biol *8*, 798-812.

Rustici, G., Mata, J., Kivinen, K., Lio, P., Penkett, C.J., Burns, G., Hayles, J., Brazma, A., Nurse, P., and Bahler, J. (2004). Periodic gene expression program of the fission yeast cell cycle. Nat Genet *36*, 809-817.

Sagolla, M.J., Uzawa, S., and Cande, W.Z. (2003). Individual microtubule dynamics contribute to the function of mitotic and cytoplasmic arrays in fission yeast. J Cell Sci *116*, 4891-4903.

Saka, Y., Sutani, T., Yamashita, Y., Saitoh, S., Takeuchi, M., Nakaseko, Y., and Yanagida, M. (1994). Fission yeast cut3 and cut14, members of a ubiquitous protein family, are required for chromosome condensation and segregation in mitosis. Embo J *13*, 4938-4952.

Salah, S.M., and Nasmyth, K. (2000). Destruction of the securin Pds1p occurs at the onset of anaphase during both meiotic divisions in yeast. Chromosoma *109*, 27-34.

Samejima, I., Lourenco, P.C., Snaith, H.A., and Sawin, K.E. (2005). Fission yeast mto2p regulates microtubule nucleation by the centrosomin-related protein mto1p. Mol Biol Cell *16*, 3040-3051.

Samejima, I., and Yanagida, M. (1994). Bypassing anaphase by fission yeast cut9 mutation: requirement of cut9+ to initiate anaphase. J Cell Biol *127*, 1655-1670.

Sanchez-Perez, I., Renwick, S.J., Crawley, K., Karig, I., Buck, V., Meadows, J.C., Franco-Sanchez, A., Fleig, U., Toda, T., and Millar, J.B. (2005). The DASH complex and Klp5/Klp6 kinesin coordinate bipolar chromosome attachment in fission yeast. Embo J *24*, 2931-2943.

Sandblad, L., Busch, K.E., Tittmann, P., Gross, H., Brunner, D., and Hoenger, A. (2006). The Schizosaccharomyces pombe EB1 homolog Mal3p binds and stabilizes the microtubule lattice seam. Cell *127*, 1415-1424.

Sato, M., Dhut, S., and Toda, T. (2005). New drug-resistant cassettes for gene disruption and epitope tagging in Schizosaccharomyces pombe. Yeast *22*, 583-591.

Sato, M., and Toda, T. (2007). Alp7/TACC is a crucial target in Ran-GTPase-dependent spindle formation in fission yeast. Nature *447*, 334-337.

Savoian, M.S., Gatt, M.K., Riparbelli, M.G., Callaini, G., and Glover, D.M. (2004). Drosophila Klp67A is required for proper chromosome congression and segregation during meiosis I. J Cell Sci *117*, 3669-3677.

Schnitzer, M.J., and Block, S.M. (1997). Kinesin hydrolyses one ATP per 8-nm step. Nature *388*, 386-390.

Schramke, V., and Allshire, R. (2003). Hairpin RNAs and retrotransposon LTRs effect RNAi and chromatin-based gene silencing. Science *301*, 1069-1074.

Schuyler, S.C., and Pellman, D. (2001). Microtubule "plus-end-tracking proteins": The end is just the beginning. Cell *105*, 421-424.

Shang, C., Hazbun, T.R., Cheeseman, I.M., Aranda, J., Fields, S., Drubin, D.G., and Barnes, G. (2003). Kinetochore protein interactions and their regulation by the Aurora kinase Ipl1p. Mol Biol Cell *14*, 3342-3355.

Shankaranarayana, G.D., Motamedi, M.R., Moazed, D., and Grewal, S.I. (2003). Sir2 regulates histone H3 lysine 9 methylation and heterochromatin assembly in fission yeast. Curr Biol *13*, 1240-1246.

Shibasaki, F., Price, E.R., Milan, D., and McKeon, F. (1996). Role of kinases and the phosphatase calcineurin in the nuclear shuttling of transcription factor NF-AT4. Nature *382*, 370-373.

Shipley, K., Hekmat-Nejad, M., Turner, J., Moores, C., Anderson, R., Milligan, R., Sakowicz, R., and Fletterick, R. (2004). Structure of a kinesin microtubule depolymerization machine. Embo J *23*, 1422-1432.

Skibbens, R.V., Rieder, C.L., and Salmon, E.D. (1995). Kinetochore motility after severing between sister centromeres using laser microsurgery: evidence that kinetochore directional instability and position is regulated by tension. J Cell Sci *108 (Pt 7)*, 2537-2548.

Skibbens, R.V., and Salmon, E.D. (1997). Micromanipulation of chromosomes in mitotic vertebrate tissue cells: tension controls the state of kinetochore movement. Exp Cell Res *235*, 314-324.

Skibbens, R.V., Skeen, V.P., and Salmon, E.D. (1993). Directional instability of kinetochore motility during chromosome congression and segregation in mitotic newt lung cells: a push-pull mechanism. J Cell Biol *122*, 859-875.

Skoufias, D.A., Andreassen, P.R., Lacroix, F.B., Wilson, L., and Margolis, R.L. (2001). Mammalian mad2 and bub1/bubR1 recognize distinct spindle-attachment and kinetochore-tension checkpoints. Proc Natl Acad Sci U S A *98*, 4492-4497.

Slep, K.C., and Vale, R.D. (2007). Structural basis of microtubule plus end tracking by XMAP215, CLIP-170, and EB1. Mol Cell *27*, 976-991.

Sodek, J., Hodges, R.S., Smillie, L.B., and Jurasek, L. (1972). Amino-acid sequence of rabbit skeletal tropomyosin and its coiled-coil structure. Proc Natl Acad Sci U S A *69*, 3800-3804.

Sproul, L.R., Anderson, D.J., Mackey, A.T., Saunders, W.S., and Gilbert, S.P. (2005). Cik1 targets the minus-end kinesin depolymerase kar3 to microtubule plus ends. Curr Biol *15*, 1420-1427.

Stade, K., Ford, C.S., Guthrie, C., and Weis, K. (1997). Exportin 1 (Crm1p) is an essential nuclear export factor. Cell *90*, 1041-1050.

Stearns, T., Evans, L., and Kirschner, M. (1991). Gamma-tubulin is a highly conserved component of the centrosome. Cell *65*, 825-836.

Stock, M.F., Guerrero, J., Cobb, B., Eggers, C.T., Huang, T.G., Li, X., and Hackney, D.D. (1999). Formation of the compact confomer of kinesin requires a COOH-terminal heavy chain domain and inhibits microtubule-stimulated ATPase activity. J Biol Chem *274*, 14617-14623.

Stommel, J.M., Marchenko, N.D., Jimenez, G.S., Moll, U.M., Hope, T.J., and Wahl, G.M. (1999). A leucine-rich nuclear export signal in the p53 tetramerization domain: regulation of subcellular localization and p53 activity by NES masking. Embo J *18*, 1660-1672.

Straight, A.F., Sedat, J.W., and Murray, A.W. (1998). Time-lapse microscopy reveals unique roles for kinesins during anaphase in budding yeast. J Cell Biol *143*, 687-694.

Stumpff, J., and Wordeman, L. (2007). Chromosome congression: the kinesin-8-step path to alignment. Curr Biol *17*, R326-328.

Sudakin, V., Chan, G.K., and Yen, T.J. (2001). Checkpoint inhibition of the APC/C in HeLa cells is mediated by a complex of BUBR1, BUB3, CDC20, and MAD2. J Cell Biol *154*, 925-936.

Sullivan, M., and Uhlmann, F. (2003). A non-proteolytic function of separase links the onset of anaphase to mitotic exit. Nat Cell Biol *5*, 249-254.

Takahashi, K., Chen, E.S., and Yanagida, M. (2000). Requirement of Mis6 centromere connector for localizing a CENP-A-like protein in fission yeast. Science *288*, 2215-2219.

Takahashi, K., Murakami, S., Chikashige, Y., Funabiki, H., Niwa, O., and Yanagida, M. (1992). A low copy number central sequence with strict symmetry and unusual chromatin structure in fission yeast centromere. Mol Biol Cell *3*, 819-835.

Tanaka, K., Mukae, N., Dewar, H., van Breugel, M., James, E.K., Prescott, A.R., Antony, C., and Tanaka, T.U. (2005). Molecular mechanisms of kinetochore capture by spindle microtubules. Nature *434*, 987-994.

Tanaka, T.U., Rachidi, N., Janke, C., Pereira, G., Galova, M., Schiebel, E., Stark, M.J., and Nasmyth, K. (2002). Evidence that the Ipl1-Sli15 (Aurora kinase-INCENP) complex promotes chromosome bi-orientation by altering kinetochore-spindle pole connections. Cell *108*, 317-329.

Tang, Z., Shu, H., Qi, W., Mahmood, N.A., Mumby, M.C., and Yu, H. (2006). PP2A Is Required for Centromeric Localization of Sgo1 and Proper Chromosome Segregation. Developmental Cell *10*, 575-585.

Tirnauer, J.S., O'Toole, E., Berrueta, L., Bierer, B.E., and Pellman, D. (1999). Yeast Bim1p promotes the G1-specific dynamics of microtubules. J Cell Biol *145*, 993-1007.

Tokai-Nishizumi, N., Ohsugi, M., Suzuki, E., and Yamamoto, T. (2005). The chromokinesin Kid is required for maintenance of proper metaphase spindle size. Mol Biol Cell *16*, 5455-5463.

Tomonaga, T., Nagao, K., Kawasaki, Y., Furuya, K., Murakami, A., Morishita, J., Yuasa, T., Sutani, T., Kearsey, S.E., Uhlmann, F., Nasmyth, K., and Yanagida, M. (2000). Characterization of fission yeast cohesin: essential anaphase proteolysis of Rad21 phosphorylated in the S phase. Genes Dev *14*, 2757-2770.

Tournier, S., Gachet, Y., Buck, V., Hyams, J.S., and Millar, J.B. (2004). Disruption of astral microtubule contact with the cell cortex activates a Bub1, Bub3, and Mad3-dependent checkpoint in fission yeast. Mol Biol Cell *15*, 3345-3356.

Tran, P.T., Marsh, L., Doye, V., Inoue, S., and Chang, F. (2001). A Mechanism for Nuclear Positioning in Fission Yeast Based on Microtubule Pushing. The Journal of Cell Biology *153*, 397-412.

Tytell, J.D., and Sorger, P.K. (2006). Analysis of kinesin motor function at budding yeast kinetochores. J Cell Biol *172*, 861-874.

Uhlmann, F., Lottspeich, F., and Nasmyth, K. (1999). Sister-chromatid separation at anaphase onset is promoted by cleavage of the cohesin subunit Scc1. Nature *400*, 37-42.

Umeda, M., Izaddoost, S., Cushman, I., Moore, M.S., and Sazer, S. (2005). The fission yeast Schizosaccharomyces pombe has two importin-alpha proteins, Imp1p and Cut15p, which have common and unique functions in nucleocytoplasmic transport and cell cycle progression. Genetics *171*, 7-21.

Uzawa, S., Li, F., Jin, Y., McDonald, K.L., Braunfeld, M.B., Agard, D.A., and Cande, W.Z. (2004). Spindle pole body duplication in fission yeast occurs at the G1/S boundary but maturation is blocked until exit from S by an event downstream of cdc10+. Mol Biol Cell *15*, 5219-5230.

Vale, R.D. (1996). Switches, latches, and amplifiers: common themes of G proteins and molecular motors. J Cell Biol *135*, 291-302.

Vale, R.D., Reese, T.S., and Sheetz, M.P. (1985). Identification of a novel force-generating protein, kinesin, involved in microtubule-based motility. Cell *42*, 39-50.

Vardy, L., and Toda, T. (2000). The fission yeast gamma-tubulin complex is required in G(1) phase and is a component of the spindle assembly checkpoint. Embo J *19*, 6098-6111.

Varga, V., Helenius, J., Tanaka, K., Hyman, A.A., Tanaka, T.U., and Howard, J. (2006). Yeast kinesin-8 depolymerizes microtubules in a length-dependent manner. Nat Cell Biol *8*, 957-962.

Venkatram, S., Jennings, J.L., Link, A., and Gould, K.L. (2005). Mto2p, a novel fission yeast protein required for cytoplasmic microtubule organization and anchoring of the cytokinetic actin ring. Mol Biol Cell *16*, 3052-3063.

Venkatram, S., Tasto, J.J., Feoktistova, A., Jennings, J.L., Link, A.J., and Gould, K.L. (2004). Identification and characterization of two novel proteins affecting fission yeast gamma-tubulin complex function. Mol Biol Cell *15*, 2287-2301.

Verollet, C., Colombie, N., Daubon, T., Bourbon, H.M., Wright, M., and Raynaud-Messina, B. (2006). Drosophila melanogaster gamma-TuRC is dispensable for targeting gamma-tubulin to the centrosome and microtubule nucleation. J Cell Biol *172*, 517-528.

Vogel, S.K., Raabe, I., Dereli, A., Maghelli, N., and Tolic-Norrelykke, I. (2007). Interphase microtubules determine the initial alignment of the mitotic spindle. Curr Biol *17*, 438-444.

Volpe, T.A., Kidner, C., Hall, I.M., Teng, G., Grewal, S.I., and Martienssen, R.A. (2002). Regulation of heterochromatic silencing and histone H3 lysine-9 methylation by RNAi. Science *297*, 1833-1837.

Walczak, C.E. (2006). Kinesin-8s: motoring and depolymerizing. Nat Cell Biol *8*, 903-905.
Walczak, C.E., Mitchison, T.J., and Desai, A. (1996). XKCM1: a Xenopus kinesin-related protein that regulates microtubule dynamics during mitotic spindle assembly. Cell *84*, 37-47.
Waters, J.C., Chen, R.H., Murray, A.W., and Salmon, E.D. (1998). Localization of Mad2 to kinetochores depends on microtubule attachment, not tension. J Cell Biol *141*, 1181-1191.
West, R.R., Malmstrom, T., and McIntosh, J.R. (2002). Kinesins klp5(+) and klp6(+) are required for normal chromosome movement in mitosis. J Cell Sci *115*, 931-940.
West, R.R., Malmstrom, T., Troxell, C.L., and McIntosh, J.R. (2001). Two related kinesins, klp5+ and klp6+, foster microtubule disassembly and are required for meiosis in fission yeast. Mol Biol Cell *12*, 3919-3932.
Westermann, S., Avila-Sakar, A., Wang, H., Niederstrasser, H., Wong, J., Drubin, D.G., Nogales, E., and Barnes, G. (2005). Formation of a dynamic kinetochore- microtubule interface through assembly of the Dam1 ring complex. Mol Cell *17*, 277-290.
Westermann, S., Cheeseman, I.M., Anderson, S., Yates, J.R., 3rd, Drubin, D.G., and Barnes, G. (2003). Architecture of the budding yeast kinetochore reveals a conserved molecular core. J Cell Biol *163*, 215-222.
Westermann, S., Drubin, D.G., and Barnes, G. (2007). Structures and functions of yeast kinetochore complexes. Annu Rev Biochem *76*, 563-591.
Westermann, S., Wang, H.W., Avila-Sakar, A., Drubin, D.G., Nogales, E., and Barnes, G. (2006). The Dam1 kinetochore ring complex moves processively on depolymerizing microtubule ends. Nature *440*, 565-569.
Wheatley, S.P., and Wang, Y. (1996). Midzone microtubule bundles are continuously required for cytokinesis in cultured epithelial cells. J Cell Biol *135*, 981-989.
Wiese, C., and Zheng, Y. (2000). A new function for the gamma-tubulin ring complex as a microtubule minus-end cap. Nat Cell Biol *2*, 358-364.
Wilde, A., Lizarraga, S.B., Zhang, L., Wiese, C., Gliksman, N.R., Walczak, C.E., and Zheng, Y. (2001). Ran stimulates spindle assembly by altering microtubule dynamics and the balance of motor activities. Nat Cell Biol *3*, 221-227.
Witt, P.L., Ris, H., and Borisy, G.G. (1980). Origin of kinetochore microtubules in Chinese hamster ovary cells. Chromosoma *81*, 483-505.
Woehlke, G., Ruby, A.K., Hart, C.L., Ly, B., Hom-Booher, N., and Vale, R.D. (1997). Microtubule interaction site of the kinesin motor. Cell *90*, 207-216.
Wolf, E., Kim, P.S., and Berger, B. (1997). MultiCoil: a program for predicting two- and three-stranded coiled coils. Protein Sci *6*, 1179-1189.
Wood, V., Gwilliam, R., Rajandream, M.A., Lyne, M., Lyne, R., Stewart, A., Sgouros, J., Peat, N., Hayles, J., Baker, S., Basham, D., Bowman, S., Brooks, K., Brown, D., Brown, S., Chillingworth, T., Churcher, C., Collins, M., Connor, R., Cronin, A., Davis, P., Feltwell, T., Fraser, A., Gentles, S., Goble, A., Hamlin, N., Harris, D., Hidalgo, J., Hodgson, G., Holroyd,

S., Hornsby, T., Howarth, S., Huckle, E.J., Hunt, S., Jagels, K., James, K., Jones, L., Jones, M., Leather, S., McDonald, S., McLean, J., Mooney, P., Moule, S., Mungall, K., Murphy, L., Niblett, D., Odell, C., Oliver, K., O'Neil, S., Pearson, D., Quail, M.A., Rabbinowitsch, E., Rutherford, K., Rutter, S., Saunders, D., Seeger, K., Sharp, S., Skelton, J., Simmonds, M., Squares, R., Squares, S., Stevens, K., Taylor, K., Taylor, R.G., Tivey, A., Walsh, S., Warren, T., Whitehead, S., Woodward, J., Volckaert, G., Aert, R., Robben, J., Grymonprez, B., Weltjens, I., Vanstreels, E., Rieger, M., Schafer, M., Muller-Auer, S., Gabel, C., Fuchs, M., Dusterhoft, A., Fritzc, C., Holzer, E., Moestl, D., Hilbert, H., Borzym, K., Langer, I., Beck, A., Lehrach, H., Reinhardt, R., Pohl, T.M., Eger, P., Zimmermann, W., Wedler, H., Wambutt, R., Purnelle, B., Goffeau, A., Cadieu, E., Dreano, S., Gloux, S., Lelaure, V., Mottier, S., Galibert, F., Aves, S.J., Xiang, Z., Hunt, C., Moore, K., Hurst, S.M., Lucas, M., Rochet, M., Gaillardin, C., Tallada, V.A., Garzon, A., Thode, G., Daga, R.R., Cruzado, L., Jimenez, J., Sanchez, M., del Rey, F., Benito, J., Dominguez, A., Revuelta, J.L., Moreno, S., Armstrong, J., Forsburg, S.L., Cerutti, L., Lowe, T., McCombie, W.R., Paulsen, I., Potashkin, J., Shpakovski, G.V., Ussery, D., Barrell, B.G., and Nurse, P. (2002). The genome sequence of Schizosaccharomyces pombe. Nature *415*, 871-880.

Wordeman, L., and Mitchison, T.J. (1995). Identification and partial characterization of mitotic centromere-associated kinesin, a kinesin-related protein that associates with centromeres during mitosis. J Cell Biol *128*, 95-104.

Xiao, C.Y., Hubner, S., and Jans, D.A. (1997). SV40 large tumor antigen nuclear import is regulated by the double-stranded DNA-dependent protein kinase site (serine 120) flanking the nuclear localization sequence. J Biol Chem *272*, 22191-22198.

Yaffe, M.P., Harata, D., Verde, F., Eddison, M., Toda, T., and Nurse, P. (1996). Microtubules mediate mitochondrial distribution in fission†yeast. Proceedings of the National Academy of Sciences *93*, 11664-11668.

Yamada, H., Kumada, K., and Yanagida, M. (1997). Distinct subunit functions and cell cycle regulated phosphorylation of 20S APC/cyclosome required for anaphase in fission yeast. J Cell Sci *110 (Pt 15)*, 1793-1804.

Yamaguchi, S., Decottignies, A., and Nurse, P. (2003). Function of Cdc2p-dependent Bub1p phosphorylation and Bub1p kinase activity in the mitotic and meiotic spindle checkpoint. Embo J *22*, 1075-1087.

Yamaguchi, S., Murakami, H., and Okayama, H. (1997). A WD repeat protein controls the cell cycle and differentiation by negatively regulating Cdc2/B-type cyclin complexes. Mol Biol Cell *8*, 2475-2486.

Yamano, H., Gannon, J., and Hunt, T. (1996). The role of proteolysis in cell cycle progression in Schizosaccharomyces pombe. Embo J *15*, 5268-5279.

Yamano, H., Kitamura, K., Kominami, K., Lehmann, A., Katayama, S., Hunt, T., and Toda, T. (2000). The spike of S phase cyclin Cig2 expression at the G1-S border in fission yeast requires both APC and SCF ubiquitin ligases. Mol Cell *6*, 1377-1387.

Yamashita, A., Sato, M., Fujita, A., Yamamoto, M., and Toda, T. (2005). The roles of fission yeast ase1 in mitotic cell division, meiotic nuclear oscillation, and cytokinesis checkpoint signaling. Mol Biol Cell *16*, 1378-1395.

Yanagida, M. (2000). Cell cycle mechanisms of sister chromatid separation; roles of Cut1/separin and Cut2/securin. Genes Cells *5*, 1-8.

Zhang, Y., and Hancock, W.O. (2004). The two motor domains of KIF3A/B coordinate for processive motility and move at different speeds. Biophys J *87*, 1795-1804.

Zhou, J., Panda, D., Landen, J.W., Wilson, L., and Joshi, H.C. (2002a). Minor alteration of microtubule dynamics causes loss of tension across kinetochore pairs and activates the spindle checkpoint. J Biol Chem *277*, 17200-17208.

Zhou, J., Yao, J., and Joshi, H.C. (2002b). Attachment and tension in the spindle assembly checkpoint. J Cell Sci *115*, 3547-3555.

Zhu, C., Zhao, J., Bibikova, M., Leverson, J.D., Bossy-Wetzel, E., Fan, J.B., Abraham, R.T., and Jiang, W. (2005). Functional analysis of human microtubule-based motor proteins, the kinesins and dyneins, in mitosis/cytokinesis using RNA interference. Mol Biol Cell *16*, 3187-3199.

Zhu, J., and McKeon, F. (1999). NF-AT activation requires suppression of Crm1-dependent export by calcineurin. Nature *398*, 256-260.

Zimmerman, S., Daga, R.R., and Chang, F. (2004a). Intra-nuclear microtubules and a mitotic spindle orientation checkpoint. Nat Cell Biol *6*, 1245-1246.

Zimmerman, S., Tran, P.T., Daga, R.R., Niwa, O., and Chang, F. (2004b). Rsp1p, a J domain protein required for disassembly and assembly of microtubule organizing centers during the fission yeast cell cycle. Dev Cell *6*, 497-509.